

**VALIDATING THE NIMA-RELATED KINASE NEK2 AS A NOVEL
CHEMOTHERAPEUTIC TARGET**

Thesis submitted for the degree of
Doctor of Philosophy
at the University of Leicester

By

Daniel Hayward B.Sc. (Hons.) (Leicester)
Department of Biochemistry
University of Leicester

February 2007

UMI Number: U601261

All rights reserved

INFORMATION TO ALL USERS

The quality of this reproduction is dependent upon the quality of the copy submitted.

In the unlikely event that the author did not send a complete manuscript and there are missing pages, these will be noted. Also, if material had to be removed, a note will indicate the deletion.



UMI U601261

Published by ProQuest LLC 2013. Copyright in the Dissertation held by the Author.
Microform Edition © ProQuest LLC.

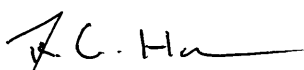
All rights reserved. This work is protected against
unauthorized copying under Title 17, United States Code.



ProQuest LLC
789 East Eisenhower Parkway
P.O. Box 1346
Ann Arbor, MI 48106-1346

DECLARATION

The accompanying thesis submitted for the degree of Doctor of Philosophy, entitled "*Validation of the NIMA-related kinase Nek2 as a novel chemotherapeutic target*" is based on work conducted by the author in the Department of Biochemistry at the University of Leicester mainly during the period May 2002 and February 2007. All of the work recorded in this thesis is original unless otherwise acknowledged in the text or by references. None of the work has been submitted for another degree in this or any other University.

Signed: 

Date: 8/2/07

Department of Biochemistry
University of Leicester
Lancaster Road
Leicester
LE1 9HN

VALIDATION OF THE NIMA-RELATED KINASE NEK2 AS A NOVEL CHEMOTHERAPEUTIC TARGET

DANIEL HAYWARD

SUMMARY

Mitotic division in human cells prompts a dramatic rearrangement of cellular architecture; chromosome condensation, nuclear envelope breakdown and bipolar spindle formation facilitates segregation of sister chromatids into daughter cells. Nek2 is a cell cycle-regulated serine/threonine kinase which is implicated in mitotic progression and establishment of a bipolar spindle. Overexpression of Nek2A in cultured human cells has resulted in an increased incidence of spindle abnormalities and aneuploidy, suggestive of defects in chromosome segregation. Currently there is considerable interest in determining whether centrosomal protein kinases that promote mitotic progression, such as Cdk1, Aurora-A, Plk1 and Nek2, are altered in tumour cells, are tumorigenic when upregulated and hence are viable chemotherapeutic targets. In this thesis I demonstrate that levels of Nek2 protein are upregulated in cell lines derived from leukaemia, breast and ovarian cancers. Importantly, I extended this analysis to primary human tumours and found Nek2 protein expression was increased in sixteen of twenty breast tumours studied, the first report of increased Nek2 protein in human neoplastic disease. I next established that the ablation of Nek2 by siRNA in cultured cervical carcinoma cells induced apoptosis. Lastly I present a series of small molecules that inhibit Nek2A *in vitro* and show the development of two cell-based assays of Nek2A activity, centrosomal disjunction and displacement of the inter-centrosomal component rootletin. Using stable cell lines inducibly expressing Nek2A I demonstrate ablation of Nek2 dependent phenotypes following treatment with a small molecule inhibitor. The ability to inhibit Nek2 in cells coupled with the observation that Nek2 depletion reduces the viability of cultured cells means Nek2 should now be considered a candidate for therapeutic intervention.

ACKNOWLEDGMENTS

I'd initially like to thank my supervisor, Andrew Fry, firstly for his encouragement when I considered registering for a higher degree and secondly for his support and guidance in completing it.

I'd also like to thank all the members of Lab 2/42 who were good colleagues when I started this thesis and great friends when I finished it.

Thanks are also due to my family for their unwavering support through many years, good and bad.

Lastly, there are a few people amongst many who listened to me when I first thought about starting this, then made me listen to them when I had doubts about finishing it. Thanks a lot Liam, Nick, Simon, Abby, Raul, Jo, Chris, Afra, Sarah and Ian.

For you, mum x

CONTENTS

Declaration	I
Summary	II
Acknowledgements	III
Table of Contents	IV
Abbreviations	X
Tables and Figures	XII

Chapter 1 Introduction

1.1	Cancer	1
1.1.1	Prevalence of cancer	1
1.1.2	Molecular pathology of cancer	2
1.1.3	The characteristics of tumour cells	4
1.2	Chemotherapy	
1.2.1	Conventional anti-proliferative therapy	8
1.2.2	Small molecule inhibitors	8
1.2.2.1	Tyrosine kinase inhibitors	8
1.2.2.2	Therapeutic antibodies	11
1.3	The eukaryotic cell cycle	12
1.3.1	The mammalian centrosome	13
1.3.1.1	Centrosome structure	13
1.3.1.2	Centrosome duplication	15
1.3.2	Centrosomes and cancer	16
1.4	Mitotic kinases	17
1.4.1	Polo-like kinases	18
1.4.1.1	Plk1	21
1.4.1.2	Plk1 and tumorigenesis	23
1.4.2	Aurora kinases	25
1.4.2.1	Aurora kinases and tumorigenesis	28
1.4.3	NIMA related kinases	30

1.4.3.1	NIMA kinase	30
1.4.3.2	NIMA homologues	31
1.4.4	Nek2	37
1.4.4.1	Nek2 substrates	42
1.4.4.2	Nek2 expression in human tumours	45
1.5	Aims and Objectives	47
 Chapter 2 Materials and methods		
2.1 Materials		
2.1.1	Chemicals	49
2.1.2	Antibodies	50
 2.2 Molecular Biology Techniques		
2.2.1	Site Directed Mutagenesis	52
2.2.2	DNA Gel Electrophoresis	52
2.2.3	Plasmid Preparation	53
2.2.4	Restriction enzyme digest	53
2.2.5	Genomic DNA extraction	53
2.2.6	Mutation analysis	53
2.2.7	Growth of bacterial cultures	54
2.2.8	Chemically competent bacteria	54
2.2.9	Bacterial Transformation	54
 2.3 Analysis of proteins		
2.3.1	SDS-PAGE	55
2.3.2	Coomassie Blue Staining	55
2.3.3	Silver Staining	55
2.3.4	Western Blotting	56
2.3.5	BCA protein assay	56
2.3.6	Recombinant protein kinases	56
2.3.7	<i>in vitro</i> Kinase Assays	57

2.3.8	High-throughput screen kinase assay	57
2.3.9	Protein Extraction	57
2.3.10	Scintillation Counting	58
2.4	Mammalian Cell Culture	
2.4.1	Maintenance of cultured cells	58
2.4.2	Storage of cell lines	59
2.4.3	Transient Transfection	59
2.4.4	Nek2 depletion by RNA interference	60
2.4.5	Immunofluorescence microscopy	60
2.4.6	Apoptosis assay	61
2.4.7	Cell viability assay	61
2.5	Immunohistochemistry	
2.5.1	Embedded cell lines	62
2.5.2	Antigen retrieval and immunohistochemistry	62
2.6	Data processing	
2.6.1	Calculating IC ₅₀ values	63
2.6.2	Calculating GI ₅₀ values	64

Chapter 3 Nek2 expression is upregulated in human cancer cell lines

3.1 Introduction

3.1.1	Genomic instability and cancer	66
3.1.2	Centrosome defects and aberrant mitosis	66
3.1.3	Kinase control of mitosis	67
3.1.4	Nek2 expression in human cancer	68

3.2 Results

3.2.1	Expression of Nek2 is elevated in cancer-derived cell lines	69
3.2.2	Increased levels of Nek2 correlate with reduced p107 in cancer cell lines	74

3.2.3	Overexpression of Nek2A induces aneuploidy in immortalized human breast cells	74
-------	---	----

3.3	Discussion	78
-----	-------------------	----

Chapter 4 Nek2 protein expression is upregulated in primary human breast tumours

4.1 Introduction

4.1.1	Nek2 upregulation in primary human tumours	84
4.1.2	Pathology of breast cancer	85

4.2 Results

4.2.1	Paraformaldehyde fixation occludes antigenic Nek2 epitopes	88
4.2.2	Antigen retrieval enables Nek2 staining following formaldehyde fixation	89
4.2.3	Detection of centrosomal antigens in cultured normal breast cells	92
4.2.4	Nek2 protein levels are increased in tumour compared to normal tissue	94
4.2.5	Nek2 upregulation persists in invasive lobular and ductal breast carcinoma	97
4.2.6	Increased Nek2 staining does not correlate with known prognostic or proliferative markers	101
4.2.7	Nek2 mutations in primary breast tumour samples and cultured tumour cell lines	102

4.3	Discussion	103
-----	-------------------	-----

Chapter 5 Nek2 depletion affects the growth and viability of cultured cells

5.1	Introduction	116
5.1.1	Nek2 in human disease	119

5.1.2	Depletion of Nek2 in cultured cells	119
5.2	Results	
5.2.1	Depletion of Nek2 in cultured cells by siRNA	121
5.2.2	Nek2 depletion restricts the growth of HeLa and U2OS cells	127
5.2.3	Induction of apoptosis in HeLa cells after Nek2 RNAi treatment	131
5.3	Discussion	136
Chapter 6	Identification of small molecule inhibitors of Nek2A	
6.1	Introduction	142
6.1.1	Measuring kinase activity in high throughput assays	145
6.1.2	Substrate selection for a Nek2 HTS	146
6.1.3	Measuring Nek2A inhibition <i>in vitro</i>	146
6.1.4	Quantifying Nek2 inhibition in cells	147
6.2	Results	
6.2.1	<i>In vitro</i> Nek2A kinase assays	148
6.2.2	NU series molecules inhibit his ₆ Nek2A <i>in vitro</i>	150
6.2.3	NU compounds have μM IC ₅₀ values against his ₆ Nek2A <i>in vitro</i>	151
6.2.4	Selectivity of NU compounds against other mitotic and NIMA-related kinases <i>in vitro</i>	153
6.2.5	NU6141 inhibits GFP-Nek2A induced centrosome disjunction	156
6.2.6	NU6141 inhibits GFP-Nek2A induced rootletin displacement	158
6.2.7	High throughput cell based assay for Nek2A inhibition	160
6.2.8	Nek2 inhibitory compounds identified in the HTS reduce HeLa and U2OS cell growth	162
6.3	Discussion	166

Chapter 7	Discussion	
7.1	Validating Nek2 as a novel drug target	175
7.2	Increased levels of Nek2 protein correlate with human disease and induce abnormalities in cultured cells	175
7.2.1	Downregulating Nek2 reduces cell viability	177
7.2.2	Nek2 is a tractable therapeutic target	178
7.3	Concluding remarks	181
Chapter 8	Bibliography	184
Appendix	Mutation analysis of the Nek2 gene	208

Abbreviations used in this manuscript

γ TuRC	γ -tubulin ring complex
ABL	Abelson kinase
aa	amino acid
APES	3-aminopropyltriethoxysilane
APS	Ammonium Persulphate
ATP	adenosine triphosphate
BCA	bicinchonic acid
BCR	breakpoint cluster region
BSA	Bovine Serum Albumin
Cdk	Cyclin-dependent kinase
CGH	comparative genomic hybridisation
CIN	chromosomal instability
CML	chronic myeloid leukaemia
DAD	D-box activating domain
DLBCL	diffuse large B-cell lymphoma
DMSO	dimethylsulfoxide
DTT	dithiothreitol
EDTA	ethylene diamine tetraacetic acid
EGTA	ethylene glycol tetraacetic acid
FCS	foetal calf serum
FFPE	formaldehyde fixed, paraffin embedded
FGF	fibroblast growth factor
FL	follicular lymphoma
GFP	green fluorescent protein
GST	glutathione-S-transferase
HA	haemagglutinin
HFK	human foreskin keratinocytes
HRP	horseradish peroxidase
HTS	high throughput screening
MAP2	Microtubule associated protein 2
MBP	Myelin basic protein

MIN	microsatellite instability
mRNA	messenger ribonucleic acid
ng	nanogram
nM	nanomolar
nmol	nanomole
NSCLC	non small-cell lung cancer
OD ₂₆₀	Optical Density (absorbance) at 260 nm
OD ₄₅₀	Optical Density (absorbance) at 450 nm
PBS	phosphate-buffered saline
PCM	pericentriolar material
PCR-SSCP	polymerase chain reaction-single strand conformational polymorphism
PK-A	Protein Kinase A
PK-C	Protein Kinase C
pmol	picomole
RISC	RNA-induced silencing complex
RNA	ribonucleic acid
RNAi	RNA interference
SDS	sodium dodecyl-sulphate
SNP	single nucleotide polymorphism
siRNA	small interfering RNA
SSCP	single strand conformational polymorphism
TBS	tris-buffered saline
μg	microgram
μl	microlitre
μm	micrometre
μM	micromolar
μmol	micromole
VEGF	vascular endothelial growth factor
v/v	volume / volume
w/v	weight / volume

Tables and Figures

Table 3.1 Expression of centrosomal proteins Nek2 and C-Nap1 in cancer cell lines	73
Table 4.1 Nek2 Staining does not correlate with known prognostic or centrosomal markers	103
Table 4.2 The N354S transposition identified in several breast tumour samples does not correlate with known prognostic markers	106
Table 6.1 Comparison of IC ₅₀ values of NU series against Nek2A generated by gel-based and flashplate assays	167
1.1 Mutations in the adenoma - carcinoma sequence	5
1.2 The acquired capabilities of cancer	6
1.3 The development of clinical kinase inhibitors	9
1.4 Centrosome structure and the centrosome duplication cycle	14
1.5 Polo homologues and the roles of Plk1 in the mammalian cell cycle	20
1.6 The roles of Aurora-A and Aurora-B in the cell cycle	27
1.7 NIMA related kinases	33
1.8 The structures of the three Nek2 splice variants	39
1.9 Nek2 activity is regulated by phosphorylation	41
1.10 Nek2 substrates	43
3.1 Nek2 polyclonal antibodies	70
3.2 Nek2 expression in cancer cell lines	71
3.3 ECL signal quantification reflects Nek2 protein levels	72
3.4 Reduced p107 correlates with increased Nek2 expression in cancer cell lines	75
3.5 Elevated Expression of Nek2A induces multinucleation in HBL100 cells	77
3.6 Possible mechanisms leading to elevated Nek2 expression	79

4.1	Structure of the mature breast	86
4.2	Abolition of centrosomal staining by Nek2 antibodies following formaldehyde fixation	93
4.3	Antigen retrieval enables Nek2 staining following formaldehyde fixation	93
4.4	Nek2 and C-Nap1 staining in HBL100 immortalized breast cells following antigen retrieval	95
4.5	Nek2 protein levels are increased in tumour compared to normal tissue	96
4.6	Nek2 is upregulated in invasive ductal carcinoma	98
4.7	Nek2 is upregulated in invasive lobular carcinoma	99
4.8	Elevated Nek2 expression in breast tumours identified with a second Nek2 antibody	100
4.9	Nek2 mutations in primary breast tumours and cancer cell lines	105
4.10	The N354S transposition does not affect the centrosomal localisation of Nek2A	108
4.11	Nek2 may promote aneuploidy by alternative pathways	113
5.1	The mechanism of RNA interference in mammalian cells	118
5.2	siRNA duplexes directed against Nek2	122
5.3	Smartpool oligoribonucleotides effectively depletes Nek2 in cultured cells	123
5.4	Single siRNA duplexes efficiently deplete Nek2 in U2OS cells	125
5.5	Single siRNA duplexes efficiently deplete Nek2 in HeLa cells	126
5.6	HeLa and U2OS cell WST assay standard curves	129
5.7	U2OS cell growth following transfection with Nek2 RNAi	130
5.8	HeLa cell growth following Nek2 RNAi treatment	132
5.9	Induction of apoptosis in Nek2 siRNA treated HeLa cells	134
5.10	Phosphoepitopes created by Nek2 may be essential for cell viability	139

6.1	The contemporary drug development process	144
6.2	Measuring Nek2A kinase activity <i>in vitro</i>	149
6.3	100 μ M NU series compounds inhibit Nek2A <i>in vitro</i>	152
6.4	NU compounds his ₆ Nek2A <i>in vitro</i> IC ₅₀	154
6.5	Specificity of mitotic kinase inhibition <i>in vitro</i> by NU compounds	155
6.6	NU6141 inhibits Nek2A induced centrosome splitting	157
6.7	NU6141 inhibits Nek2A induced rootletin displacement	159
6.8	A high throughput cell based assay for Nek2: InCell Analysis of Nek2-induced centrosome splitting	161
6.9	Growth inhibition of U2OS cells by HTS compounds CC004731 and CC004733	164
6.10	Growth inhibition of HeLa cells by HTS compounds CC004731 and CC004733	165
6.11	Structure and selectivity of selected NU Compounds	170
7.1	Nek2 drug discovery project test cascade	179
7.2	Possible consequences of Nek2 inhibition	183

CHAPTER 1

INTRODUCTION

1.1 Cancer

1.1.1 Prevalence of cancer

Cancer, the abnormal growth of new tissue, is a major contributor to global mortality. In 2005, 7.6 million people died of cancer, 13.5% of the 58 million recorded deaths worldwide. Deaths from cancer are predicted to continue rising, with an estimated 9 million people dying in 2015 and 11 million annual deaths by 2030 (W.H.O., 2006). In the United Kingdom, this translated to more than 153,000 deaths from cancer in 2004, a rate of approximately 251 deaths per 100,000 people (O.N.S., 2004).

The growth of cells in the adult human body is tightly regulated, being largely restricted to cell types that renew tissues and structures such as hair follicles, skin and the lining of the gastrointestinal tract. Though all human cell types once possessed the ability to grow and divide, chiefly during embryogenesis and puberty, this proliferative ability is lost in most adult tissues. However, those cells that have formed mature tissues and organs can inappropriately regain the ability to divide. The checks that normally prevent cell growth are lost, a single cell proliferates and new tissue begins to form, resulting in a mass referred to as a tumour (Latin, literally “swelling” (Barnhart, 2003). Tumours are broadly classified as benign or malignant depending on the degree to which they affect surrounding tissues (Weinberg, 2006). Benign tumours remain confined to their site of origin and, though the additional mass can exert pressure on adjacent vital organs, they are rarely life threatening. In marked contrast are malignant tumours, which grow aggressively, invade surrounding tissues and establish secondary smaller tumours which disrupt the function of distant organs. These secondary, metastatic, growths are responsible for the poor prognosis of malignant tumours. Approximately 90% of cancer related deaths are due to metastases (Weinberg, 2006).

The term cancer encompasses a range of pathologies related by unrestrained cellular proliferation. There are many tissues comprising the human body and hence an equal number of different cancers. The majority of tumours arise through proliferation of epithelial cells. Internally, these are sheets of cells that line body cavities such as the gastrointestinal tract; externally they comprise the skin.

Histologically, epithelial tissues appear similar in transverse section; sheets of epithelial cells atop a basement membrane with an underlying supporting matrix of connective tissue referred to as the stroma, or mesenchyme (Knowles and Selby, 2005). Convoluted to form glands or stratified in layers, epithelia also comprise many organs such as the liver (Weinberg, 2006). Epithelia are of interest in tumour biology as the most common human cancers, carcinomas, arise here. In keeping with the prevalence of epithelial tissue in the human body, carcinomas encompass tumours occurring in the stomach, intestines, breast, lungs and liver and are responsible for 80% of global cancer mortality. A further distinction can be drawn depending on the nature of the epithelium the carcinoma develops in. Carcinomas arising in secretory epithelia are referred to as adenocarcinoma whilst those which originate in cells of protective epithelia, such as the skin, are designated squamous cell carcinomas (Weinberg, 2006).

1.1.2 Molecular pathology of cancer

The development of a tumour from initially normal tissue appears to be a multistep process. The stepwise development of tumours is suggested by the increasing incidence of disease with the age of the patient (Knowles and Selby, 2005; O.N.S., 2004). This time dependency suggests somatic cells gradually accrue incremental mutations that free them from growth restriction, whether by errors in DNA replication or exposure to mutagens in the environment. The mutations allow normal cells to proliferate and, in the case of malignant tumours, ultimately invade surrounding tissue.

At a molecular level, the presence of mutations underpinning carcinomas was first advanced as the two-hit hypothesis. The two hits referred to the loss of dominant tumour suppressor genes, each “hit” being the loss of one allele (reviewed in (Knudson, 2001)). A study of patients with a rare childhood cancer of the retina, retinoblastoma, compared the incidence of bilateral and unilateral retinoblastoma. In general, bilateral retinoblastoma is familial and unilateral retinoblastoma is sporadic. Hereditary retinoblastoma patients have already suffered the first “hit” *in utero*, an inherited mutation in one allele of the retinoblastoma (RB) gene. Development of the retinal tumours in these patients occurs more rapidly and in

both eyes simultaneously, prompted by a single acquired disruption of the sole intact RB allele, the second and final “hit”. In contrast, patients developing unilateral retinoblastoma do so at a slower rate. These patients require a cell to receive two successive mutations, hits, of the recessive RB gene before the disease manifests. Subsequent cloning of the retinoblastoma gene and characterisation of the product, RB, showed it to be transcriptional repressor governing cell cycle progression. Loss or mutation of RB allows a cell to proliferate without reliance on external growth signals (Friend et al., 1986; Khidr and Chen, 2006).

The incremental development of tumours does not rely exclusively on loss of tumour suppressor genes nor on the multistep acquisition of mutations (Knudson, 1986). The transition from normal to malignant cells can require as few as a single event in chronic myelogenous leukaemia (CML) or more than four in colorectal carcinoma (Knudson, 2001; Ren, 2005). The pathology of colorectal carcinoma underlines the incremental nature of cancer. Distinct stages of neoplastic growth can be observed in the colonic mucosa. Epithelial cells within the secretory epithelium proliferate to form a neoplastic polyp termed an adenoma. Adenomas themselves are benign but progress in a time-dependent manner to malignant invasive carcinoma (Fearon and Vogelstein, 1990; Underwood, 2002). In contrast to the loss of the tumour suppressor RB in retinoblastoma, the histopathology of the adenoma-carcinoma series belies a sequence of genetic changes within the tumour cells. These changes encompass both loss of tumours suppressor genes, as in retinoblastoma, and the activation of oncogenes. Examining the karyotype of adenomas and carcinomas revealed gross losses of chromosomal arms and deletions of intrachromosomal regions, notably those of 5q, 17p and 18q. These deletions were initially suggested to contain the familial adenomatous polyposis (FAP) gene, deleted in colorectal cancer (DCC) and p53 tumour suppressor genes, respectively (Fearon and Pierceall, 1995; Fearon and Vogelstein, 1990). In addition to loss or disruption of tumour suppressors, adenocarcinomas gain activation of a RAS family member, commonly K-RAS (Fearon and Vogelstein, 1990). Later research has shown loss of the adenomatous polyposis coli (APC) gene product, usually by a truncating missense mutation, to occur in 85% of

sporadic colorectal cancer (Hisamuddin and Yang, 2004). The refining of genotyping has allowed the progression of colorectal carcinoma to be characterised beyond the gross rearrangements detectable by chromosome staining. The adenoma carcinoma sequence involves at least five mutational events (Knudson, 2001) (Figure 1.1). Broadly, these comprise an initiating APC mutation that causes the accumulation of β -catenin. The excess β -catenin interacts with the transcription factor TCF4 to inappropriately activate a panel of genes including c-myc. Further defects in SMAD2/SMAD4, components of the TGF- β signalling pathway, allow growth of the adenoma. Latterly, p53 mutations facilitate the progression from adenoma to carcinoma (Knowles and Selby, 2005).

1.1.3 The characteristics of tumour cells

The genetic lesions that can induce cellular proliferation, or obviate mechanisms repressing it, are as varied as the pathways normally governing cell growth and division. Despite the diverse genetic underpinnings of carcinoma development, it is suggested that in order to form a tumour, neoplastic cells must acquire the same biological capabilities, regardless of route. These characteristics are enumerated by Hanahan and Weinberg as six traits relating to proliferation, the transition to a larger tumour and the establishment of metastases (Figure 1.2) (Hanahan and Weinberg, 2000). The authors suggest that tumour cells gain independence in growth signalling, proliferate without limit and are refractory to anti-growth and apoptic signalling. Additionally, the new tumour tissue must become vascularized and able to metastasize. The independence in growth signalling can occur either by overexpression of growth factor receptors, such as the EGFR receptor *ERBB2*, overexpressed in 30% of early breast carcinomas (reviewed in (Bange et al., 2001)) or by mutations in growth signalling pathways downstream of the receptor such as the RAS-RAF pathway (Davies et al., 2002a). Conversely, inactivation of the anti-proliferative retinoblastoma protein Rb, either by mutation of the protein itself or signalling pathways converging on it, renders cells insensitive to anti-growth signals (Khidr and Chen, 2006). Loss or mutation of the proapoptotic sensor of DNA damage, p53, is reported in more than 50% of human cancers. Apoptotic signalling is also likely abrogated in tumours by upregulation of the pro-

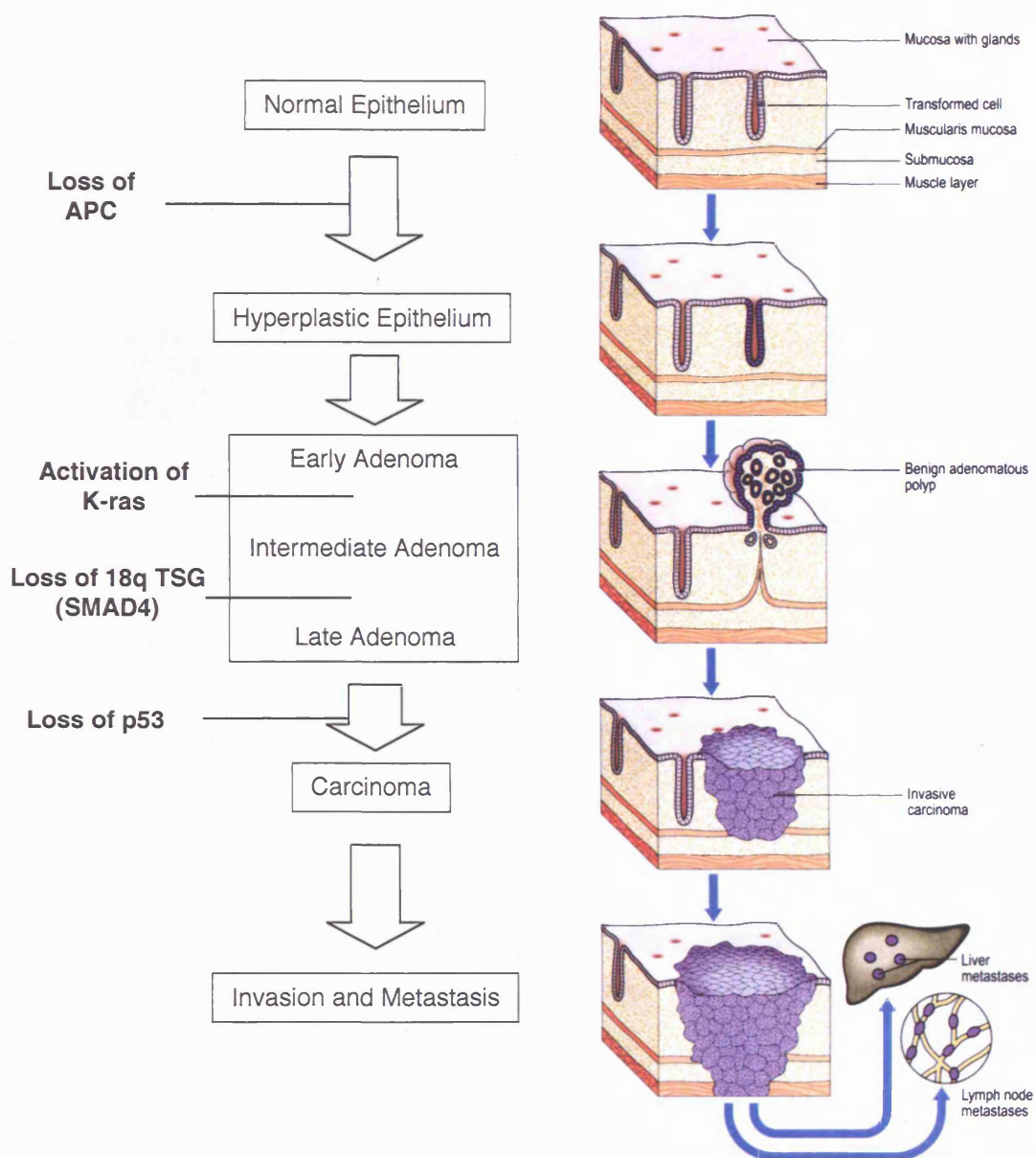
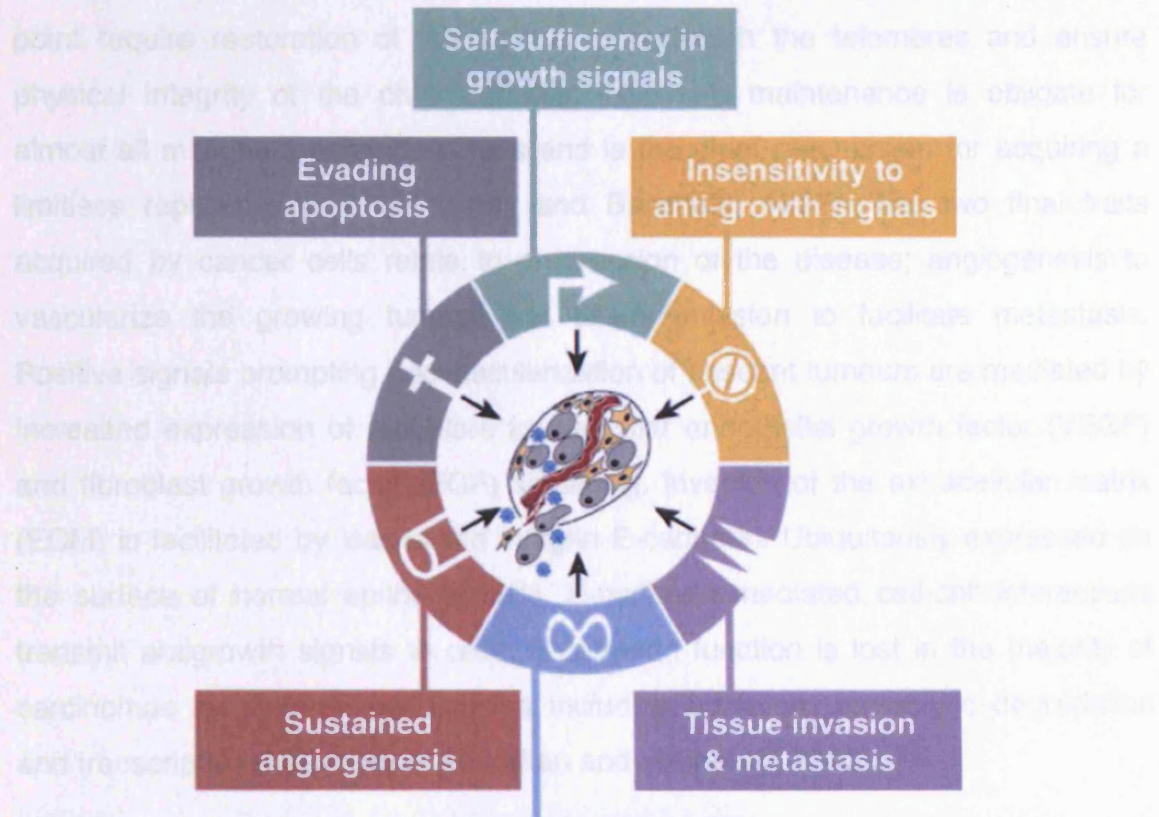


Figure 1.1 Mutations in the adenoma - carcinoma sequence

Common deletions and activations in the multi-step model of colorectal tumour proposed initially by Fearon and Vogelstein. Initiating APC mutations occur in 85% of sporadic colorectal cancers, deregulating Wnt pathway signalling. Subsequent promotion through the adenoma sequence is accompanied by K-ras activation and losses of regions of chromosome 18q. Loss of p53 allows progression to carcinoma. Adapted from Knowles and Selby (2005) and Underwood (2002)

survival PI3-kinase-AKT pathway (Hanahan and Weinberg, 2000). Tumour cells cultured in vitro that successfully evade p53 or Rb mediated growth inhibition will reach a lethal replicative "crisis" after 30-70 divisions. This is due to loss of telomeres, repetitive DNA sequences that cap chromosome ends. The ensuing end to end fusion of uncapped chromosomes proves lethal. Divisions past this point require restoration of telomeres and chromosome maintenance is obligatory for almost all malignant cells.



Cancer is a disease of inappropriate growth which cells should be able to suppress. This new growth can disrupt vital organs, or spread, disseminating itself throughout the body, ultimately ensuring the host's death or survival. It is now widely accepted that the progression to malignancy involves

Figure 1.2 The acquired capabilities of cancer
Six characteristics acquired by cancer cells to evade immune surveillance, develop into a primary tumour then form secondary metastatic growths. These traits are considered universal amongst carcinoma cells that endure to form a tumour, regardless of the mutations that underpin them. Taken from Hanahan and Weinberg (2000).

survival PI3 kinase-AKT pathway (Hanahan and Weinberg, 2000). Tumour cells cultured *in vitro* that successfully sidestep p53 or Rb mediated growth inhibition still reach a lethal replicative “crisis” after 60-70 divisions. This is due to loss of telomeres, repetitive DNA sequences that cap chromosome ends. The ensuing end to end fusion of uncapped chromosomes proves lethal. Divisions past this point require restoration of telomerase to replenish the telomeres and ensure physical integrity of the chromosomes. Telomere maintenance is obligate for almost all malignant carcinoma cells and is the chief mechanism for acquiring a limitless replicative potential (Shay and Bacchetti, 1997). The two final traits acquired by cancer cells relate to progression of the disease; angiogenesis to vascularize the growing tumour and tissue invasion to facilitate metastasis. Positive signals prompting neovascularization of nascent tumours are mediated by increased expression of receptors for vascular endothelial growth factor (VEGF) and fibroblast growth factor (FGF) signalling. Invasion of the extracellular matrix (ECM) is facilitated by loss of the integrin E-cadherin. Ubiquitously expressed on the surface of normal epithelial cells, E-cadherin mediated cell-cell interactions transmit antigrowth signals to cells. E-cadherin function is lost in the majority of carcinomas by several mechanisms including mutation, proteolytic degradation and transcriptional repression (Hanahan and Weinberg, 2000).

Cancer is a disease of tissue hyperplasia, inappropriate growth where there should be none. This new tissue displaces and disrupts vital organs, at worst disseminating itself throughout the body, critically impairing the host’s ability to survive. It is now readily apparent that this proliferation is instituted and underpinned by alterations of tumour cells at the molecular level. The majority of current cancer therapies, however, predate the diagnostic technologies that elucidated these genetic alterations. Current chemotherapy regimes treat the proliferation of tumour cells, not the mutations that cause them.

1.2 Chemotherapy

1.2.1 Conventional anti-proliferative therapy

The most damaging effect of cancer is the replacement or disruption of normal tissue with tumour tissue. Broadly speaking carcinoma cells proliferate, form a tumour *in situ* then invade additional tissues. The goal of cancer therapy is to effect cure and local control. A tumour can be resected to remove malignancy from healthy tissue and chemical therapies can be used to reduce or destroy primary tumours or distant metastases. Current treatments used as an adjuvant to surgery and radiotherapy are blunt. Therapy such as paclitaxel treatment is non-specific, arresting any proliferating cells in mitosis and inducing apoptosis. There are a range of side effects associated with the mechanism of action. The arrest of all the proliferating cell populations in the body suppresses the immune system, prevents renewal of the gastro-intestinal mucosa and kills hair follicles. Paclitaxel also induces peripheral neuropathy, impeding microtubule dependent transport along axons (Knowles and Selby, 2005). Small molecule inhibitors raised against a defined, tumour specific lesion would avoid the pitfalls of antiproliferative drug therapy.

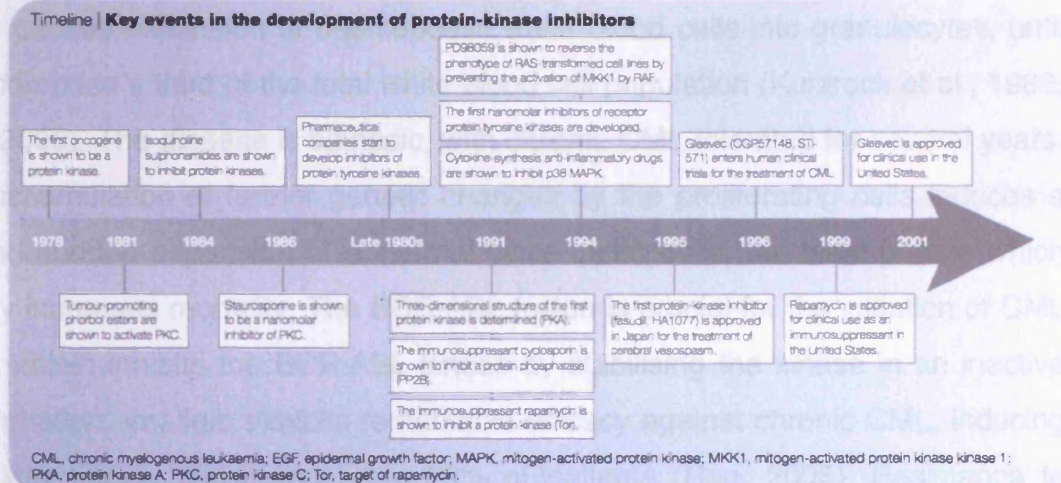
1.2.2 Small molecule inhibitors

Kinases are susceptible to inhibition by small molecules in several ways, most notably those that compete with ATP for binding at the catalytic pocket or stabilise the kinase in an inactive conformation. This tractability has led to a burgeoning number of kinases as drug targets. The human genome has over 500 kinases and some 25 are the subject of clinical trials with putative inhibitors, with several compounds currently licensed for clinical use (Dancey and Sausville, 2003). The kinase targets of licensed small molecule inhibitors are mostly those involved in aberrant cellular proliferation, such as cancer (Figure 1.3).

1.2.2.1 Tyrosine Kinase inhibitors

The initial and most successful of the current small molecule inhibitors is imatinib mesylate (Gleevec, Novartis) used to treat chronic myelogenous leukaemia (CML). In this disease a translocation occurs between the breakpoint cluster region (BCR) and Abelson (ABL) kinase genes on chromosomes 22 and 9, respectively. The

A



B

Kinase targeted	Inhibitor	Company	Disease	Status
Tyrosine kinases				
ABL (KITR, PDGFR)	Gleevec (Glivec, STI-571)	Novartis	Cancer	FDA approval, May 2001
EGFR	ZD1839 (Iressa)	AstraZeneca	Cancer	Phase III
	OSI774	OSI Pharmaceuticals/Roche/Genentech	Cancer	Phase III
EGFR, ERB2R	C11033	Pfizer	Cancer	Phase I
	EKB599	Wyeth-Ayerst	Cancer	Phase I
	GW2016	GlaxoSmithKline	Cancer	Phase I
	PK1166	Novartis	Cancer	Phase I
VEGFR (PDGFR, FGFR)	SU6668	Pharmacia Corporation	Cancer	Phase I
VEGFR	PTK787/ZK222584	Novartis/Schering-Plough	Cancer	Phase II
VEGFR (EGFR)	ZD6474	AstraZeneca	Cancer	Phase I
NGFR	CEP2583	Cephalon	Cancer	Phase II
Serine/threonine kinases				
PKC, KITR, PDGFR?	PKC412	Novartis	Cancer, retinopathy	Phase I
CDKs?	Flavopiridol	Aventis	Cancer	Phase II
CDK2	CYC202	Cyclacel	Cancer	Phase I
MKK1	PD184352	Pfizer	Cancer	Phase I
RAF?	BAY43-906	Onyx Pharmaceuticals/Bayer	Cancer	Phase I
CHK1, PKC, others?	UCN-01	Kyowa Hakko	Cancer	Phase I
mTOR	CCI779	Wyeth-Ayerst	Cancer	Phase II
	RAD001	Novartis	Cancer	Phase I
	Rapamycin (Sirolimus)	Wyeth-Ayerst	Immunosuppression	FDA approval, 1999
ROCK?	HA1077 (AT877, fasudil)	Asahi Chemical Industry	Cerebral vasospasm	Approved in 1995 (Japan)
PKC β	LY333531	Eli Lilly	Diabetic retinopathy	Phase III
p38/SAPK2a	SB281832	GlaxoSmithKline	Rheumatoid arthritis	Phase I
	BIRB0796	Boehringer Ingelheim	Rheumatoid arthritis	Phase II
	Ro320-1195	Roche	Rheumatoid arthritis	Phase I
MLK	CEP-1347	Cephalon	Neurodegeneration	Phase I

ABL, Abelson tyrosine kinase; CDK, cyclin-dependent kinase; CHK1, checkpoint kinase 1; EGFR, epidermal-growth-factor receptor; ERB2R, ERB2 receptor; FDA, US Food and Drug Administration; FGFR, fibroblast-growth-factor receptor; KITR, c-KIT receptor; MKK1, mitogen-activated protein kinase kinase 1; MLK, mixed-lineage protein kinase; mTOR, target of rapamycin (mammalian); NGFR, nerve-growth-factor receptor; p38, p38, mitogen-activated protein kinase; PDGFR, platelet-derived-growth-factor receptor; PKC, protein kinase C; ROCK, RHO-dependent protein kinase; SAPK, stress-activated protein kinase; VEGFR, vascular-endothelial-growth-factor receptor.

Figure 1.3 The development of clinical kinase inhibitors

A. A timeline depicting the evolution of protein kinase inhibitors, including imatinib (Gleevec) the first targeted anti-cancer therapy. **B.** Clinical kinase inhibitors approved, or seeking regulatory approval, for the treatment of human disease. Reproduced from Cohen (2002).

fusion gene encodes a constitutively active tyrosine kinase, termed BCR-ABL, which causes expansion of haemopoietic white blood cells into granulocytes, until they comprise a third of the total white blood cell population (Kurzrock et al., 1988; Ren, 2005). The disease is biphasic, with chronic CML tolerated for several years. The accumulation of further genetic changes by the proliferating cells induces a second sudden expansion of abnormal white blood cells, the blast phase, which rapidly increases mortality. The BCR-ABL fusion is crucial for the initiation of CML and imatinib inhibits the BCR-ABL kinase by stabilising the kinase in an inactive conformation. Imatinib exhibits remarkable efficacy against chronic CML, inducing complete cytogenetic response in 80% of patients (Ren, 2005). Resistance to Imatinib does evolve in CML, commonly through a mutation of the kinase, M351T, that prevents the inhibitor binding. Amplification of the BCR-ABL gene and active efflux of the inhibitor have also been observed in patients refractory to imatinib (Daub et al., 2004). Similarly, administration of imatinib proves ineffective in CML patients in blast crisis or acute lymphoblastic leukaemia (ALL) patients with the 9-22 translocation (Ren, 2005). Imatinib also inhibits signal transduction mediated by the c-Kit and platelet-derived growth factor receptor (PDGFR). The inhibition of c-Kit has led to imatinib being used in the treatment of gastrointestinal stromal tumours (GIST). GIST commonly exhibits gain of function C-KIT mutations (Kitamura et al., 2003).

The success of imatinib as a single agent treatment demonstrated the clinical worth both of kinase inhibitors and the rational of treating the causal mutations of proliferative disease. Therapies directed against other tyrosine kinases implicated in cell transformation, notably subtypes of the erbB receptor tyrosine kinase epidermal growth factor receptor (EGFR), are also entering clinical use. The ATP competitive small molecules gefitinib (Iressa; Astra Zeneca) and erlotinib (Tarceva; Genentech) both inhibit anti-apoptotic signal transduction by binding EGFR. Erlotinib has been approved for treatment of metastatic non-small cell lung cancer, though it only demonstrates efficacy as a single agent in patients that have previously failed to respond to conventional chemotherapy (Levitzki, 2003) (Dancey and Sausville, 2003).

Initial concerns that kinase inhibitors would lack specificity due to the common requirement for ATP binding have also been dispelled in part. A recent examination of the binding of 20 kinase inhibitors against 119 protein kinases showed distinct profiles of specificity for each inhibitor (Fabian et al., 2005). Though ATP pockets are structurally similar it is thought that binding to adjacent residues outside the pocket confers inhibitor specificity (Cohen, 2002).

1.2.2.2 Therapeutic antibodies

Small molecules are not the sole therapeutic agents targeting receptor EGFRs. A humanised monoclonal antibody directed against the receptor tyrosine kinase ErbB2, trastuzumab (Herceptin; Genentech) has proved effective at treating breast cancer. Binding of trastuzumab to ErbB2 induces endocytic internalisation of the receptor and consequently removes the proliferative signal mediated by EGF binding, resulting in cell cycle arrest (Knowles and Selby, 2005). In the United Kingdom, trastuzumab is currently prescribed as an adjuvant to a conventional chemotherapy regime, commonly paclitaxel, or as monotherapy where previous chemotherapy regimes have failed. Trastuzumab is only prescribed to those patients with advanced breast cancer demonstrably overexpressing the ErbB2 receptor (NICE, 2002). Trastuzumab has recently been licensed as an adjuvant for treatment of early-stage breast cancer (NICE, 2006). Though tyrosine kinase inhibitors, whether antibody or small molecule, currently enjoy some clinical success there are drawbacks. Trastuzumab and likely all tyrosine kinase inhibitors affect cardiac function. ErbB2 appears to prevent cardiac myocyte apoptosis, administration of trastuzumab removes this protection and induces left ventricular cardiomyopathy (Mann, 2006).

The use of imatinib to treat CML or trastuzumab as therapy in breast cancer is in response to defined genetic lesions within the carcinoma cells, the chimeric BCR-ABL kinase or overexpression of the ErbB2 receptor, respectively. Profiling tumour cells, or cancer derived cell lines, continues to identify mutated or overexpressed proteins and these proteins will provide new targets for cancer therapy. One class of kinases that are currently the subject of pharmaceutical interest are those that

govern the timing and fidelity of chromosome segregation during cell division, the mitotic kinases.

1.3 The eukaryotic cell cycle

Somatic cells progress through four stages to divide into two new daughter cells. These stages comprise an initial growth of the cell immediately following the previous division termed gap₁ (G₁). A bout of DNA synthesis (S) duplicates the genome in preparation for the next division before a second gap phase (G₂) allows further cell growth. Lastly, the duplicated chromosomes are segregated and the cell invaginates, partitioning the replicated genome and cytoplasm into two nascent daughter cells. This act of duplication is termed mitosis, or M phase. In cultured HeLa cells the entire cell cycle lasts around 22 hours, with mitosis executed in approximately one hour and G₁, S and G₂ (collectively termed interphase) occupying the remaining time. In response to anti-proliferative extracellular signals cells can exit the cell cycle at G₁ into a quiescent fifth state, G₀, before later resuming growth and division (Alberts et al., 2002).

Mitosis witnesses a dramatic rearrangement of the interphase cell. Chromosomes condense, the nuclear envelope breaks down and a large microtubule scaffold, the mitotic spindle, assembles to physically segregate paired sister chromatids. In common with the cell cycle as a whole, mitosis can be considered in stages. These stages were derived initially from light microscope observations of structures within the mitotic cells. Interphase gives way to prophase as replicated chromosomes condense. The nuclear envelope rapidly breaks down, allowing the chromosomes access to the burgeoning spindle and marking prometaphase. Metaphase proper sees chromosomes aligned on the spindle, equidistant from the poles of the cell. The paired chromatids which comprise the duplicated chromosomes separate during anaphase, travelling towards opposite ends of the cell, a process completed at telophase. During cytokinesis, the final stage of mitosis, the segregated chromosomes are encapsulated at the poles of the cell as the nuclear envelope reconstitutes. The process of division instituted in telophase completes, creating two daughter cells, each with a single nucleus (Alberts et al., 2002).

1.3.1 The mammalian centrosome

The mitotic spindle is a large scaffold which forms during mitosis to allow physical segregation of duplicated chromosomes into the nascent daughter cells. The spindle is a bipolar structure, facilitating an equal separation of DNA and preserving the ploidy of the progeny. The bipolarity of the spindle in mammalian cells is predominantly due to microtubule nucleating organelles at each spindle pole, the centrosomes.

1.3.1.1 Centrosome structure

The centrosome of the somatic mammalian cell is a small perinuclear organelle, approximately 1-2 μm in diameter. The centrosome is composed of two distinct structures, two linked tubulin barrels enveloped by a diffuse matrix of proteins called the pericentriolar material (PCM) (Figure 1.4A) (Doxsey, 2001). The PCM comprises structural and regulatory proteins ranging from 13 kDa to 461 kDa and is enriched for coiled coil proteins (Andersen et al., 2003). The diaphanous PCM is also the site of microtubule nucleation, both of the microtubule network in interphase and the astral microtubules of the spindle in mitosis. Microtubule nucleation and binding to the PCM is mediated by a circular structure, the γ -tubulin ring complex (γ -TuRC). γ TuRC appears to function as a microtubule minus-end cap and, though present in the cytoplasm, predominantly nucleates microtubules at the centrosome (Wiese and Zheng, 2000).

The two centrioles enveloped by the PCM are cylinders comprised of nine “blades” of triplet microtubules composed of glutamylated α - and β -tubulin. Centrioles measure approximately 200 nm by 400 nm (Lange and Gull, 1996). Centrioles normally duplicate by semi-conservative replication, with one centriole serving as a template for construction of the other. Depending on the stage of the cell cycle each centrosome hence contains an older, “mother”, centriole and a newer “daughter”. Structurally, the mother centriole can be distinguished by the presence of distal and sub-distal appendages as well as the antigens ϵ -tubulin and cenexin (Figure 1.4B) (Doxsey, 2001; Lange and Gull, 1996). Though the protein

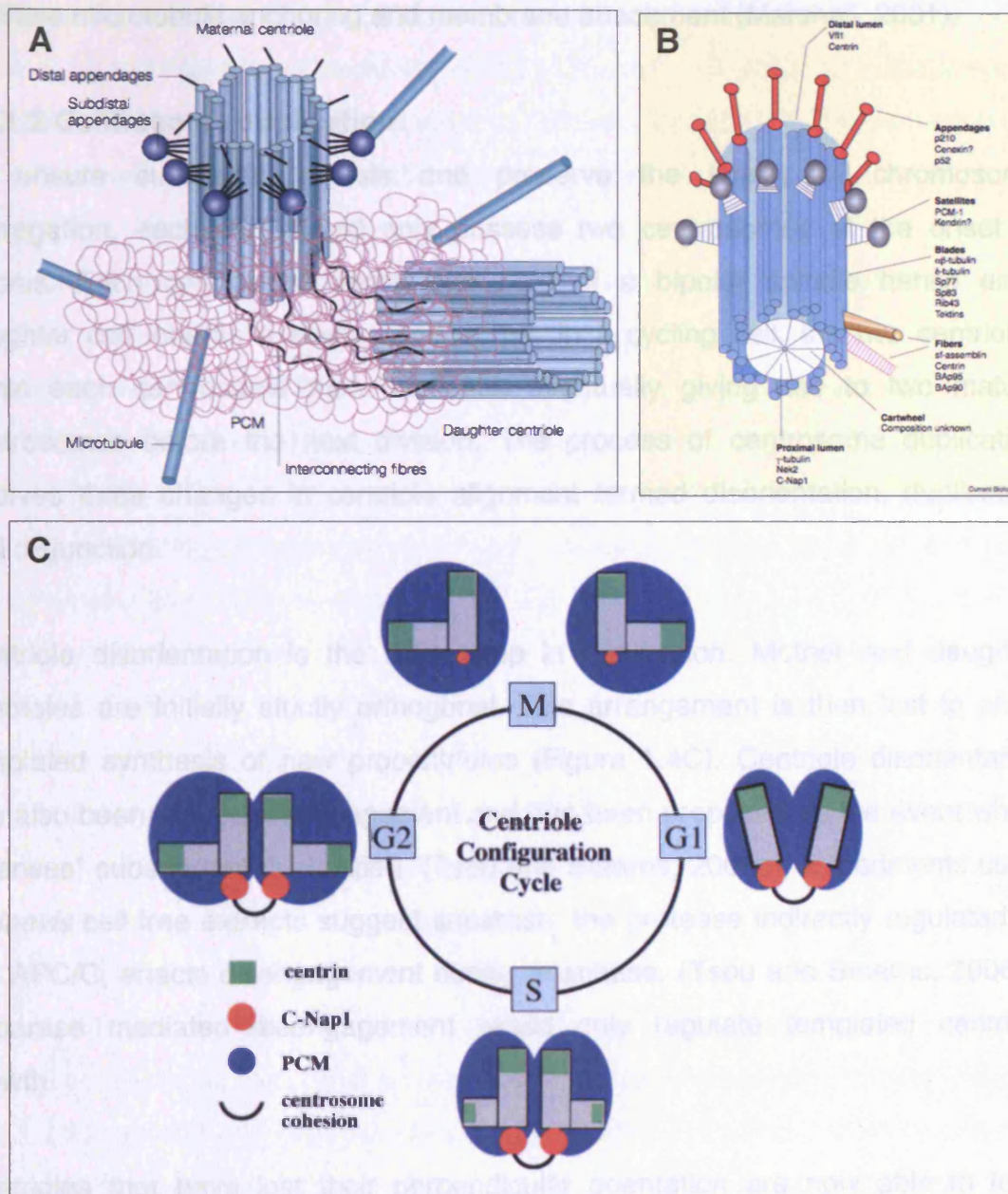


Figure 1.4 Centrosome structure and the centrosome duplication cycle

A. The mammalian centrosome comprises two tubulin barrels, the centrioles, surrounded by an amorphous cloud of proteins, the pericentriolar material (PCM). **B.** The two centrioles differ in their physical structure and composition. The maternal centriole bears distal and sub-distal appendages and antigens such as cenexin not present on the daughter centriole. **C.** Centrosomes duplicate by templated replication. Once cytokinesis is complete, each cell inherits a single centrosome comprising two centrioles. These centrioles are initially tightly tethered to one another. A realignment of these paired centrioles, disorientation, allows them to serve as templates for synthesis of new centrioles during S phase, creating two new centrosomes. At the onset of mitosis the centrosomes move apart to form the spindle poles in an event termed disjunction. Taken from Doxsey (2001) and Marshall (2001).

composition of these appendages is not completely clear they are thought to facilitate microtubule anchoring and membrane attachment (Marshall, 2001).

1.3.1.2 Centrosome duplication

To ensure successful mitosis and preserve the fidelity of chromosome segregation, each cell should only possess two centrosomes at the onset of mitosis. Each centrosome forms one pole of a bipolar spindle hence each daughter cell inherits a single centrosome. In a cycling cell, the two centrioles within each centrosome then duplicate, eventually giving rise to two mature centrosomes before the next division. The process of centrosome duplication involves three changes in centriole alignment termed disorientation, duplication and disjunction.

Centriole disorientation is the initial step in duplication. Mother and daughter centrioles are initially strictly orthogonal. This arrangement is then lost to allow templated synthesis of new procentrioles (Figure 1.4C). Centriole disorientation has also been termed disengagement and has been proposed as the event which “licenses” subsequent duplication (Tsou and Stearns, 2006a). Experiments using *X. laevis* cell free extracts suggest separase, the protease indirectly regulated by the APC/C, enacts disengagement during anaphase. (Tsou and Stearns, 2006b). Separase mediated disengagement would only regulate templated centriole growth.

Centrioles that have lost their perpendicular orientation are now able to form templates for the synthesis of procentrioles. The extension of procentrioles occurs concomitantly with DNA replication in S phase and is initiated at the G₁/S transition (Figure 1.3C). In somatic mammalian cells, Cdk2/Cyclin A activity is required for duplication (Meraldi et al., 1999). In *Xenopus* egg extracts and cultured *C. griseus* cells Cdk2/Cyclin E is implicated in initiating centriole duplication (Lacey et al., 1999; Matsumoto et al., 1999). The addition of antibodies against nucleophosmin blocked its phosphorylation by Cdk2/Cyclin E and centriole duplication in NIH3T3 cell extracts (Tarapore et al., 2002). Latterly, Plk4 has been identified as a core centriolar antigen. Overexpression of active but not kinase dead Plk4/Sak has

been shown to induce centriole duplication in U2OS and HeLa cells, though only in the presence of active Cdk2. Conversely, ablation of Plk4 in HeLa cells by RNAi resulted in a progressive loss of centrioles with each cell division (Habedanck et al., 2005). Cdk2 activity is also required to stabilise *MmMps1*, a kinase necessary for centrosome duplication in mouse cells (Hinchcliffe and Sluder, 2001a).

Throughout interphase, the original mother and daughter cells are connected by a putative tether. Both electron micrographs and the purification of paired centrosomes from cultured cells suggest a physical intercentrosomal link (Fry, 2002). The fibrous linkage is not entirely defined but it is thought that the structural protein C-Nap1, localised to the proximal ends of the centrioles, provides a platform for fibres of a second coiled-coil protein, rootletin (Bahe et al., 2005; Mayor et al., 2002; Mayor et al., 2000). Severing or remodelling of this link in response to phosphorylation is necessary to allow centrosome disjunction. The mitotic kinase Nek2 induces this rearrangement in cultured cells and phosphorylates both C-Nap1 and rootletin *in vitro* (Bahe et al., 2005; Faragher and Fry, 2003; Fry et al., 1998b). Kinesin motors then act to pull the centrosomes apart following Nek2 induced severance (Sharp et al., 2000).

1.3.2 Centrosomes and cancer

The centrosome plays a critical role in mitotic spindle formation and chromosome segregation as it is the primary site of microtubule nucleation in cells (Bornens, 2002; Doxsey, 2001). Normal cells enter mitosis with two properly duplicated centrosomes that ensure bipolarity, as well as correct axial positioning, of the spindle. Cancer cells from a wide variety of tumour types exhibit multipolar spindles and these are often associated with abnormal centrosome number or architecture. (Kuo et al., 2000; Lingle et al., 1998; Pihan et al., 1998; Pihan et al., 2001; Sato et al., 2001). In addition, prematurely split centrosomes, unusually positioned centrosomes and centrosomal proteins with aberrant levels of phosphorylation have all been detected in tumour cells (Lingle et al., 1998; Lingle and Salisbury, 1999). Supernumerary centrosomes, and thereby aneuploidy, may be generated either by a direct uncoupling of the centrosome duplication cycle from the cell division cycle or through an indirect failure of cell division that leads to tetraploidization (Brinkley,

2001; Lingle et al., 1998; Lingle and Salisbury, 1999; Nigg, 2002; Pihan and Doxsey, 1999). Cells lacking p53 or Rb pocket proteins fail to eliminate tetraploid cells allowing them to progress to the next mitosis where multipolar spindles can form (Borel et al., 2002).

Centrosome defects, aneuploidy and chromosomal instability (CIN) were detected in early, even pre-invasive, tumours (Ghadimi et al., 2000; Lingle et al., 2002; Pihan et al., 2003a). An analysis of osteosarcoma cell lines showed supernumerary centrosomes in p53 mutant lines. Supernumerary centrosomes correlated with an increased incidence of abnormal mitoses and aneuploidy (Al-Romaih et al., 2003). A similar relationship was identified in cultured pancreatic cancer cell lines (Sato et al., 2001). Centrosome amplification has been shown to be prognostic for some human cancers. Bladder cancer patients with a high proportion of centrosome hyperamplification in their tumours had an increased chance of disease progression or recurrence after treatment (Yamamoto et al., 2004). Similarly, assessment of 103 primary invasive breast tumours by pericentrin immunohistochemistry found regions of centrosome amplification within 92 of the samples. The greatest centrosome amplification was observed in aggressive, oestrogen independent disease with lymph node involvement (Schneeweiss et al., 2003).

There is considerable interest in identifying whether centrosomal proteins are either mutated or abnormally expressed in cancer cells. The sequential reordering of the cell, throughout the cell cycle and during mitosis, is coordinated by a series of interlocking molecular switches, protein kinases. These switches act by the phosphorylation of defined substrates that ensure the correct order and timing of cell division. A number of cell cycle regulated protein kinases have been localized to the centrosome including Cdk1, Plk1 and Aurora-A. Each of these kinases is active in mitosis and required for mitotic progression and correct bipolar spindle formation (Nigg, 2001).

9

1.4 Mitotic kinases

The function of a protein within the cell, whether structural or catalytic, can be grossly regulated by rates of transcription, translation and degradation. Increases

in abundance may induce a corresponding increase in activity, conversely higher rates of degradation reduce the amount of available protein. A second, post-translational method of modulating protein function is by the reversible addition of phosphate groups by protein kinases. The gain or loss of phosphate groups can induce changes in protein charge, activity and conformation, in turn regulating enzymatic activity, polymerisation and complex formation. In this way, kinases control many aspects of the cell cycle, notably the timing and execution of events preceding and during mitosis.

The canonical regulators of the cell cycle are the bipartite cyclin-dependent kinases (Cdks) and their attendant cyclins (Norbury and Nurse, 1992). Several different Cdk-cyclin complexes are active throughout the cell cycle. The different combinations of Cdk and cyclin regulate diverse processes. Cdk1-cyclinB regulates the onset of mitosis, inducing nuclear envelope breakdown (NEBD) in part by phosphorylation of nuclear lamins and chromosome condensation by phosphorylation of histones H1 and H3. Phosphorylation of motor proteins such as Eg5 by Cdk1-cyclinB create phosphoepitopes that allow their recruitment to the centrosome at the onset of mitosis, inducing centrosome separation as the mitotic spindle forms (Nigg, 1995; Nigg, 2001). Correspondingly, other Cdk-cyclin complexes initiate different aspects of the cell cycle. Cdk2-cyclinE and Cdk2-cyclinA govern DNA replication, for example.

Cdk1-cyclinB is the dominant mitotic kinase, with an increase in activity obligate for correct mitotic entry in eukaryotes (Norbury and Nurse, 1992). Conversely, the degradation of cyclinB and concomitant reduction in cdk1-cyclinB activity is necessary for mitotic exit (Nasmyth, 2005). Cdk1-CyclinB is not the sole mitotic kinase, there are at least three other distinct kinase families that control the order, timing and fidelity of mitosis, the Polo-like kinases (Plks), Aurora kinases and NIMA-related kinases (Neks).

1.4.1 Polo-like kinases

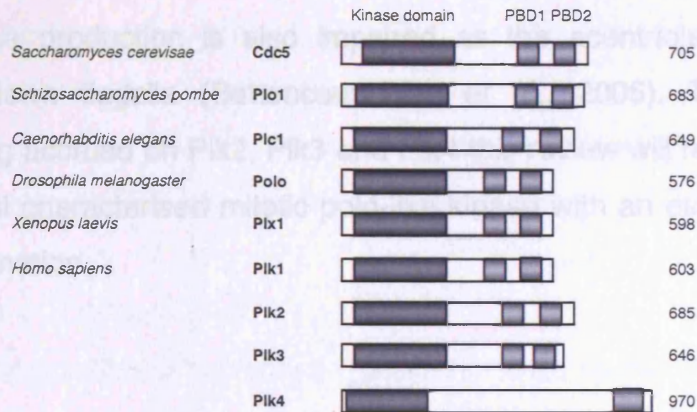
Polo kinase, the founding member of the Plk family, was identified in *D. melanogaster* as the product of the *polo* gene necessary for correct function and

development of centrosomes during larval development. Larvae of homozygous *polo* mutants exhibited metaphase spindle defects in 70% of cells, commonly tetrapolar and multipolar spindles, compared to a background rate of 4% in wild-type larvae. The high incidence of multipolar spindles further affects DNA segregation in meiotic divisions, with *polo*^{-/-} spermatids normally aneuploid (Sunkel and Glover, 1988).

Based on homology to *polo*, multiple Plks have been identified in mammals, *X. laevis*, the nematode *C. elegans* and the budding and fission yeasts *S. cerevisiae* and *S. pombe*, respectively (Figure 1.5). Plks are grouped by their structural similarity, an amino terminal serine/threonine kinase domain with a carboxy terminal regulatory domain containing highly conserved polo box motifs. Polo box motifs are thought to facilitate binding to phosphoepitopes in Plk substrates (Barr et al., 2004). Polo box motifs, or domains (PBDs), have been shown to bind phospho-serine or phospho-threonine epitopes in a range of mitotic Plk substrates such as cdc25 and ninein-like protein (Nlp). Cdk1 and the NIMA-related kinase Nek2 have been proposed as candidate kinases which prime Plk1 binding to cdc25 and Nlp, respectively (Elia et al., 2003a; Elia et al., 2003b; Rapley et al., 2005).

In humans, there are currently four Plks identified through their homology with *polo*, Plks 1-4. Plk1, chiefly active during mitosis, is the most well characterised with less known about Plk2/Snk and Plk3/Fnk. In humans, Plk2 is most active at the G₁/S transition and has a postulated cell cycle role in regulating centriole duplication at the G₁/S transition (Warnke et al., 2004). Cells cultured from Plk2 knockout mice embryos similarly have a delay entering S-phase (Ma et al., 2003). Plk3 is largely thought to interact with cdc25 prior mitosis, phosphorylating it in a similar manner to Plk1. Ectopic expression of Plk3 is also lethal to cultured cells (Myer et al., 2005). Plk4/Sak exhibits homology to the kinase domain of *polo* but lacks the conserved PBDs of Plk1-3, suggesting an evolutionary divergence (Lowery et al., 2005). The most clearly defined role for Plk4 is in regulating centrosome duplication. Depletion of Plk4 by RNAi in human cells reduces centriole numbers with each successive cell division, conversely overexpression

A



B

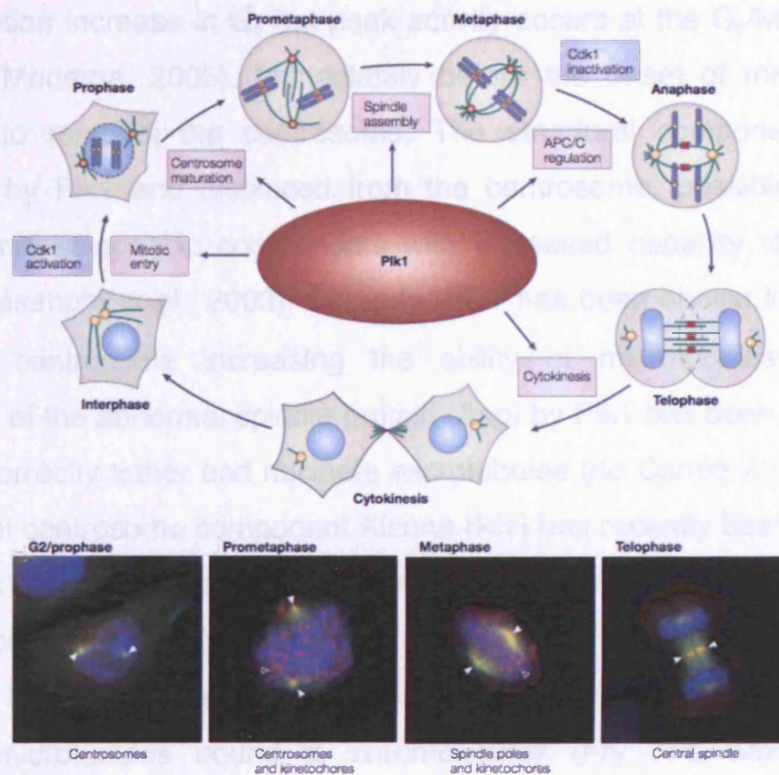


Figure 1.5 Polo homologues and the roles of Plk1 in the mammalian cell cycle

A. Diagrammatic view of Polo homologues from eukaryotic model systems. Kinase domains are shaded dark grey, the bipartite Polo box domains (PBD1 and PBD2) light grey. The number in bold denotes the size of the protein in amino acids. Adapted from Dai (2005). **B.** Schematic view of the diverse interactions of Plk1 with spindle components, Cdk1 and the APC/C. Structures associated with Plk1 at a given stage of the cell cycle appear red. Immunofluorescence microscopy demonstrates the changing localization of Plk1 (red) in mitosis as it moves from the centrosomes to kinetochores and spindle poles before finally associating with the central spindle. DNA appears blue and α -tubulin green. Taken from Barr et al. (2004).

induces novel aggregates of centriolar antigens (Habedanck et al., 2005). Centriolar loss is echoed in *D.melanogaster* cells with mutated or siRNA ablated Plk4/Sak. Axoneme production is also impaired as the acentriolar spermatids cannot correctly form flagella (Bettencourt-Dias et al., 2005). Though more information is being accrued on Plk2, Plk3 and Plk4 this review will restrict itself to Plk1, the most well characterised mitotic polo-like kinase with an established role in cellular transformation.

1.4.1.1 Plk1

In common with Cdk1, Plk1 is most active both prior to and during mitosis. Levels of Plk1 transcription increase in G₂ but peak activity occurs at the G₂/M transition (van Vugt and Medema, 2005). Immediately before the onset of mitosis Plk1 activity begins to remodel the centrosome. The structural component Nlp is phosphorylated by Plk1 and displaced from the centrosome, possibly to allow recruitment of mitosis-specific components with increased capacity to nucleate microtubules (Casenghi et al., 2003). Similarly, Plk1 has been shown to recruit γ -tubulin to the centrosome increasing the ability of microtubules to bind. Phosphorylation of the abnormal spindle protein (Asp) by Plk1 has been implicated in its ability to correctly tether and nucleate microtubules (do Carmo Avides et al., 2001). The novel centrosome component Kizuna (Kiz) has recently been shown to interact with Plk1 to ensure spindle pole integrity. Depletion of Kiz in HeLa cells results in the spindle pole fragmenting into multiple γ -tubulin positive foci. In the absence of Kiz it is suggested that the PCM fragments in response to tension generated by microtubules bound to chromosomes (Fry and Baxter, 2006; Oshimori et al., 2006).

Distinct from roles in spindle formation by enhancing microtubule nucleation at the centrosome, Plk1 cooperates with Cdk1 to induce the onset of mitosis. Binding via its PBD, Plk1 phosphorylates the activating phosphatase cdc25c. Activated cdc25c in turn removes the inhibitory phosphorylation on Cdk1 residues threonine 14 and tyrosine 15, increasing Cdk1-cyclin B activity. In parallel, Plk1 activity reduces a second inhibitory cdk1 signal by phosphorylating wee1, the kinase in part responsible for creating Cdk1 phosphotyrosine 15, causing its degradation

(for comprehensive review see (van Vugt and Medema, 2005)). It is suggested that Cdk1 acts as a priming kinase in both these events, creating the initial phosphoepitope necessary for subsequent Plk1 binding and phosphorylation. Additionally, the DNA damage checkpoint, a halt to mitotic entry in response to DNA strand breaks, targets Plk1 because of its role in amplifying Cdk1-cyclinB activity via wee1 degradation and cdc25c activation (van Vugt and Medema, 2005).

Aside from the G₂/M transition, Plk1 activity also contributes to mitotic progression, specifically the metaphase-anaphase transition and mitotic exit. A series of late mitotic events including chromatid separation, cyclinB degradation and centrosome disengagement are all coordinated by the APC/C (Nasmyth, 2005; Tsou and Stearns, 2006b). The APC/C, a multi-subunit E3 ubiquitin ligase, ubiquitinates substrates that are then degraded by the 26S proteasome (Castro et al., 2005; Peters, 1999). Plk1 has been shown to phosphorylate APC/C subunits 1, 3, 5, and 6 and thereby increase its ubiquitination activity *in vitro*. The APC/C inhibitor Emi1 is also bound and degraded by SCF- β -TrCP in response to Plk1 phosphorylation, further enhancing APC/C activity indirectly (van Vugt and Medema, 2005).

Lastly, Plk1 activity is implicated in the correct formation of the spindle midzone, contractile ring and execution of cytokinesis, roles mirrored by its changing location during mitosis. Plk1 localises to the spindle poles and kinetochores from prophase to metaphase then redistributes to the central spindle in anaphase (Nigg, 2001; van Vugt and Medema, 2005). Plk1 has been shown to phosphorylate NudC and the kinesin-related motor protein Mklp2 at the spindle midzone. Ablation of Mklp2 or NudC by siRNA disrupts cytokinesis, as does removal of the Plk1 phosphorylation site in Mklp2 (van Vugt and Medema, 2005). Polo kinase also interacts with motor proteins during cytokinesis in *D. melanogaster*. Polo mutants fail to localise the *pavarotti* kinesin like protein gene product Pav-KLP, similarly polo localisation at the spindle mid-zone is lost in *pavarotti* mutants (Carmena et al., 1998). In contrast to a requirement for polo and Plk1 for cytokinesis there is also evidence that the proteolytic degradation of Plk1

is necessary for mitotic exit. Plk1 is a target for degradation by APC/C^{cdh1}, the complex it is partially responsible for activating. HeLa cells transfected with Plk1 carrying a mutated D-box destruction motif exhibit a delay in exiting mitosis (Lindon and Pines, 2004). The authors reconcile a need for Plk1 destruction for mitotic exit with its requirement for cytokinesis by suggesting that though Plk1 is necessary for assembly of contractile ring components such as Mklp2, excess Plk1 impairs their ability to bundle microtubules to allow cytokinesis (Lindon and Pines, 2004; Pines and Lindon, 2005).

Plk1 regulates centrosome maturation, spindle polarity and can induce tetraploidy by cytokinesis failure. The unequal segregation of hyperploid genomes is a direct route to the aneuploidy which is a hallmark of solid human tumours (Knudson, 1986; Weinberg, 2006). It is no surprise, therefore, that Plk1 has been implicated in cellular transformation and tumorigenesis.

1.4.1.2 Plk1 and tumorigenesis

The demonstration that levels of Plk1 RNA were increased in human tumours was coincident with the initial cloning of the PLK gene and its putative assignment as the *H. sapiens* homologue of Mouse Plk1, *D. melanogaster* Polo and *S. cerevisiae* cdc5 (Golsteyn et al., 1994; Holtrich et al., 1994). Plk1 mRNA levels were shown to be low in peripheral blood lymphocytes but increased as the cells were induced to proliferate *in vitro*. Plk1 transcripts were also higher in 86% of tumours including lung, breast, and colon when compared to adjacent normal tissue (Holtrich et al., 1994). Subsequent microinjection of Plk1 constructs into NIH-3T3 cells showed Plk1 to be classically transforming *in vitro*. Exogenous expression of Plk1 increased growth rates, induced growth in low serum conditions, conferred anchorage independence and tumour formation in nude mice (Smith et al., 1997). Building on detection of increased Plk1 in tumours, the same authors reported high levels of Plk1 expression in non-small-cell lung cancer (NSCLC) correlated with reduced survival. Five year survival for NSCLC patients with high levels of transcripts was halved, from 51% of the cohort to 24% (Wolf et al., 1997). A similar reduction in three year survival was also observed in oesophageal tumours strongly expressing Plk1 mRNA. Only 24% of patients in the high expression

group survived for three years compared with 59% of those with low amounts of transcript (Tokumitsu et al., 1999). Similarly, Plk1 expression has been detected in gliomas and associated with increased clinical stage in endometrial and ovarian carcinoma (Dietzmann et al., 2001; Takai et al., 2001a; Takai et al., 2001b). Plk1 may also function as a prognostic marker for disease spread in skin cancer. Immunohistochemistry demonstrated increased Plk1 protein levels in thin melanomas with metastases compared to those without (Kneisel et al., 2002).

It can readily be seen that Plk1 overexpression in carcinoma is closely associated with the disease stage, metastasis and clinical outcome. Conversely, a reduction in Plk1 reduces cell viability. Reduction of Plk1 in cervical, breast and NSCLC derived culture cell lines by antisense oligonucleotides reduced proliferation and induced apoptosis (Spankuch-Schmitt et al., 2002a; Spankuch-Schmitt et al., 2002b). Similarly depletion of Plk1 induced apoptosis in cultured prostate cancer cells (Reagan-Shaw and Ahmad, 2005).

The close association of upregulated Plk1 with disease, low levels in non-cycling cells and the induction of apoptosis when the protein is depleted all suggest Plk1 as a putative target in cancer therapy. Preliminary attempts to treat tumours in animal models by depleting Plk1 have proved encouraging. Electroporation with anti-Plk1 phosphorothioate antisense oligodeoxynucleotides *in situ* induced regression of mouse xenograft tumours derived from lung, breast and pharyngeal tumour cell lines (Elez et al., 2003). The expression level of a second polo-like kinase, Plk2, has also been found to modulate the response of cultured cells to the classical anti-cancer agent taxol, with Plk2 depletion increasing apoptosis 48 hours after taxol treatment (Burns et al., 2003). A novel non-ATP competitive Plk1 inhibitor, ON01910, has also been shown to inhibit growth of the 57 cell lines that comprise the national cancer institute (NCI) cancer cell line panel at nanomolar concentrations (Gumireddy et al., 2005).

1.4.2 Aurora kinases

The second main class of mitotic kinases to be considered are the aurora kinases. Described initially in *S. cerevisiae*, a screen for temperature sensitive mutants that showed chromosome gains identified a series of genes designated increase-in-ploidy (lpl) (Chan and Botstein, 1993). lpl1 was later determined to be a serine/threonine kinase, homologous to the *D. melanogaster* gene aurora. Aurora mutant embryos fail to undergo centrosome separation and form monopolar spindles as a result (Glover et al., 1995). The human homologue of aurora was originally identified as a serine/threonine kinase encoded on a region of chromosome 20q13 commonly amplified in human neoplasms and as such was designated breast tumour amplified kinase 1 (BTAK1) (Sen et al., 1997). Near simultaneously, the aurora homologue on 20q13 was also designated Aurora2 and serine/threonine kinase 15 (STK15) (Bischoff et al., 1998a; Zhou et al., 1998b). For clarity, the current accepted nomenclature for human aurora homologues, Aurora-A, B and C, will be adopted. Accordingly STK15/BTAK1/Aurora 2 will be referred to as Aurora-A (Nigg, 2001).

The Aurora family expands with the complexity of the parent organism. The unicellular fungi each have a single Aurora kinase, lpl1 in *S. cerevisiae* and Aurora related kinase 1 (ARK1) in *S.pombe* (Petersen et al., 2001). There are two paralogues in *C.elegans*, AIR-1 and AIR-2, two in *D. melanogaster*, Dm Aurora-A and -B, two in *X. laevis*, Xl Aurora-A and -B and three in humans, Aurora-A, -B and -C (for review see (Carmena and Earnshaw, 2003; Keen and Taylor, 2004)). Whilst the Aurora kinase family members are linked by the strong homology of their N-terminal kinase domains, the roles of the individual kinases within an organism are divergent.

In mammalian cells, Aurora-A and Aurora-B are currently the most well characterised aurora homologues and both are involved in mitotic entry and progression. Aurora-A phosphorylates cdc25b on serine 353, activating it and in turn promoting mitotic entry by Cdk1/cyclin B activation (Dutertre et al., 2004). Aurora-A is associated with centrosomes from G₂ phase into M and has a central role in centrosome maturation and spindle formation, as evidenced by the

monopolar phenotype of *Drosophila* Aurora mutants (Glover et al., 1995). The spindle defects are thought to arise not through failures in centrosome separation but rather through defects in protein recruitment to the centrosome. *C. elegans* embryos treated with Aurora-A RNAi do initially undergo centrosome separation though the separated centrosomes rapidly coalesce. *CeAurora-A* is also required for γ -tubulin and motor protein recruitment to the PCM (Hannak et al., 2001). Aurora-A associated with the PCM becomes activated at mitosis by binding of its substrate targeting protein for XKLP2 (TPX2). Binding of TPX2 to Aurora A displaces the inhibitory phosphatase PP1 γ , allowing autoactivation of Aurora by phosphorylation of threonine 295. Ran-GTP at the spindle induces TPX2 release from importin α,β which in turn activates Aurora-A; the local Ran-GTP gradient originating from chromosomes activates Aurora-A at the spindle poles (Carmena and Earnshaw, 2003). Aurora-A activity is also curtailed by APC/C^{cdh1} mediated degradation during mitotic exit. In *Xenopus*, APC/C^{cdh1} binding is via a “silent” D-box destruction motif activated by a nearby D-box activating domain (DAD) (Castro et al., 2002).

Aurora-B has a distinct subcellular localisation from that of Aurora-A, localising chiefly to centromeres and the mitotic spindle as a chromosome passenger (Figure 1.6). *C.elegans* Aurora-B (AIR-2) is active prior to mitotic entry, phosphorylating histone H3 serine 10 (Hsu et al., 2000). In humans Aurora-B appears to integrate with the spindle checkpoint, mediating accurate chromosome segregation. Unattached kinetochores carry a complex of proteins that mediate the inhibition of anaphase until all the chromosomes are bi-oriented. Current models suggest kinetochore bound Mad, Bub1 and Mad2 are stable components of the spindle checkpoint, with a proportion of diffusible Mad2 directly binding cdc20 and inhibiting the APC/C mediated anaphase transition. The kinases Mps1, Bub1 and BubR1 are known to be necessary to translate the unbound kinetochores into the diffusible “wait” signal (Shah et al., 2004). The kinesin-like protein CENP-E interacts with microtubules to transmit the physical act of microtubule capture at the kinetochore into silencing of downstream signalling by BubR1 (Mao et al., 2003; Mao et al., 2005). Aurora-B is necessary for the correct localisation of BubR1, Mad2 and CENP-E to the kinetochore, with Aurora-B inhibition by the

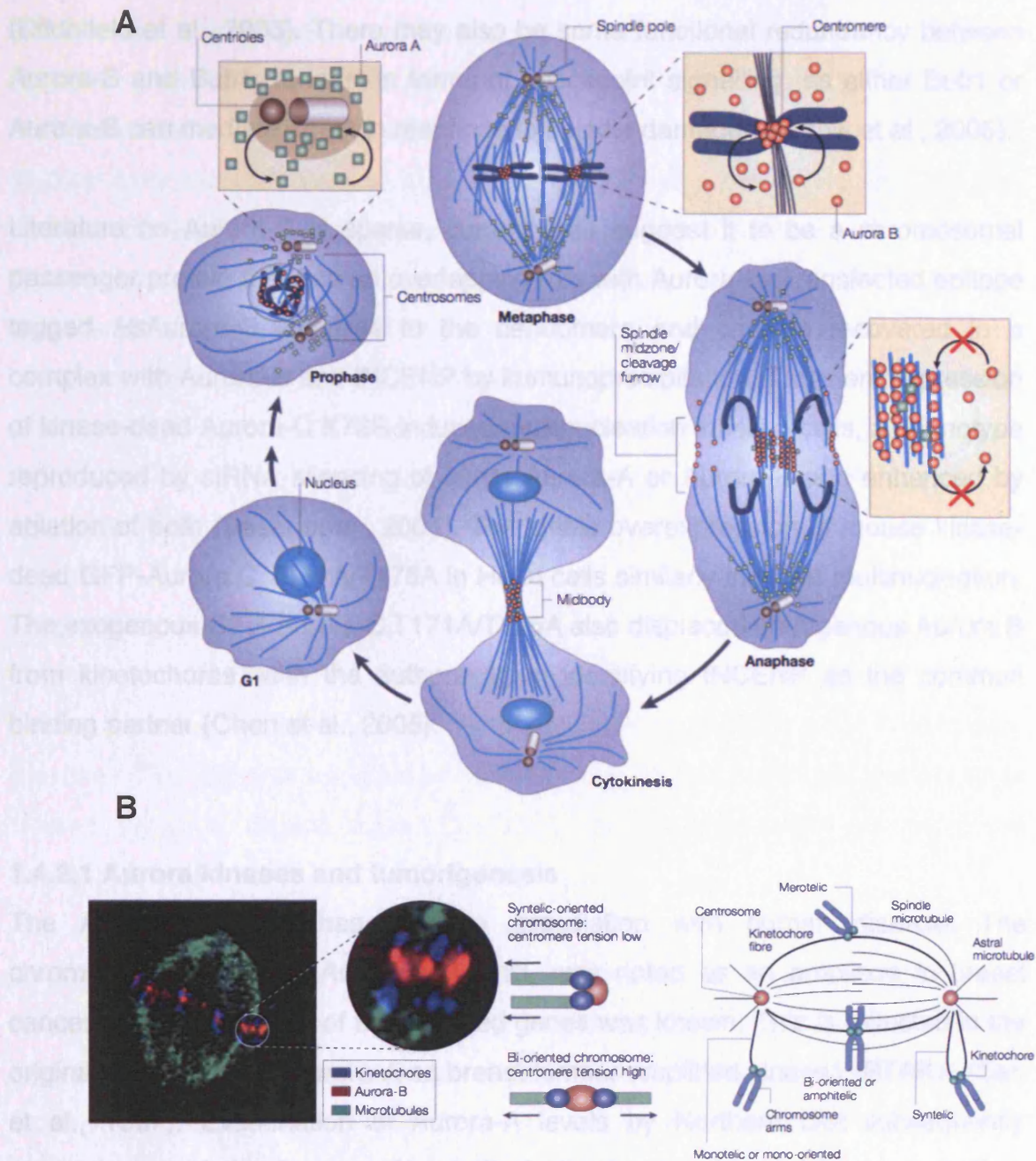


Figure 1.6 The roles of Aurora-A and Aurora-B in the cell cycle

A. In prophase, Aurora-A (green squares) is predominantly centrosomal and Aurora-B (red circles) is nuclear. At metaphase Aurora-B is concentrated at kinetochores, reflecting its role in the spindle checkpoint, whilst Aurora-A decorates microtubules. Progressing through anaphase to cytokinesis Aurora-B is found first at the spindle midzone then the midbody. Aurora-A also localises to the midbody during cytokinesis. Taken from Carmena and Earnshaw (2003). **B.** Aurora-B resolves the syntelic attachment of chromosomes to microtubules, ensuring accurate chromosome segregation. Aurora-B is involved in sensing the tension generated by kinetochores attached to microtubules from opposing poles, bi-orientation. Bi-orientation extinguishes Aurora-B signaling, inactivating the spindle checkpoint and allowing chromosome segregation. Taken from Keen and Taylor (2004).

inhibitor ZM4477439 or ablation by RNAi abrogating the spindle checkpoint (Ditchfield et al., 2003). There may also be some functional redundancy between Aurora-B and Bub1, at least in terms of checkpoint signalling, as either Bub1 or Aurora-B can mediate arrest in response to spindle damage (Morrow et al., 2005).

Literature on Aurora-C is sparse, current data suggest it to be a chromosomal passenger protein that has an overlapping role with Aurora-B. Transfected epitope tagged *HsAurora-C* localises to the centromere and can be recovered in a complex with Aurora-B and INCENP by immunoprecipitation. Transient expression of kinase-dead Aurora-C K72R induced multinucleation in HeLa cells, a phenotype reproduced by siRNA silencing of either Aurora-A or Aurora-B and enhanced by ablation of both (Sasai et al., 2004). The stable overexpression of mouse kinase-dead GFP-Aurora C T171A/T175A in HeLa cells similarly induced multinucleation. The exogenous GFP-Aurora C T171A/T175A also displaced endogenous Aurora B from kinetochores, with the authors again identifying INCENP as the common binding partner (Chen et al., 2005).

1.4.2.1 Aurora kinases and tumorigenesis

The Aurora-A kinase has a close association with human disease. The chromosomal region of Aurora-A, 20q13, was noted as an amplicon in breast cancer before the nature of the encoded genes was known. This is reflected in the original designation of Aurora-A as breast tumour amplified kinase1 (BTAK1) (Sen et al., 1997). Examination of Aurora-A levels by Northern blot subsequently showed upregulation in more than half of all primary colorectal tumours studied. Moreover, expression of constitutively active *HsAurora-A* T288D transformed rat fibroblasts (Bischoff et al., 1998b). Wild-type *HsAurora-A* was also noted to transform mouse NIH-3T3 cells and additionally induced supernumerary centrosomes and changes in ploidy (Zhou et al., 1998b). HeLa cells transfected with wild-type *HsAuroraA* were also refractory to paclitaxel, with a fifty percent reduction in apoptosis compared to mock transfected cells (Anand et al., 2003). An immunohistochemical analysis of human bladder cancers found increased Aurora-A protein expression frequently accompanied higher grade disease. Patients with

bladder tumours expressing high levels of Aurora-A experienced reduced overall survival and more rapid occurrence of metastatic disease (Sen et al., 2002). Elevated protein levels of Aurora-A were also detected in 22 of 38 pancreatic tumours compared to matched normal tissue (Li et al., 2003). The majority of studies have examined levels of Aurora-A, the kinase associated with the 20q amplification in disease. Increased expression of Aurora-B was noted, though not investigated, in transformed cell lines (Bischoff et al., 1998a). A more recent widespread analysis of mRNA levels in multiple primary human tumours found overexpression of both Aurora-A and Aurora-B, though not Aurora-C. Aurora-B expression always mirrored that of Aurora-A, both high or both low, leading the authors to speculate a feedback mechanism may exist between the two paralogues (Keen and Taylor, 2004).

Aurora-A exhibits widespread upregulation in multiple human tumours and a close association with higher grade disease and aneuploidy. Upregulated Aurora-A further correlates with reduced patient survival and higher incidence of metastatic disease. This defined association with human tumours and the tractability of kinases as drug targets makes Aurora-A an attractive target for anticancer therapy.

A recent review of Aurora kinase inhibitors in development identified more than ten different molecules from a range of pharmaceutical companies, with several reported to have commenced phase 1 clinical trials (Matthews et al., 2006). The most well characterised disclosed compounds are currently VX-680 (Vertex Pharmaceuticals, Cambridge, MA), ZM447439 (AstraZeneca, Alderley Park, UK) and Hesperadin (Boehringer Ingelheim, Albany, NY). All three compounds produce broadly similar phenotypes in treated cultured cells; exit from mitosis without cytokinesis, endoreduplication and polyploidy (Mortlock et al., 2005). The observed disruption of cytokinesis and reduction in phosphorylation of histone H3 residue serine 10 are consistent with these molecules acting via inhibition of Aurora-B (Carmena and Earnshaw, 2003; Keen and Taylor, 2004; Nigg, 2001). The exact response to chemical Aurora inhibition depends on the cell line used and more precisely p53 status. Cultured cells with wild-type p53 treated with VX-

680 or ZM447439 arrest with a 4n or 8n DNA content, whereas cells lacking functional p53 continue to endoreduplicate, lose viability and apoptose (Ditchfield et al., 2003; Gizatullin et al., 2006). Currently, there is considerable debate on the existence of a tetraploid, or post-mitotic, checkpoint in mammalian cells (Andreassen et al., 2001; Uetake and Sluder, 2004). Regardless of its exact nature the action of current Aurora inhibitors does appear to be mediated by a p53 dependent post-mitotic checkpoint. Experiments with VX-680 suggested that in addition to wild-type p53 and intact RB, the induction of p21^{Waf1/Cip} is necessary to mediate a G₁ arrest and prevent further endoreduplication (Gizatullin et al., 2006; Margolis et al., 2003). Without consideration of the underlying mechanism, Aurora-B inhibitors induce growth arrest or apoptosis of cultured cancer cell lines. ZM447439 inhibited growth of a range of cultured cells (Ditchfield et al., 2003). Encouragingly, VX-680 also induced regression of HL60 (leukaemia), MIA PaCa-2 (pancreatic) and HCT-116 (colon) derived xenograft tumours in nude mice (Harrington et al., 2004). Though Aurora inhibitors are not classically anti-mitotic they would be expected to arrest cycling somatic cells, dependent on dose. The administration of VX-680 intraperitoneally to nude mice or intravenously to nude rats was well tolerated with minimal toxicity and reduction in body weight (Harrington et al., 2004).

1.4.3 NIMA related kinases

1.4.3.1 NIMA kinase

A genetic screen in the filamentous fungus *Aspergillus nidulans* identified genes required for progression through the cell division cycle. Two gross classes of temperature sensitive mutants were identified. These genes were termed either *nim* whereby at the restrictive temperature mutations result in a block in interphase and the cells are never in mitosis, or *bim*, where mutants were blocked in mitosis, with condensed chromosomes and mitotic spindles, never progressing to interphase (Morris, 1975).

One of the 26 *nim* mutants isolated, *nimA*, arrested in late G₂ with duplicated spindle pole bodies (SPBs) and, upon shifting to the permissive temperature, rapidly entered mitosis, undergoing chromosome condensation and spindle

formation (Oakley and Morris, 1983). Cloning of *nimA* suggested a mature transcript of 3.6Kb which was later shown to encode a serine/threonine kinase designated NIMA (Lu et al., 1993; Osmani et al., 1987). NIMA activity was demonstrated to be obligate for mitotic entry, with cells requiring both active cdc2 and NIMA for chromosome condensation and spindle formation. Cdc2 activity remains independent of NIMA, however, with cdc2 activated even in the absence of NIMA. Conversely, aberrant expression of NIMA could induce a “pseudo-mitotic” state of chromosome condensation from any point in the cell cycle. In addition to regulating the cell cycle NIMA is itself tightly regulated. Levels of *nimA* mRNA are low throughout G₁ and S phase, rising through G₂ to peak immediately before the onset of mitosis (Osmani et al., 1987). This pattern is mirrored by the gene product, NIMA, which is most abundant and active at the same point before decreasing as cells exit mitosis. The increase in NIMA activity is commensurate with an increase in NIMA serine/threonine autophosphorylation (Lu et al., 1993).

The genetic screen of *A. nidulans* also identified compensatory mutations, notably that of the gene BIME. *nimA/BimE* double mutants allow an increase in the level of NIMA to approximately 20% of wild-type; sufficient to overcome the late interphase arrest and enter mitosis but not to complete it correctly. *BimE* encodes a subunit of the APC/C, that targets NIMA for proteolysis. Reduction of BIME reduces the suppression of NIMA, presumably by interfering with its degradation, allowing a partial recovery from the effect of the *nimA* mutation (Ye et al., 1998).

1.4.3.2 NIMA homologues

The demonstration that NIMA kinase activity is essential for correct mitosis in *A. nidulans* prompted a search for NIMA-like pathways in other eukaryotes. The presence of signalling pathways employing NIMA-like proteins in other organisms was likely as the expression of NIMA in both the fission yeast *Schizosaccharomyces pombe* and the human HeLa cervical carcinoma cell line induced similar pseudo-mitotic chromatin condensation to that originally observed in *A. nidulans* (Lu et al., 1993; O'Connell et al., 1994). Several NIMA-like kinase genes and gene families were identified in fungi, yeast and higher eukaryotes,

generally employing low stringency screening of genomic libraries by PCR of the conserved kinase domains.

A second filamentous fungus, *Neurospora crassa*, yielded a kinase with the greatest sequence identity to NIMA. The *nim-1* gene product, NIM-1, bears 75% sequence identity to NIMA across the 295 residue kinase domain but more importantly is the sole functional homologue of NIMA identified to date, whereby introduction of *nim-1* to *A. nidulans nimA* mutants restores normal mitosis, abolishing the late G₂ arrest (Pu et al., 1995). In terms of descending sequence identity, the next most similar kinase to NIMA is KIN3, identified in the budding yeast *Saccharomyces cerevisiae* (Jones and Rosamond, 1990) which exhibits 48% sequence identity though neither complements *nimA* or shows a marked phenotype upon mutation of the gene or overexpression of the gene product (Barton et al., 1992; Kambouris et al., 1993) suggesting either a redundancy of KIN3 function or a role in a different pathway in that system.

The fission yeast, *S. pombe*, also possesses a NIMA related kinase, termed Fin1, transcribed from the gene fission yeast *nimA1*, *fin1*, which is 44% identical across amino acid residues 121-289 (Krien et al., 1998). Functionally, Fin1 overexpression induces *cdc2* independent chromatin condensation in *S. pombe* irrespective of the cell cycle stage, much like that observed for NIMA in *A. nidulans*. Fin1 has latterly been shown to be necessary for spindle formation. *S. pombe* mutant in *fin1* failed to nucleate spindle microtubules from one of their spindle pole bodies (SPBs) and Fin1 has further been shown to regulate recruitment of the polo kinase Plo1 to the SPB (Grallert and Hagan, 2002). In addition, Fin1 recruitment to nascent SPBs has been shown to restrain septation via interaction with the septum initiation network (SIN) inhibitors Byr4 and Cdc16 (Grallert et al., 2004).

Whereas *S. pombe*, *S. cerevisiae* and *N. crassa* each possess a single NIMA homologue, in higher eukaryotes there has been a marked expansion of kinases exhibiting homology to the NIMA catalytic domain. There are 11 NIMA related kinases, Neks, currently identified in vertebrates (Figure 1.7). Accompanying the

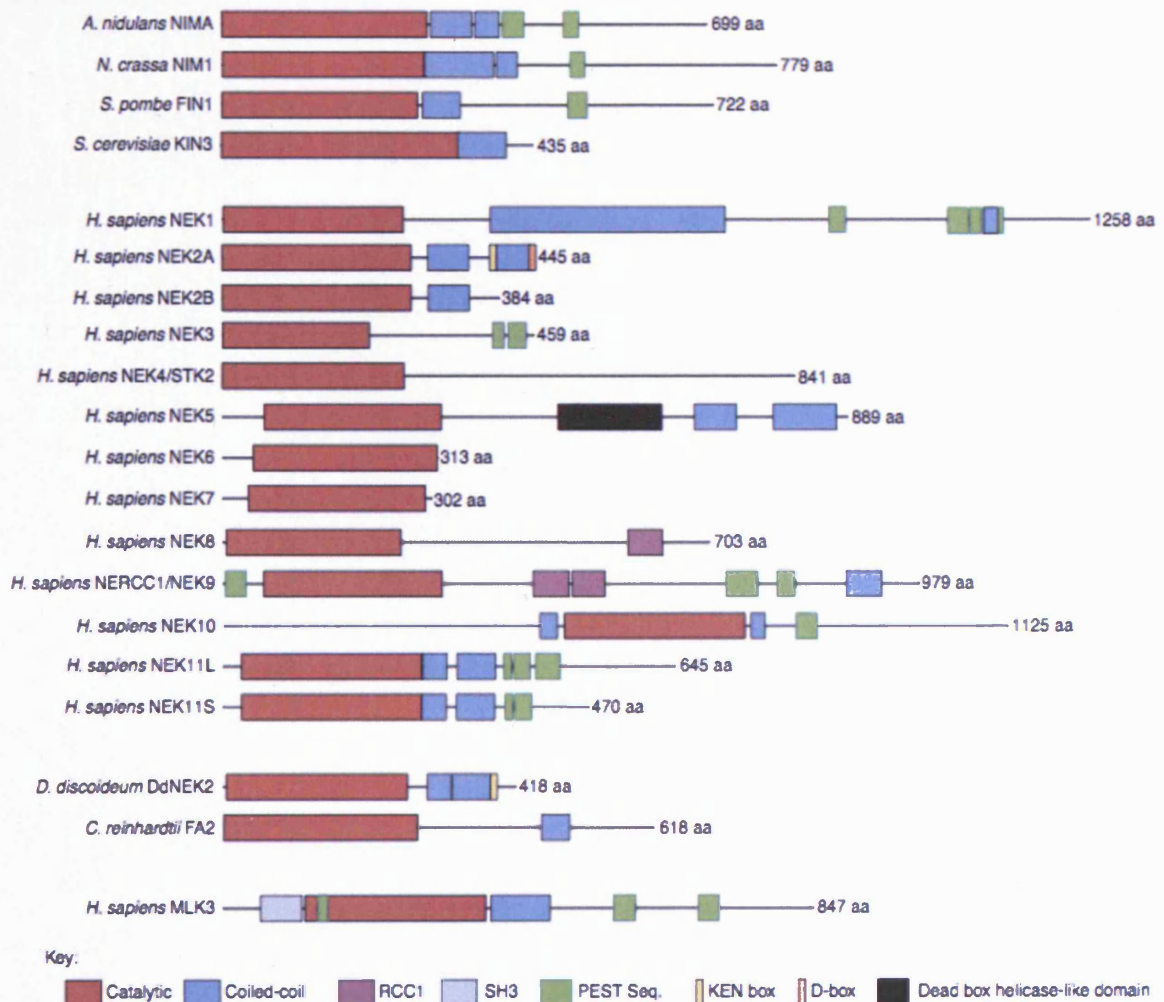


Figure 1.7 NIMA related kinases

The NIMA kinase family has seen an expansion to eleven members in *H. sapiens*. Two homologues have also been identified in the green algae *Chlamydomonas reinhardtii* and the amoeba *Dictostylium discoideum*. The family is defined by homology to the NIMA kinase domain with various C-terminal motifs facilitating protein-protein interactions (Coiled coil, RCC1) or regulation via proteolytic degradation (PEST, KEN, D-box). Reproduced from O'connell et al. (2003).

expansion of the NIMA family has been a corresponding diversification of roles and not all the Neks have a defined function in mitosis.

Murine Nek1, the first vertebrate Nek isolated, was identified by screening a murine cDNA expression library with anti-phosphotyrosine antibodies. Nek1 is a dual specificity serine/threonine tyrosine kinase shown by *in-situ* hybridisation to be most heavily expressed in meiotic tissues and without an absolute role in mitosis (Letwin et al., 1992). Mutations in Nek1 have been implicated in the pathology of polycystic kidney disease (PKD) in mouse models (Upadhyaya et al., 2000) and human Nek1 further interacts via its coiled-coil domain with two proteins, the kinesin-like motor protein KIF3A and the tumour suppressor tuberlin, implicated in PKD development (Surpili et al., 2003). Additional interactions were also noted between Nek1 and the DNA damage repair/checkpoint proteins, MRE11 and 53BP1, and recent work has suggested a role in response to ionizing radiation induced DNA damage (Polci et al., 2004).

Nek3 similarly lacks a clear role in mitosis or any other marked impact upon the cell cycle in both human and mouse with levels of the protein constant through the cell cycle and no clear phenotypes manifested by either overexpression or disruption by antibody microinjection (Tanaka and Nigg, 1999). Human Nek3, though not cell cycle regulated, does show higher expression in testis, ovary and brain tissue reminiscent in part of murine Nek1 expression in meiotic tissue types (Kimura and Okano, 2001b).

Homology search of the human genome with the NIMA catalytic domain further identified two closely related novel serine/threonine kinases, both with severely truncated non-catalytic C-termini. The first was designated *HsNek6*, exhibiting 97% sequence identity to the previously isolated murine Nek6 (Hashimoto et al., 2002; Li et al., 1999), and a second, Nek7 which in addition to NIMA homology also shares 77% identity with Nek6 (Kimura and Okano, 2001a). Nek6 had been shown to phosphorylate both histones H1 and H3 *in vitro* suggesting a role in chromosome condensation (Kimura and Okano, 2001a). The first physiological role suggested for both Nek6 and Nek7 followed their identification as the kinase

activity copurifying with p70 S6 Kinase (S6K). Nek6 was suggested to be responsible for phosphorylating recombinant ribosomal p70 S6K on residue Thr412 *in vitro* and activating it *in vivo* (Belham et al., 2001). Latterly, doubts have emerged over the specificity of S6K phosphorylation by Nek6 *in vitro*. Mutation of the Nek6 consensus sight does not ablate Thr412 phosphorylation and S6K activation *in vivo* (Lizcano et al., 2002).

Intriguingly, both Nek6 and Nek7 have been implicated in a signalling cascade with a further NIMA related kinase, Nek9, and that individually and cooperatively these kinases have a role in mitotic progression. Nek9 (also termed Nercc1 (Roig et al., 2002) and Nek8 (Holland et al., 2002)) was initially co-immunoprecipitated from an embryonic kidney cell line as a 120 kDa protein bound strongly to transfected FLAG-Nek6 via residues 732-891. *In vivo* Nek9 is activated during mitosis and undergoes a concomitant decrease in electrophoretic mobility reminiscent of phosphorylation. As with NIMA, Nek9 has also been shown to be an *in vitro* Cdk1 substrate. In keeping with a mitotic function, microinjection of Nek9 antibodies into cultured cells during prophase disrupts spindle formation, metaphase chromosome alignment and the fidelity of segregation (Roig et al., 2002). In addition, Nek9 is also suggested to modulate interphase progression by interacting with the chromatin remodeller FACT and interact with the proteins BicD2 and RanGTP via its RCC1 coiled-coil motif (Holland et al., 2002; Roig et al., 2002; Tan and Lee, 2004).

The extremely tight binding of Nek9 to Nek6 belies a functional relationship that also extends to Nek7. Phosphorylation of serine 206 of Nek6 and serine 196 of Nek7 confers a 25-fold activation *in vitro* and Nek9 is able to perform this modification. Co-expression of FLAG-Nek9 with GST-Nek6 and GST-Nek7 in cultured cells followed by immunoprecipitation shows a parallel 2 fold increase in Nek6 activity and reduction in electrophoretic mobility. This effect is not seen when a kinase inactive mutant of Nek9 is substituted for the wild type (Belham et al., 2003). The cell cycle regulation of Nek6 was initially suggested by the observation that protein levels of Nek6 are increased in rat hepatoma cells arrested in mitosis with nocodazole (Belham et al., 2003) Though in HeLa cells this increased mitotic

abundance is not observed, the autophosphorylation and activity of Nek6 is markedly upregulated. Activity peaks in mitosis and decreases again in G₁ and S-phase. Nek6 activity has also been shown to be essential for mitotic progression, MDA-MB-231 breast tumour cells stably expressing a kinase inactive K74M K75M mutant Nek6 arrest in metaphase with a significant induction of apoptosis, similarly depletion of Nek6 in HeLa cells by the transfection of Nek6 siRNA caused a G₂/M arrest and increased apoptosis (Yin et al., 2003).

The roles of Nek8 and Nek11 are currently poorly defined in man. hsNek8 is a 75 kDa protein identified via search of the human genome database and named in accordance with its sequence similarity to mouse Nek8. *HsNek8* mRNA is reported to be upregulated in 58% of primary breast tumour tissue with the greatest increase observed in invasive ductal (IDC) (Bowers and Boylan, 2004). Nek11 occurs in two isoforms, most likely alternative splice variants encoded from chromosome 3q21-22. The resulting proteins are 74 and 55 kDa and are termed Nek11_{Long} (Nek11L) and Nek11_{Short} (Nek11S). Nek11L is the most abundant isoform and is regulated in a cell cycle dependent manner with mRNA and protein levels low in G₁, increasing through S to peak in G₂/M. Functionally, Nek11 appears to be activated by genotoxic stress and may act in the S-phase checkpoint (Noguchi et al., 2002). In addition, Nek11 is reported to colocalise with Nek2A in the nucleoli of U2OS and HeLa S3 cells and both proteins are recoverable in a complex by immunoprecipitation. Nek2A phosphorylates the C-terminus of Nek11 *in vitro*, increasing its activity (Noguchi et al., 2004).

The NIMA related kinase family also encompasses non-vertebrate homologues. The green algae *Chlamydomonas reinhardtii* initially yielded a single Nek, a 65 kDa protein named Fa2p. Though not essential for cell cycle progression in *C. reinhardtii*, the subcellular localisation of HA-tagged Fa2p is altered as cells progress from prophase through mitosis into interphase. HA-Fa2p moves first from the basal bodies to spindle poles during metaphase and anaphase then reassociates with nascent basal bodies in the subsequent interphase. *C. reinhardtii* mutants for *fa2* arrest at G₂ though this appears to be a kinase independent phenotype (Mahjoub et al., 2004).

Recent sequence analysis has identified six further NIMA related kinases in *Chlamydomonas*. Termed *Chlamydomonas* NIMA related kinases (CNKs) the role of these proteins remains undetermined (Bradley et al., 2004). The slime mold *D. discoideum* Nek2 shares 43% amino acid identity with hsNek2 and whilst a core centrosome component it does not appear subject to cell cycle regulation. Overexpression of DdNek2 does induce MTOC abnormalities however, with either active or inactive GFP-DdNek2 inducing supernumerary or abnormal centrosomes. The phenotype is independent of kinase activity and it may simply be that the kinase acts in a structural manner to allow the accretion of further centrosome components (Graf, 2002). Antibodies raised to *D. melanogaster* Nek2 strongly stain the centrosome and midbody in cultured S2 cells. Depletion of *DmNek2* by RNAi induces spindle abnormalities and an increase in the proportion of metaphase cells. Conversely, overexpression of *DmNek2* induces centrosome fragmentation (Prigent et al., 2005).

1.4.4 Nek2

The NIMA related kinases have been implicated in diverse roles in the cell and aside from a common association with MTOCs a truly coherent picture has yet to emerge from the literature. The closest homologue and currently best studied NIMA related kinase is Nek2. Identified by degenerate PCR screen of HL-60 promyelocytic cell line cDNA library, Nek2 has 47% sequence identity to the catalytic domain of NIMA. The cell cycle distribution of Nek2 is broadly similar to that of NIMA; abundance is low in G₁, increasing through S phase to peak at the G₂/M transition, whereas peak activity of NIMA actually occurs in mitosis (Fry et al., 1995; Schultz et al., 1994).

The abundance and activity of Nek2 is regulated chiefly at the transcriptional and post-translational level. Chromatin immunoprecipitation (ChIP) assays demonstrated that Nek2 mRNA levels are maintained at a low level in G₀ and G₁ by binding of transcription factor E2F4, an observation confirmed by RT-PCR (Twomey et al., 2004). Gene expression is silenced by E2F4 promoting a closed chromatin conformation via the Rb-like proteins p107/p130, with p107/p130 ^{-/-} mouse embryonic fibroblasts (MEFs) showing elevated Nek2 mRNA (Ren et al.,

2002). Conversely, Nek2 transcription is induced by the forkhead transcription factor, FoxM1, which increases in S phase to induce expression of a range of G₂/M specific genes including cyclinB₁ (Laoukili et al., 2005).

Once expressed, Nek2 pre-mRNA is subject to alternative splicing to produce two isoforms, Nek2A and Nek2B, which differ in their extreme C-termini. (Figure 1.8). Recently a third isoform, initially referred to as Nek2-T, has been isolated from a testis cDNA library that carries an internal in frame deletion (Fardilha et al., 2004). Initially thought to be a testis specific isoform, Nek2-T mRNA expression has since been shown in tissues other than testis. Nek2-T has been renamed Nek2C in light of this revised tissue distribution (Wu, 2006). In common with NIMA, the conserved catalytic domain of Nek2 is N-terminal with regulatory domains throughout the C-terminus. The divergence between Nek2A and Nek2B preserves catalytic activity whilst affecting their regulation and, ultimately, cell cycle expression.

In addition to the leucine zipper which facilitates homodimerisation (Fry et al., 1999) Nek2A carries two degradation motifs, a KEN box and a C-terminal MR dipeptide which are targets of the APC/C (Hayes et al., 2006). Nek2B, which lacks these motifs, persists throughout mitosis (Hames and Fry, 2002; Hames et al., 2001). This subtle difference in the regulation of Nek2A and Nek2B hints at differing substrates and perhaps roles. This speculation is borne out in part by evidence that Nek2B is required for mitotic exit, at least in HeLa cells (Fletcher et al., 2005). In embryos of the African clawed cane toad *Xenopus laevis* Nek2B is necessary for nascent centrosome maturation in the *X. laevis* zygote. This role may be solely structural, independent of kinase activity (Fry et al., 2000; Twomey et al., 2004). In *X. laevis* embryos Nek2B, the sole Nek2 isoform present, is responsible for centrosome maintenance. Injection of Nek2B antibodies or supplementation with excess kinase-dead Nek2B induced centrosome fragmentation and disrupted bipolar spindle formation (Uto and Sagata, 2000).

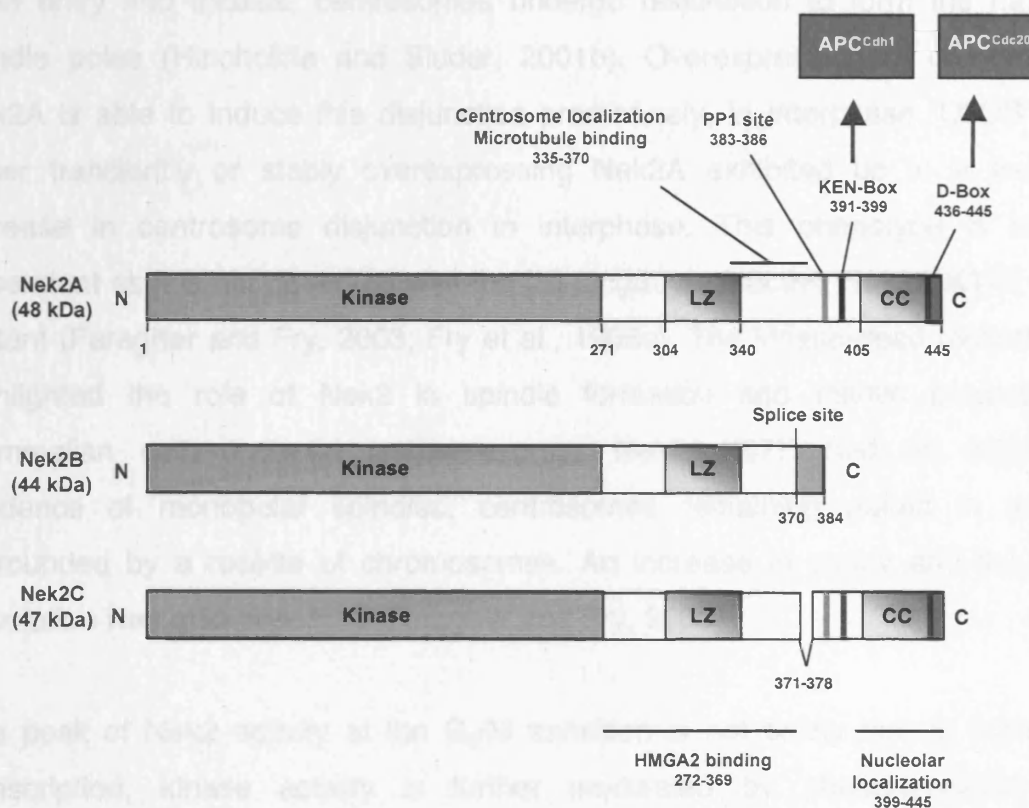


Figure 1.8 The structures of the three Nek2 splice variants

Three splice variants of human Nek2 have been described: Nek2A, Nek2B and Nek2C. The splice variants all carry an identical N-terminal catalytic kinase domain followed by a leucine zipper (LZ) dimerization motif. Nek2A and Nek2C contain an additional coiled-coil (CC) at the extreme C-terminus. A splice site after amino acid 370 leads to an alternative C-terminus in Nek2B and a short internal truncation in Nek2C. Both Nek2A and Nek2C retain motifs essential for interaction with PP1 and for protein degradation mediated by APC/CCdc20 or APC/CCdh1. The non-catalytic domains of Nek2 also confer centrosome and nucleolar localization and the capacity to interact with microtubules and the chromatin architectural protein HMGA2. Reproduced from Hayward and Fry (2005).

Nek2 is a core centrosomal antigen, localising independently of microtubules throughout the cell cycle both in fixed live cells and isolated centrosomes (Fry et al., 1998c). Nek2B has a defined role in the structural maintenance of centrosomes whilst Nek2A governs centrosome cohesion. Centrosomes, two orthogonal centrioles surrounded by a diffuse matrix of proteins (section 1.3.1), are usually arranged as paired organelles throughout interphase. In a normal cell cycle upon entry into mitosis, centrosomes undergo disjunction to form the nascent spindle poles (Hinchcliffe and Sluder, 2001b). Overexpression of recombinant Nek2A is able to induce this disjunction prematurely, in interphase. U2OS cells either transiently or stably overexpressing Nek2A exhibited up to a five-fold increase in centrosome disjunction in interphase. This phenotype is kinase dependent as it is not observed with the full-length yet inactive Nek2A-K37R point mutant (Faragher and Fry, 2003; Fry et al., 1998c). The kinase-dead mutant also highlighted the role of Nek2 in spindle formation and mitotic progression. Mammalian cells induced to overexpress Nek2A-K37R had an increased incidence of monopolar spindles, centrosomes remaining paired in mitosis surrounded by a rosette of chromosomes. An increase in ploidy and the G₂/M population was also observed (Faragher and Fry, 2003).

The peak of Nek2 activity at the G₂/M transition is not solely due to increased transcription, kinase activity is further modulated by phosphorylation and dephosphorylation (Figure 1.9). Nek2 was fractionated from mammalian cells via ultracentrifugation as a salt-resistant homodimer, associating via the leucine zipper. This coiled coil mediated dimerisation facilitated the autophosphorylation essential for full activity (Fry et al., 1999; Helps et al., 2000). The C-terminus of Nek2A was also identified as a binding partner of the phosphatase PP1 in a yeast two-hybrid screen and confirmed by the reciprocal coimmunoprecipitation of full length GST-Nek2A and PP1. Residues 383-386 of Nek2A comprise a canonical KVHF PP1 binding domain whereby the mutation F386A abolishes PP1 binding (Helps et al., 2000). The KVHF motif is located after the splice site at which Nek2A and Nek2B diverge. While Nek2A and Nek2C retain the KVHF motif, it is lost in Nek2B which is not therefore a substrate of PP1 (Hames and Fry, 2002). Nek2 autophosphorylation leads to an increase in kinase activity and the reverse

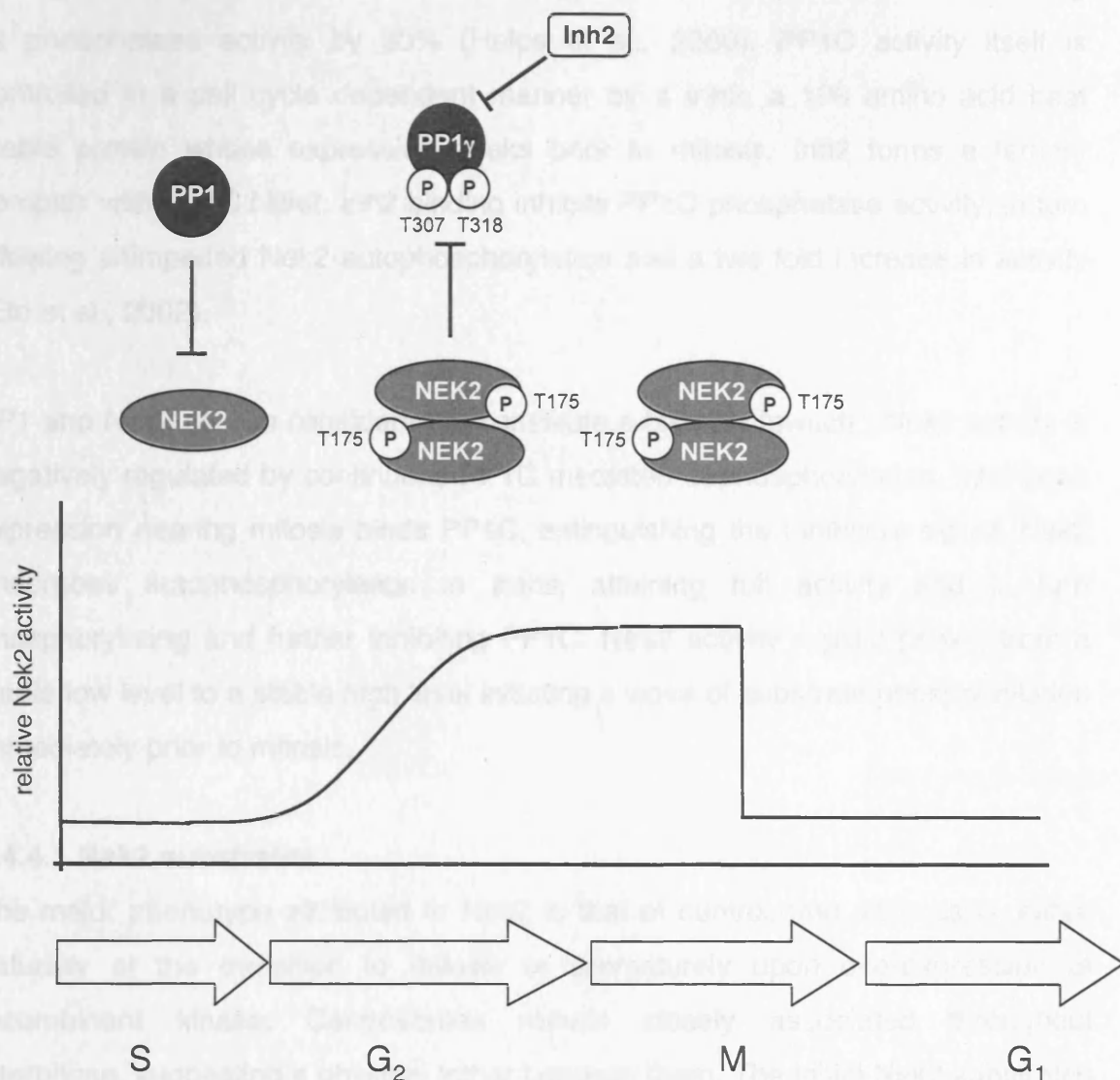


Figure 1.9 Nek2 activity is regulated by phosphorylation

In addition to transcriptional regulation Nek2 activity is modulated by its phosphorylation status. During G₁ and S phase Nek2 is inhibited by the phosphatase PP1. During G₂ PP1 is in turn inhibited by Inhibitor 2, allowing Nek2 to undergo autophosphorylation on residue threonine 175 and increase its catalytic ability. Autophosphorylated Nek2 then phosphorylates PP1, abrogating its inhibitory ability. Peak Nek2 activity occurs at the G₂/M transition. The interaction between PP1, Inh2 and Nek2 constitutes a bistable switch, allowing Nek2 activity to rapidly toggle from a stable low level to a stable high level. Nek2A activity falls towards the end of mitosis due to APC/C mediated proteolysis.

appears to be true; PP1 dephosphorylation reduces GST-Nek2A activity by 65%. Equally, PP1 γ is a substrate of Nek2, phosphorylation of T307 and T318 reducing its phosphatase activity by 30% (Helps et al., 2000). PP1C activity itself is controlled in a cell cycle dependent manner by a Inh2, a 198 amino acid heat stable protein whose expression peaks prior to mitosis. Inh2 forms a ternary complex with PP1C:Nek2. Inh2 binding inhibits PP1C phosphatase activity, in turn allowing unimpeded Nek2 autophosphorylation and a two fold increase in activity (Eto et al., 2002).

PP1 and Nek2 can be considered to constitute a bistable “switch”; Nek2 activity is negatively regulated by continuous PP1C mediated dephosphorylation. Inh2 peak expression nearing mitosis binds PP1C, extinguishing the inhibitory signal. Nek2 undergoes autophosphorylation in *trans*, attaining full activity and in turn phosphorylating and further inhibiting PP1C. Nek2 activity rapidly peaks, from a stable low level to a stable high level initiating a wave of substrate phosphorylation immediately prior to mitosis.

1.4.4.1 Nek2 substrates

The major phenotype attributed to Nek2 is that of centrosome disjunction, either naturally at the transition to mitosis or prematurely upon overexpression of recombinant kinase. Centrosomes remain closely associated throughout interphase, suggesting a physical tether between them. The initial Nek2 substrates were identified as components of this link (Figure 1.10).

Centrosomal-Nek2 associated protein 1 (C-Nap1, also isolated in tandem as Cep250 (Mack et al., 1998)) was identified in a yeast two hybrid screen which sought to identify Nek2 interacting proteins (Fry et al., 1998b). Using full length Nek2 as bait eight positive clones were obtained, four of which corresponded to the C-terminus of a 280 kDa low abundance, ubiquitous, novel coiled-coil protein. C-Nap1 localises to centrosomes by immunofluorescence microscopy. Higher resolution immuno-electron microscopy (IEM) of U2OS cells restricted this staining to the proximal ends of centrosomes. A microtubule independent core component of the centrosome throughout interphase, C-Nap1 is displaced from mitotic spindle

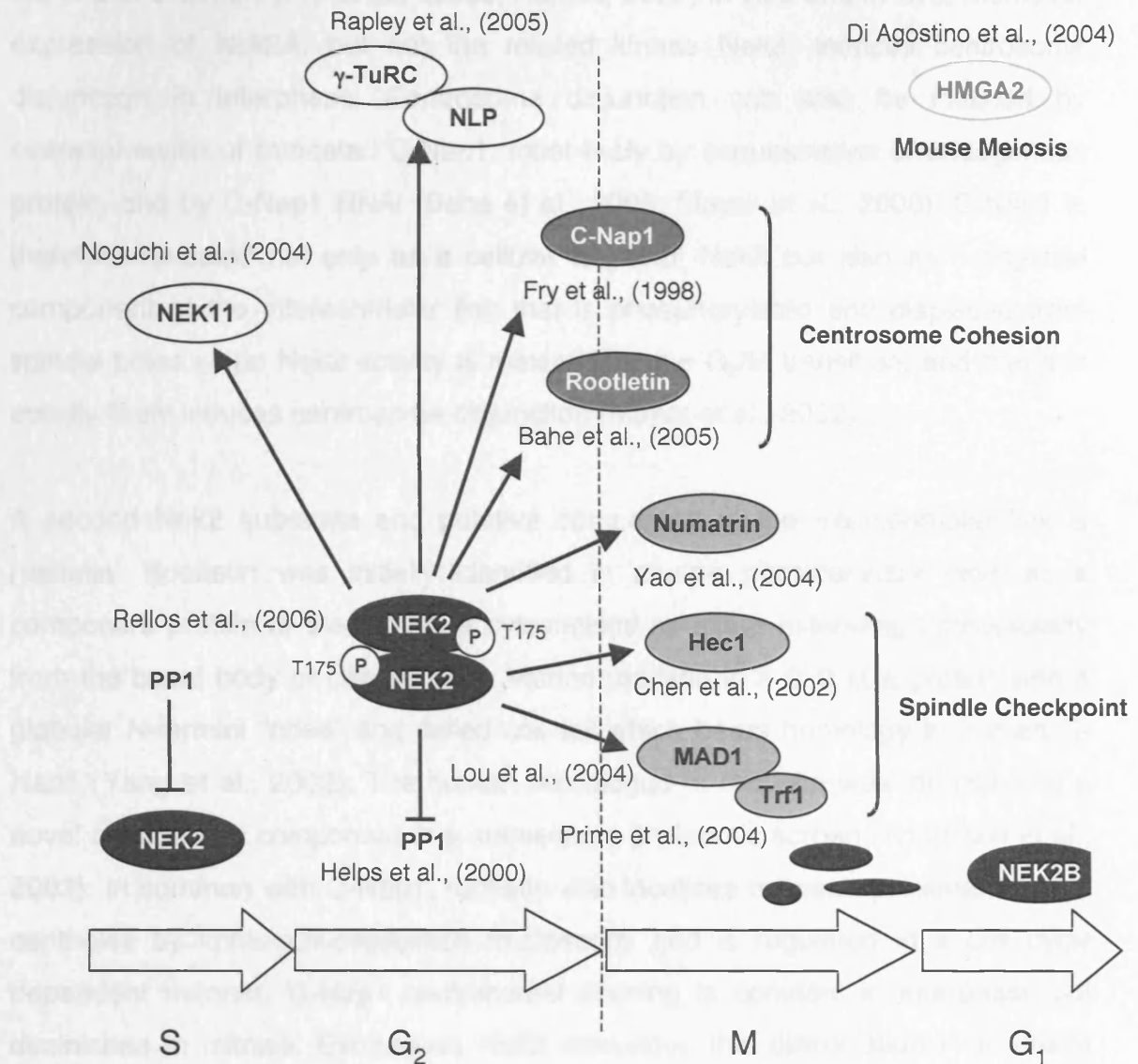


Figure 1.10 Nek2 substrates

Nek2 has been shown to bind and phosphorylate a range of proteins both *in vitro* and in cultured cells. The majority of interactions can be broadly grouped into those governing centrosome cohesion and spindle checkpoint signaling. A distinct role for Nek2 in mouse meiosis has been suggested by its interaction with HMGA2, depicted separately from its mitotic functions. Relevant references are shown adjacent to the interactions.

poles as evidenced by a reduction in immunofluorescent staining before reaccumulation following telophase. Nek2 is able to phosphorylate C-Nap1 at both the N and C termini (Fry et al., 1998c; Hames, 2002) in vitro and in vivo, moreover expression of Nek2A, but not the related kinase Nek3, induces centrosome disjunction in interphase. Centrosome disjunction can also be induced by overexpression of truncated C-Nap1, most likely by sequestration of endogenous protein, and by C-Nap1 RNAi (Bahe et al., 2005; Mayor et al., 2000). C-Nap1 is therefore revealed not only as a cellular target of Nek2 but also as a physical component of the intercentriolar link that is phosphorylated and displaced from spindle poles when Nek2 activity is maximal, at the G₂/M transition, and that this activity likely induces centrosome disjunction (Mayor et al., 2002).

A second Nek2 substrate and putative component of the intercentriolar link is rootletin. Rootletin was initially identified in murine photoreceptor cells as a component protein of the rootlet, a cytoskeletal structure extending intracellularly from the basal body of ciliated cells. Murine rootletin is a 220 kDa protein with a globular N-termini “head” and coiled coil tail which bears homology to human C-Nap1 (Yang et al., 2002). The human homologue of rootletin was identified as a novel centrosome component in a subsequent proteomic screen (Andersen et al., 2003). In common with C-Nap1, rootletin also localises between proximal ends of centrioles by immunofluorescence microscopy and is regulated in a cell cycle dependent manner. C-Nap1 centrosomal staining is constant in interphase but diminished in mitosis. Exogenous Nek2 stimulates this dissociation in a kinase dependent manner. Rootletin recovered after co-expression with active Nek2 also shows reduced mobility suggesting phosphorylation (Bahe et al., 2005). In keeping with a role for rootletin as a component of the intercentriolar link, rootletin interacts with C-Nap1. The current proposed model is that C-Nap1, confined to the proximal ends of centrioles, interacts with the globular head of rootletin whilst the C-terminal tails mesh to form a dynamic link. Commensurate with this arrangement, depletion either of C-Nap1 or rootletin induced centrosome splitting. Whereas depletion of C-Nap1 displaced rootletin the reverse is not true (Bahe et al., 2005). In summary, Nek2, modulated by PP1, phosphorylates both C-Nap1 and rootletin at the G₂/M

transition to induce their displacement from centrioles, leading to dissolution of the intercentriolar linkage and subsequent centrosomal disjunction.

Distinct from its role in regulating bipolar spindle formation, Nek2 is also implicated in maintaining the fidelity of chromosome attachment to the spindle during mitosis. Current models suggest spindle checkpoint signalling is mediated by a fluid complex of proteins accumulating at the kinetochore of chromosomes in prometaphase. Amphitelic attachment to the spindle causes an inhibitory signal to be extinguished, allowing procession into anaphase as the last chromosome attaches correctly. Nek2 is reported to interact with two members of spindle checkpoint protein complexes, Mad1 and Hec1. Hec1 (highly expressed in cancer –1) is a coiled coil phosphoprotein that is required for recruitment of Mps1 kinase and Mad1/Mad2 complexes to the kinetochore (Martin-Lluesma et al., 2002). Nek2 has been shown to specifically bind Hec1 and phosphorylate serine 165 in human cells, an event also demonstrated to be essential for correct chromosome segregation in *Saccharomyces cerevisiae* (Chen et al., 2002). Nek2A was also identified as a novel interactor with Mad1 in a yeast two-hybrid screen, probably via the Nek2A leucine zipper (Lou et al., 2004a).

Nek2A has also been implicated in chromosome condensation during meiosis via an interaction with the architectural chromatin protein high mobility group A2 (HMGA2). Nek2 phosphorylates HMGA2 *in vitro* and it is proposed that in mouse spermatocytes this phosphorylation decreases the affinity of HMGA2 for DNA, causing its release from chromatin and eventual chromosome condensation (Di Agostino et al., 2004).

1.4.4.2 Nek2 expression in human tumours

Reports implicating Nek2 in human disease first appeared following studies of mRNA levels in tumour derived cell lines by microarray analysis. Assessment of some 1,700 hundred genes identified marked upregulation of Nek2 in cell lines derived from Ewings tumours, a paediatric osteosarcoma (Wai et al., 2002).

An increase in Nek2 mRNA is also observed directly in human non-Hodgkin lymphoma and is strongly associated with disease progression. Profiling successive patient samples showed that as follicular lymphoma (FL) advances to the more aggressive diffuse large B-cell lymphoma (DLBCL) mRNA levels of Nek2 rise (de Vos et al., 2003b). Comparison of matched lymph nodes resected from five patients before and after the transformation showed Nek2 mRNA increase in four samples. The transformation to DLBCL signals a decreased response to drug therapy and a concomitantly bleak patient prognosis with a median survival of only 22 months (de Vos et al., 2003b).

1.5 AIMS AND OBJECTIVES

The goal of this research is to determine whether the NIMA-related mitotic kinase Nek2 can be considered a target for therapeutic intervention in human cancer. Existing centrosomal kinases that govern mitotic progression such as Plk1 and Aurora-A have been shown to be upregulated in a range of cancers and to transform cultured cells. In this project I focus on whether Nek2 is also implicated in human malignancy and the feasibility of reducing the activity of the kinase with small molecule inhibitors.

The project aims are as follows;

1. To investigate whether Nek2 protein levels are upregulated in human cancer cell lines.
2. To investigate whether Nek2 protein is upregulated or downregulated in primary human tumours.
3. To determine the effect of Nek2 downregulation on the growth and viability of cultured cells.
4. To perform a high-throughput screen (HTS) that can be used to identify small molecule inhibitors of Nek2

CHAPTER 2

MATERIALS AND METHODS

2.1 MATERIALS

2.1.1 Chemicals

All chemicals were of analytical grade purity or higher and purchased from Sigma (Poole, UK) unless otherwise indicated below.

Reagent	Supplier
Deoxynucleotides (dATP,dCTP,dGTP,dTTP)	Amersham Pharmacia Biotech (Buckinghamshire, UK)
EDTA EGTA NaCl KCl Na ₂ HPO ₄ KH ₂ PO ₄ Glacial acetic acid	Fisher Scientific (Loughborough, UK)
D-MEM with Glutamax MEM RPMI 1640 Optimem Foetal Calf Serum Lipofectamine 2000 Oligofectamine GST-Plk1 Gene Tailor Site-directed Mutagenesis Kit Oligonucleotide Primers	Invitrogen (Paisley, UK)
Cdk1-his ₆ /GST-Cyclin B his ₆ Nek2A his ₆ Nek6 his ₆ Nek7 his ₆ Aurora-A	Upstate (Dundee, UK)
GST-Nek2A	Stressgen (San Diego, USA)

ProTran Nitrocellulose membrane	Schleicher & Schuell (Dassel, Germany)
3MM Chromatography Paper	Whatman (Maidstone, UK)
Qiafilter Plasmid Maxipreps Qiafilter Plasmid Miniprep Genomic DNA extraction kit	Qiagen (Hilden, Germany)
Protogel liquid acrylamide (30% w/v)	National Diagnostics (Hessle, UK)
Marvel (skimmed milk powder)	Premiere Beverages (Stafford, UK)
RNAi Oligoribonucleotides	Dharmacon (Lafayette, USA)
BCA Protein Assay	Pierce (Rockford, USA)
Bacto-agar Bacto-tryptone Yeast Extract	Oxoid (Basingstoke, UK)
Dalton VII protein molecular weight markers	Sigma (Poole, UK)
Precision plus protein kaleidoscope standards	Bio-Rad (Hemel Hempstead, UK)
DNA 100 bp molecular weight ladder DNA 1 kb molecular weight ladder	NEB (Hitchin, UK)
DNA 100 bp Generuler plus molecular weight ladder	MBI Fermentas (York, UK)
BSA (Fraction V)	Fluka (Gillingham, UK)
FuGene 6	Roche (Lewes, UK)
Super RX X-Ray film	Fuji Photo. Film (Dusseldorf, Germany)
Histoclear	VWR (Lutterworth, UK)
Envision Detection system	DAKO (Ely, UK)
Pertex	Cellpath plc. (Hemel Hempstead, UK)
WST-1 Cell Proliferation Assay	Merck Chemicals (Nottingham, UK)

2.1.2 Antibodies

Antibody	Dilution ([antibody])	Supplier
anti-C-Nap1	1:750 (1 μ g/ml)	Fry <i>et al</i> 1998b
anti-Nek2 (AR40)	1:500 (2 μ g/ml)	Fry <i>et al</i> 1998a
anti-Nek2 (peptide)	1:250 (1 μ g/ml)	Fry <i>et al</i> 1999
anti-Nek2 (monoclonal)	1:850 (1 μ g/ml)	Abcam
anti-Nek2 (monoclonal)	1:250 (1 μ g/ml)	BD Biosciences
anti- γ -tubulin (mouse)	1:2000 (6.5 μ g/ml)	Sigma
anti- γ -tubulin (rabbit)	1:500	Sigma
anti- α -tubulin (mouse)	1:2000	Sigma
anti- α -tubulin (rabbit)	1:200	Sigma
anti-p130	1:100 (1 μ g/ml)	Santa Cruz
anti-p107 (SC318)	1:100 (2 μ g/ml)	Santa Cruz
anti-myc (mouse)	1:1000	Cell Signalling
anti-cleaved caspase 3 (ASP175)	1:100	Cell Signalling
anti-rabbit IgG Alexa488	1:200 (10 μ g/ml)	Molecular Probes
anti-mouse IgG Alexa488	1:200 (10 μ g/ml)	Molecular Probes
anti-rabbit IgG Alexa594	1:200 (10 μ g/ml)	Molecular Probes
anti-rabbit IgG Alexa594	1:200 (10 μ g/ml)	Molecular Probes
anti-mouse IgG HRP	1:500	Sigma
anti-rabbit IgG HRP	1:500	Sigma
anti-GFP antibody	100 ng/ml	AbCam
Normal rabbit IgG	2 μ g/ml	DAKO (Ely, UK)
Normal mouse IgG	2 μ g/ml	DAKO (Ely, UK)

Final antibody concentrations, where known, are stated in brackets after the working dilution.

2.2 MOLECULAR BIOLOGY TECHNIQUES

2.2.1 Site-directed mutagenesis

The Genetailor site-directed mutagenesis system was used to introduce nucleotide changes in plasmid vectors and hence the amino acids they encode. Briefly, 100 ng of target plasmid was methylated with 4 units of DNA methylase by incubation at 37°C for 1 hour. 12.5 ng of methylated template was then subject to amplification by PCR (initial denaturation 2 minutes at 94 °C then 94 °C, 30 seconds, 55 °C, 30 seconds, 68 °C, 7 minutes for 25 cycles with a final extension of 10 minutes at 68 °C) using Expand Hi-Fidelity polymerase (3.5 U polymerase, 300 nM each primer, 200 μ M dNTPs, 500 μ M MgCl₂). Amplification was confirmed by gel electrophoresis and 1/25th of the reaction volume used to transform 50 μ l DH5 α -T1R (F-, ϕ 80lacZ Δ M15, Δ (lacZYA-argF), U169, recA1, endA1, hsdR17(rk-, mk+), phoA, supE44, thi-1, gyrA96, relA1, tonA) and appropriate selective media used to identify transformant colonies. Mutants were confirmed by DNA sequencing and large scale DNA preparations made as necessary. To introduce the N354S transposition the plasmid pCMVmycNek2A (described in (Fry et al., 1998c)) was amplified with the primers Nek2A N354S F (AGCAGAAATCTGTTGAAGAGCTACAGCTTG) and Nek2A N354S R (TCTTCAACAGATTTTCTGCTCTAGCCAGTTT). Sequences are 5'-3' as written and the nucleotide change with respect to wild-type Nek2 is shown in bold.

2.2.2 DNA gel electrophoresis

DNA in loading buffer (50% v/v Glycerol, 100 mM EDTA, 0.3% v/v Bromophenol blue) was resolved by electrophoresis on a gel of 1% (w/v) agarose dissolved in 1xTBE (89 mM Tris-HCL, 89 mM Boric acid, 1mM EDTA pH 8.0) supplemented with ethidium bromide (0.5 μ g/ml) alongside 0.5 μ g of the 100bp or 1Kb DNA molecular weight marker as appropriate (MBI Fermentas). The gel was immersed in 1x TBE and DNA resolved by electrophoresis at 80V. Gels were subject to UV transillumination (302 nm) and images acquired with a Gene Genius CCD gel documentation system (Syngene, Cambridge, UK).

2.2.3 Plasmid preparation

Small and large scale preparations of DNA were made using Qiagen miniprep and Qiafilter maxiprep kits, respectively, according to the manufacturers' instructions. Essentially overnight cultures of the appropriate transformed bacterial strain were grown overnight in LB medium (Bacto-tryptone 10 g/l, Yeast extract 5 g/l, NaCl 10 g/l) at 37°C, plasmid DNA extracted and purified, and eluted with H₂O. Maxiprep yield was quantified by measuring OD₂₆₀ and diluted to a final concentration of 1 µg/µl.

2.2.4 Restriction enzyme digest

Purified DNA was digested in the appropriate buffer conditions and temperature as specified by the manufacturer. Routinely, 2 µg DNA was digested with 5 U restriction endonuclease for 1 hour at 37°C in a water bath before visualization by agarose gel electrophoresis.

2.2.5 Genomic DNA extraction

Archival breast tumour tissue flash frozen in liquid nitrogen was obtained from the CRUK Paterson Institute for Cancer Research (PICR, Manchester, UK) and processed at the University of Leicester (Leicester, UK). Total genomic DNA was extracted from frozen breast tumour tissue using the QIAamp DNA mini kit according to the manufacturer's instructions. Essentially, 50 mg frozen tissue was ground under liquid nitrogen with a pestle and mortar. The resulting powdered tissue was treated with RNase A and proteinase K at final concentrations of 1 mg/ml and 60 mAU/ml, respectively. DNA was extracted with QIAamp spin columns before elution into 10 mM Tris·HCl, 0.5 mM EDTA pH 9.0 and storage at -80°C.

2.2.6 Mutation analysis

Analysis of the Nek2 genomic sequence was undertaken by CRUK Mutation Detection Facility (Sheffield, UK). Basically, genomic DNA extracted at Leicester was quantified by Nanodrop spectrophotometer (Nanodrop technologies, Wilmington, USA) and the exons analysed by PCR amplification and single-strand conformational polymorphism (SSCP) detection. Identified polymorphisms were confirmed by sequencing and compared to the SNP database (dbSNP, NCBI,

Washington, USA).

2.2.7 Growth of bacterial cultures

LB (Luria-Bertani) media was prepared and sterilised by autoclaving (15 minutes, 121°C) with the addition of 2% agar (w/v) for plates if necessary. Selective media was supplemented with 100 µg/ml ampicillin, 50 µg/ml kanamycin or 34 µg/ml chloramphenicol as appropriate.

2.2.8 Chemically competent bacteria

DH5α *E. coli* were streaked on LB agar plates and incubated overnight at 37°C. 2 ml LB medium was inoculated with a single isolated colony and incubated at 37°C, 225 rpm for 9 hours. The entire starter culture was used to inoculate a further 500ml LB containing 10mM MgCl₂. This 500 ml culture was incubated at room temperature with gentle shaking until an OD₆₀₀ of 0.5 was reached or 46 hours had elapsed, then cooled rapidly in ice water. The bacterial cells were collected by centrifugation at 3000 rpm, 0°C, in a pre-chilled Sorvall GS3 rotor. The culture media was decanted and the pellet resuspended in 150 ml ice cold transformation buffer (15 mM CaCl₂, 250 mM KCl, 10mM PIPES, 55 mM MnCl₂, pH 6.7), centrifuged again as before and resuspended in 40 ml ice cold transformation buffer. 5ml DMSO was added and mixed by gentle swirling before aliquoting and immediate storage at –80°C.

2.2.9 Bacterial transformation

Aliquots of chemically competent *E. coli* DH5α (F⁻, φ80lacZΔM15, Δ(lacZYA-argF), U169, recA1, deoR, endA1, hsdR17(rk⁻, mk⁺), phoA, supE44, thi-1, gyrA96, relA1) were thawed from –80°C on ice. 100 ng DNA was added and mixed by gentle stirring before incubation on ice for 30 minutes. Plasmid uptake was induced by incubation at 42°C for 1 minute in a waterbath followed by reincubation on ice for 5 minutes. Prewarmed LB media was added and the transformation incubated at 37°C, 225 rpm for 1 hour before aliquots were spread onto the appropriate selective media.

2.3 ANALYSIS OF PROTEINS

2.3.1 SDS-PAGE

Proteins were resolved using the Mini Protean 2 polyacrylamide gel system (Bio-Rad) with a discontinuous Tris.HCl buffer system comprising a stacking (0.5 M Tris.HCl pH 8.8, 0.4% SDS (w/v)) and resolving (1.5 M Tris.HCl pH 6.8, 0.4% SDS (w/v)) gel with an SDS running buffer (0.1% SDS, 0.3% Tris, 1.44% glycine). Stacking and resolving gels were polymerised by the addition of 0.8% and 2.4% (v/v) TEMED and 0.015% and 0.045% (v/v) of 10% APS respectively. Gels were run at a standard of 180V for 1 hour. The percentage acrylamide in the resolving gel varied between 8% and 15% to separate proteins of 36 – 94 kDa and 10 – 43 kDa, respectively.

2.3.2 Coomassie Blue staining

Following electrophoresis the stacking gel was discarded and the resolving gel soaked in Coomassie Brilliant Blue solution (0.25% Coomassie Brilliant Blue (w/v), 40% IMS, 10% acetic acid (v/v)) for a minimum of 30 minutes. Protein bands were visualized by washing in destaining solution (25% IMS, 7.5% acetic acid (v/v)) to remove background gel staining. Gels were dried onto 3MM paper (Whatmann) at 80°C under vacuum. Radiolabelled proteins were then visualized by autoradiography as necessary.

2.3.3 Silver staining

Protein samples were resolved by SDS-PAGE and the stacking gel discarded. The resolving gel was incubated first in 50% methanol (v/v) 10% acetic acid (v/v) for 15 minutes. The gel was subsequently transferred to a solution of 25% methanol (v/v) 10% acetic acid (v/v) for a further 15 minutes and lastly a solution of 5µg/ml DTT, 0.1% AgNO₃ in H₂O for 15 minutes. The gel was then rinsed briefly in distilled H₂O before development in 3% (w/v) Na₂CO₃/460 µl/l formaldehyde until the appropriate intensity of staining was achieved. The reaction was stopped in 1% acetic acid (v/v) for 5 minutes and washed in 5 changes of distilled water.

2.3.4 Western blotting

Resolved proteins were transferred to nitrocellulose membrane for immunodetection by semi-dry electrophoretic blotting. Briefly, the resolving gel, ProTran nitrocellulose membrane (Schleicher and Schuell) and 3MM chromatography paper were equilibrated in Western blotting buffer (25 mM Tris, 192 mM glycine, 10% methanol (v/v)) for 5 minutes. The resolving gel was placed on the membrane and in turn sandwiched between buffer-soaked chromatography paper and rolled to displace air bubbles. Proteins were transferred in a Hoefer Semi-phor blotting apparatus (Pharmacia) at 1 mA/cm² membrane for 1 hour. Post-transfer, proteins were visualized on the membrane with ponceau red solution (0.1% Ponceau S (w/v), 5% acetic acid (v/v)) and Dalton VII molecular weight markers (Sigma) annotated in pencil as necessary. Before immunoblotting, the membrane was incubated in 5% (w/v) skimmed milk powder in PBS (137 mM NaCl, 2.7 mM Na₂HPO₄, 1.4 mM KH₂PO₄), 0.1% (v/v) Tween-20 to block non-specific antibody binding. The blocked membrane was then incubated with primary antibody (1 µg/ml) for several hours at room temperature or +4°C overnight in 5% (w/v) skimmed milk powder in PBS, washed three times in 1x PBS/0.1% Tween-20 to remove unbound antibody before incubation with an HRP-conjugated secondary antibody. Unbound secondary antibodies were removed by washing in PBS/Tween-20 as before and bound HRP conjugates visualized by development with either ECL or ECL+ (Amersham Pharmacia) and exposure to film.

2.3.5 BCA protein assay

Total protein content of solutions was determined by BCA assay, which exploits the quantitative colorimetric interaction of reduced copper sulphate, bicinchoic acid and peptide bonds. 5 µl of protein solution was incubated with 1 ml BCA assay reagent at 60°C for 30 minutes, allowed to cool and the absorbance determined at 562 nm. A serial dilution of BSA standards similarly assayed allowed construction of a standard curve relating absorption to protein concentration.

2.3.6 Recombinant protein kinases

The recombinant His₆Nek2A T175E F386A kinase was produced by transfection of insect Sf9 cells with the supernatant containing pBlueBac -Nek2A T175E F386A

derived baculoviruses at a multiplicity of infection of 5. Infected cells were cultured for 72 hours post infection before total cell lysates were made in NEB buffer according to 2.3.9. All other recombinant kinases were obtained from the manufacturer, Upstate (Dundee, UK) or as otherwise indicated in the text.

2.3.7 *In vitro* kinase assays

Recombinant kinase was mixed with the control substrate β -casein at final concentrations of 2 ng/ μ l and 0.5 μ g/ μ l, respectively, on ice. Kinase buffer (50 mM Hepes KOH pH 7.4, 5 mM MnCl_2 , 5 mM β -glycerophosphate, 5 mM NaF, 4 μ M ATP, 1mM DTT, 20nCi $\gamma^{32}\text{-P-[ATP]}$ / μ l) was added and the components mixed on ice by gentle pipetting. Complete reaction mixtures were transferred to a waterbath at 30°C for 30 minutes, removed to ice and the reactions stopped by the addition of 3X sample buffer (62.5 mM Tris.HCl pH 6.8, 2% w/v SDS, 5% v/v β -mercaptoethanol, 10% v/v glycerol, 0.01% v/v bromophenol blue) and incubation at 90°C for 3 minutes. Reaction tubes were centrifuged briefly to collect condensate and either resolved by SDS-PAGE immediately or stored at -20°C as appropriate.

2.3.8 High-throughput screen kinase assay

The high-throughput screen, conducted at the Institute for Cancer Research (Sutton, UK), employed kinase assays in 384-well scintillant coated Flashplates (Perkin Elmer, USA). Briefly, a 384-well basic Flashplate was coated with 25 μ g/ml MBP overnight at +4°C. Excess, unbound, substrate was removed by washing with 1 x PBS. Inhibitor dissolved in DMSO was added at a final concentration of 32 μ M followed by 40 pg of GST-Nek2A per well (Stressgen, USA), ATP at a final concentration of 2 μ M and 0.2 μ Ci $\gamma^{33}\text{P-[ATP]}$ per well. The complete reaction mixture was incubated at room temperature for 4 hours. The reaction was halted and unincorporated $\gamma^{33}\text{P-[ATP]}$ removed with a sodium pyrophosphate / 1 x PBS wash. The plates were counted on a Topcount microtitre plate reader (Packard, USA).

2.3.9 Protein extraction

Whole cell lysates of asynchronous cell populations were made in either RIPA (50 mM Tris.HCl pH 7.4, 1% Nonidet P-40 (v/v), 0.25% sodium deoxycholate (w/v), 1

mM EDTA, 150 mM NaCl, 1 mM EDTA, 1 mM PMSF, 1 μ g/ml leupeptin, 1 μ g/ml pepstatin A, 1% aprotinin (v/v), 1mM Na₃VO₄, 1mM NaF) or NEB buffer (50 mM HEPES-KOH pH 7.4, 5 mM MnCl₂, 10 mM MgCl₂, 5 mM EGTA, 2 mM EDTA, 100 mM NaCl, 5 mM KCl, 0.1% Nonidet P-40 (v/v), 30 μ g/ml Rnase A, 30 μ g/ml Dnase I, 1 mM phenylmethylsulfonyl fluoride (PMSF), 1 μ g/ml leupeptin, 1 μ g/ml pepstatin A, 1% aprotinin (v/v), 20 mM β -glycerophosphate, 20 mM NaF (Fry and Nigg, 1997)). Briefly, cells were washed in cold 1x PBS and lysed directly in RIPA buffer on ice for 30 minutes, centrifuged at +4°C, 14,000 rpm to remove insoluble material and total protein concentration of the resulting supernatant determined by BCA assay. NEB lysates were prepared by washing harvested cells in ice-cold 1x PBS, 1 mM PMSF, pelleting and resuspending in NEB. Lysates were incubated on ice for 30 minutes, passed through a 27G needle 10 times and centrifuged at 14,000 rpm at +4°C and the resulting supernatant quantified by BCA assay. 50 μ g of lysate for each cell line was resolved by SDS-PAGE and analysed by Western blotting.

2.3.10 Scintillation counting

The relevant Coomassie Blue stained phosphoprotein bands were excised from dried SDS-PAGE gels and immersed in 3 ml Optiphase HiSafe 2 liquid scintillant (Wallace - Perkin Elmer) and the amount of ³²P incorporation determined by quantification in either a TriCarb 2000CA Liquid Scintillation Analyzer (Packard) using program 14 or a LS6500 (Beckman Coulter), user option 2.

2.4 MAMMALIAN CELL CULTURE

2.4.1 Maintenance of cultured cells

Cell lines were maintained in a humidified 5% CO₂ atmosphere at 37°C and passaged before reaching confluence. Growth media was aspirated from adherent cells which were then washed with 1x PBS and detached in 1x PBS, 0.5M EDTA before seeding into pre-warmed growth media at the appropriate density. The construction of U2OS cells inducibly expressing GFP-Nek2A or GFP-Nek2A K37R has been described previously (Faragher and Fry, 2003). Expression of GFP-Nek2A was induced by the addition of doxycyclin to the culture media at a final concentration of 1 μ g/ml with further supplementation every 48 hours. Cervical

(HeLa), Breast (HBL100, ZR75-1, MDA-MB-231, MDA-MB-468, T47D), Prostate (PC3, DU145, PNT2-C2), Ovarian (SKOV3, OVCAR5), Leukaemic (K562, KCL22, U937, HL60, Ros, Riva, REC) cancer cell lines and umbilical vein primary cells (HUVEC) were cultured in either Dulbecco's Modified Eagle's Media (DMEM) (Invitrogen) supplemented with 10% heat inactivated foetal calf serum (FCS, Invitrogen) and 2mM Glutamine (Invitrogen) (HBL100, MDA-MB-231, MDA-MB-468, T47D, U2OS), RPMI (Invitrogen) supplemented with 10%FCS and Glutamine to 4mM (ZR75-1, SKOV3, OVCAR5, DU-145, PNT2-C2) or 2mM (K562, KCL22, U937, HL60, Ros, REC, Riva) or Hams F12 (Invitrogen) with 7% FCS, 4mM Glutamine (PC-3).

Cells were obtained from ECACC (Porton down, UK; HeLa, U20S), DSMZ (Braunschweig, Germany; KCL22), Dr. R. Chopra (PICR, UK; K562, U937, HL60), Prof. R. Walker (University of Leicester, UK; HBL100, MDA-MB-231, MDA-MB-468, T47D, ZR75-1), Dr. N. Smith (PICR, UK; SKOV3, OVCAR5), Mr. N. Clarke (PICR, UK; PC3, DU145, PNT2-C2) and Dr. M. Dyer (University of Leicester, UK; Ros, REC, Riva).

2.4.2 Storage of cell lines

Adherent cells were washed in 1x PBS and detached in 1x PBS, 0.5M EDTA. Both suspension and adherent cells were then collected by centrifugation at 1100 rpm for 5 minutes at room temperature, supernatant discarded and the resulting pellet resuspended in 90% FCS/10% DMSO and transferred to cryotubes (Nunc). Cryotubes were placed in an isopropanol filled cell freezer then chilled to -80°C overnight. Frozen cryotubes were transferred to liquid phase liquid nitrogen for long term storage.

2.4.3 Transient transfection

Adherent cells were seeded 1×10^5 cells/cm² 24 hours prior to transfection. 24 hours later 3 μg maxiprep DNA was mixed with 1 μl FuGene 6 reagent according to manufacturers' instructions, added dropwise to cells cultured in the appropriate complete media and incubated until expression was assayed by preparation of cell lysates and Western blotting or immunofluorescence microscopy. To allow

immunofluorescent staining cells were seeded onto 22 mm diameter sterile acid-etched No1 coverslips.

2.4.4 Nek2 depletion by RNA interference

U2OS or HeLa cells were seeded at $1 \times 10^4/\text{cm}^2$ in DMEM supplemented with 10% FCS or MEM supplemented with 1% NEAA, 10% FCS, respectively, 24 hours prior to transfection. Cells were transfected with either individual or pooled RNA duplexes directed against Nek2 (Dharmacon) at a final concentration of 50 nM in serum and antibiotic free media. Oligofectamine (Invitrogen) and RNAi duplex were diluted in Optimem (Invitrogen) according to manufacturers instructions with a final ratio of $1 \mu\text{l}$ Oligofectamine : 125 pmol RNAi. The relevant antibiotic free media supplemented with 30% FCS was added 4 hours post transfection. Nek2 depletion was assayed each subsequent 24 hours as necessary by western blot or immunofluorescence.

2.4.5 Immunofluorescence microscopy

Adherent cells were fixed in -20°C methanol for a minimum of 15 minutes before rehydration in three 5 minute washes in 1x PBS. Non-specific binding was blocked by incubating the rehydrated coverslip in 1x PBS / 1% BSA (w/v) for 15 minutes. Droplets of primary antibody diluted in 1x PBS / 3% BSA (w/v) were arrayed on Nescofilm (Nippon. Shoji Kaisha Ltd) and blocked coverslips inverted onto the droplets and incubated for a minimum of 60 minutes at room temperature. Coverslips were washed 3 times in 1x PBS to remove unbound antibody before incubation with the appropriate secondary antibody diluted in 1x PBS / 3% BSA / $0.3 \mu\text{g/ml}$ Hoechst 33258 for a minimum of 60 minutes at room temperature in the dark. Unbound secondary antibody was similarly removed with 3 sequential 1x PBS washes, residual PBS removed by a single immersion in H_2O and coverslips placed on glass slides on mountant (80% glycerol (v/v), 3% n-propyl gallate (w/v) in H_2O). Images were obtained with a Nikon TE300 inverted microscope using a series of oil immersion lenses and captured with an Orca ER camera (Hamamatsu inc.) and OpenLab 5.0 software (Improvison). Images were processed and quantified where necessary using Photoshop 7 (Adobe) and OpenLab 5.0, respectively.

To allow automated immunofluorescence microscopy on the IN Cell 1000 platform (GE Healthcare, Cardiff, UK) U2OS GFP-Nek2A cells were seeded in poly-L-lysine coated 96 well plates (Nunc) at approximately 1×10^4 cells/cm² 24 hours prior to induction. Doxycyclin was added to the growth media at a final concentration of 1 μ g/ml and the cells returned to the incubator for a further 24 hours before fixation in -20°C methanol for a minimum of 15 minutes. Cells were stained with a mouse anti- γ -tubulin primary antibody an Alexa 488 conjugated secondary antibody in the same manner as above. Plate wells were filled with 1x PBS following the last wash step, sealed and shipped to GE Healthcare for analysis.

2.4.6 Apoptosis assay

Adherent cells were fixed in -20°C methanol for a minimum of 15 minutes before rehydration in 3 x 5 minute washes in 1x TBS. Non specific binding was blocked by incubating the rehydrated cells on the coverslip in 1x TBS / 1%BSA (w/v) for 15 minutes. Droplets of cleaved Caspase 3 antibody (Cell signalling) diluted 1:100 in 1x TBS / 3% BSA (w/v) were arrayed on Nescofilm (Nippon. Shoji Kaisha Ltd) and blocked coverslips inverted onto the droplets and incubated overnight at $+4^{\circ}\text{C}$. Coverslips were washed 3 times in 1x TBS to remove unbound antibody before incubation with the goat anti-rabbit Alexa 488 conjugated secondary antibody diluted 1:200 in 1x TBS/1%BSA/0.3 μ g/ml Hoechst 33258 for a minimum of 60 minutes at room temperature in the dark. Unbound secondary antibody was similarly removed with 3 sequential 1x TBS washes, residual TBS removed by a single immersion in H₂O and coverslips placed on glass slides on mountant (80% glycerol (v/v), 3% n-propyl gallate (w/v) in H₂O). Images were obtained with a Nikon TE3000 inverted microscope using a series of oil immersion lenses and captured with an Orca ER camera (Photometrics inc.) and OpenLab 5.0 software (Improvison). Images were processed using Photoshop 7 (Adobe).

2.4.7 Cell Viability assay

HeLa or U2OS cells were seeded in flat bottom 96 well plates and treated with Nek2 or control RNAi (2.4.4). To assay cell viability 10 μ l of freshly made WST-1 assay reagent (Merck Biosciences, UK) was added to each well and incubated at

37°C for 2 hours in a humidified cell culture incubator, supplemented with 5% CO₂. Cells reduce the WST-1 reagent to a coloured formazan salt in direct proportion to their viability. The formazan product was quantified directly in the plate wells by measuring the OD₄₅₀ in a microplate reader (Model 3550, Bio-Rad, Hercules, CA). Viability measurements were taken at the time of transfection and each subsequent 24 hours up to a maximum of 96 hours. Background absorbance corresponding to untreated cells without WST-1 reagent was subtracted from reading. RNAi treatment and viability assays were performed in triplicate.

To determine cell viability in response to inhibitor treatment the protocol was modified slightly. Cells were seeded at 6×10^3 cells / cm² in 96 well plates. 24 hours after seeding cells were treated with serially diluted inhibitors dissolved in DMSO at a final concentration of 100 µM, 10 µM, 1 µM, 100 nM, 10 nM, 1 nM or DMSO alone as a carrier control. Cell viability was calculated as a percentage of DMSO treatment alone.

2.5 IMMUNOHISTOCHEMISTRY

2.5.1 Embedded cell lines

Cell lines inducibly expressing GFPNek2A were induced with 1 µg/ml doxycycline for 24 hours before harvesting and fixation in 4% paraformaldehyde (w/v). Fixed cells were collected by centrifugation and the pellet embedded in 1% agar. Agar pellets were infiltrated with warmed, liquid paraffin wax, allowed to cool then sectioned in 4 µm slices and mounted on APES coated slides.

2.5.2 Antigen retrieval and immunohistochemistry

Archival formaldehyde-fixed, paraffin wax-embedded tumour samples were obtained from a research collection held at the PICR. 4 µm thick sections of formaldehyde-fixed, paraffin wax-embedded samples of resected tumour, normal breast tissue or embedded cell lines were mounted on APES coated slides by pathologists at the PICR. Sections were dewaxed in three washes of xylene and rehydrated in graded alcohols; 100, 95, 90 and 70% ethanol for 10, 5, 5 and 5 minutes, respectively, before incubation in PBS. Slides were then incubated in a pressure cooker in 10 mM citrate buffer, pH 6.0, for 2 or 3 minutes at full pressure

to recover antigenic Nek2 epitopes. Slides were probed with antibodies raised to Nek2 (Zymed or AR40, 2 $\mu\text{g/ml}$) or normal rabbit serum as an appropriate control (DAKO, 2 $\mu\text{g/ml}$). Bound antibodies were detected with an HRP-conjugated secondary antibody system (Envision, DAKO) and DAB development according to the manufacturers protocol. Developed slides were counterstained in haematoxylin, dehydrated through graded alcohols, incubated in histoclear (National Diagnostics) and mounted in Pertex (Cellpath). Slides were examined on an Axioskop light microscope (Zeiss) and images processed with Axiovision (Zeiss) and Photoshop (Adobe) software.

2.6 DATA PROCESSING

2.6.1 Calculating IC_{50} values

Dose response curves for inhibitor-kinase combinations were produced by performing *in vitro* kinase assays and measuring the degree of β -casein phosphorylation by scintillation counting. *In vitro* kinase assays were performed as described (2.3.6) with the addition of inhibitor dissolved in DMSO. Inhibitors were used in the assay at final concentrations of 250 μM , 100 μM , 10 μM , 1 μM , 100 nM and 10 nM and comprised 2.5% of the assay volume. An equivalent volume of DMSO was used to control for non-specific inhibition of the kinase. Complete reactions were resolved by SDS-PAGE (2.3.1), the gel stained with coomassie brilliant blue (2.3.2) and dried under vacuum. The phosphoprotein band corresponding to ^{32}P - β -casein (approximately 30 kDa) was excised from the dried gel and subject to scintillation counting (2.3.8). Background counts corresponding to a complete assay lacking kinase were subtracted from all the scintillation values. The scintillation counts for each inhibitor concentration were then expressed as a percentage of the kinase assay without inhibitor (DMSO alone). Percentage activity was plotted against log [inhibitor] and linear regression used to fit a hill slope (gradient 1) dose response curve using GraphPad Prism 4.00 for Mac OSX (Graphpad Software Inc., San Diego, CA). The IC_{50} value was defined as the inhibitor concentration reducing kinase activity to half maximal.

2.6.2 Calculating GI₅₀ values

Dose response curves for cell viability at a given inhibitor concentration were produced by incubating sub-confluent HeLa or U2OS cells with serially diluted inhibitors dissolved in DMSO. Following incubation for 72 hours cell viability was measured by WST-1 assay (2.4.7). Briefly, U2OS or Hela cells were seeded in complete media at 6×10^3 cells / cm² in 96 well flat-bottomed microtitre plates. Inhibitor dissolved in DMSO, or DMSO alone, and comprising 1% of the total culture media volume was added directly to each well at final concentrations of 100 μ M, 10 μ M, 1 μ M, 100 nM, 10 nM and 1 nM. Cells were returned to a humidified 5% CO₂ atmosphere at 37°C for 72 hours before the addition of WST-1 as described previously. The concentration of inhibitor that reduced viability to 50% of maximal (GI₅₀) was calculated by linear regression to fit a dose-response curve (variable hill slope, bottom asymptote constrained = 0) to the viability values. Background absorbance corresponding to culture medium with WST-1 reagent in the absence of cells was subtracted from each reading. Inhibitor treatment and viability assays were performed in triplicate.

CHAPTER 3

NEK2 EXPRESSION IS UPREGULATED IN HUMAN CANCER CELL LINES

3.1 INTRODUCTION

Nek2 is regulated in a cell cycle dependent manner, with gross levels of the protein governed by transcriptional regulation and proteolysis. To determine whether Nek2 is implicated in human disease, I first looked at Nek2A and Nek2B protein expression in a panel of normal and cancer derived cell lines to determine whether protein levels are significantly altered in cancer cells.

3.1.1 Genomic instability and cancer

Aneuploidy, the possession of more or less than the correct number of chromosomes, is the single most common feature of solid human tumour cells and is generally associated with poor prognostic outcome (Heim and Mitelman, 1995; Magennis, 1997). The underlying mechanisms for the generation of aneuploidy, although poorly understood, are likely to include defects in the mitotic machinery used to segregate duplicated chromosomes between daughter cells (Pihan and Doxsey, 1999). Persistent loss of control over chromosome segregation leads to chromosome instability (CIN), which is defined as the rate of karyotypic change that occurs within a tumour over time. Ominously, CIN leads to a heterogenous population of cells with respect to genetic content and provides the tumour with a mechanism to select for cells with more malignant or drug resistant properties (Lengauer et al., 1998).

3.1.2 Centrosome defects and aberrant mitosis

The centrosome plays a critical role in mitotic spindle formation and chromosome segregation as it is the primary site of microtubule nucleation in cells (Bornens, 2002; Doxsey, 2001). Normal cells enter mitosis with two properly duplicated centrosomes that ensure bipolarity, as well as correct axial positioning, of the spindle. Cancer cells from a wide variety of tumour types exhibit multipolar spindles and these are often associated with abnormal centrosome number or architecture (Lingle et al., 1998; Pihan et al., 1998; Pihan et al., 2001). In addition, prematurely split centrosomes, unusually positioned centrosomes and centrosomal proteins with aberrant levels of phosphorylation have all been detected in tumour cells (Lingle and Salisbury, 1999). Supernumerary centrosomes, and thereby aneuploidy, may be generated either by a direct uncoupling of the centrosome duplication cycle from the

cell division cycle or through an indirect failure of cell division that leads to tetraploidization (Brinkley, 2001; Nigg, 2002; Pihan et al., 1998). Cells lacking p53 or Rb pocket proteins fail to eliminate tetraploid cells allowing them to progress to the next mitosis where multipolar spindles can form (Borel et al., 2002). As a result of centrosome defects, aneuploidy and CIN being detected in early, even pre-invasive, tumours (Lingle et al., 2002; Pihan et al., 2003a), there is considerable interest in identifying whether centrosomal proteins are either mutated or abnormally expressed in cancer cells.

3.1.3 Kinase control of mitosis

A number of cell cycle regulated protein kinases have been localized to the centrosome including Cdk1, Plk1 and Aurora-A. Each of these kinases is active in mitosis and required for mitotic progression and correct bipolar spindle formation (Nigg, 2001). Overexpression of active and catalytically-inactive versions of Plk1 and Aurora-A lead to mitotic defects, the generation of aneuploid cells and supernumerary centrosomes. Plk1 and Aurora-A also exhibit elevated mRNA and protein expression in a wide variety of tumours and cancer cell lines and can induce transformation upon overexpression in model systems (Bischoff et al., 1998a; Smith et al., 1997; Zhou et al., 1998a). Another centrosomal kinase that is regulated in a cell cycle-dependent manner is Nek2 (NIMA-related kinase 2) (Fry, 2002). Nek2 is expressed in human cells as two splice variants, Nek2A and Nek2B, both of which localize to the centrosome (Hames and Fry, 2002). The combined abundance and activity of the two forms peaks in S and G2 phase of the cell cycle, while Nek2A is specifically targeted for proteasomal destruction in mitosis (Hames et al., 2001). Nek2A also has a binding site for the catalytic subunit of PP1, and hyperactivation of Nek2A at the onset of mitosis is thought to be dependent upon inactivation of PP1 (Helps et al., 2000).

Overexpression of active Nek2A leads to premature centrosome splitting (Fry et al., 1998c; Meraldi and Nigg, 2001), while overexpression of kinase-dead Nek2A causes the formation of centrosomal abnormalities, monopolar spindles and aneuploidy (Faragher and Fry, 2003). Additionally, depletion of endogenous Nek2A in cultured cells by siRNA inhibits centrosome splitting on entry into mitosis (Fletcher et al.,

2005). These data, combined with the characterization of C-Nap1, a centrosomal substrate of Nek2, suggest a physiological role for Nek2A in regulating the separation of centrosomes at the G2/M transition.

3.1.4 Nek2 expression in human cancer

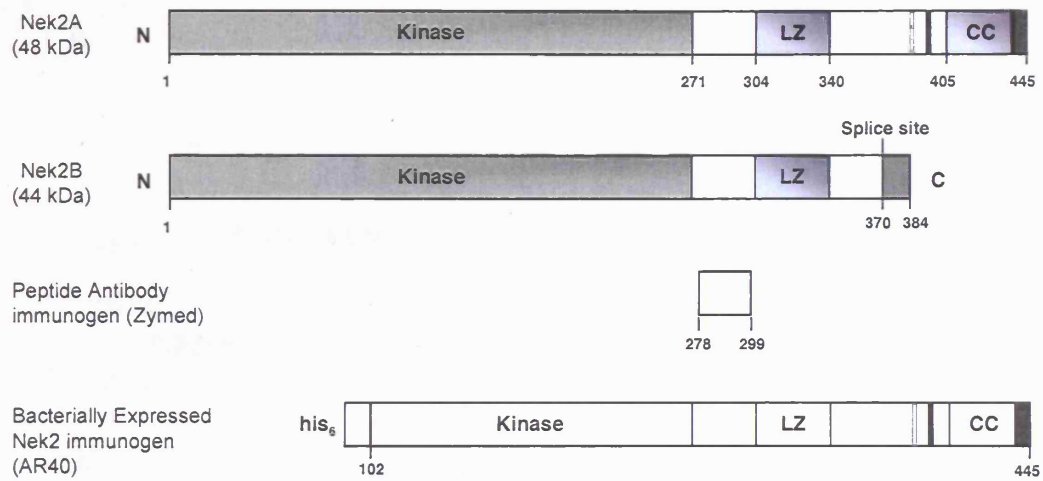
Despite its importance in centrosome regulation and spindle formation, detailed analysis of Nek2 expression in tumours has not been performed. The only relevant data comes from two microarray studies that looked at the expression of a range of genes in certain cancer models. The first of these studies employed an oligonucleotide array to examine the expression levels of 1700 genes in 11 cell lines derived from childhood tumours. The 11 cell lines assayed included 7 derived from Ewing tumours (a paediatric osteosarcoma), 3 derived from neuroblastoma and 1 derived from a malignant melanoma of soft parts (MMSP). Nek2 was one of a group of genes upregulated in the Ewing tumour cell lines (Wai et al., 2002). Similarly, an examination of gene expression levels in follicular lymphomas identified Nek2 as being upregulated in aggressive disease. The pathology of follicular lymphoma (FL) is characterised by a long, chronic, phase which transitions to an acute, aggressive diffuse large B-cell lymphoma (DLBCL) with an accompanying decrease in patient survival. Nek2 is expressed at a four-fold higher level in DLBCL compared to FL (de Vos et al., 2003b). In this chapter I use specific Nek2 antibodies to quantify Nek2 expression in cell lines derived from a variety of different cancer types and examine the effect of overexpressing myc-Nek2A in non-transformed breast cells.

3.2 RESULTS

3.2.1 Expression of Nek2 is elevated in cancer-derived cell lines

To determine whether the protein expression level of the Nek2 kinase is altered in human cancer, I first performed Western blots on extracts prepared from a panel of human cancer cell lines with a polyclonal anti-Nek2 antibody. I used two antibodies that also detected Nek2 in methanol fixed human cells. Both were polyclonal rabbit antibodies that were raised to immunogens comprising either a small peptide, amino acids 278-299 (Fry et al., 1999), or a larger hexahistidine tagged fragment, amino acids 102-445 (Fry et al., 1998c) and referred to as anti-peptide or AR40 antibodies respectively (Figure 3.1A). These antibodies were capable of detecting both Nek2A and Nek2B. The anti-peptide and AR40 antibodies both detected centrosomes in fixed cells (Figure 3.1B), colocalising with the centrosomal marker γ -tubulin (data not shown). Western blots were performed on extracts of peripheral T lymphocytes, primary human umbilical vein endothelial cells (HUVECs) and immortalised breast and prostate epithelial cells (HBL100 and PNT2-C2, respectively). These four non-transformed cell types showed very similar levels of expression of Nek2 proteins, with Nek2A consistently expressed at higher levels than Nek2B. In contrast, Nek2 protein levels were elevated in 10 out of 17 (59%) cancer cell lines including those of ovarian (SKOV3 and OVCAR5), leukaemic (K562, KCL22, RIVA and Rec), breast (MCF-7 and MDA-MB-468), prostate (PC3) and cervical (HeLa) origin (Table 3.1). The highest Nek2 expression levels, greater than two-fold more than in untransformed cells, were found in the SKOV3, K562, KCL22, RIVA and Rec cell lines (Table 3.1, Figure 3.2). Those cell lines having increased expression of Nek2A generally showed similar increases in Nek2B suggesting either amplification of the gene or upregulated transcription. None of the cell lines tested had altered expression of the centrosomal Nek2 substrate, C-Nap1 (Table 3.1). To ensure that the amount of Nek2 detected in Western blotted cancer cell lysate was accurately reflected by ECL detection, we blotted increasing amounts of K562 total cell lysate and quantified the resulting ECL signal by densitometry (Figure 3.3). The ECL signal accurately reflected the level of Nek2 protein depending on the amount of cancer cell lysate used.

A



B

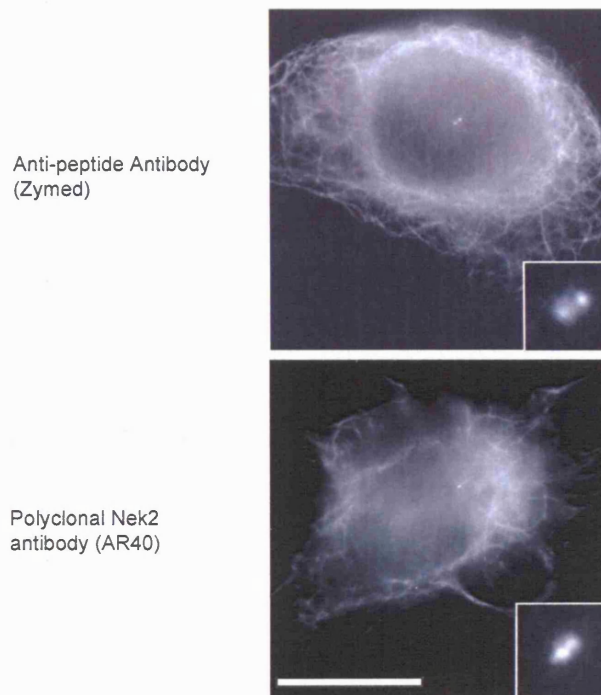


Figure 3.1 Nek2 Polyclonal Antibodies

A. Polyclonal rabbit antibodies were raised to immunising Nek2 synthetic peptides or bacterially expressed fragments comprising amino acids 278-299 and 102-445 and affinity purified. These sequences include regions before the splice site at the C-terminus of Nek2 and hence the antibodies recognise both isoforms, Nek2A and Nek2B. **B.** The resulting anti-peptide and AR40 antibodies recognise Nek2 at the centrosome in methanol fixed cells. Microtubules are stained with primary antibodies to α -tubulin. Centrosomes appear as punctate dots at the centre of the microtubule network in interphase cells (magnified, inset). Scale bar 10 μ m.

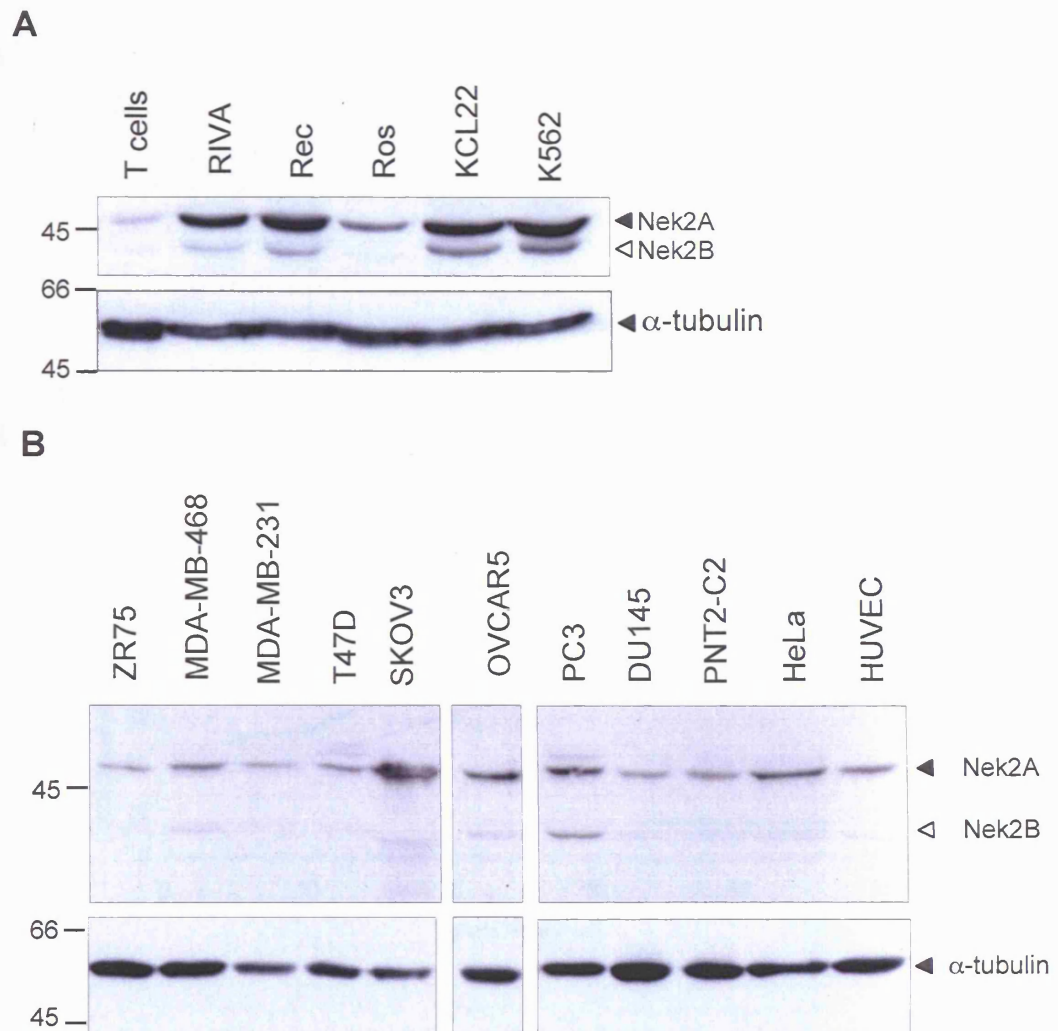


Figure 3.2 Nek2 expression in cancer cell lines

A. Representative Western blots of leukemic and **B.** breast, ovarian and prostate cancer derived cell lysates. 50 μ g total cell lysate was separated on SDS-polyacrylamide gels, Western blotted and probed with Nek2 (anti-peptide antibody; 1 μ g/ml) or α -tubulin (1 μ g/ml) antibodies and developed with ECL (Amersham). T-cells and HUVEC are untransformed primary cells, PNT2-C2 are immortalized, non-transformed cells.

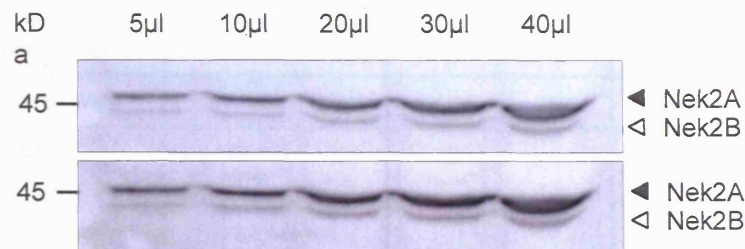
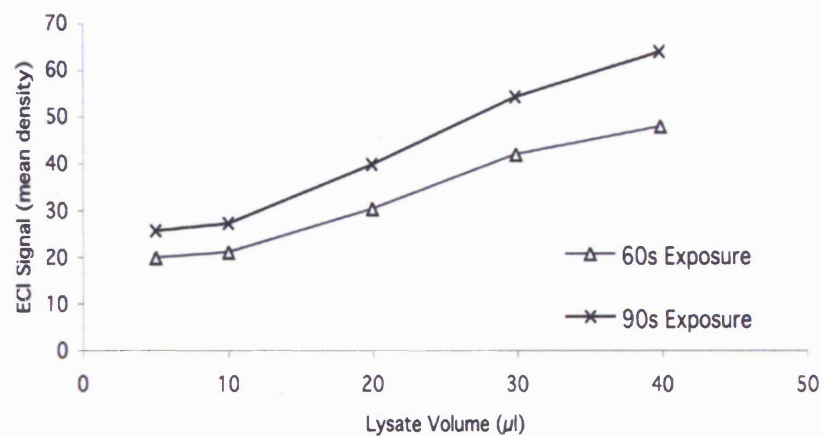
A**B**

Figure 3.3 ECL signal quantification reflects Nek2 protein levels

Increasing amounts of K562 total cell lysate were resolved by SDS-PAGE, transferred to nitrocellulose, probed with a monoclonal antibody to Nek2 (BD Transduction Labs) and bound antibodies detected with ECL plus (Pharmacia). 60 and 90 second exposures shown (A). Autoradiographs from (A) were scanned, the ECL signal was quantified with NIH image 1.62 and the mean pixel density plotted against volume of lysate loaded (B). The quantification reflects the amount of protein loaded and the relationship is linear between 10 and 30 μl (approximately 12-38 μg total protein) of total cell lysate. The quantification is conservative at higher protein levels, underestimating the protein present and hence any fold-change deduced from those levels.

Tissue Origin	Cell Line	Nek2	C-Nap1
Umbilical Vein	HUVEC	+	ND
Breast	HBL100	+	+
	ZR75	+	+
	MDA-MB-231	+	+
	MDA-MB-468	++	+
	T47D	+	ND
	MCF7	++	ND
Prostate	PNT2-C2	+	ND
	PC3	++	ND
	DU145	+	ND
Ovary	SKOV3	+++	+
	OVCAR5	++	ND
Blood	T cells	+	ND
	K562	+++	+
	KCL22	+++	ND
	U937	+	+
	HL60	+	+
	Ros	+	+
	RIVA	+++	+
	Rec	+++	+
Cervix	HeLa	++	ND

Table 3.1 Expression of centrosomal proteins Nek2 and C-Nap1 in cancer cell lines

The expression levels of Nek2 and C-Nap1 were determined by Western blotting total lysates of asynchronous cell populations equalised for protein content. Protein levels are presented with respect to that observed in HUVEC primary cells. Relative expression levels were determined by densitometric scanning over the linear range of enhanced chemiluminescent autoradiographs using NIH Image 1.62 and denoted as follows; +, expressed at equivalent abundance to that seen in HUVECs; ++ overexpressed up to 2 fold, +++ >2 fold overexpressed; -, expressed at lower abundance than in HUVECs. Each cell line was analyzed in at least three independent experiments. ND, not determined

3.2.2 Increased levels of Nek2 correlate with reduced p107 in cancer cell lines

In a recent microarray study, Nek2 was identified as a potential E2F4 transcription factor target gene (Ren et al., 2002). E2F4 acts as a transcriptional repressor during G₁ and G₀ through recruitment of the Rb pocket proteins, p107 and p130. These tumour suppressors, in turn, recruit histone deacetylases which promote a closed state of chromatin preventing access to transcriptional activators. Importantly, Nek2 mRNA is elevated in mouse embryo fibroblasts lacking both p107 and p130 supporting the hypothesis that Nek2 transcription is tightly regulated under normal cell cycle conditions (Ramos-Vara, 2005). We then examined whether the increased levels of Nek2 observed in the cancer-derived cell correlated with a reduction in the level of p107. Whole cell NEB buffer lysates of six leukaemic cell lines and four breast cancer-derived cell lines were resolved by SDS-PAGE and Western blotted with antibodies to p107 (Santa Cruz). Four cell lines, U937, K562, HBL100 and MB-MDA-468, exhibited reduced levels of p107. Three of these cell lines, U937, K562 and MB-MDA-468, showed increased levels of Nek2 protein. Interestingly, in the case of the U937 leukaemic cell line, only the Nek2B isoforms appears to be upregulated. Cell lines with reduced levels of p107 generally showed a marked increase in Nek2 expression (Figure 3.4), suggesting that transcriptional regulation via E2F4 recruitment of p107/p130 is extended to cultured cells of tissue lineages other than fibroblasts. This inverse relationship is tentative. The levels of Nek2 detected in the Rec and RIVA leukaemic lines are lower than reported elsewhere in this chapter (Figure 3.2). Careful repetition is required.

3.2.3 Overexpression of Nek2A induces aneuploidy in immortalized human breast cells

To determine whether altered Nek2 expression might contribute to aneuploidy and CIN in breast cancer, we analysed the consequences of ectopic expression of Nek2A in non-transformed breast cells. HBL100 cells are derived from normal breast epithelia but are immortal due to the presence of SV40 large T antigen (deFromental et al., 1985). Immunofluorescence microscopy revealed that <1% untransfected HBL100 cells had supernumerary centrosomes or abnormal nuclei, whereas a breast cancer cell line (MDA-MB-468) had ~5% cells with

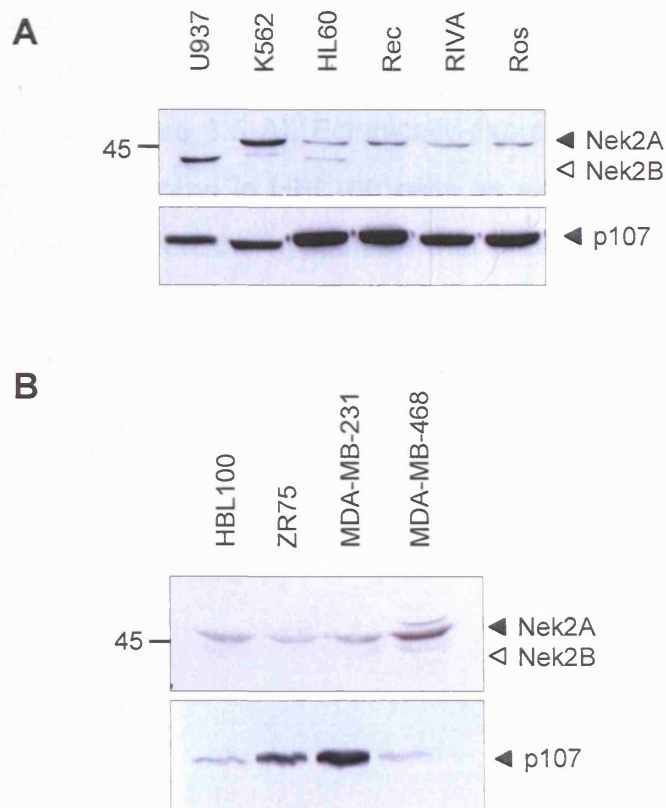


Figure 3.4 Reduced p107 correlates with increased Nek2 expression in cancer cell lines

Representative western blots of leukaemia and breast cancer derived cell lines. **(A)** 50 μ g of six leukaemic cell lines was resolved by SDS-PAGE, transferred to nitrocellulose membrane and probed for Nek2 (anti-peptide antibody, 1 μ g/ml) and p107 (SC318, 2 μ g/ml) and detected by ECL (Amersham). **(B)** Similarly, one immortalized breast epithelial cell line (HBL100) and three breast cancer derived cell lines were lysed and probed for Nek2 and p107. A reduction in levels of p107 correlates with an increase in levels of Nek2, commensurate with its reported role as a transcriptional regulator of Nek2.

supernumerary centrosomes (data not shown). Following 72 hours transfection with myc-tagged Nek2A, ~9% HBL100 cells (n=900) exhibited gross nuclear abnormalities being either multinucleated or with extra chromosomal material (Figure 3.5 A). Staining with antibodies against γ -tubulin (Figure 3.5 B-E) and C-Nap1 (data not shown) revealed that the multinucleated cells invariably contained extra centrosomes suggesting that they arose through an aborted mitosis or failed cytokinesis. Cells transfected with myc-tagged lamin A showed only ~1% nuclear defects (n=1200; Figure 3.5 A). Ectopically-expressed Nek2A co-localized with γ -tubulin at the centrosome in HBL100 cells as expected (Figure 3.5 B-E). These results therefore support the hypothesis that elevated Nek2 levels can contribute to errors in mitotic progression and/or chromosome segregation that generate aneuploid cells.

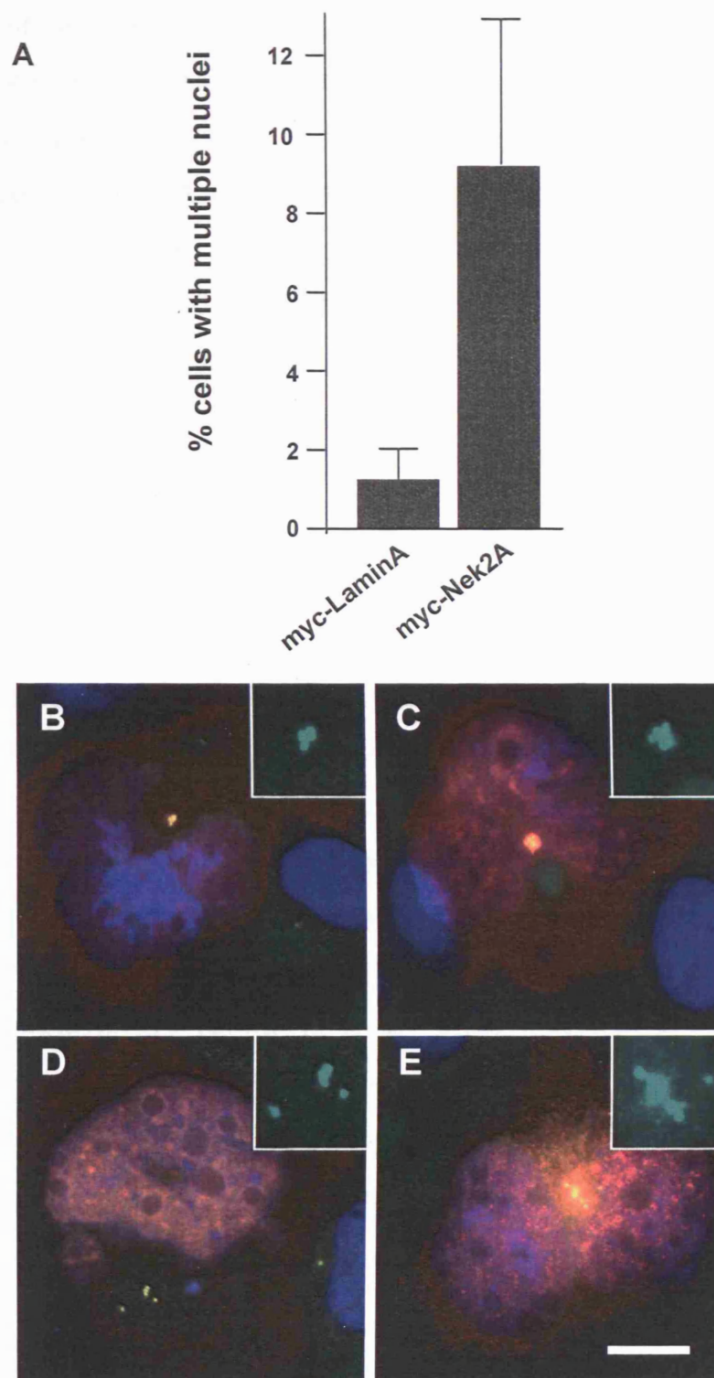


Figure 3.5 Elevated Expression of Nek2A induces multinucleation in HBL100 cells
A Histogram showing percentage of multinucleated cells ($n=100-300$, $p=0.01$) following 72 hours transfection of either myc-LaminA or myc-Nek2A. Error bars represent standard deviation and the p value is 0.01 (student's paired T- test). **B-E** Merged images of multinucleated HBL100 cells expressing myc-Nek2A stained with antibodies against the myc tag (red) and γ -tubulin (green, enlarged inset). DNA was stained with Hoechst 33258 (blue). Scale bar in E, 5 μ m. Images and analysis courtesy of Andrew Fry, adapted from Hayward et al., (2004).

3.3 DISCUSSION

The majority of tumour cells in human cancers exhibit centrosome abnormalities. These typically include increased centrosome size, number and microtubule nucleation capacity (Lingle and Salisbury, 1999; Pihan et al., 1998; Pihan et al., 2001). Importantly, centrosome aberrations correlate with or even precede the generation of aneuploidy and the acquisition of a CIN phenotype in breast and prostate tumours (Lingle et al., 2002; Pihan et al., 2003a). This has led to the hypothesis that deregulation of centrosome function could be a major contributory factor to the genetic instability and loss of tissue differentiation that drive most cancer progression.

This chapter shows elevated protein expression of the centrosomal kinase Nek2 in cancer cell lines. This adds to previous mRNA studies demonstrating elevated Nek2 expression in Ewing tumour cell lines and diffuse large B-cell lymphomas (de Vos et al., 2003b; Wai et al., 2002). Having analysed 17 cancer cell lines, we found upregulated expression in breast, ovarian, leukaemic, prostate and cervical cancer cells. The level of upregulation was 2- to 5-fold with respect to its abundance in primary or immortalized untransformed cell lines. Similar levels of protein overexpression were reported for Aurora-A in pancreatic, breast and colorectal tumour cell lines (Bischoff et al., 1998a; Li et al., 2003; Zhou et al., 1998b). The HBL100 and PNT2-C2 immortalized cell lines do contain SV40 antigens that could alter expression from E2F responsive genes (Berthon et al., 1995; deFromental et al., 1985). However, these cell lines had equivalent expression of Nek2 to the two primary cell types and significantly less than related cancer cell lines.

The underlying cause for an increase in Nek2 expression is unclear, though a series of mechanisms including loss of transcriptional control, gene amplification and reduced proteolysis could be responsible (Figure 3.6). The Nek2 locus, 1q32.1, has been shown to be amplified in both breast tumours and gastric carcinoma. The use of comparative genomic hybridisation (GCH) allows changes in gene copy numbers between normal and tumour tissue to be determined. CGH analysis of 44 archival breast tumours showed a common amplification of region 1q32, the locus of the

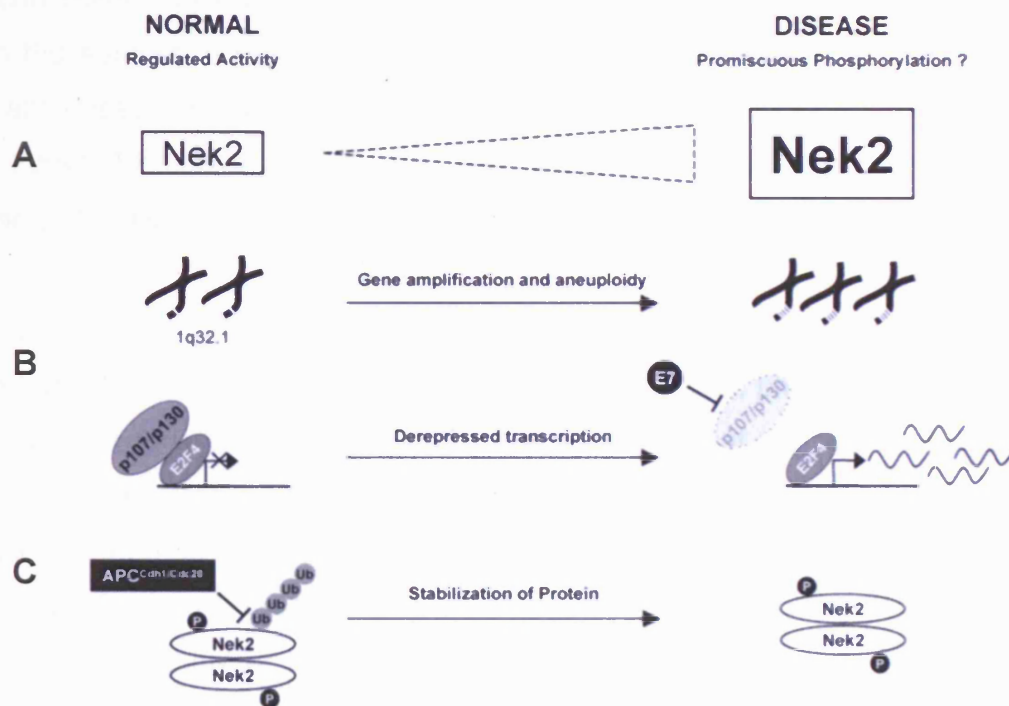


Figure 3.6 Possible mechanisms leading to elevated Nek2 expression

A. Comparative genomic hybridisation studies reveal gain of up to six copies of the Nek2 locus 1q32.1 in breast carcinoma. **B.** Expression of human papillomavirus (HPV) E7 protein leads to increased Nek2 expression in human keratinocytes. This is likely to result from E7 sequestration of the Rb pocket proteins, p107 and p130, which repress Nek2 expression via the E2F4 transcription factor. Loss of p107 and/or p130 protein would equally relieve the repression of Nek2 transcription. **C.** Nek2A protein, which exists as an autophosphorylated dimer, is subject to proteasomal degradation in M, G1 and G0 following ubiquitylation mediated by APC/C^{Cdc20} or APC/C^{Cdh1}. Failure to degrade Nek2A, possibly as a result of destruction site mutation or downregulation of APC/C activity, would increase Nek2A protein stability and hence abundance

human Nek2 gene (Schultz et al., 1994), with 32 patient samples showing a gain of up to six copies (Loo et al., 2004). Though 1q32 gain was widespread, the degree of amplification varied slightly between histopathological tumour types, being more common in IDC and invasive lobular carcinoma (ILC). A similar gain of 1q32 has also been demonstrated in gastric cancer by CGH. Analysis of 35 primary gastric adenocarcinomas revealed a previously unreported gain of 1q32.3 in 10 cases leading the authors to propose Nek2 as a candidate gene; this common gain was significantly associated with lymph node positive disease and poor prognosis (Weiss et al., 2004). Multiple copies of the Nek2 gene may be expected to lead to an increase in the level and activity of Nek2 protein (Figure 3.6A).

Previous analysis of the abundance of Nek2 mRNA in synchronized cells showed a reduced amount in G1 and M phase compared to S and G2 phase (Hayward et al., 2004). This result is in agreement with the observation that the promoter region of the human Nek2 gene binds the E2F4 transcriptional repressor. This would be expected to lead to a decrease in Nek2 transcription in G1 and G0 through recruitment of the p107/p130 pocket proteins. Indeed, cells lacking p107 and p130 exhibit elevated levels of Nek2 mRNA (Ren et al., 2002). Due to the significant number of mitotic and G2/M checkpoint proteins shown to have E2F4 binding sites, loss of p107 and p130 tumour suppressor proteins may well cause upregulation of many cell cycle regulators. Infection with the human papillomavirus type 16 (HPV 16) is associated with cervical neoplasia and infected cells exhibit supernumerary centrosomes and polyploidy. Two HPV antigens, E6 and E7, bind the Rb family proteins p107 and p130. Microarray analysis of human foreskin keratinocytes (HFKs) infected with a retroviral construct expressing HPV16 E6 and E7 identified upregulated G2/M phase proteins, including Nek2 (Patel et al., 2004). As loss of Rb pocket proteins also promotes survival of tetraploid cells it is possible that these tumour suppressors may be critical in preventing the accumulation of centrosome abnormalities and aneuploidy. Latterly, the forkhead transcription factor FoxM1 has been shown to regulate a range of genes with peak expression at the G2/M transition, including Nek2 (Laoukili et al., 2005). Increased levels of FoxM1, which have been reported in breast cancer (Wonsey and Follettie, 2005), would be expected to increase expression of the genes it regulates, including Nek2.

Nek2 abundance is also governed by cell cycle-dependent protein degradation. Both Nek2A and Nek2B are short-lived proteins in cultured cells. However, while levels of both Nek2A and Nek2B increase during S and G₂, Nek2A is specifically degraded upon mitotic entry, Nek2B persisting until the subsequent G₁ (Fry et al., 1995; Hames et al., 2001). The early mitotic destruction of Nek2A results from proteasomal degradation following ubiquitylation mediated by the anaphase promoting complex/cyclosome (APC/C). Recognition of Nek2A by the APC/C depends upon two C terminal destruction motifs that are recognised by the APC/C adaptor proteins Cdh1 and Cdc20 (Figure 3.6A). Additionally a further APC/C mediated degradation during mitosis, independent of Cdh1, is enacted via the terminal two residues of Nek2A. The APC/C recruits Nek2A directly via binding the terminal MR residues, even in the absence of Cdc20, which renders Nek2 degradation insensitive to the mitotic checkpoint (Hayes et al. 2006). Mutation of the residues in Nek2 which allow binding of the APC/C or disruption of the proteolytic machinery would both contribute to the increased expression of Nek2 observed in cancer cell lines.

Previous studies have shown that Nek2 contributes to assembly and maintenance of centrosomes and to bipolar spindle formation (Faragher and Fry, 2003; Twomey et al., 2004; Uto and Sagata, 2000). Inappropriately high expression of Nek2 might therefore interfere with either centrosome integrity or chromosome segregation. In non-dividing cells, this could contribute to the loss of differentiated cell morphology and breakdown in tissue architecture typical of invasive breast carcinomas (Lingle et al., 2002; Lingle et al., 1998). In dividing cells, this could lead to aneuploidy and CIN. Indeed, overexpression of Nek2A in the non-transformed HBL100 cell line did induce the generation of multinucleated cells at a level that was nine-fold higher than control transfections. As these multinucleated cells also had supernumerary centrosomes, it seems reasonable to predict that they have failed cytokinesis, perhaps as a result of some earlier defect in mitosis. In addition to disrupting proper spindle formation, altered expression of Nek2 might interfere with other mitotic processes. Nek2 has been reported to interact with the kinetochore proteins Hec1 and Mad1 suggesting a role in the spindle checkpoint (Chen et al., 2002a; Lou et al., 2004b). These

experimental data provide the first report of altered Nek2 protein expression in cancer cell lines derived from a range of tissues. Further, they show overexpression of Nek2A in a breast epithelial cell background induces supernumerary centrosomes and changes in ploidy, two hallmarks of human cancer. Logically, the examination of Nek2 expression levels should now be extended to primary human tumours.

CHAPTER 4

NEK2 PROTEIN EXPRESSION IS UPREGULATED IN PRIMARY HUMAN BREAST TUMOURS

4.1 INTRODUCTION

The transformation of a normal cell to a neoplastic state, acquiring the ability to proliferate beyond normal growth restrictions, is a multi-step process, evading programmed cell death, acquiring proliferative capability and invading and disrupting surrounding tissue (Hanahan and Weinberg, 2000). A frequent hallmark of this transformation process is the loss of genomic regulation producing gross changes in ploidy and the associated gain of oncogenes and loss of tumour suppressors (Heim and Mitelman, 1995).

The fidelity of genomic replication is governed, in part, in somatic cells by the formation of a bipolar mitotic spindle, the structural apparatus nucleated at each apex by centrosomes, which ensures duplicated chromosomes are segregated equally into nascent daughter cells (Gadde and Heald, 2004). As centrosomes can regulate spindle formation, so the kinases that govern centrosome replication in turn influence DNA segregation. Consequently there is considerable current interest in centrosomal kinases as therapeutic targets to retard chromosomal instability and aneuploidy. Two classes of mitotic kinases, the polo-like kinases (Plks) and Aurora kinases, both contain members shown to be transforming and oncogenic upon overexpression (Bischoff et al., 1998a; Smith et al., 1997). Attention has now shifted to a third class of serine/threonine kinase, the NIMA related kinases (Neks) and specifically Nek2, currently the most characterised of the human Nek kinases (Fry, 2002).

4.1.1 Nek2 upregulation in primary human tumours

Having determined that Nek2 is overexpressed in cultured cancer cell lines derived from a range of tissues including blood, ovary and breast, I sought to examine levels of Nek2 protein expression in solid tumours. In addition to the observed upregulation of Nek2 in a breast cancer derived cell line, there have also been several prior reports of altered centrosome morphology, number and composition in primary breast tumours (Lingle et al., 1998; Lingle and Salisbury, 1999). These alterations are implicated in driving chromosomal instability and tumour aggression (D'Assoro et al., 2002; Lingle et al., 2002; Salisbury et al., 2004). With an established role for Nek2A in the regulation of centrosomes and an observed

upregulation in tumour derived cell lines, the examination of levels of the protein in primary breast tumours was the next logical step.

4.1.2 Pathology of breast cancer

Breast cancer is the fourth most prevalent carcinoma in the United Kingdom, accounting for 8% of all cancer mortality and 16.8% of female cancer mortality in 2004 (O.N.S., 2004). Malignancies arise in epithelial cells lining the network of ducts and tubules that convey milk to the nipple or, less commonly, within cells of the nipple itself.

At a histological level, the basic structure of the breast begins to form during embryogenesis when epithelial cells invade indentations at the interface of the epithelium and stroma. The epithelium proliferates and subsequently separates into 15-20 branches of epithelial duct. The ducts open onto the area destined to form the aureolus and nipple in a primitive version of the lobuloalveolar duct network. Structural development of the breast is then largely static until puberty when the duct network enlarges, forming primary and secondary ducts lined with epithelial cells and ending within the breast in blind sacs initially called terminal end buds which then develop into the terminal duct lobulalveolar units (TDLUs), or ductules. A concomitant expansion of the collagenous connective tissue supports this increased epithelial architecture. The mature adult mammary gland hence consists of lobules from which exit lactiferous ducts that converge to larger extralobular ducts that open to the surface of the nipple, each bundle of converging lobules termed a lobe (Clarke and Howell, 2001). The overall structure resembles a bunch of grapes (Figure 4.1)

Histologically the ducts and alveoli within lobules are lined with two types of epithelial cells arranged in layers and bounded by a basal membrane, the vessels are lined first with secretory luminal cells and below those, basal myoepithelial cells that have smooth muscle characteristics, allowing contraction and subsequent expulsion of expressed milk during lactation. Immunologically the different cell types can be distinguished by cell surface marker expression as well as relative position within the duct. Myoepithelial cells express cytokeratins CK5

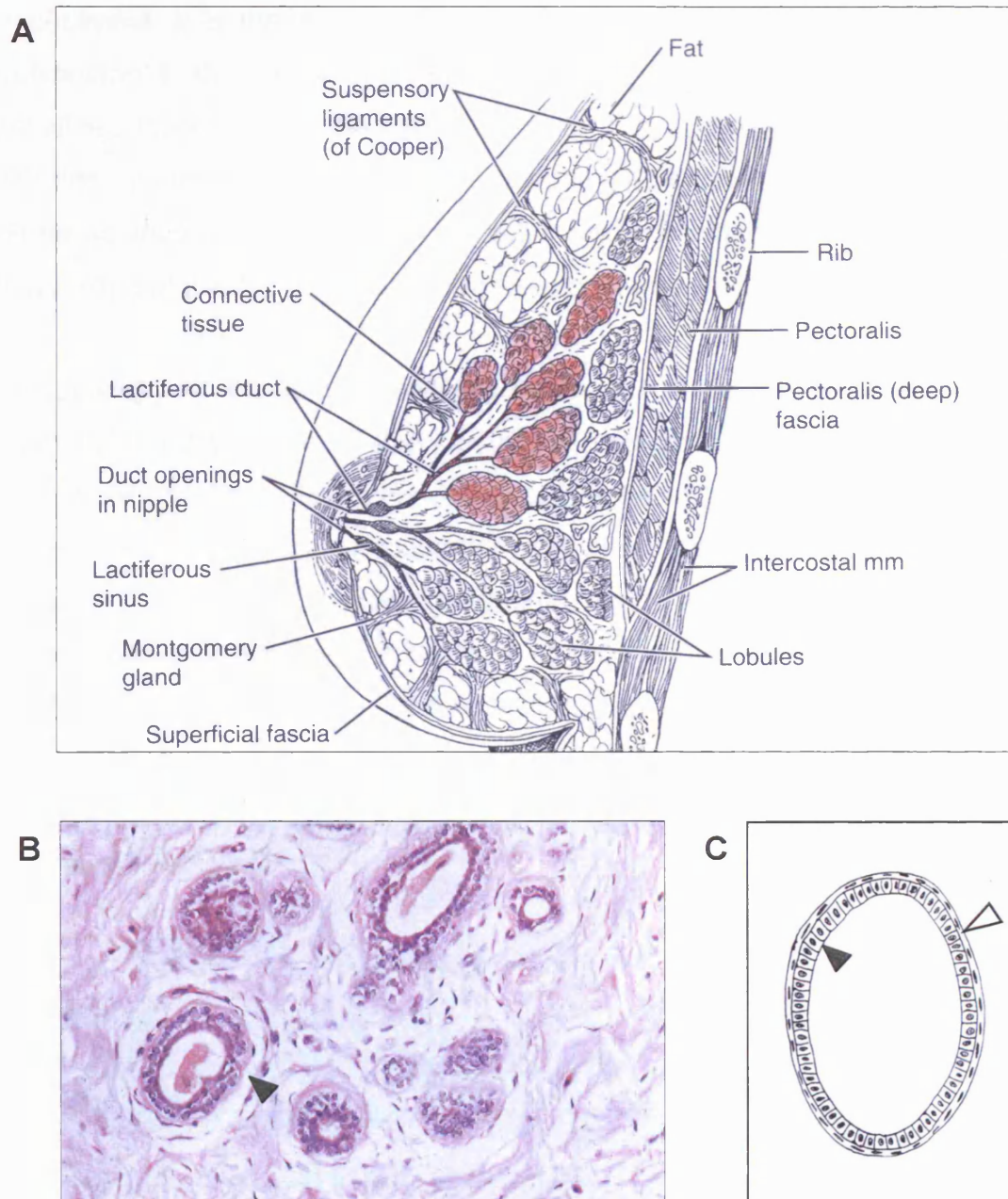


Figure 4.1 Structure of the mature breast

A. Sagittal cross section of the mature breast. A lobe, a unit comprising lobules and ducts, is shown shaded in red. Adapted from Roses, D.F. (1999) **B.** Transverse section of a lactiferous duct stained with haematoxylin and eosin. The myoepithelial and luminal cells bounded by a basement membrane can be seen (arrowed). **C.** A transverse section of a duct shown in cartoon depicting luminal cells (closed arrow) surrounded by contractile myoepithelial cells (C, open arrow). Adapted from Ahmed, A. (1992).

and CK14 and smooth muscle actin, whereas the luminal cells express a different subset of cytokeratins, CK8, CK18, CK19 and, more pertinently in terms of tissue regulation, the nuclear oestrogen and progesterone receptors (ER α and PR respectively). It is the luminal cell population that is responsible for 90% of the proliferation in the non-lactating breast and this expansion is due to endocrine signalling; responses to the cyclical variations in oestrogen and progesterone secreted by the ovaries during the normal menstrual cycle. Cells bearing ER α or PR do not themselves proliferate but rather signal to adjacent luminal cells which in turn expand (Clarke et al., 2004; Clarke and Howell, 2001).

The plasticity of the luminal cell population is reflected in the origin of most common breast tumours. Breast carcinomas, almost without exception, express luminal cell characteristics rather than those of the myoepithelium or stroma. The majority of tumours originate in luminal cells within the ductules or lobes and this gives the nomenclature to breast carcinoma, being described as *ductal* or *lobular* in origin and, subsequently, as either *in situ* or *invasive* depending upon whether the proliferating cells have crossed the basement membrane to invade the surrounding tissue, respectively. The distinction is chiefly histopathological, with ductal carcinoma cells appearing as clusters whilst lobular carcinoma cells appear as strands in single file.

4.2 RESULTS

4.2.1 Paraformaldehyde fixation occludes antigenic Nek2 epitopes

Prior to storage the majority of archival tissue samples are first fixed in paraformaldehyde then embedded in blocks of paraffin wax. This treatment preserves some cellular epitopes and structure whilst the wax acts as a physical support both to preserve tissue ultrastructure and to facilitate the sectioning of the sample into layers sufficiently thin to allow light microscopy.

The formaldehyde used in tissue preservation creates crosslinks between the amino groups of proximal amino acids. However, while this network of crosslinks acts to preserve gross protein structures within a cell or tissue, it can also modify the tertiary and quaternary structure of proteins. This modification can obscure the specific immunogenic epitopes recognised by antibodies, rendering them undetectable. Whilst Nek2 is readily detected by the anti-peptide and AR40 antibody in whole cell lysates and cells fixed in methanol (Faragher and Fry, 2003; Fry et al., 1999; Fry et al., 1998c), it was not known whether either antibody would stain Nek2 in formaldehyde fixed samples.

To determine whether formaldehyde fixation obscures antigenic Nek2 epitopes, I first examined formaldehyde fixed monolayers of adherent cultured cells. HBL100 cells were seeded onto acid treated glass coverslips, cultured overnight and then fixed in either -20°C methanol or 3.7% (v/v) paraformaldehyde before processing for immunofluorescence microscopy (Fry and Faragher, 2001). The fixed cells were incubated separately with three polyclonal antibodies raised to Nek2, the anti-peptide (Zymed) antibody and two further antibodies raised to larger Nek2 fusion proteins, R31 and R40 (Figure 4.2). In interphase U2OS cells Nek2 is present in both the nucleus and the cytoplasm, though is most concentrated at the centrosome (Fry et al., 1998c). This Nek2 staining pattern is reproduced in HBL100 cells with the Zymed anti-peptide, R31 and R40 antibodies; a low level of diffuse signal throughout the cell with two bright punctate dots corresponding to the centrosome. This staining pattern is preserved in cells fixed in methanol (4.2 A, C and E) but completely ablated in cells fixed in formaldehyde (4.2 B, D and F).

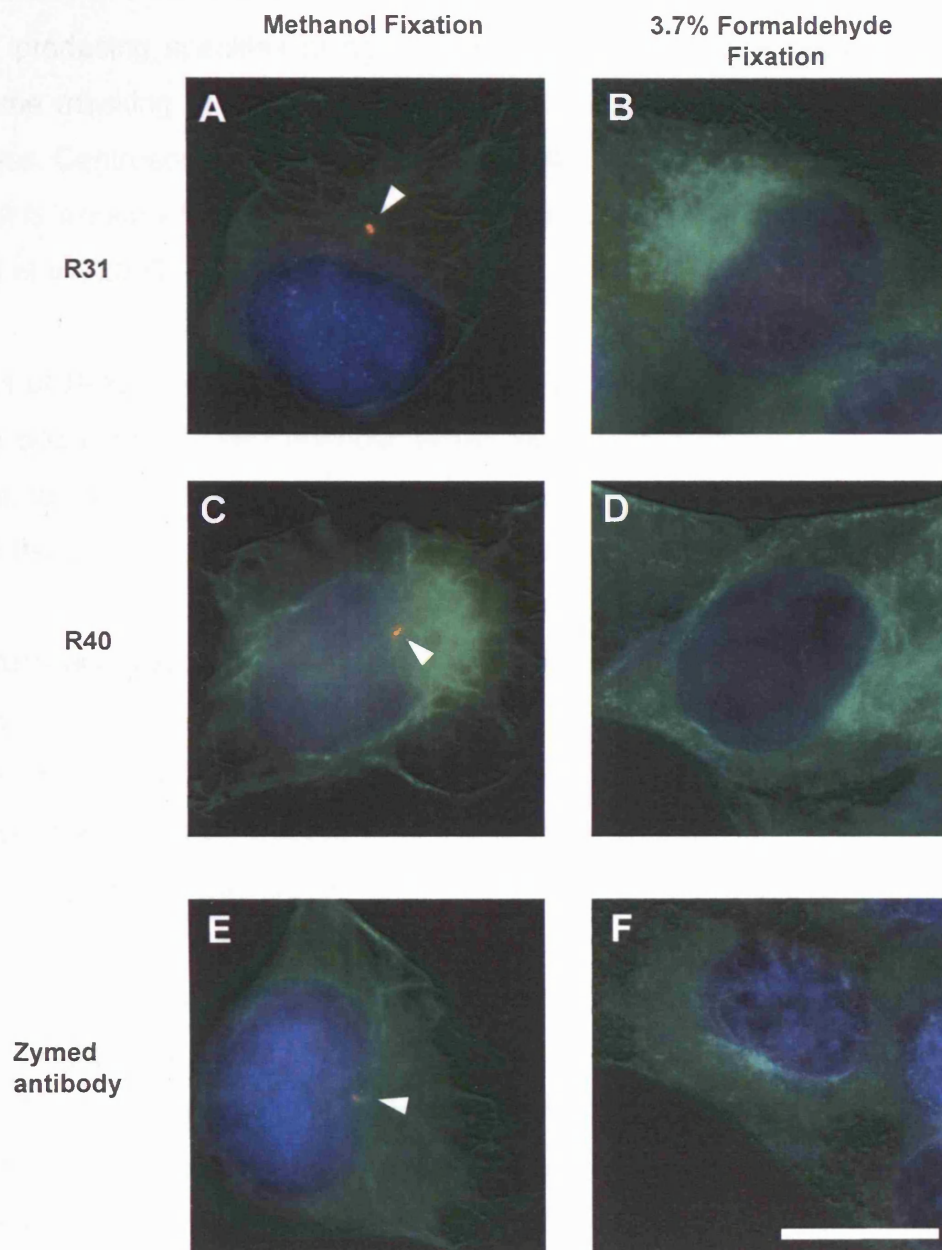


Figure 4.2. Abolition of centrosomal staining by Nek2 antibodies following formaldehyde fixation

HBL100 breast tissue derived cell lines fixed in -20°C methanol (A, C and E) or 3.7% formaldehyde (B, D, and F) for 10 mins were probed with rabbit polyclonal antibodies to Nek2: R31 (A, B), R40 (C, D), Zymed (E, F) and visualized with biotinylated anti-rabbit antibodies and streptavidin Texas red. Cells were co-stained with monoclonal α -tubulin antibodies visualized with Alexa fluor 488 anti-mouse Abs and with Hoechst 33258. Centrosomes appear red, microtubules green and DNA blue. Scale bar, 10 μm .

The ability to detect Nek2 at the centrosome is lost by all three of the antibodies tested and in addition the formaldehyde fixation also affects the α -tubulin staining pattern, producing speckles along the interphase microtubule network, probably due to the masking of some epitopes recognised by a subset of the polyclonal antibodies. Centrosomal staining of the *Drosophila melanogaster* Nek2 homologue *DmNek2* is similarly lost following formaldehyde fixation of cultured S2 insect cells (Prigent et al., 2005).

The loss of Nek2 staining in formaldehyde fixed cultured cells strongly suggested that the occlusion of Nek2 epitopes would also occur in archival tissue samples and that, to be able to determine the expression of Nek2 in tumours, treatment to unmask the crosslinked epitopes would be required.

4.2.2 Antigen retrieval enables Nek2 staining following formaldehyde fixation

In order that tissue samples may be archived for examination after their initial extraction, they must be treated to preserve morphological detail, the location of cellular components and prevent autolysis and subsequent sample degradation. Fixation of the sample in an aqueous solution of formaldehyde and embedding in paraffin wax has been the method of choice for over a century, favoured for its superior retention of morphological detail over other fixatives such as ethanol. A consequence of the long history of formaldehyde fixation is that the majority of the criteria for the pathological diagnosis of disease have evolved using tissues fixed in this manner. The necessity to standardise samples for diagnosis and the legacy of archival tissue has led formaldehyde to endure when combinations of more modern solvents would perhaps result in an improved fixative. The chief advantage of formaldehyde fixation, rigorous preservation of three dimensional cellular and tissue ultrastructure, has also proved to be a hindrance to more modern, molecular, assessments of disease in tissue samples (Ramos-Vara, 2005; Shi et al., 2001).

As mentioned above, treating tissues with formaldehyde chemically modifies macromolecules, inducing covalent intermolecular and intramolecular crosslinks.

The aldol group of formaldehyde reacts with exposed hydrogen atoms on the macromolecule, commonly with amine groups of proteins, to form a covalent bond (Shi et al., 1997). The ability of aldehyde molecules to polymerise then allows chains of aldehyde molecules, termed methylene bridges, to form between groups bearing hydrogen atoms on adjacent proteins, carbohydrates and nucleic acids. Whilst it is suggested that amino groups are the most common targets of formaldehyde crosslinks, aromatic rings, imino, amido, peptide, guanidyl and carboxyl groups may all be able to supply the necessary hydrogen (Montero, 2003). The capacity for a large network of interconnected macromolecules readily becomes apparent. The covalent cross-links formed between adjacent chemical groups after formaldehyde fixation stably preserve cellular and tissue architecture but do so at the expense of chemically modifying the structure of proteins comprising the tissue, inadvertently masking protein epitopes. The process of exposing these occluded epitopes is termed antigen retrieval.

Initial methods of recovering antigens employed a proteolytic digestion of the fixed sample, notably demonstrated by the detection of Hepatitis B proteins in liver biopsies following trypsin treatment (Huang, 1975; Huang et al., 1976). The use of proteases prior to immunostaining allowed more antigens to be studied in fixed tissue and is still employed. However, proteolysis is non-specific and can destroy antigenic epitopes as well as degrading tissue structure (Ramos-Vara, 2005). A later development used high temperature incubation of the tissue sample in aqueous buffer. This proved more versatile, increasing the specific staining associated with 39 of the 52 polyclonal and monoclonal antibodies initially tested and has since been widely adopted (Shi et al., 1991). The antigen retrieval is likely achieved by hydrolysis of some methylene bridges and a partial renaturation of the protein. The reaction is driven largely by thermal energy, the incubation time required reducing in proportion to the increasing temperature (Shi et al., 2001).

To determine whether antigen retrieval would allow detection of Nek2 protein in formaldehyde fixed, paraffin embedded (FFPE) tissues I employed a U2OS T-rex cell line which inducibly overexpresses myc-Nek2A in response to doxycycline (Faragher and Fry, 2003). The U2OS:myc-Nek2A cells were induced to

overexpress myc-Nek2A for 24 hours, fixed in formaldehyde then embedded in paraffin wax. The overexpressed myc-Nek2A fusion protein was used to validate the antigen retrieval procedure, as the Nek2A immunostaining should be greatest in the retrieved samples overexpressing Nek2A and least in the uninduced, unretrieved cells. To retrieve the antigens occluded by formaldehyde fixation, I used high temperature incubation in sodium citrate buffer, a technique routinely used to recover nuclear antigens such as PR, ER and the proliferation marker Ki67 for immunohistochemistry (Esteva and Hortobagyi, 2004).

The antigen retrieval technique successfully recovered Nek2 antigenic epitopes (Figure 4.3). Prior to retrieval the FFPE cells showed no immunoreactivity when incubated with either the Zymed antipeptide Nek2 antibody (Figure 4.3 A, B) or rabbit IgG at the same concentration (Figure 4.3 E, F); only the purple haematoxylin nuclear counterstain was evident. Repeating the immunocytochemistry after antigen retrieval resulted in a markedly different Nek2 staining pattern. While the control rabbit immunoglobulins did not produce any 3',3'-diaminobenzidine (DAB) staining in the embedded cells (Figure 4.3 G, H), a clear Nek2 signal was evident in both the uninduced and induced cells (Figure 4.3 D, E). The Nek2 staining was greatest in the cells overexpressing myc-Nek2A (4.3 E) though detection of endogenous Nek2 was also evident in the uninduced cells (4.3 D) albeit at a lower level as expected. The degree of staining for both endogenous and exogenous Nek2 was not uniform in each cell as Nek2 is regulated in a cell cycle dependent manner with Nek2 being degraded in G₁ cells (Hayes et al., 2006). The conditions that successfully retrieved Nek2 in FFPE treated cultured cells could now be applied to breast tumour samples.

4.2.3 Detection of centrosomal antigens in cultured normal breast cells

Antigen retrieval allowed the detection of Nek2, both overexpressed and endogenous, in cultured cells. I sought to determine whether the unmasking of antigens at the centrosome was restricted to Nek2 or whether another centrosomal antigen and Nek2 substrate, C-Nap1 (Fry et al., 1998a), could also be detected. An immortalized normal human breast cell line, HBL100, was formaldehyde fixed and paraffin embedded in the same manner as the U2OS:myc-

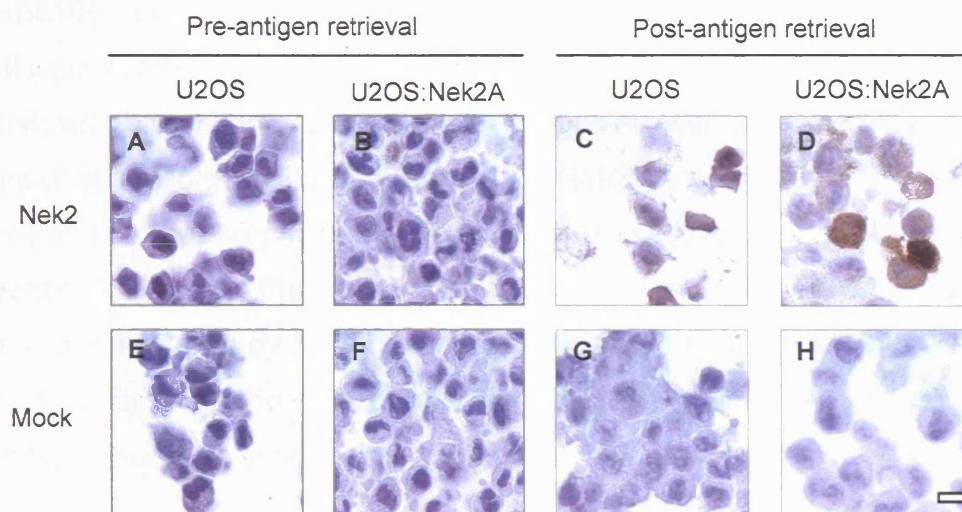


Figure 4.3 Antigen Retrieval enables Nek2 staining following formaldehyde fixation

U2OS osteosarcoma cells stably transformed with a construct expressing kinase dead Nek2A-K37R-myc-His (U2OS:Nek2A; B, D, F and H) or the parental U2OS cell line (U2OS; A, C, E and G) were fixed with formaldehyde before embedding in paraffin wax. Sections were then cut and stained with the Zymed antipeptide antibodies raised to Nek2 (A-D; 3.75 µg/ml) or control IgGs (E-H) before (A, B, E, F) or after (C, D, G, H) antigen retrieval. DAB staining (brown) indicates that Nek2 is recognized in the stable cell line only after processing for antigen retrieval (D). The cell-to-cell variability of staining reflects the cell cycle dependent expression of Nek2A. Scale bar, 10 µm.

Nek2A cells, then subjected to antigen retrieval and immunohistochemistry with antibodies raised to Nek2 and C-Nap1.

C-Nap1 (centrosomal Nek2 associated protein 1) is a 280 kDa protein which forms part of the putative link between paired centrosomes. Correspondingly, it is most concentrated in this region and is an excellent marker for centrosomes (Fry et al., 1998a). HBL100 cells incubated with control rabbit IgG antibodies after antigen retrieval did not exhibit any staining (Figure 4.4 A,D), but clear staining patterns were evident with both the Nek2 and C-Nap1 antibodies, with punctate dots highly reminiscent of centrosomes weakly evident in the Nek2 stained sample (Figure 4.4 C, arrowed) and more distinctly in the C-Nap1 stained cells (Figure 4.4 D,E). This staining pattern is similar to that seen when the localisation of Nek2 and C-Nap1 is examined in cultured cells by indirect immunofluorescence (Fry et al., 1998a). The detection of C-Nap1 at the centrosome suggests the conditions for antigen retrieval of Nek2 would be suitable for centrosomal antigens generally.

4.2.4 Nek2 protein levels are increased in tumour compared to normal breast tissue

The differential expression of Nek2 detected in the induced and uninduced myc-Nek2A stable cell lines allowed me to optimise the antigen retrieval procedure, confident that the staining pattern was due to detection of Nek2. The further staining of C-Nap1 suggested that other centrosomal antigens were similarly unmasked. The conditions determined with the stable cell lines and the antipeptide antibody could therefore be used to assess the levels of Nek2 protein in primary breast tumours.

I examined the Nek2 protein expression levels of 20 FFPE archival primary breast tumours that included both *in situ* and invasive ductal and lobular carcinoma. Strikingly, I found that Nek2 protein expression was significantly elevated in the majority of these breast tumour samples. Elevated Nek2 expression was clearly detected in invasive ductal carcinoma (IDC, Figure 4.5 A, solid arrows 1 and 2) and ductal carcinoma *in situ* (DCIS, Figure 4.5 A, solid arrow 3 and Figure 4.5 B, solid arrow) tumour cells as compared to normal breast ductal

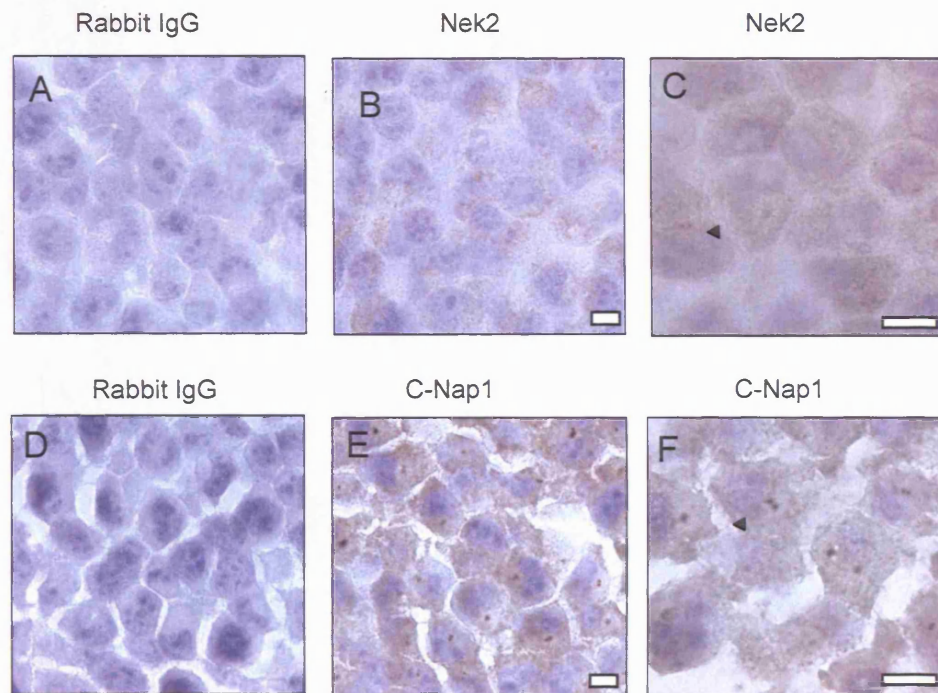


Figure 4.4 Nek2 and C-Nap1 staining in HBL100 immortalized breast cells following antigen retrieval.

HBL100 cultured breast cells were fixed with formaldehyde, embedded in paraffin wax, processed for antigen retrieval and stained with Zymed anti-peptide antibodies raised against Nek2 (3.75 $\mu\text{g/ml}$; B and C), C-Nap1 (4 $\mu\text{g/ml}$; E and F) or mock-stained (A and D). Primary antibodies were visualised with avidin-biotin-peroxidase conjugates and 3,3'-diaminobenzidine (DAB) development (brown). The cells were lightly counterstained with haematoxylin (purple). Panels B and E were Paired interphase centrosomes can clearly be seen after staining with C-Nap1 antibodies (E and F, arrows) and at higher magnification with Nek2 (C, arrow). Scale bars in B, C, E and F, 10 μm .

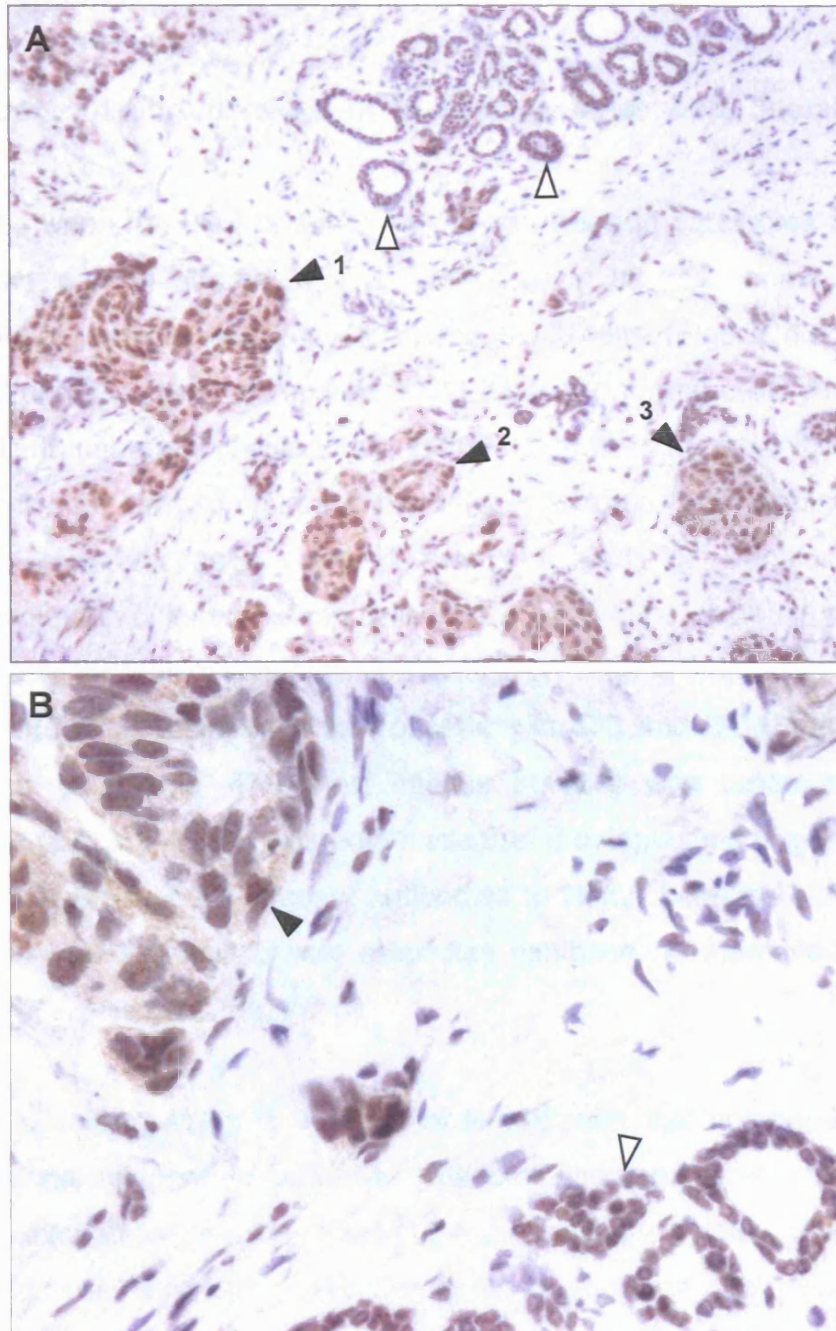


Figure 4.5 Nek2 protein levels are increased in tumour compared to normal tissue
 Invasive ductal carcinoma (IDC) breast tumour sections were cut and stained with Zymed anti-peptide antibodies raised to Nek2 ($2\mu\text{g/ml}$) following antigen retrieval. **A.** Images taken at low magnification. **B.** Images taken at high magnification. Antibody staining reveals the marked upregulation of Nek2 in tumour (solid arrows) compared to normal tissue (empty arrows). Nek2 upregulation is observed in both IDC (A, solid arrows, 1 and 2) and DCIS (A, solid arrow, 3).

cells or stromal cells within the same sections. These latter cells showed weak levels of staining as would be expected for a ubiquitously expressed protein (Hames and Fry, 2002).

4.2.5 Nek2 upregulation persists in invasive lobular and ductal breast carcinoma

The contrast between the high levels of Nek2 expression in carcinoma cells and the lower basal level in stroma cells is marked in *in situ* carcinoma and this overexpression persists in invasive carcinoma. IDC cells (Figure 4.6 A, solid arrow) stain strongly for Nek2 compared to the adjacent normal cells. Analysis of additional patient samples showed the same pattern; a marked increase in staining of carcinoma cells compared to the adjacent stroma. The staining pattern for Nek2 in carcinoma cells mirrored that observed for transfected and endogenous protein in cultured human cells in that there is no obvious preference for an exclusively nuclear or cytoplasmic localization (Figure 4.6 B, solid arrow) (Fry et al., 1998c). The staining pattern observed in IDC and DCIS extended to invasive lobular carcinoma. The most intense staining was restricted to the carcinoma cells (Fig. 4.7 A) and was both nuclear and cytoplasmic (Fig 4.7 B) and dependent on the presence of primary antibodies to Nek2. Several DCIS tumour sections incubated with Nek2 zymed antibodies exhibited no increased staining and hence Nek2 expression (Fig. 4.7 D).

To verify the staining pattern that I had observed with the anti-peptide Nek2 antibody, a second independent polyclonal antibody was used. This antibody was raised to a bacterially-expressed fragment representing approximately the C-terminal two-thirds of the Nek2A protein (Fry et al., 1998c). Again following antigen retrieval, carcinoma cells in DCIS tumours stained strongly for Nek2, whereas the normal ductal tissue and stromal cells did not (Figure 4.8 A), serial sections stained with control rabbit immunoglobulins showed no staining (4.8 B).

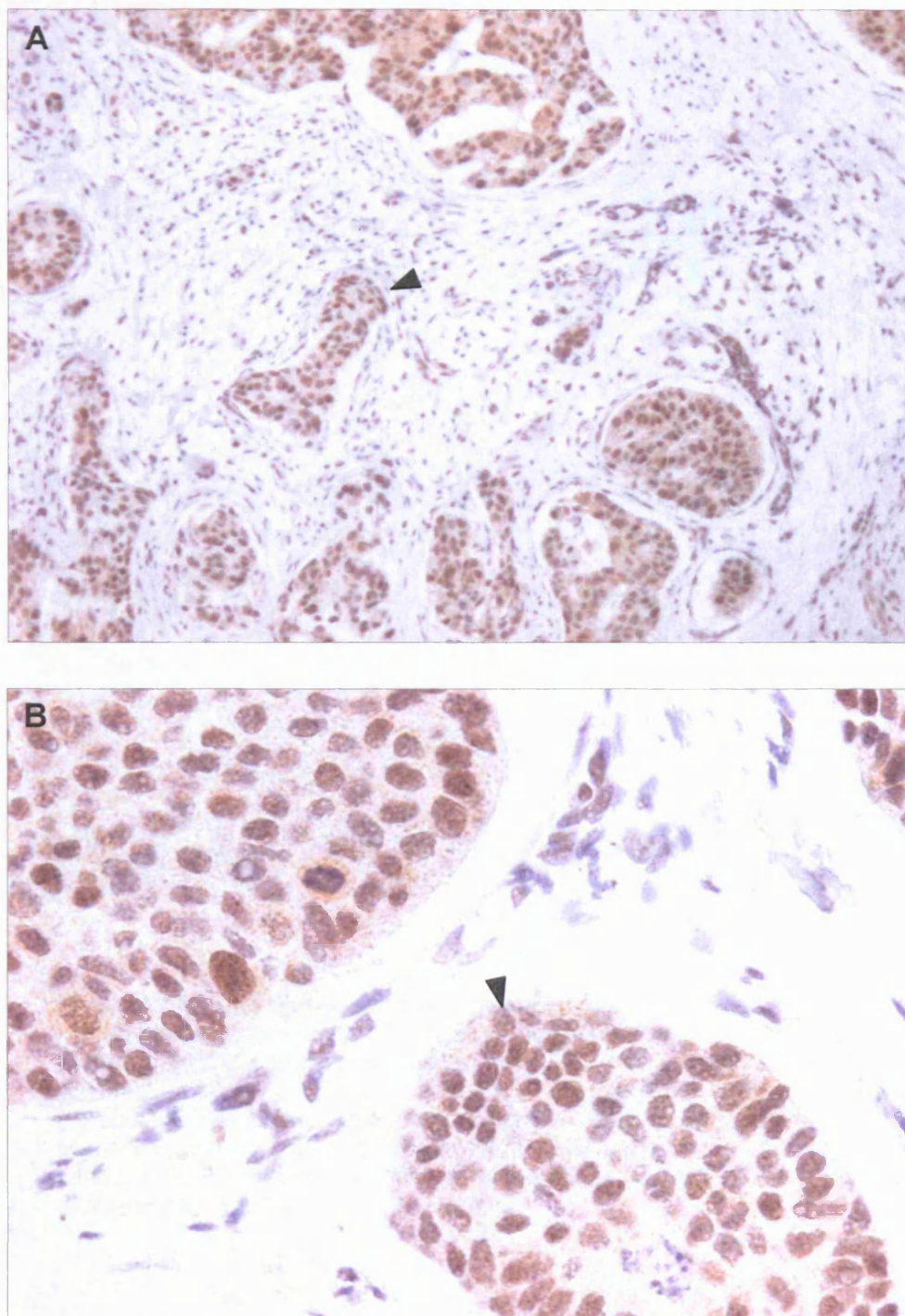


Figure 4.6 Nek2 is upregulated in invasive ductal carcinoma

Invasive ductal carcinoma (IDC) breast tumour sections were cut and stained with Zymed anti-peptide antibodies raised to Nek2 ($2\mu\text{g/ml}$) following antigen retrieval. Images taken at low (A) and high (B) magnification. Antibody staining reveals the marked upregulation of Nek2 in tumour cells.

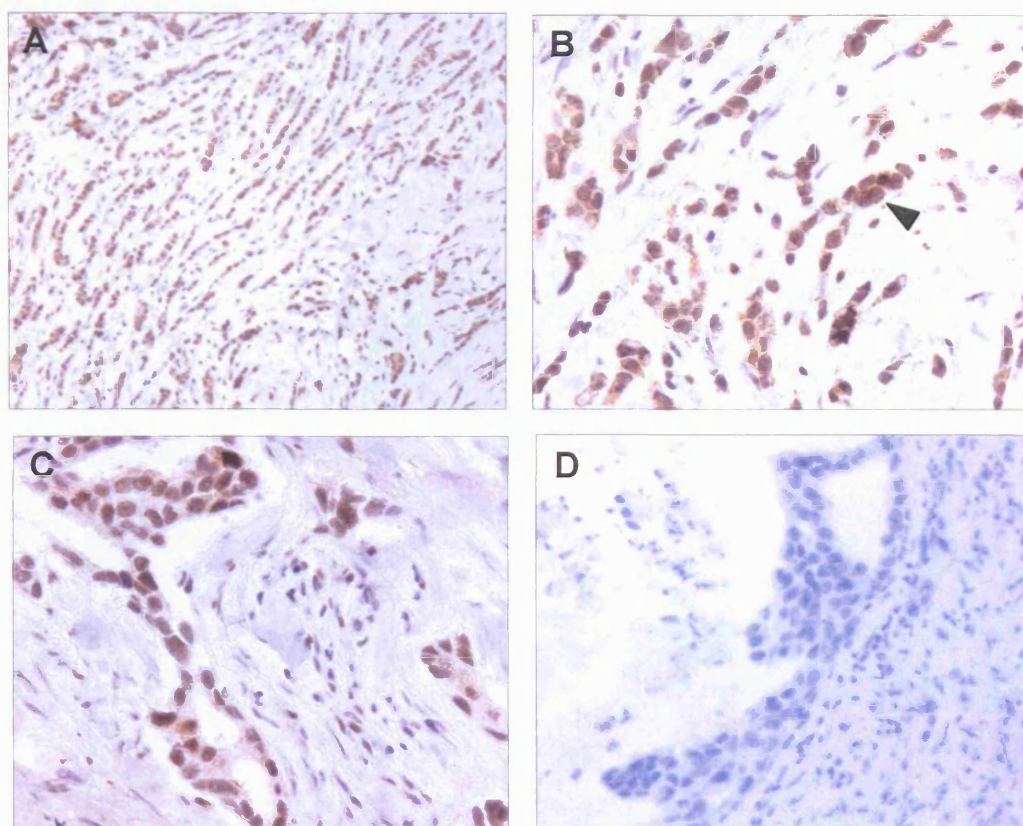


Figure 4.7 Nek2 is upregulated in invasive lobular carcinoma

Invasive lobular carcinoma (ILC) breast tumour sections were cut and stained with Zymed anti-peptide antibodies raised to Nek2 ($2 \mu\text{g/ml}$) following antigen retrieval.

A. Images taken at low and **B.** high magnification. The normal breast morphology has broken down with carcinoma cells dispersed throughout the tissue and antibody staining reveals the marked upregulation of Nek2 in these tumour cells. Tumour sections stained with Nek2 anti-peptide antibodies which **C.** express Nek2 at a high level or **D.** low level.

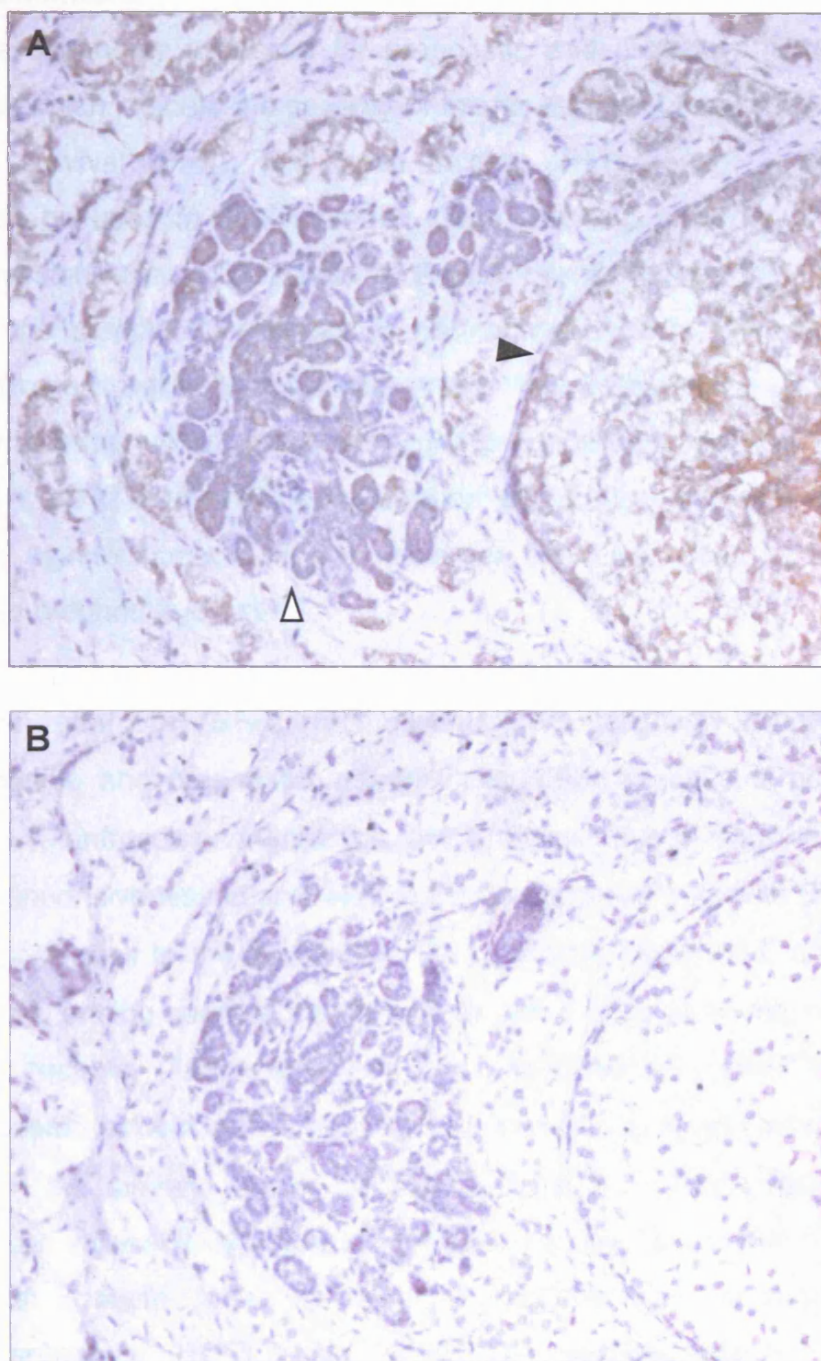


Figure 4.8 Elevated Nek2 expression in breast tumours identified with a second Nek2 antibody

A Sequential breast tumour sections stained with a second independent polyclonal antibody raised to Nek2 (R40 2 $\mu\text{g/ml}$) or **B** mock antibody (control IgG) following antigen retrieval. The specific staining pattern observed with the peptide antibody is reproduced. Carcinoma cells within an enlarged duct (**A**, solid arrow) stain strongly for Nek2 whilst adjacent normal tissue (**A**; open arrow) stains weakly.

4.2.6 Increased Nek2 staining does not correlate with known prognostic or proliferative markers

Tumours are commonly assessed for prognostic and predictive characteristics, that is factors which indicate the severity of the disease and hence likely period of disease-free survival (DFS), and those factors which govern response to a treatment can be used to direct therapy. The canonical scheme for assessing tumour aggression is an examination of the tumour section by light microscopy and scoring the sample for changes in nuclear morphology, differentiation and proportion of mitotic cells. Tumours are graded 1 to 3 depending on the sum of these characteristics, with 3 being the worst prognosis (Elston and Ellis, 1991; Galea et al., 1992). Immunohistochemistry of tumour sections is similarly employed to assess tumours at the molecular level and used to reveal both predictive and prognostic antigens.

The oestrogen receptor α (ER α) indicates a tumour's sensitivity to oestrogen and is both predictive and prognostic; patients with ER α negative tumours having reduced DFS (Cianfrocca and Goldstein, 2004). ER α status is most valuable as a predictor of responsiveness to anti-oestrogenic therapy. Patients with ER α positive tumours respond well to the competitive ER α inhibitor Tamoxifen, an oestrogen analogue, experiencing nearly a fifty percent reduction in disease recurrence. The progesterone receptor (PR) is also able to transactivate ER α and demonstrates that in the absence of strong ER α staining a hormone dependent pathway may still be present in the tumour. Ligand binding to Epidermal growth factor receptor (EGFR) induces signal transduction cascade such as the Ras-Raf and PI3 kinase pathways that activate genes necessary for proliferation, angiogenesis and inhibition of apoptosis. EGFR overexpression is associated with poor prognosis and resistance to radiotherapy and chemotherapy (Herbst, 2004). Tumours with a high fraction of proliferating cells have a greater chance of recurrent disease and the degree of proliferation can be determined by staining the section for the nuclear antigen Ki67, which is not expressed in senescent, G₀, cells (Esteva and Hortobagyi, 2004). I compared my staining data with the prognostic marker staining previously determined for these tumours by pathologists at the PICR. I

found no clear correlation between increased levels of Nek2 staining and the current panel of prognostic molecular markers in the tumour samples (Table 4.1).

4.2.7 Nek2 mutations in primary breast tumour samples and cultured tumour cell lines

Nek2 expression was found to be significantly elevated in primary human breast tumours. Whether due to a loss of transcriptional regulation, reduced degradation or gene amplification, protein levels of the kinase were markedly higher in carcinoma cells than adjacent normal tissue (Hayward et al., 2004). In parallel, we were moved to ask whether increased Nek2 kinase activity in disease could be achieved more subtly by activating mutations within the gene.

Activating mutations in serine/threonine kinases are well documented in human cancers. For example, an isoform of the mitogenic RAF kinase, B-raf, which carries somatic mutations in the kinase domain of the BRAF gene in 66% of malignant melanomas. The activating missense mutation, V599E, accounts for 80% of those mutations (Davies et al., 2002a). Similarly, somatic mutations in PIK3CA, a PI3 kinase catalytic subunit within the PI3 kinase signalling pathway, have been reported in 74 of 234 (32%) colorectal tumours studied with mutations also present in 25% and 27% of glioblastomas and gastric tumours examined, respectively. As with B-raf, these mutations were clustered, centred around two residues in the helical and kinase domains (Samuels et al., 2004). Expression of one of these mutations, H1047R, in cultured cells increased the lipid kinase activity above that observed with expressed wild-type kinase and has been shown to abrogate apoptosis and reduce growth factor dependence (Samuels et al., 2005).

Activating mutations also have been observed in the tyrosine kinases, including the receptor tyrosine kinase KIT (CD117) which harbours activating mutations in 88.2% of gastrointestinal tumours studied (Heinrich et al., 2003) and the human flt3 receptor where a duplication event within the FLT3 gene was present as a somatic mutation in 17% of cases of acute myelogenous leukaemia (AML) studied (Horiike et al., 1997; Nakao et al., 1996).

Patient	Nek2 (%)	ER (%)	PR (%)	EGFR (+/-)	Ki67 (%)	Tumour type	Grade
8225	No stain	97	12	-	21.9	IDC	1
8226	91.0	95	95	-	44.6	IDC	2
8401	88.3	0	0	-	35.8	ILC	NK
8403	86.8	33	0	-	58.4	IDC	3
2243	90.2	78	2	-	41.7	IDC	NK
2304	72.9	95	49	-	39.3	IDC	3
2575	No stain	0	0	++	30.3	IDC	3
3000	98.0	98	37	-	16	IDC	3
2282.1	92.9	0	0	++++	52	IDC	3
2196	93.9	70	24	-	6.9	IDC	3
2210	91.6	91	8	-	9.8	IDC	3
2585	81.6	0	0	+	46.7	IDC	3
2262.2	93.7	97	98	-	18.9	ILC	3
6238	No Stain	20	30	+	7.4	IDC	3
1223.2	76.0	90	15	-	37.6	IDC	3
7911	No stain	0	0	-	88.1	IDC	3
1570.2	83.0	0	0	-	34.8	IDC	3
7956	94.5	0	0	-	70.3	IDC	3
7916	75.2	80	8	-	69.9	IDC	3
1955	97.7	3	0	-	51.1	IDC	3

Table 4.1 Nek2 staining does not correlate with known prognostic or proliferative markers

The table indicates the percentage of cells (n>1000) exhibiting elevated levels of Nek2 expression in 20 breast tumour samples and compares this to expression levels of ER α , PR, EGFR and Ki67. Random fields of tumour sections were selected and the number of cells overexpressing Nek2 within the tumour tissue scored. The expression levels of ER α , PR, EGFR, Ki67, tumour type and grade, where known, were previously determined by pathology staff at the Paterson Institute for Cancer Research (Manchester, UK)

Determining whether Nek2 harbours activating mutations would prove interesting, firstly, because if a mutation confers kinase hyperactivity then screening for that mutation may be prognostic and, secondly, because a mutation within the kinase that is synonymous with tumour cells would provide an extremely attractive therapeutic window, amenable to specific therapy by small molecule inhibitors tailored to bind solely the disease-associated kinase (Baselga and Arribas, 2004).

To examine the status of the NEK2 gene in human disease I obtained frozen primary breast tumours samples from the CRUK Paterson institute (Manchester, UK) ground the tissue under liquid nitrogen and purified genomic DNA using Qia-Amp spin columns (Qiagen, UK) The samples comprised frozen tumour shards from ten patients who had previously been diagnosed with breast cancer and encompassed cases of both ductal and lobular carcinoma. Genomic DNA extracted in Leicester was transferred to the CRUK Mutation Detection Facility, St. James Hospital, Leeds. Researchers at the CRUK Mutation Detection Facility screened the Genomic DNA extracted at Leicester alongside genomic DNA from ten breast tumour derived cell lines already held there: MCF7, MDA-MB-415, MDA-MB-361, MDA-MB-468, MDA-435, BT20, SKBR3, T47D, MDA-MB-231 and ZR75.

In each of the twenty tumour and cell line samples the eight exons which comprise *HsNEK2* (Hames and Fry, 2002) were first screened by polymerase chain reaction-single strand conformational polymorphism (PCR-SSCP) analysis. This identified polymorphisms in three exons and one intron which were further investigated by DNA sequencing. The mutations detected in exons 3 and 8 were both silent whereas the adenine to guanine transposition in exon 7 at position 1061 encodes a missense mutation, substituting a serine residue for the asparagine at residue 354 (Figure 4.9A). Interestingly, the N354S mutation was restricted to the breast tumour samples, found in 3 of the 10 tumours analysed. Staff at the Paterson Institute had previously determined the degree of ER, PR, Ki67, EGFR and ErbB2 immunostaining for the breast tumours subjected to PCR-SSCP and sequence analysis. No association between the N354S mutation and these current prognostic markers was evident (Table 4.2).

A

cDNA Reference	Protein Reference	Position	Predicted Effect	Frequency (n=20)
c.504 T>C	p.H168H	Exon 3 codon 168	Silent Variation	13 samples
intronic	intronic	IVS 5 + 14 G>T	none predicted	2 samples
c.1061 A>G	p.N354S	Exon 7 codon 76	Asparagine(N) > Serine(S)	3 samples
c.1317 A>G	p.R439R	Exon 8 codon 206	Silent variation	6 samples

B

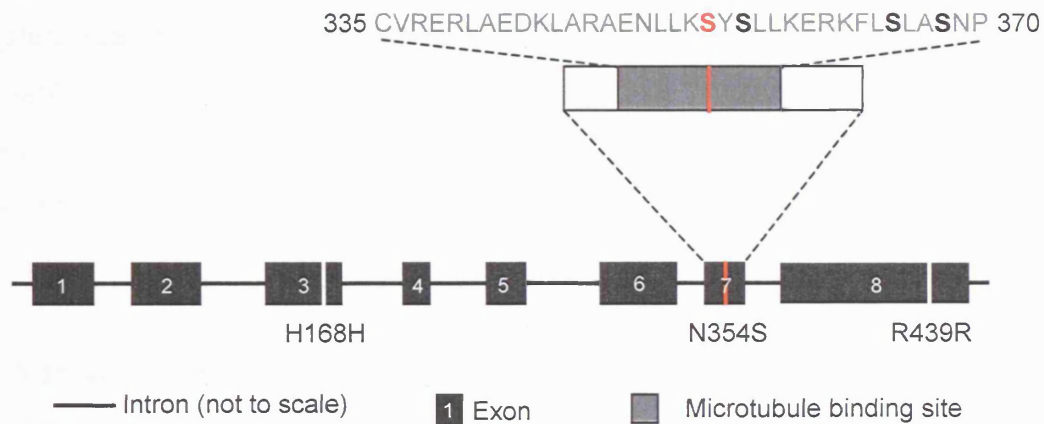


Figure 4.9 Nek2 mutations in primary breast tumours and cancer cell lines

A. Genomic DNA was extracted from 10 FFPE archival breast tumours and 10 breast cancer derived cell lines. Mutations in the Nek2 gene were profiled by SSCP and confirmed by sequencing. Mutations in exons 3, 7 and 8 and intron 5 were identified. The mutations in exons 3 and 8 are silent whereas that identified in exon 7 results in the substitution of asparagine at residue 354 for serine. **B.** The silent mutations in exons 3 and 7 are indicated by white bars within the exons. The position of the residue is indicated below the exon. The mutation in exon 7 lies in a region of Nek2 known to be necessary for microtubule binding and centrosomal localisation, shaded grey in the expanded exon. The amino acid sequence of the microtubule binding region is shown above the exon. The existing serine residues are shown in bold and the novel residue found in three breast tumour samples is shown in red. Mutation analysis was performed at the CRUK mutation detection facility, St. James hospital, Leeds.

Patient	ER (%)	PR (%)	Ki67 (%)	EGFR (-/+)	Exon 7 Mutation
2737	95	0	31.3	-	None
2785	0	0	12.8	-	N354S
2799	0	0	25.2	-	N354S
2819	90	13	38.6	-	None
2914	94	89	13.1	-	None
3206	0	0	52.9	-	None
3227	0	0	33.3	+ / ++	None
3420	80	25	15	-	None
3076	21	61	28.3	-	None
3509	1	0	33.5	+	N354S

Table 4.2 The N354S transposition identified in several breast tumour samples does not correlate with known prognostic markers

The table compares the presence of the N354S transposition in exon 7 to expression levels of ER, PR, EGFR and Ki67 previously determined by staff at the Paterson institute, Manchester, UK.

The N354S mutation was located within a region defined as necessary for centrosomal localization, residues 335–370 (Hames et al., 2005) (Figure 4.9B). There is an existing serine at position 356 and this residue has been identified by tryptic digest and mass spectroscopy of a bacterially expressed kinase as being autophosphorylated (Rellos et al., 2006). The introduction of a serine residue was of interest as Nek2 is a serine/threonine kinase which has been suggested to use dimerisation and autophosphorylation as a mechanism for regulating its activity (Fry et al., 1999). The possibility therefore existed that phosphorylation of the novel serine could affect either Nek2 microtubule binding and hence centrosome localization or kinase activity as a whole.

To assess the effects of the N354S mutation in cultured cells, plasmids encoding myc-Nek2A:N354S and myc-Nek2A:K37R, N354S were constructed and

transfected into U2OS cells which were then fixed and processed for immunofluorescence microscopy. To determine localization of the exogenous myc-Nek2 protein cells were stained with antibodies raised against the centrosomal marker γ -tubulin and the myc epitope. myc-Nek2A:N354S was still able to localize to the centrosome, colocalising with γ -tubulin in interphase cells in an identical manner to myc-Nek2A (Figure 4.10 A-F).

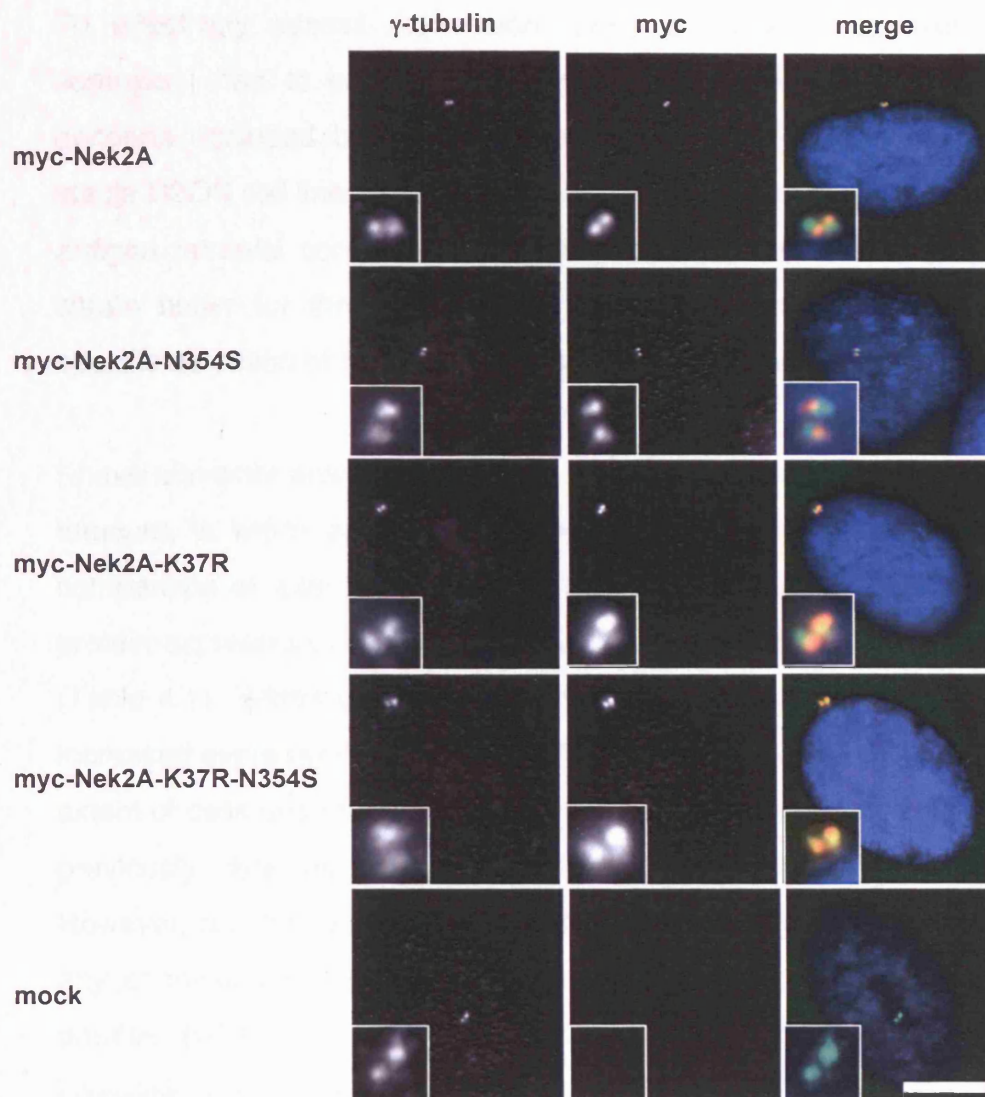


Figure 4.10 The N354S transposition does not affect the centrosomal localisation of Nek2A

U2OS cells were transfected with myc-Nek2A, myc-Nek2A-N354S and the inactive myc-Nek2A-K37R and myc-Nek2A-K37R-N354S constructs and cultured for 24 hours before being fixed in ice cold methanol and processed for immunofluorescence microscopy. Fixed cells were stained with antibodies against the *myc* epitope to detect exogenous Nek2A and γ -tubulin to discriminate centrosomes (shown in red and green, respectively, in the merged images). The myc-Nek2A-N354S and myc-Nek2A-K37R-N354S fusion proteins are able to localise to the centrosome in the same manner as myc-Nek2A and myc-Nek2A-K37R. Centrosomes are shown magnified, inset. Scale bar 5 μ m.

4.3 DISCUSSION

To effectively assess expression levels of Nek2 in archived human tumour samples I had to employ an antigen retrieval procedure to restore the Nek2 epitopes occluded by paraformaldehyde fixation (Shi et al., 1997). Employing stable U2OS cell lines that inducibly overexpress Nek2A I was able to optimise the antigen retrieval conditions. Incubating the archived tumour sections in 10 mM citrate buffer for three minutes at high temperature and pressure allowed the specific detection of Nek2 with minimal background staining.

I have currently analysed 20 breast tumour samples, including DCIS, IDC and ILC tumours, in which areas of both tumour and normal tissue could be detected for comparison of expression levels. 16 (80%) exhibited significantly elevated Nek2 protein expression, whereas 4 (20%) gave no more staining than the normal tissue (Table 4.1). Within those tumours that showed elevated Nek2 expression, all had increased expression in more than 70% of tumour cells ($n > 1000$). We compared the extent of cells overexpressing Nek2 in these breast cancers with data that had been previously obtained on oestrogen, progesterone and EGF receptor expression. However, no obvious correlation was apparent between the expression of Nek2 and any of these markers. For example, of the 16 tumours that were strongly Nek2 positive ($>70\%$), 9 were ER α positive ($>70\%$) whereas 7 were ER α negative. Likewise, some tumours that were Nek2 positive were PR and EGFR positive whereas others were PR and EGFR negative. Clearly, though, my current sample size is too small to draw any strong conclusion about the correlative expression of these markers. Finally, no correlation was detected between expression of Nek2 and Ki67, a marker for cell proliferation. Whilst one might predict that cells expressing Nek2 would be proliferating, we note that there was no obvious correlation either between expression of proliferation markers (Ki67 or PCNA) and the overexpression of the other mitotic kinases, Plk1 and Aurora-A (Knecht et al., 2000; Kneisel et al., 2002; Takahashi et al., 2000; Takai et al., 2001c)

The mechanisms leading to increased Nek2 protein levels in primary tumours are likely to be similar to those suggested for tumour derived cell lines in chapter 3, essentially perturbation of transcriptional regulation, reduced proteolysis or gene

amplification. In addition to increased expression, I considered whether an increase in net Nek2 kinase activity could be achieved more subtly, by activating mutations within the kinase. Genomic DNA was extracted from 10 tumour derived cell lines and 10 primary breast tumours. Mutations were identified by SSCP and confirmed by single strand DNA sequencing. Six of the samples, two breast tumours and four cell lines, contained no mutations as compared to the genomic reference sequence (Genbank AC096637.1). The remaining 14 samples contained a mixture of synonymous and non-synonymous mutations with silent changes detected in codon 168 of exon three and codon 206 of eight as well as a silent variation located within intron seven. None of these three nucleotide changes produce a concomitant change in the encoded protein. The effect of these mutations on Nek2 pre-mRNA splicing has not been quantified experimentally but software analysis of the variations in exons three and eight suggest that a splicing pattern different from that of the wild-type gene may result (C. Taylor, personal communication).

The heterozygous adenine to guanine mutation identified at genomic sequence position 160537 results in a non-synonymous change of amino acid 354, substituting a serine residue for the asparagine present in the reference sequence. This mutation, which lies in the c-terminal non-catalytic domain, was of interest for two reasons. Firstly, the activity of Nek2 is regulated in part by phosphorylation and dephosphorylation and so the novel serine residue could act as a substrate for regulatory phosphorylation. Secondly, the transposition lies within a region defined as being necessary for localisation of Nek2 to the centrosome.

The cell cycle regulation of serine/threonine kinase activity by phosphorylation is well established, most notably for the canonical cyclin dependent kinases (Cdks). Phosphorylation of Cdk1 by the kinase wee1 inhibits Cdk1 activity, until dephosphorylation by cdc25 activates the kinase to facilitate mitotic entry. A similar mechanism extends to other Cdk/cyclin complexes (for review (Nakao et al., 1996)). In an opposite manner, Nek2A is believed to be activated by autophosphorylation *in vitro* and inactivated by the phosphatase PP1c (Fry et al., 1999; Helps et al., 2000). The N354S mutation may allow an extra phosphorylation event that affects Nek2 activity, either positively or negatively. The activity of a given Nek2 mutation can be

assessed in cultured cells by measuring the induction of a phenotype observed in several cell types upon overexpression: premature centrosome disjunction (Faragher and Fry, 2003).

To determine whether the N354S mutation activates Nek2 the kinase could be immunoprecipitated from transfected cells and used to phosphorylate a control substrate *in vitro*. This approach has previously identified activating Nek2 mutations (Rellos et al., 2006). Examination of the immunofluorescence data also shows that the N354S change does not disrupt localisation of Nek2A to the centrosome, despite being located in a region necessary for microtubule binding and centrosomal localisation. The N354S mutation identified in three breast tumour patients has no marked effect on Nek2A subcellular localisation in one cultured cell type. However, this does not assess more subtle and perhaps equally important effects, such as the avidity and specificity of Nek2A binding to known substrates. The N354S transposition could also initiate novel interactions that could perhaps be beneficial to the initiation or maintenance of a tumour. The most pressing investigation is to determine whether the a160537g mutation underlying the N354S transposition is actually a polymorphism. To test this, genomic DNA should be extracted from matched normal tissue from the three breast cancer patients with the mutation to determine whether it is restricted to the tumour tissue. The polymorphism is listed in a database of known polymorphisms, the dbSNP, and this suggests it may simply be a naturally occurring variation within the population.

Unfortunately, the patients that have had tumours assessed for Nek2 protein expression by immunohistochemistry are distinct from those that have been screened for mutations in the NEK2 gene. The formaldehyde fixation commonly used to preserve archived samples for immunohistochemistry makes extraction of intact genomic DNA more difficult. Assuming that the N354S mutation is somatic it would be of interest to determine whether it correlates with Nek2 protein upregulation. In common with Nek2 upregulation, the N354S mutation does not correlate with tumour grade, histopathological type or existing prognostic markers (Table 4.2).

Nek2 is upregulated in human breast tumours and so consideration should now be given to how an increase in Nek2 kinase activity could contribute to tumour initiation or progression. It is well established that centrosome abnormalities, both structural and numerical, are strongly associated with chromosomal instability and aneuploidy and have also been linked with a poor prognosis in human cancer (Al-Romaih et al., 2003; D'Assoro et al., 2002; Kramer et al., 2003; Lingle et al., 2002; Lingle and Salisbury, 1999; Pihan et al., 2001; Sato et al., 2001). Increased levels of Nek2 in cultured human cells have been shown to affect spindle polarity, ploidy and centrosome number and upregulated Nek2 in fungal, insect and protozoan systems induced centrosome fragmentation and likely cytokinesis failures.

The impact of increased levels of Nek2 in human tumours is most likely to be manifested by disrupting bipolar spindle formation to induce multipolar spindles and aneuploidy. Upregulation of Nek2 has been shown to affect both centrosome structure and number in cultured cells and additionally may prevent cells with multiple centrosomes clustering them to produce bipolar spindles, all mechanisms likely to increase the incidence of multipolar mitoses (Figure 4.11). Overexpression of myc-*hsNek2A* in human U2OS cells affected centrosome structure, causing dispersal of centrosomes and microtubule nucleation from multiple sites (Fry et al., 1998c). This pattern of additional microtubule nucleation sites upon Nek2 overexpression is mirrored in the fungi *Dictyostelium discoideum* whereby *DdNek2* induces multiple aster formation (Graf, 2002). Transfection of the *Drosophila melanogaster* homologue of Nek2, *dmNek2*, into S2 insect cells and a subsequent 3-4 fold elevation of *DmNek2* protein levels induced multiple spindle poles and fragmented centrosomes in mitosis at 3 times the rate of control cells (Prigent et al., 2005). Distinct from the loss of centrosome structural integrity induced by excess Nek2, there is also evidence that a failure of cytokinesis associated with increased levels of the Nek2 homologues, *DmNek2* and *TbNRKC*, results in tetraploid cells with multiple centrosomes or basal bodies in *D. melanogaster* and *T. brucei*, respectively (Prigent et al., 2005) (Pradel et al., 2006).

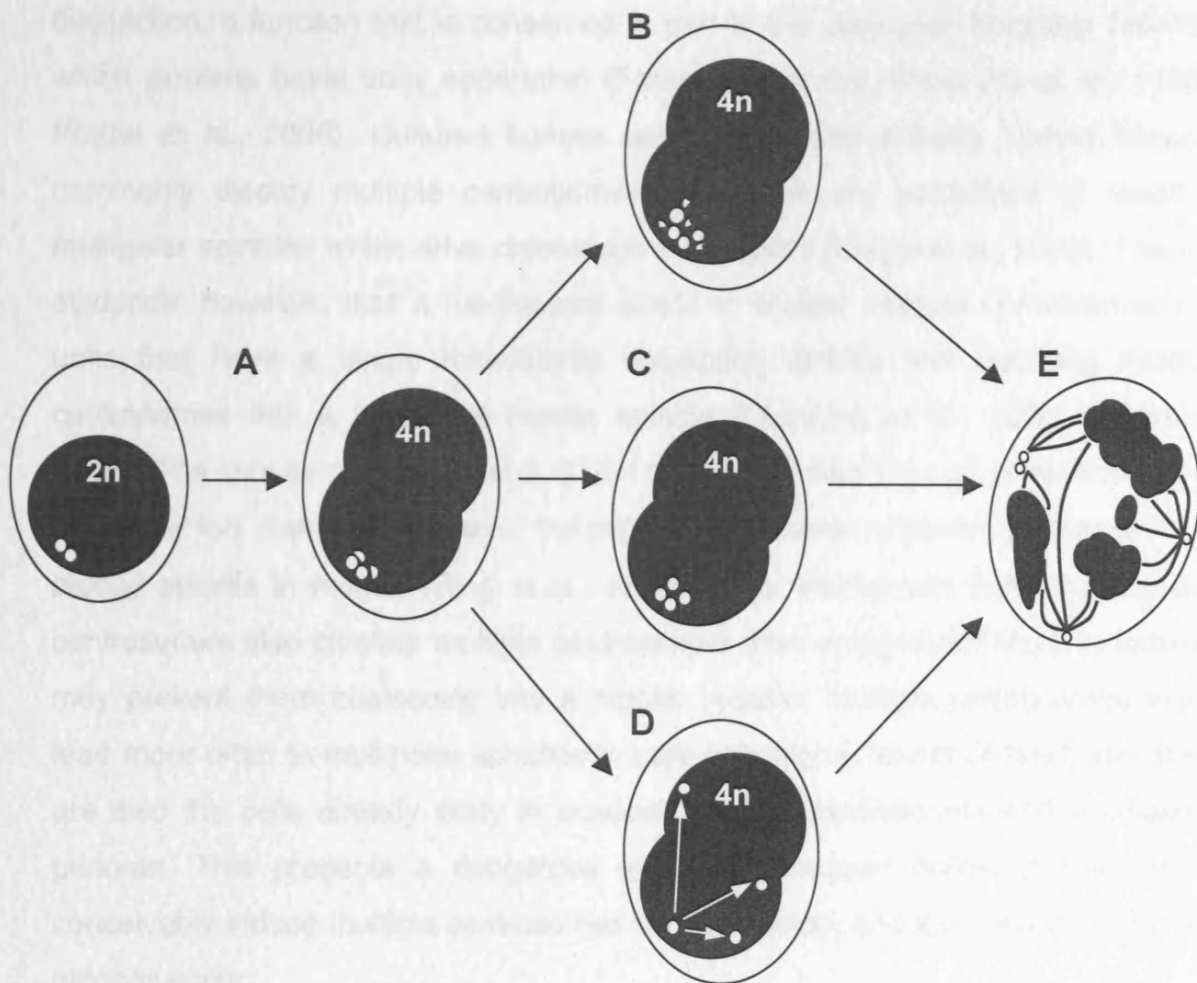


Figure 4.11 Nek2 may promote aneuploidy by alternative pathways

A. Increased levels of Nek2 in cultured cells and model insect systems promotes an increase in ploidy, most likely through a failure in cell division **C**. The resulting cells have a polyploid genome and multiple centrosomes. **B.** Furthermore, upregulated Nek2 has been shown to fragment centrosomes or, **D**, prevent the clustering of multiple centrosomes into a bipolar spindle. **E.** Increased levels of Nek2 in human tumours may act synergistically to induce polyploidy and ensure that the polyploid genome undergoes a multipolar mitosis, leading to aneuploid daughter cells.

The most well characterised phenotype of Nek2A activity in cultured cells is the rearrangement of the molecular tether joining centrosomes to allow centrosome disjunction, a function that is conserved in part in the protozoan homolog *TbNRKC* which governs basal body separation (Faragher and Fry, 2003; Fry et al., 1998c; Pradel et al., 2006). Cultured human cancer cells and primary human tumours commonly display multiple centrosomes and these are postulated to result in multipolar spindles which drive chromosome instability (Lingle et al., 2002). There is evidence, however, that a mechanism exists to cluster multiple centrosomes into units that have a single microtubule nucleating activity and resolving multiple centrosomes into a functional bipolar spindle (Quintyne et al., 2005; Saunders, 2005). The mouse neuroblastoma N1E-115 cell line has tens of centrosomes, as judged by foci staining positive for the centrosomal marker γ -tubulin, yet constructs a bipolar spindle in mitosis (Ring et al., 1982). If the mechanism that tethers paired centrosomes also clusters multiple centrosomes then upregulated Nek2 in tumours may prevent them coalescing into a bipolar spindle. Multiple centrosomes would lead more often to multipolar spindles in cells with higher levels of Nek2 and these are also the cells already likely to possess multiple centrosomes and a tetraploid genome. This presents a dangerous synergy, increased levels of Nek2 could conceivably induce multiple centrosomes and polyploidy, and then ensure multipolar mitoses occur.

The presence of a polyploid genome segregated by supernumerary MTOCs induced by elevated Nek2, whether composed of fragmented or whole centrosomes, would be a significant mechanism for the genomic plasticity and resulting aneuploidy which characterise human tumours.

CHAPTER 5

NEK2 DEPLETION AFFECTS THE GROWTH AND VIABILITY OF CULTURED CELLS

5.1 INTRODUCTION

Examination of the function of Nek2A in the cell cycle has been elucidated in part by the use of stable cell lines which inducibly overexpress an inactive point mutant, Nek2A-K37R, fused to either the *myc* epitope or GFP fluorophore to allow discrimination of exogenous from native protein. The presence of inactive Nek2A kinase was demonstrated to interfere with bipolar spindle formation, chromosome segregation and cytokinesis. Induction of kinase-dead Nek2A resulted in a four-fold increase in abnormal spindles after 24 hours and, after 72 hours, a two-fold increase in multinucleation (Faragher and Fry, 2003). The overexpression of inactive Nek2A is suspected to act in a dominant-negative manner, disrupting the function of the remaining endogenous, active protein with the observed phenotypes due to an overall reduction or impairment of kinase activity. The presence of exogenous inactive protein may also have effects unrelated to loss of Nek2A activity as the inactive but intact protein is able to titrate binding partners such as PP1c, the APC/C and PCM1 (Hames et al., 2005; Hayes et al., 2006; Helps et al., 2000).

An alternative method for studying the function of a protein in model systems, which avoids some of the artefactual effects associated with dominant-negative mutants, is to remove the endogenous protein rather than interfering with it. Though genetic deletions are straightforward in model eukaryotes such as yeast, loss-of-gene function in higher eukaryotes are more laborious, relying on the generation of gene “knockouts” by recombination and targeting of a specific allele. This approach is time consuming and expensive. More recently, techniques have been developed which allow the rapid removal of gene products in a range of cultured human and animal cells as well as complete organisms by targeting the transcribed RNA, a method termed RNA interference (RNAi). Initially employed in cultured mouse fibroblast cells, it was found that thymidine kinase activity could be persistently reduced by transfection of a cassette carrying the thymidine kinase gene coding sequence cloned in the reverse orientation. The transcribed nonsense DNA strand interfered with the endogenous messenger RNA (mRNA) (Izant and Weintraub, 1984). The technique was extended to other organisms and in doing so a refinement of the properties necessary to suppress a specific gene

occurred. RNAi experiments in the model nematode, *Caenorhabditis elegans*, determined that a duplex of RNA is more effective than antisense RNA alone. In addition, transfection of *C. elegans* suggested that an amplifying mechanism underpinned the mRNA suppression, with a few molecules of duplex effectively ablating an excess of transcript, rather than simple stoichiometric interference (Fire et al., 1998). The dsRNA-mediated suppression of endogenous transcripts proved to be equally effective in cultured human cells. Shorter sequences (siRNAs) were more potent still, with 21 nucleotide duplexes reducing expression of endogenous Lamin A/C protein in HeLa cells by 90% and similar results obtained in CHO and HEK293 cells (Elbashir et al., 2001). The efficacy of shorter duplexes also avoided activation of the interferon response. This is a sequence independent effect that globally represses translation due to dsRNA greater than 30 nucleotides binding and activating protein kinase PKR in the cytoplasm (Manche et al., 1992). The same dsRNA-mediated suppression of a target gene can also be achieved by transfecting constructs expressing small hairpin RNA (shRNA) transcribed RNA polymerase III which are processed intracellularly to siRNAs (Figure 5.1) (Brummelkamp et al., 2002).

The application of RNAi to commonly cultured mammalian cell lines greatly simplifies the reagents required for studies of gene function, sidestepping the need for generation of recombinant knockout animal strains or immunisation of animals to produce specific antisera for microinjection studies. Suppressing duplexes can be chemically synthesized to any gene for which the coding sequence is known. This ready availability of gene specific reagent aids target validation. RNAi mediated depletion of Nek2 in cultured cells is being undertaken in parallel with an HTS to identify small molecule inhibitors of Nek2A. The phenotypes of cells treated with Nek2 siRNAs can be used to determine the likely consequences of treating cells with small molecule inhibitors of Nek2. Expression levels of Nek2 have been shown to be increased in a variety of human cancers. Though a causal role for Nek2 in human cancer has not yet been shown, a therapeutic Nek2 inhibitor would likely be used to treat the subset of tumours that overexpress Nek2.

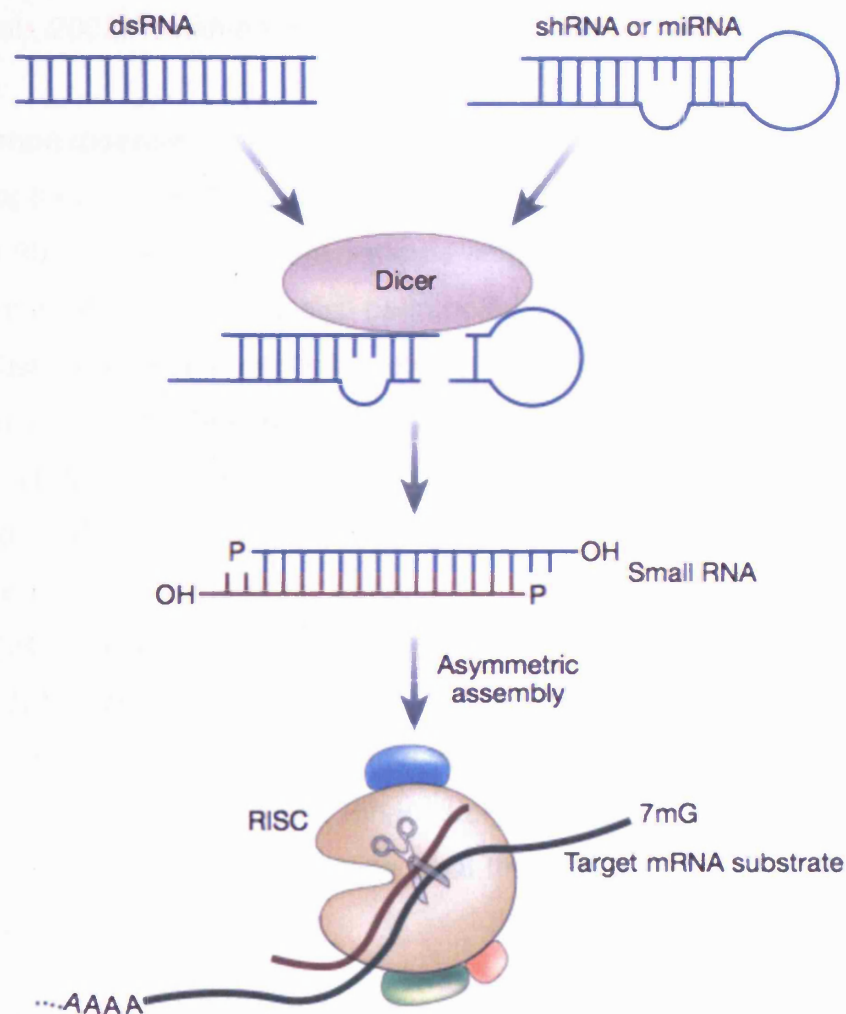


Figure 5.1 The mechanism of RNA interference in mammalian cells

Exogenous long double stranded RNA (dsRNA) or small hairpin RNA (shRNA) are processed into siRNA by the enzyme Dicer before incorporation into the RNA induced silencing complex (RISC) which targets mRNA, guided by the sequence of the siRNA antisense strand (shown in brown). Though the complementary strand (blue) is described as non-targeting, the symmetry of the two strands means it can be incorporated in the RISC and induce off-target silencing. Adapted from Hannon, G.J. and Rossi J.J., 2004.

Cancer is a hyperproliferative disease, unrestrained cell growth results in new tissue, a tumour. Ideally, depleting Nek2 in cultured cells should result in a phenotype desirable for treating malignancies; an anti-proliferative or pro-apoptotic effect (Aherne et al., 2002; Workman, 2001).

5.1.1 Nek2 in human disease

As shown in chapters 3 and 4, Nek2 is upregulated in human cancer, being overexpressed in 80% of primary breast tumours studied (Hayward et al., 2004). Increased levels of NEK2 mRNA have also been noted in paediatric osteosarcoma and a form of diffuse large B-cell lymphoma refractory to chemotherapy (de Vos et al., 2003a; Wai et al., 2002). Genomic amplifications of the Nek2 locus, 1q32.1-3 (Hames and Fry, 2002) have been detected in breast tumours and though they have yet to be correlated with increased Nek2 protein expression would provide the underlying mechanism for the gross upregulation observed in breast tumours (Loo et al., 2004; Weiss et al., 2004). Transfection of myc-Nek2A into untransformed HBL100 breast epithelial cells also recapitulated some aspects of malignancy, including supernumerary centrosomes and changes in ploidy (Hayward et al., 2004; Lingle et al., 1998; Pihan et al., 2003a). With a tentative role in human disease, I then sought to determine what the effects of ablating Nek2 in cultured cells would be.

5.1.2 Depletion of Nek2 in cultured cells

Reports of Nek2 depletion and the ensuing phenotypes in the literature are sparse. Depletion of the Nek2A homologue *TbNRKC*, with a 640bp hairpin RNA, inhibited basal body separation but not cell viability in the protozoa *T. brucei* (Pradel et al., 2006). This is analogous to the impaired centrosome separation observed in cultured human cells expressing inactive Nek2 (Faragher and Fry, 2003). Reduction of the *D. melanogaster* Nek2 homologue, *DmNek2*, in S2 cells by dsRNA resulted in spindle defects and centrosome fragmentation, correlating with the role of *hsNek2* as a core structural component of the centrosome (Fry, 2002; Fry et al., 2000; Prigent et al., 2005; Uto and Sagata, 2000). Nek2 has also been tentatively implicated in regulating chromosome segregation by interaction with the spindle checkpoint components, Mad1 and Hec1, and suppression of embryonic

M. musculus Nek2A indeed induced segregation defects (Lou et al., 2004b; Martin-Lluesma et al., 2002; Sonn et al., 2004).

Depletion of Nek2 in the cervical carcinoma HeLa cell line identified diverging roles for Nek2A and Nek2B. Depletion of Nek2A interfered with centrosome separation, while depletion of Nek2B impaired mitotic exit (Fletcher et al., 2005). Transfection of HeLa cells with siRNA that depleted both Nek2A and Nek2B simultaneously induced growth arrest and apoptosis. Growth inhibition of HeLa cells was observed immediately following siRNA treatment and persisted for at least five days. The rate of apoptosis was also greatest at five days after treatment, occurring in 20% of cells (Fletcher et al., 2004). Employing a pool of siRNA duplexes directed against Nek2, we examined whether growth restriction and apoptosis extended to other cell lines.

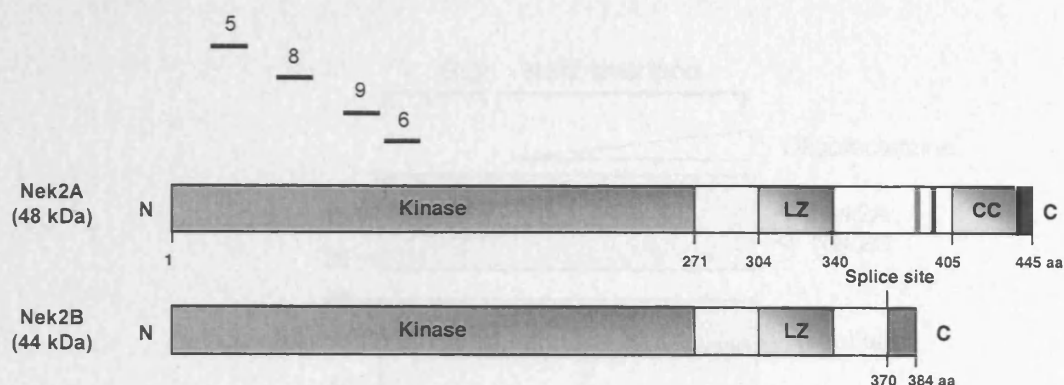
5.2 RESULTS

5.2.1 Depletion of Nek2 in cultured cells by siRNA

To effectively deplete Nek2 in cultured cells I obtained four pooled oligoribonucleotides from a commercial supplier (Dharmacon, CO, USA). The pool, termed a “smartpool” by the manufacturer, comprised four 21 nucleotide duplexes; 19 paired bases with a 2 nucleotide 3' overhang. All the duplexes targeted the 5' end of the mRNA before the alternative splice site at which Nek2A and Nek2B diverge (Figure 5.2 A) (Hames and Fry, 2002). Each duplex in the pool was expected to suppress both Nek2A and Nek2B as a result. Two negative control duplexes were employed, GL2 directed against *P. pyralis* firefly luciferase and Lamin A/C directed against the respective nuclear lamins (Figure 5.2 B). The GL2 duplex is non-targeting, diverging from predicted human mRNA sequences by at least four nucleotides. Lamin A/C effectively depletes nuclear lamins A and C, two isoforms of the same abundant lamin gene, and this depletion is not reported to result in any noticeable phenotype (Elbashir et al., 2001).

The duplexes were transfected into cultured HeLa and U2OS cells by supplementation of the growth media in the presence of a lipid carrier, oligofectamine (Invitrogen, Paisley, UK) and the degree of suppression measured by western blotting. Though RNAi acts upon mRNA the goal is destruction of the mature protein as this is the effector within the cell and hence the endpoint I chose to measure. Nek2 is known to have a short intracellular half-life and so destruction of the mRNA was predicted to lead to a rapid loss of Nek2 protein (Hames et al., 2001). To optimise the suppression of Nek2, I varied the ration of duplex:oligofectamine carrier. 125 pmols of smartpool duplexes (equimolar amounts of each of the four duplexes directed against Nek2) were mixed with increasing amounts of oligofectamine transfection reagent, 0.25 μ l, 0.5 μ l, 1 μ l and 2 μ l then added to sub-confluent HeLa or U2OS cells for twenty four hours. In each case the final concentration of duplex in the growth media was 50 nM. Total cell lysates were collected, resolved by SDS-PAGE, Western blotted and levels of Nek2 expression assayed by probing with an anti-Nek2 monoclonal antibody (BD Clontech). Nek2 expression was dramatically reduced in both HeLa (Figure 5.3, A)

A



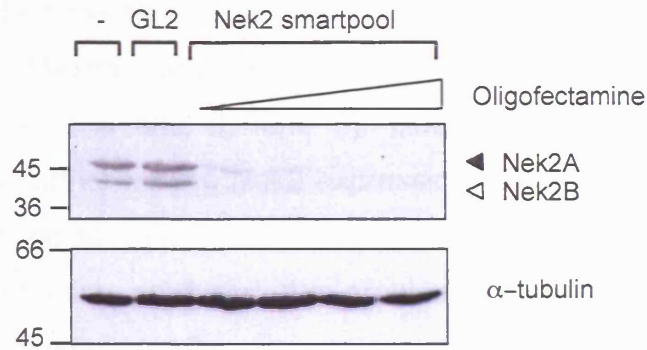
B

siGenome duplex 5	¹⁰⁷ GGAAAGAACTTGACTATGG
siGenome duplex 8	¹⁹⁵ AAACATCGTTCGTTACTAT
siGenome duplex 9	²⁷⁶ GGATCTGGCTAGTGTAAAT
siGenome duplex 6	³¹¹ GAAAGGCAATACTTAGATG
Control duplex GL2	CGTACGCGGAATACTTCGA <i>Photinus pyralis</i> luciferase (U47296)
siGenome Lamin A/C	⁶⁰⁸ AACTGGACTTCCAGAAGAACA

Figure 5.2 siRNA duplexes directed against Nek2

A. Four separate duplexes directed against Nek2 were obtained, all targeted to the region encoding the N-terminal kinase domain and hence effective against both Nek2A and Nek2B. **B.** The sequences of the sense strands of the oligonucleotide duplexes complementary to Nek2. The superscript denotes the corresponding position of the duplex within the cDNA with respect to the adenine of the first translated methionine. The sequences of the control duplex homologous to lamin A/C and the non-targeting control duplex GL2 are shown. Directed against firefly luciferase, GL2 has a minimum of four mismatches against known *H. sapiens* genes. The accession number is shown in brackets.

A



B

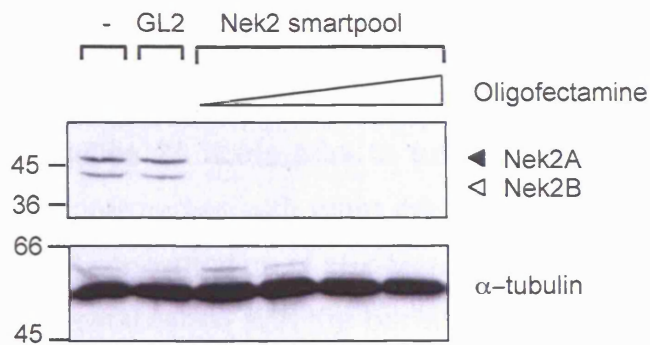


Figure 5.3 Smartpool oligoribonucleotides effectively depletes Nek2 in cultured cells

A. HeLa and **B.** U2OS cells were seeded in tissue culture dishes at a density of 1×10^4 cells/cm² twenty four hours before treatment with the non-targeting control duplex GL2 or pooled Nek2 duplexes at a final concentration of 50 nM. Twenty four hours after RNAi treatment cells were lysed in NEB buffer. Cell lysates were resolved by SDS-PAGE, Western blotted with an anti-Nek2 monoclonal antibody (BD Clontech) and visualised by ECL plus (Amersham). Membranes were stripped and reprobed with a rabbit anti-α-tubulin antibody (Sigma) to demonstrate uniform loading of protein in each well and that no general inhibition of translation had occurred. Untreated cells (-) are shown for comparison

and U2OS (Figure 5.3, B) cells treated with the pool of Nek2 duplexes when compared to the untreated cells (5.3 A and B, lanes 3 and 1, respectively). Transfection with the non-targeting GL2 control (5.3 A and B, lane 2) did not affect the levels of either Nek2 or the loading control, α -tubulin, demonstrating that Nek2 ablation is specific to the pooled Nek2 duplexes. Increasing the volume of oligofectamine used to transfect the Nek2 duplexes brought only a further slight reduction in Nek2 expression. Maximal suppression was obtained with 125 pmols duplex : 1 μ l oligofectamine (5.3 A and B, lane 5). Doubling the volume of oligofectamine to 2 μ l did not further reduce Nek2 expression (5.3 A and B, lane 6). Oligofectamine can be toxic to cultured cells, hence 125 pmols of duplex combined with 1 μ l oligofectamine produced the greatest reduction in Nek2 expression with the least likelihood of toxicity.

The level of Nek2 protein expression was readily reduced in both HeLa and U2OS cells by an equimolar mix of four duplexes directed against Nek2. I next attempted to determine whether the efficacy of the smartpool duplexes was preserved when they were used individually. HeLa and U2OS cells were seeded at 1×10^4 cells / cm^2 in 60 cm diameter culture dishes 24 hours prior to transfection. The culture media was then replaced and supplemented with either the control GL2 duplex or individual Nek2 duplexes at a final concentration of 50 nM, using the ratio of 1 μ l of oligofectamine : 125 pmols RNA established with the pooled oligoribonucleotides. Transfected cells were cultured for a further 24 hours before being collected and total cell lysates made. In parallel, cells were seeded onto glass coverslips, transfected as previously and cultured for up to 72 hours post transfection before being fixed in cold methanol and processed for immunofluorescence microscopy.

The smartpool duplexes used individually effectively suppress Nek2 protein expression, though the degree of suppression achieved differed with the duplex used. Western blots of total cell lysates showed Nek2 duplexes 6 and 8 led to the greatest ablation of Nek2 protein in both U2OS (Figure 5.4 A, lanes 6 and 7) and HeLa cells (Figure 5.5 A, lanes 6 and 7). Transfection of duplex 9 reduced cellular levels of Nek2 to approximately that of the pooled duplexes in both HeLa and

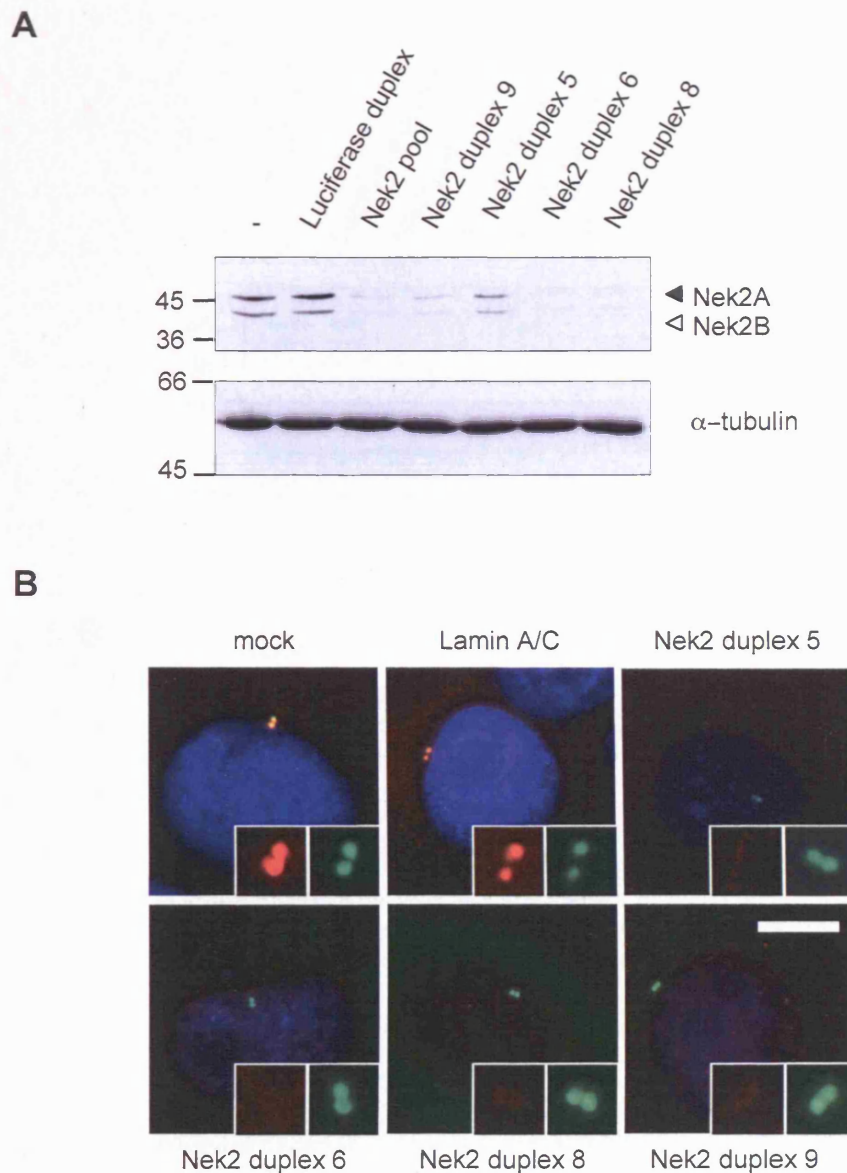


Figure 5.4 Single siRNA duplexes efficiently deplete Nek2 in U2OS cells

The four duplexes comprising the smartpool efficiently deplete Nek2 when used individually. **A.** Asynchronous U2OS cells were either untreated (-), treated with pooled or individual duplexes directed against Nek2 for 24 hours, collected and equal amounts of cell lysate resolved by SDS-PAGE and transferred to nitrocellulose membrane. Membranes were probed with monoclonal Nek2 antibodies (BD), stripped and reprobed with α -tubulin antibodies as a loading control (Sigma). **B.** U2OS cells treated with Nek2 duplexes for 72 hours, fixed and processed for immunofluorescence microscopy. Cells are stained with primary antibodies against Nek2 (red) and γ -tubulin (green) and DNA was stained with Hoechst 33258. Magnified images (inset) show clear loss of centrosomal Nek2 in cells treated with Nek2, but not control, duplex. Scale bar, 5 μ m.

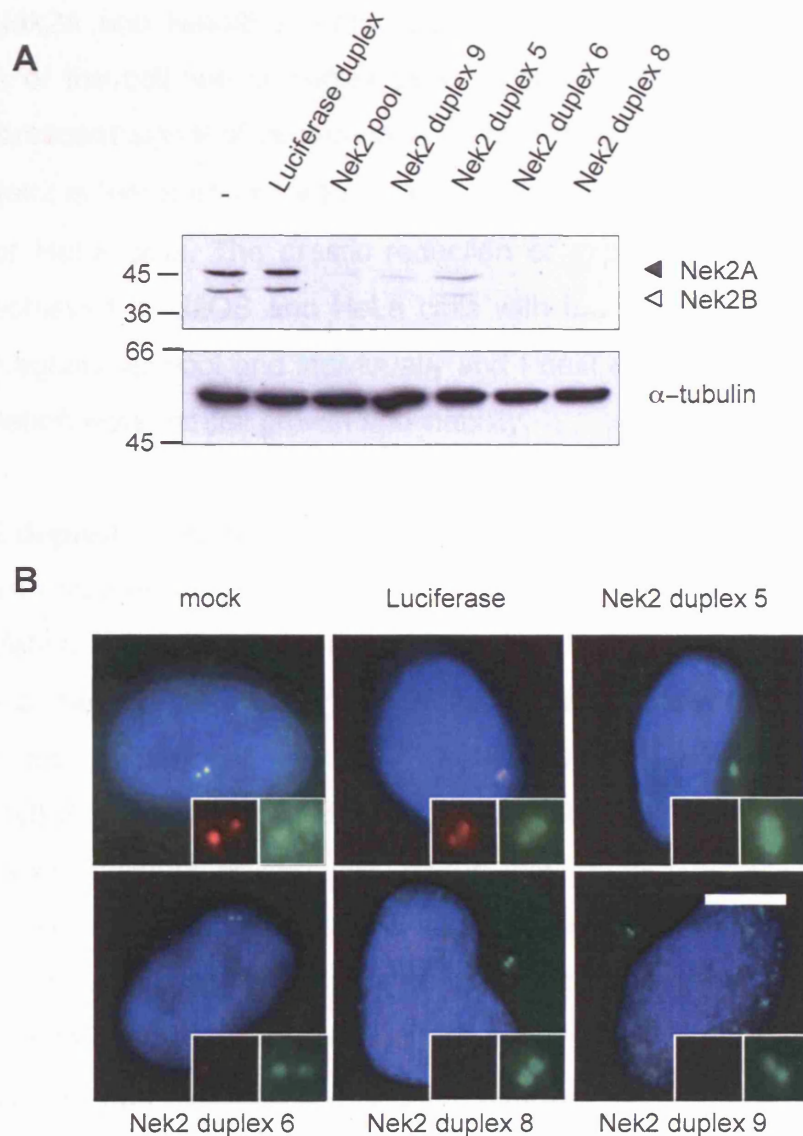


Figure 5.5 Single siRNA duplexes efficiently deplete Nek2 in HeLa cells

The four duplexes comprising the smartpool efficiently deplete Nek2 when used individually. **A.** Asynchronous HeLa cells were treated with pooled or individual duplexes directed against Nek2 at a final concentration of 50 nM for 24 hours, collected and equal amounts of cell lysate resolved by SDS-PAGE and transferred to nitrocellulose membrane. Membranes were probed with monoclonal Nek2 antibodies (BD Clontech), stripped and reprobed with α -tubulin antibodies as a loading control (Sigma). **B.** HeLa cells treated with Nek2 duplexes at a final concentration of 50 nM for 24 hours, fixed and processed for immunofluorescence. Cells are stained with primary antibodies against Nek2 (AbCam, red) and γ -tubulin (Sigma, green) and DNA was stained with hoechst 33258. Magnified images (inset) show clear loss of centrosomal Nek2 in cells treated with Nek2, but not control, duplex. Scale bar, 5 μ m.

U2OS cells (compare lanes 4 and 5, Figures 5.4 A and 5.5 A). Duplex 5 was the least effective of the four present in the pool, though it did markedly reduce protein levels of Nek2A and Nek2B in both cell lines compared to the control duplex. Regardless of the cell line or duplex used, depletion of Nek2 did not affect the immunofluorescent signal of centrosomal γ -tubulin (Figures 5.4 B and 5.5 B, inset images). Nek2 is therefore not required for γ -tubulin recruitment to the centrosome in U2OS or HeLa cells. The drastic reduction of expressed Nek2A and Nek2B could be achieved in U2OS and HeLa cells with four oligoribonucleotides, used both as an equimolar pool and individually and I next asked what the implications of this depletion were for cell growth and viability.

5.2.2 Nek2 depletion restricts the growth of HeLa and U2OS cells

To measure changes in cell viability and growth in response to RNAi-mediated Nek2 depletion I used a colorimetric assay that measures an aspect of mitochondrial metabolism directly proportional to cell viability: the reduction of the colourless tetrazolium salt sodium (2-(4-Iodophenyl)-3-(4-nitrophenyl)-5-(2,4-disulfophenyl)-2H-tetrazolium (WST-1) to soluble, highly coloured formazan, with an absorbance maxima of 450 nm. Historically, growth assays employed the tetrazolium salt 3-(4,5-dimethylthiazol-2-yl)-2,5-diphenyltetrazoliumbromide (MTT), which was thought to be reduced by succinate dehydrogenase to the coloured formazan salt (Mosmann, 1983). Though an effective measure of cell viability, the coloured product was insoluble and required a further solubilization step before the assay endpoint could be determined. The later adoption of 2,3-bis(2-methoxy-4-nitro-5-sulfophenyl)-5-[(phenylamino)carbonyl]-2H-tetrazolium (XTT) resulted in a soluble formazan salt, simplifying the assay. WST-1 shared this advantage, in that it was also reduced to a soluble product, but had the advantage over XTT of a larger linear range and greater stability of the formazan product. WST-1 is thought to be reduced at the plasma membrane by NADP or NAPH in a mechanism which involves superoxide (Berridge et al., 2005; Berridge et al., 1996). To measure cell viability and hence growth I used the WST-1 salt. U2OS or HeLa cells were seeded at 1×10^4 / cm² in sterile flat bottomed micro-titre plates and incubated for 24 hours before treatment with Nek2 or control RNAi. Viability was assessed at the time of RNAi treatment and each subsequent 24 hours by the addition of 10 μ l of

WST reagent (WST-1 salt combined with the intermediate electron acceptor phenazine methosulfate (PMF)) directly to each plate well and incubation at 37°C in a humidified cell culture incubator for 2 hours. Absorbance at 450 nm was measured in a multiwell plate reader. The reduction of WST-1 correlated well with HeLa and U2OS cell number at this density, whereas at higher densities WST-1 reduction reached a plateau and no longer reflected cell number (Figure 5.6 A and B, respectively).

Treatment of the U2OS osteosarcoma cell line with Nek2 RNAi restricted cell growth completely as determined by the reduction of WST-1. The OD₄₅₀ did not increase with time following Nek2 RNAi treatment, suggesting no further cell growth occurred and hence no increase in capacity to reduce the WST-1 reagent (Figure 5.7 A). The growth inhibition was observed in cells treated with the Nek2 smartpool mixture comprising all four duplexes (Figure 5.7 A, broken line, star) and each duplex individually (Figure 5.7A broken lines, open circle, square, triangle and cross). However, the same degree of inhibition was observed when U2OS cells were treated with the non-targeting control GL2 duplex (Figure 5.7 A, solid line, cross) at the same final concentration, 50 nM, as the pooled or individual Nek2 duplexes. Untreated U2OS cells or cells treated with oligofectamine in the absence of any oligoribonucleotides continued to grow at approximately the same rate (Figure 5.7 A, solid line, solid square and broken line, bar respectively). Plotting the same data while omitting the individual duplexes for clarity (Figure 5.7 B) clearly shows the growth inhibition effects are only obtained with duplex treated cells and are near identical with the Nek2 and GL2 duplexes. A similar growth inhibition was also obtained with the control Lamin A/C duplex (data not shown). This suggested the growth inhibition was a non-specific effect, unrelated to the duplex sequence and hence could not be specifically ascribed to Nek2 depletion.

To examine whether the response to Nek2 RNAi treatment was cell line specific I treated the HeLa cervical carcinoma derived cell line in an identical manner; seeding the cells 24 hours prior to treatment, incubating with Nek2 or control GL2 duplex at a final concentration of 50 nM and measuring growth by WST assay at the time of treatment and each 24 hours thereafter. The growth inhibition seen in

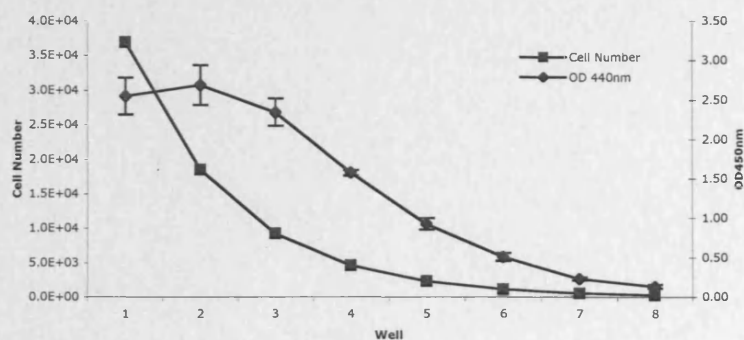
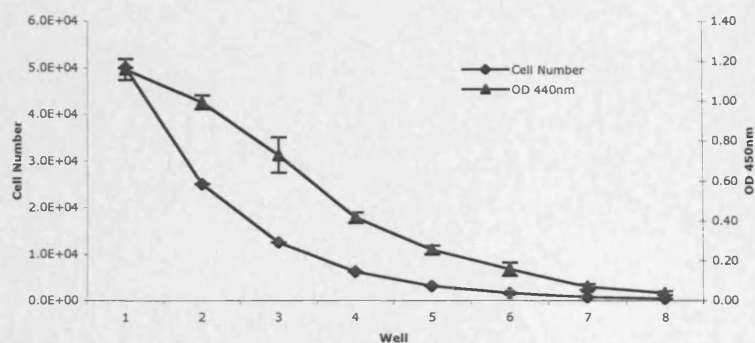
A**B**

Figure 5.6 HeLa and U2OS cell WST assay standard curves

Serially diluted **A.** HeLa and **B.** U2OS cells were seeded in 96 well plates and incubated for 24 hours before the addition of 10 μ l of WST assay reagent. Cells were then incubated at 37°C for a further two hours before measuring the resulting absorbance at 450 nm. A seeding density of 1×10^4 was chosen for both HeLa and U2OS cells. Error bars represent standard deviation from the mean of absorbance measured in triplicate.

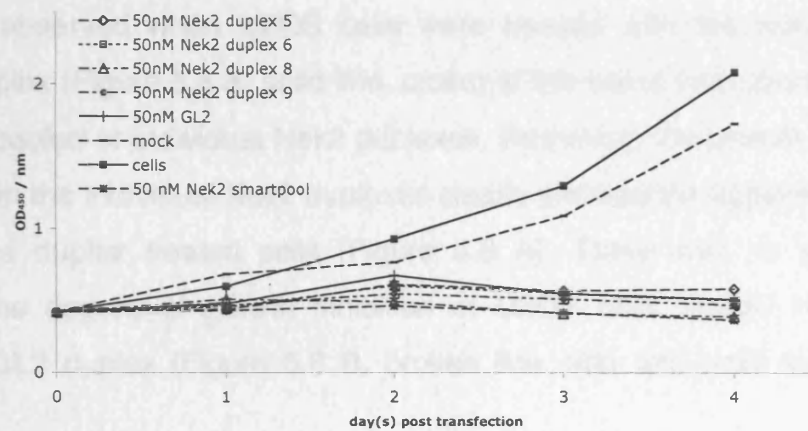
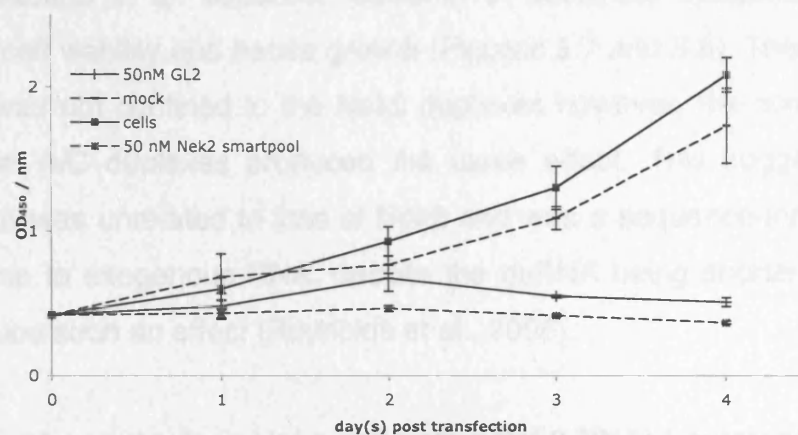
A**B**

Figure 5.7 U2OS cell growth following transfection with Nek2 RNAi

A. Cells were seeded at 1×10^4 cells / cm^2 in 96 well microtitre plates 24 hours prior to transfection with Nek2 or GL2 siRNA at a final concentration of 50 nM. Cell growth was measured initially and each subsequent 24 hours after transfection by WST-1 assay. **B.** Omitting the growth curves of cells treated with individual Nek2 duplexes for clarity highlights the growth inhibition induced by GL2 and Nek2 RNAi. Error bars are standard deviation derived from triplicate measurements of absorbance.

U2OS cells was also observed in HeLa cells treated with the Nek2 smartpool mixture (Figure 5.8 A, broken line, star) and each duplex individually (Figure 5.8 A broken lines, open circle, square, triangle and cross). Again, the same degree of inhibition was observed when U2OS cells were treated with the non-targeting control GL2 duplex (Figure 5.8 A, solid line, cross) at the same final concentration, 50 nM, as the pooled or individual Nek2 duplexes. Removing the growth curves of cells treated with the individual Nek2 duplexes clearly showed the apparent growth inhibition of the duplex treated cells (Figure 5.8 A). There was no significant difference in the degree of growth inhibition of U2OS cells treated with Nek2 Smartpool or GL2 duplex (Figure 5.8 B, broken line, star and solid line, cross, respectively).

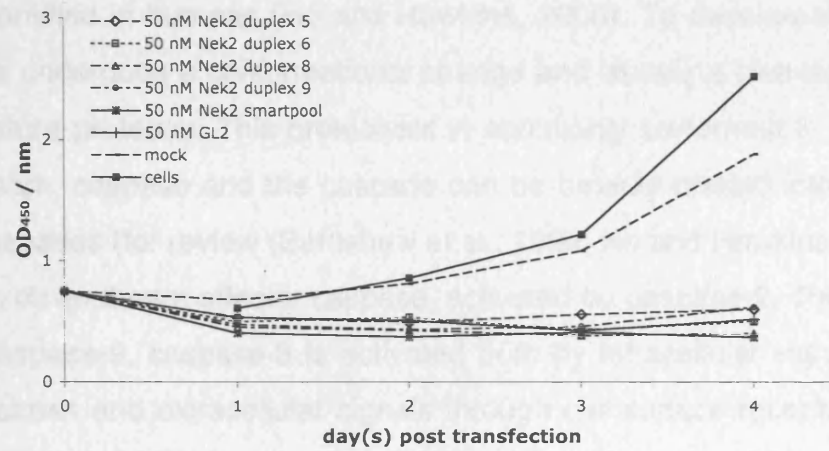
Transfecting two different cell lines, U2OS and HeLa, with oligoribonucleotides which demonstrably ablated both isoforms of Nek2 (Figures 5.4 and 5.5 respectively) resulted in an apparent reduction of succinate metabolism which correlates with cell viability and hence growth (Figures 5.7 and 5.8). This inhibition of cell growth was not confined to the Nek2 duplexes however, the non-targeting GL2 and Lamin A/C duplexes produced the same effect. This suggested that growth inhibition was unrelated to loss of Nek2 and was a sequence-independent cellular response to exogenous RNA, despite the dsRNA being shorter than that reported to induce such an effect (Reynolds et al., 2006).

5.2.3 Induction of apoptosis in HeLa cells after Nek2 RNAi treatment

Treatment of HeLa or U2OS cell lines with either Nek2 or control, luciferase, duplex appeared to prevent further cell growth. We decided to measure the degree of apoptosis every 24 hours after Nek2 and GL2 treatment in fixed HeLa cells.

Apoptosis is the programmed death of a cell in response to internal or external stimuli. It is morphologically distinct from necrosis and is characterised by cytoplasmic shrinkage, membrane disruption and an accompanying chromatin condensation and fragmentation. The net result is the breakdown of the cell into fragmented high molecular weight DNA packaged into membrane enclosed vesicles that are then normally engulfed by macrophages. At the molecular level,

A



B

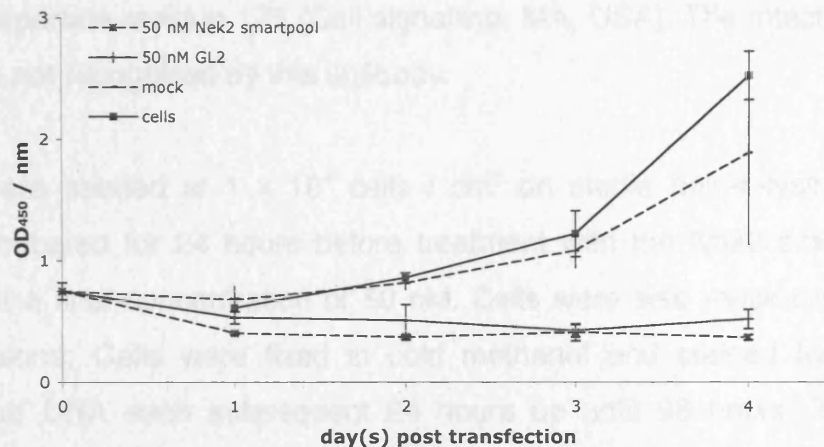


Figure 5.8 HeLa cell growth following Nek2 RNAi treatment

A. Cells were seeded at 1×10^4 cells / cm^2 in 96 well microtitre plates 24 hours prior to transfection with Nek2 or GL2 siRNA at a final concentration of 50 nM. Cell growth was measured initially and each subsequent 24 hours after transfection by WST-1 assay. **B.** Omitting the growth curves of cells treated with individual Nek2 duplexes for clarity clarifies the growth inhibition induced by GL2 and Nek2 RNAi. Error bars are the standard deviation about the mean derived from triplicate measurements of absorbance.

apoptosis is characterised by a wave of proteolysis throughout the cell, the end point of a proteolytic cascade. The components of this cascade are a number of cysteine-dependent aspartate directed proteases, caspases, and there are currently 14 identified in humans (Ho and Hawkins, 2005). To become activated, the procaspase undergoes a conformational change and usually a cleavage event to yield the mature protease. This proteolysis is commonly performed in *trans* by another, upstream, caspase and the cascade can be broadly divided into initiator and effector caspases (for review (Earnshaw et al., 1999; Ho and Hawkins, 2005)). Caspase-3 is a downstream effector caspase, activated by caspase-9. Through its cleavage by caspase-9, caspase-3 is activated both by intracellular signals from mitochondrial stress and extracellular signals through cell surface receptors such as the tumour necrosis factor receptor TNFR1 (Nunez et al., 1998). Located downstream of two converging apoptotic signalling pathways, activated caspase-3 is an excellent marker of apoptosis. To detect apoptosis in RNAi treated HeLa cells, I used an antibody which recognised caspase-3 which has been activated by cleavage at aspartate residue 175 (Cell signalling, MA, USA). The intact, inactive, procaspase is not recognised by this antibody.

HeLa cells were seeded at 1×10^4 cells / cm² on sterile poly-L-lysine coated coverslips, incubated for 24 hours before treatment with the Nek2 smartpool or GL2 duplex at a final concentration of 50 nM. Cells were also mock treated with lipid carrier alone. Cells were fixed in cold methanol and stained for cleaved caspase-3 and DNA each subsequent 24 hours up until 96 hours. To induce apoptosis in a duplex independent manner and confirm the specificity of cleaved caspase-3 staining HeLa cells were treated with staurosporine at a final concentration of 1 μ M. Staurosporine is a pan-kinase inhibitor that induces apoptosis and cleavage of caspase-3 at nanomolar concentrations in cultured mammalian cells (Bijur et al., 2000; Jacobsen et al., 1996). All HeLa cells treated with staurosporine for 48 hours stained strongly for cleaved caspase 3 (Figure 5.9 A).

The mean background rate of apoptosis in mock treated U2OS cells, as judged by cleaved caspase-3 staining, was 0.7% after 24 hours rising to a maximum of 5% at

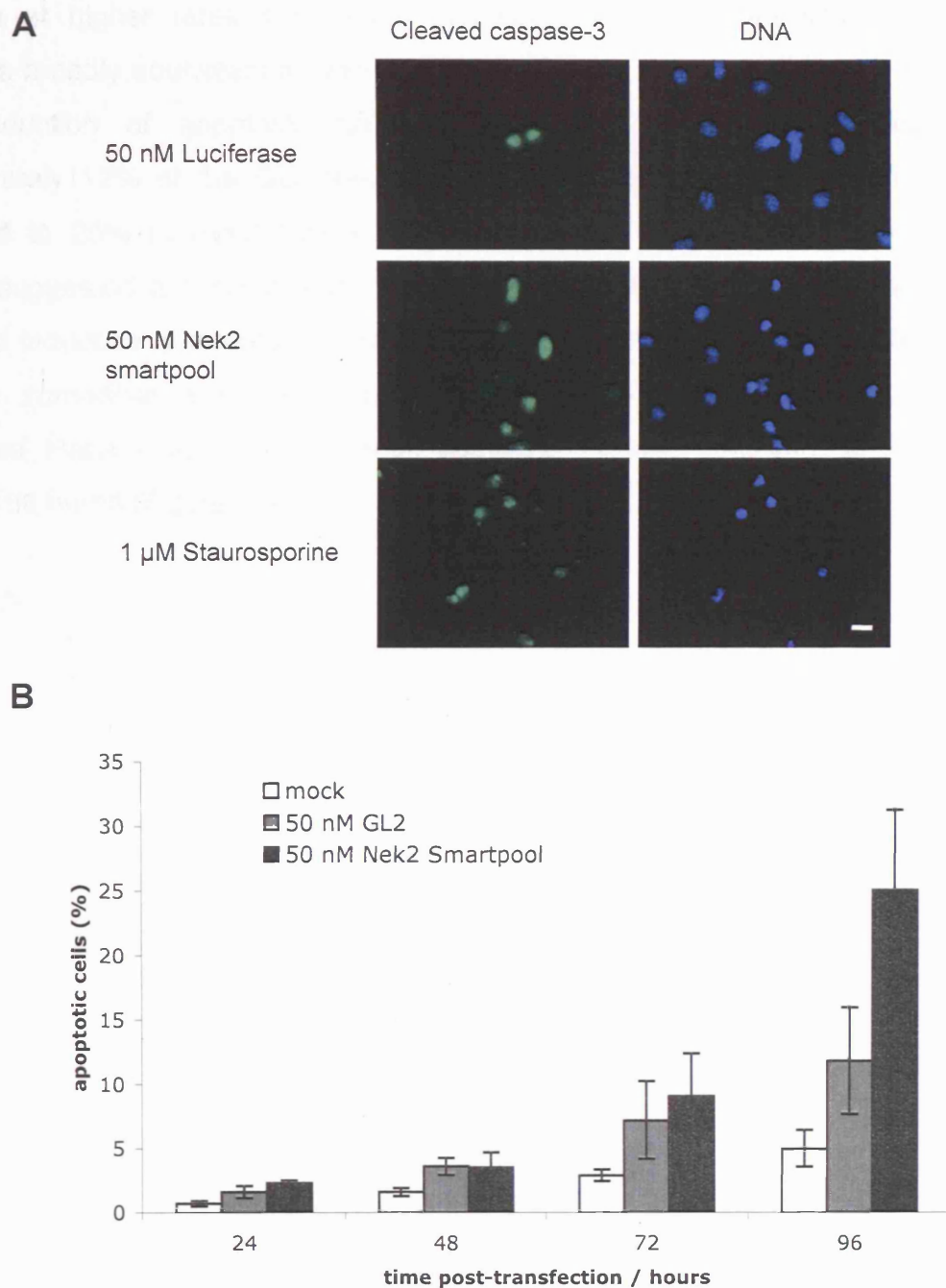


Figure 5.9 Induction of apoptosis in Nek2 siRNA treated HeLa cells

A. HeLa cells were seeded onto sterile glass coverslips 24 hours before transfection with pooled Nek2 or GL2 duplexes at a final concentration of 50 nM. Cells were fixed every 24 hours after transfection. Apoptotic cells were stained for cleaved caspase-3 (green) and DNA (blue). Scale bar 20 μ m. **B.** Nek2 RNAi induces apoptosis, as evidenced by increased cleaved caspase-3 staining, at a rate twice that of treatment with control duplex. Error bars represent standard errors derived from three independent experiments.

96 hours (Figure 5.9 B). Treatment with both GL2 and Nek2 duplexes induced apoptosis at higher rates than mock treatment at the 24, 48 and 72 hour timepoints broadly equivalent at twice that of the mock treated cells. However, the mean induction of apoptosis differed significantly at the final timepoint, approximately 12% of the GL2 treated HeLa cells were apoptotic at 96 hours compared to 25% of Nek2 treated cells (Figure 5.9 B). This clear difference strongly suggested a specific response to Nek2 depletion in HeLa cells with an increased induction of apoptosis. This specific response to Nek2 RNAi treatment contrasts somewhat with the growth assays in which both Nek2 and GL2 transfected HeLa cells showed equal, complete, growth inhibition up to and including 96 hours (Figure 5.8).

5.3 DISCUSSION

I have shown that several siRNA duplexes arrayed against four sites within the Nek2 mRNA effectively deplete both isoforms of the mature protein, Nek2A and Nek2B, when transfected into HeLa and U2OS cultured cells. The depletion of Nek2 protein is marked and specific, no ablation was observed with either the lamin or GL2 duplexes which are directed against human lamin A/C or *p.pyralis* luciferase, respectively. Having achieved an effective, reproducible repression of Nek2 in two cultured cell lines, I then determined what effect the depletion had on cell viability.

Depletion of the mitotic serine/threonine kinase Plk1 by siRNA inhibits cell growth and induces apoptosis in a range of cell types including cultured prostate cancer derived cell lines and human mammary epithelial cells (Liu et al., 2006; Reagan-Shaw and Ahmad, 2005; Spankuch-Schmitt et al., 2002b). In a similar manner, RNAi repression of the mitotic Aurora-A kinase in cultured breast cancer cells inhibits growth (Katayama et al., 2003).

The first consequence of Nek2 RNAi I examined was the effect upon growth of cultured U2OS osteosarcoma and HeLa cervical cancer derived cell lines. Rather than counting cell numbers directly to determine growth I measured an aspect of cellular mitochondrial metabolism that correlates well with cell viability and hence number. Using cells seeded in 96-well microtitre plates, I measured viability by the addition of the formazan WST-1 salt which is reduced to a coloured product by cellular redox pathways. The WST assay had the advantage of simplicity, reagent was added directly to the media and the assay endpoint measured in a plate reader without intervening wash steps. The use of 96 well plates facilitated easy replicate measurements. Treating U2OS or HeLa cells with pooled or single Nek2 duplexes completely inhibited growth (Figure 5.7 and 5.8). There was no significant increase in cell number, as measured by WST reduction, after Nek2 duplex treatment. However, the growth inhibition was not specific to the Nek2 duplexes. Transfection of U2OS or HeLa cells with the control GL2 duplex, an oligoribonucleotide that is directed against firefly luciferase and is nominally non-targeting in human cells, produced the same effect; growth was completely

inhibited. These data would suggest that the observed growth inhibition was not sequence specific and not reliant on depletion of Nek2 but a gross response to exogenous RNA. This is possible though both the Nek2 and GL2 duplexes are both shorter and employed at a lower concentration than that thought to be required to induce the non-specific interferon mediated response (for review (Cullen, 2006; Pei and Tuschl, 2006)). Additionally, a recent report published as this work was being undertaken demonstrated growth inhibition of HeLa cells in response to Nek2 depletion (Fletcher et al., 2004). In this study HeLa cells were treated with Nek2, GL2 or GL3 duplex and growth assayed by direct counting. Nek2 duplex inhibited growth, the GL2 and GL3 luciferase duplexes did not. The sequence independent inhibition of growth after RNAi treatment also contrasts with the data on apoptosis, a response only observed in HeLa cells after Nek2 treatment (Figure 5.9). The possibility exists that the mechanism of the WST assay was affected by exogenous RNA duplexes rather than the cell viability that the assay measured.

WST-1 is a tetrazolium salt that is reduced to an orange coloured formazan product and along with the related compounds MTT and XTT forms the basis for colorimetric assays of cell growth. It was initially thought that WST-1 was reduced intracellularly by mitochondrial succinate metabolism in the same manner as XTT and MTT (Berridge et al., 1996). Latterly this view has been revised, attempts to detect reduced WST-1 intracellularly have failed and it is thought that though WST-1 reduction occurs in a cell dependent manner, this reduction occurs by superoxide extracellularly or at the cell surface (Berridge et al., 2005). The possibility exists that the negatively charged siRNA duplex occludes or occupies sites at the cell surface usually bound by the negatively charged WST-1 salt. This may impede WST-1 reduction and hence apparent cell growth. This would explain the discrepancy between the growth inhibition by the GL2 duplex measured with the WST assay reported in this work and the published data where no such inhibition was observed (Fletcher et al., 2004). Repeating the growth curves by manually counting cells would determine whether the siRNA is interfering with WST-1 metabolism or cell growth.

In addition to examining the overall growth rate of RNAi treated cells we measured cleaved caspase-3 activity as a measure of apoptosis in HeLa cells following siRNA transfection. In contrast to the growth curve which showed no difference in response to Nek2 or GL2 RNAi, a clear difference emerged when the rate of apoptosis was measured. For the first 72 hours post-transfection the rates of apoptosis in Nek2 and GL2 treated cells is comparable. However, 96 hours after transfection 25% of the HeLa cells were apoptotic compared to only 11.8% of the GL2 treated cells a significant difference. The timing and the degree of apoptosis are comparable to published data which showed a marked increase of apoptosis between 72 and 120 hours after Nek2 depletion by RNAi (Fletcher et al., 2004). Nek2 is subjected to a cell cycle dependent regulation, such that levels of Nek2A mRNA and mature protein are undetectable in mitosis with Nek2B disappearing in the subsequent G₁ (Hames and Fry, 2002; Hames et al., 2001; Hayward et al., 2004). Nek2 is depleted and replenished with each cell cycle, yet cells artificially depleted of Nek2 by RNAi did not undergo significant apoptosis in the first 24 hours. This would be expected if Nek2 kinase activity was obligate during the subsequent cell cycle. The significant induction of apoptosis did not occur until 96 hours after Nek2 siRNA treatment. This lethality may reflect the absence of phosphoepitopes created by Nek2. Daughter cells arising from Nek2 RNAi treated progenitors would not carry any centrioles modified by Nek2 phosphorylation 72 hours after treatment (Figure 5.10) and it is after this time point that significant levels of apoptosis occurred. Nek2A has been demonstrated to interact with and phosphorylate a number of structural and regulatory components of the centrosome including C-Nap1, rootletin, PP1c, Plk1 and Hec1 (Chen et al., 2002a; Fry, 2002; Lou et al., 2004b; Pugacheva and Golemis, 2005; Rapley et al., 2005) and Nek2B has been implicated in achieving timely mitotic exit in HeLa cells (Fletcher et al., 2005). Modification of these and other cryptic substrates by Nek2A or Nek2B could be essential for mitotic progression and lethal when absent.

The apoptosis induced by Nek2 RNAi in HeLa cells is encouraging in terms of choosing Nek2 as a target for cancer therapy. If increased levels of Nek2 drives or facilitates cancer cell proliferation, then apoptosis induced by Nek2 depletion would be expected to be cytostatic with respect to those tumour cells

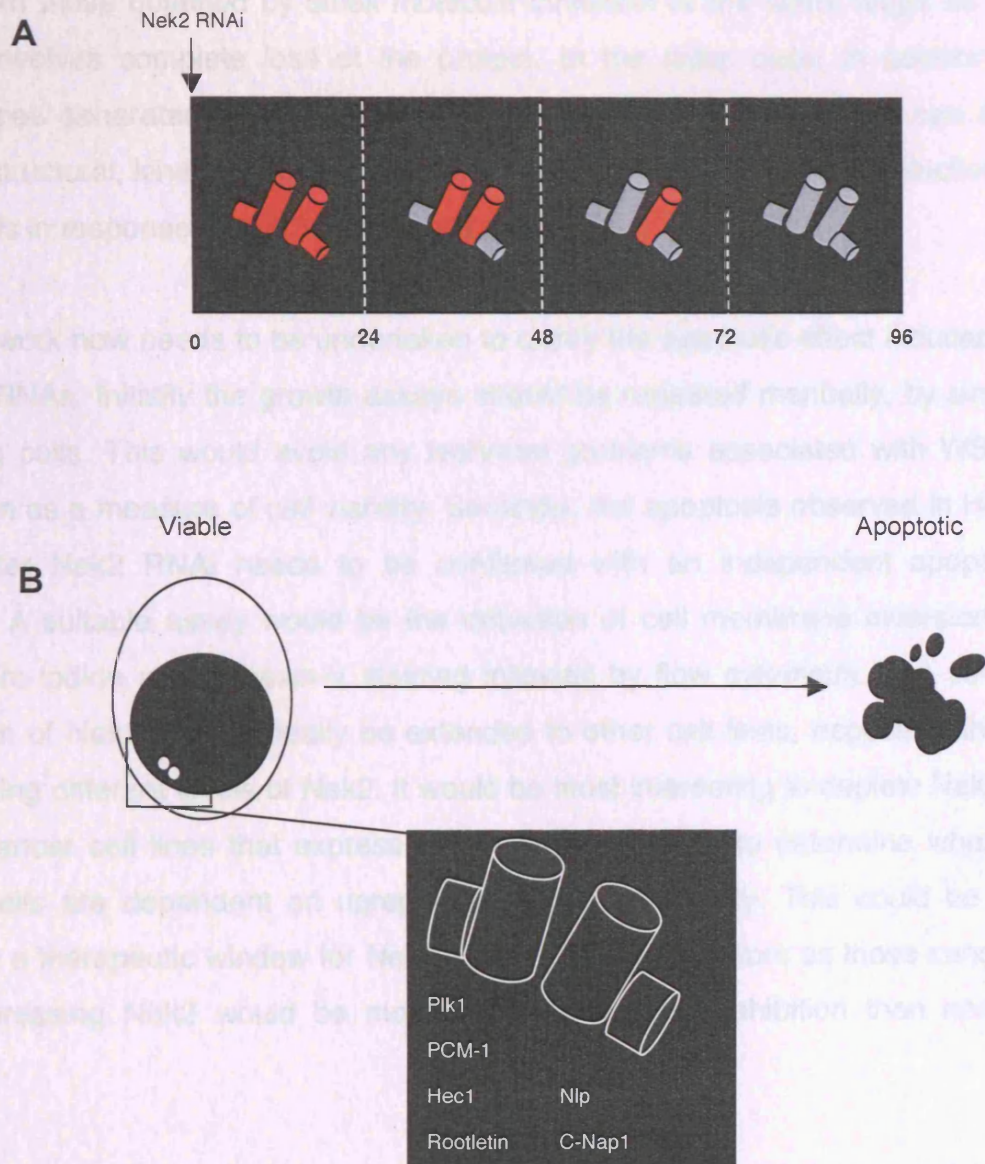


Figure 5.10 Phosphopeptides created by Nek2 may be essential for cell viability

A. Daughter cells arising from Nek2 RNAi treated progenitors would not carry any centrioles modified by Nek2 phosphorylation (depicted as red shaded centrioles and procentrioles) 72 hours after treatment. If Nek2 phosphorylated substrates were essential for cell cycle progression then cell viability would be expected to decrease as cells undertake subsequent divisions. **B.** Nek2 is known to interact with a range of structural and regulatory components which could require modification for correct function.

overexpressing Nek2. Phenotypes observed after RNAi depletion of a kinase can differ from those obtained by small molecule inhibition of the same target as the former involves complete loss of the protein. In the latter case, in addition to phenotypes generated by loss of Nek2 kinase activity, RNAi depletion can also disrupt structural, kinase-independent, roles of Nek2. Nonetheless, the induction of apoptosis in response to Nek2 depletion is promising.

Further work now needs to be undertaken to clarify the apoptotic effect induced by Nek2 siRNAs. Initially the growth assays should be repeated manually, by simply counting cells. This would avoid any technical problems associated with WST-1 reduction as a measure of cell viability. Secondly, the apoptosis observed in HeLa cells after Nek2 RNAi needs to be confirmed with an independent apoptotic marker. A suitable assay would be the detection of cell membrane inversion by propidium iodide and Annexin-V staining followed by flow cytometry. The siRNA depletion of Nek2 should ideally be extended to other cell lines, especially those expressing different levels of Nek2. It would be most interesting to deplete Nek2 in those cancer cell lines that express higher levels of Nek2 to determine whether those cells are dependent on upregulated Nek2 for viability. This could be the basis of a therapeutic window for Nek2 small molecule inhibitors as those cancers overexpressing Nek2 would be more sensitive to Nek2 inhibition than normal tissue.

Finally, the morphology of centrosomes needs to be examined more carefully in Nek2 depleted cells. Nek2 is known to be a core component of the centrosome and depletion of Nek2 by RNAi in *drosophila* leads to centrosome maturation defects (Fry, 2002; Prigent et al., 2005). The loss of spindle pole integrity could increase the incidence of multipolar mitosis, inducing aneuploidy and resulting in the loss of viability observed following Nek2 siRNA treatment.

CHAPTER 6

IDENTIFICATION OF SMALL MOLECULE INHIBITORS OF NEK2A

6.1 INTRODUCTION

The initiation and progression of cancer is underpinned by a series of mutations which allow cells to escape normal growth restrictions (Hanahan and Weinberg, 2000; Knudson, 2001). Targeting the defects which drive tumour formation may allow more specific therapies than current blunt, cytotoxic, treatments which attack proliferating cells. Defects which involve the aberrant expression of a kinase can be treated with small molecules that inhibit the kinase activity and remove the drive to malignancy. This approach is well illustrated in the development of imatinib to treat CML by inhibiting the BCR-ABL tyrosine kinase. Imatinib stabilises BCR-ABL in an inactive conformation, blocking the proliferative signal that initiates CML (Ren, 2005).

To identify candidate kinase inhibitors, the enzyme can be screened *in vitro* against a large compound collection. Compounds which reduce kinase activity can then be pursued as leads for further development to increase the potency and specificity of inhibition. The rate at which the vast compound libraries possessed by pharmaceutical companies could be screened was increased by the simultaneous employment of automation and the reduction in *in vitro* assay volume. Automated liquid handling systems and homogenous, machine readable, assays allowed the inhibitory activity of thousands of compounds to be rapidly tested. Compound collections stored in 384 well plates and assays performed in volumes smaller than 50 μ l allows thousands of assay points to be measured each day. Screening rates at or greater than 10,000 compounds each day (high throughput) and 100,000 compounds daily (ultra-high throughput) became feasible (Sundberg, 2000).

High throughput screens have been instrumental in the discovery of new lead compounds to inhibit novel targets in disease. Inhibitors of Aurora (ZM447439, VX680), EGFR (gefitinib, erlotinib), c-Kit and BCR-ABL (imatinib) employed HTS in their development (Aherne et al., 2002; Ditchfield et al., 2003). Overexpression of the mitotic kinases Plk1 and Aurora has been shown to correlate with disease progression and poor prognosis. Correspondingly, small molecule inhibitors of Plk1 and Aurora have been identified which reduced the viability of cancer derived

cell lines (Ditchfield et al., 2003; Gumireddy et al., 2005). The NIMA related kinases are a fourth class of kinases which govern mitotic progression alongside the Cdks, the Polo-like kinases and Aurora kinases. Nek2, a member of the NIMA related kinases, is also overexpressed in human breast tumours and a range of tumour derived cell lines (see chapters 3 and 4). The locus of the Nek2 gene, 1q32.1, has also been shown to be amplified in subsets of breast tumours and gastric adenocarcinomas (Loo et al., 2004; Weiss et al., 2004).

The most well characterised role for Nek2A in human cells is the induction of centrosome separation immediately prior to mitosis and subsequent bipolar spindle formation. Overexpression of myc-Nek2A in breast epithelial cells resulted in aneuploid cells with supernumerary centrosomes (Hayward et al., 2004). U2OS osteosarcoma cells stably overexpressing GFP-Nek2A underwent premature centrosome disjunction. Prolonged overexpression of myc-Nek2A in the same osteosarcoma cell line induced aneuploidy (Faragher and Fry, 2003). Conversely, overexpression of a kinase dead mutant, GFP-Nek2A K37R, for 24 hours altered centrosome morphology and induced a four-fold increase in spindle abnormalities. Downregulation of Nek2 in HeLa cells by RNAi induced immediate growth arrest and after 72 hours, apoptosis ((Fletcher et al., 2004): and see chapter 5). siRNA silencing of one Nek2 isoform, Nek2B, also delayed mitotic exit in GFP-centrin HeLa cells (Fletcher et al., 2005).

Elevated levels of Nek2 protein and gene amplification have been observed in breast tumours, gastric adenocarcinoma, osteosarcomas and lymphoma. Transfection of Nek2A into cultured cells induced supernumerary centrosomes and aneuploidy, common hallmarks of solid tumours. Ablation of Nek2 in cultured HeLa cells inhibited growth and increased the rate of apoptosis. Taken together, this validation data is sufficiently strong to suggest Nek2 as a novel target for therapeutic intervention.

This chapter details the development of a high throughput screen (HTS) to identify small molecules that inhibit Nek2A *in vitro*. An HTS forms the initial step of a test cascade for drug discovery (Figure 6.1). The test cascade serves to identify and

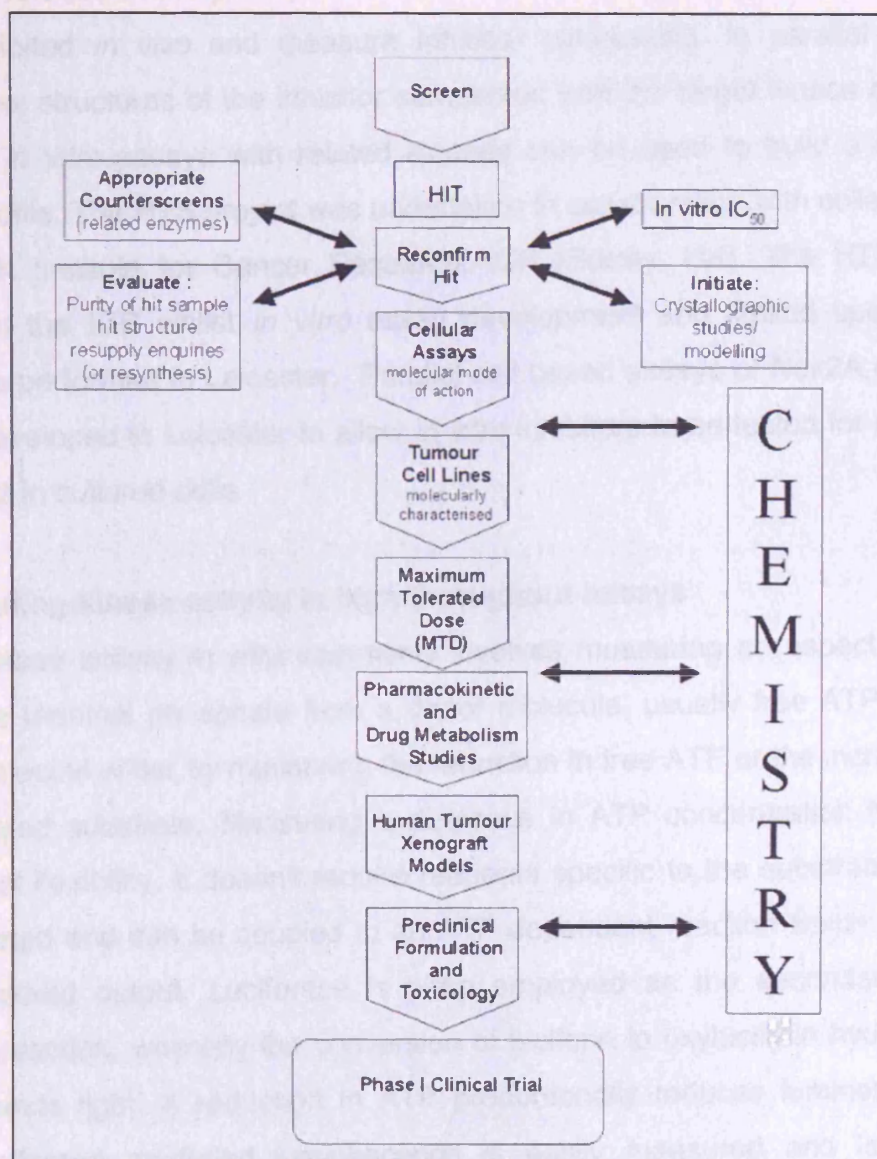


Figure 6.1 The contemporary drug development process

Drug development follows a defined protocol. High throughput screening (HTS) initiates this process which becomes more refined as the project continues. Inhibitors identified in the HTS are designated "hits". Hits with favourable chemical and physical properties are termed "leads" and pursued for further development. The characterisation of leads becomes more stringent, with assays to determine whether the target of inhibition is modulated *in vitro*, in cultured cells and in animals. Reproduced from Garrett et al., (2003).

refine crude inhibitors and becomes increasingly defined as the project progresses. A large compound collection is screened against the target of interest to identify putative “hits”, molecules inhibiting Nek2. These hits are then reconfirmed to check that the molecules have not degraded in storage. Reconfirmed hits are subsequently tested in cell-based assays both to confirm the target is inhibited *in vivo* and measure inhibitor cytotoxicity. In parallel to hit reconfirmation, structures of the inhibitor complexed with the target kinase can be determined. *In vitro* assays with related kinases can be used to build a limited specificity profile. The HTS project was undertaken in collaboration with colleagues at the CRUK Institute for Cancer Research, ICR (Surrey, UK). The HTS was performed at the ICR whilst *in vitro* assay development and limited specificity profiles were performed in Leicester. Parallel cell based assays of Nek2A activity were also developed in Leicester to allow *in vitro* inhibitors to be tested for activity against Nek2 in cultured cells.

6.1.1 Measuring kinase activity in high throughput assays

Assaying kinase activity *in vitro* commonly involves measuring an aspect of the transfer of a terminal phosphate from a donor molecule, usually free ATP, to an acceptor molecule either by measuring the reduction in free ATP or the increase in phosphorylated substrate. Measuring a decrease in ATP concentration has the advantage of flexibility. It doesn't require reagents specific to the substrate being phosphorylated and can be coupled to an ATP dependent reaction which has an easily measured output. Luciferase is often employed as the secondary ATP dependent reaction, whereby the conversion of luciferin to oxyluciferin hydrolyses ATP and emits light. A reduction in ATP proportionally reduces luminescence. Though luciferase mediated luminescence is easily measured and is easily coupled to the activity of disparate kinases it is more prone to artefacts when employed in high throughput screens. The luciferase itself is subject to inhibition, generating false positive results when the reduced luminescence is not due to the unimpeded kinase but the abrogated luciferase activity (von Ahsen and Bomer, 2005). To measure Nek2A activity *in vitro* we chose instead to directly measure substrate phosphorylation without a secondary reporter system by using ATP in which the terminal γ phosphate contains the radioisotope ^{32}P (phosphorus (^{32}P)) or

³³phosphorus (³³P). The spontaneous decay of ³²P or ³³P emits β-particles hence kinase activity can be determined by determining the amount of radioisotope transferred to the substrate.

6.1.2 Substrate selection for a Nek2A HTS

The isolation of recombinant Nek2A kinase from baculoviral infected Sf9 insect cells allowed characterisation of its *in vitro* substrate specificity and comparison of its biochemical properties with those of NIMA. Nek2A strongly phosphorylated the milk protein β-casein, myelin basic protein (MBP) and microtubule associated protein 2 (MAP2) and further showed avidity for a peptide comprising residues 42-72 of phospholemman (Fry et al., 1995). Phospholemman is a 72 amino acid component of the myocardial plasma membrane and substrate for PKA and PKC (Palmer et al., 1991). Incubation of substrates in parallel with the catalytically inactive point mutant Nek2A-K37R demonstrated that the kinase activity derived from the insect cell lysate was solely due to the baculoviral encoded Nek2A and not from a copurifying endogenous kinase. Both MBP and β-casein have been employed as *in vitro* substrates in Nek2A kinase assays.

6.1.3 Measuring Nek2A inhibition *in vitro*

The activity of Nek2A *in vitro* is proportional to the amount of radiolabelled phosphate incorporated into the substrate, assuming the substrate is present in excess. Similarly, molecules acting as kinase inhibitors would reduce Nek2A activity, phosphorylation and hence radioisotope incorporation. To accurately measure this phosphorylation, the substrate must be resolved from unincorporated ³²P-γ-ATP and autophosphorylated kinase and this is achieved in one of two ways depending on the number of putative inhibitors being assayed. Assay development in Leicester employed a homogenous *in vitro* assay whereby Nek2A was incubated with β-casein in the presence of increasing concentrations of inhibitor and the reaction resolved by SDS-PAGE. The other reaction components are excluded by size and ³²P-β-casein quantified by excision from the gel and incubation with liquid scintillant.

Pilot experiments conducted at the ICR to establish the HTS assay conditions used proximity scintillation counting. Briefly, scintillant coated microtitre plates, “flashplates”, are in turn coated with myelin basic protein (MBP). Kinase and inhibitor or appropriate control were added to the wells in reaction buffer containing ^{33}P - γ -ATP, incubated and the plate wells washed. Only the radiolabelled MBP substrate bound to the well wall has sufficient proximity to the scintillant to generate a signal.

6.1.4 Quantifying Nek2 inhibition in cells

The major phenotype observed upon overexpression of Nek2A is premature centrosome disjunction (Faragher and Fry, 2003; Fry et al., 1998c). Under normal conditions centrioles undergo disorientation and duplication concomitant with S phase but the centrosomes remain in close proximity until a cascade of phosphorylation induces centrosome disjunction upon entry to mitosis. The ability to recover paired centrosomes from cultured cells by differential centrifugation has long suggested a physical tether and the molecular nature of that tether is now being elucidated.

Two putative components of the intercentrosomal link are the large structural proteins C-Nap1 and rootletin. Both have been shown to be phosphorylated by Nek2A *in vitro* and *in vivo* are phosphorylated endogenously during the G₂/M transition when Nek2 activity is maximal (Bahe et al., 2005; Fry et al., 1998c). It is suggested that the phosphorylation of C-Nap1 and rootletin results in their displacement, allowing centrosome disjunction to occur (Yang et al., 2006). Immunofluorescent staining of fixed cells shows rootletin is similarly displaced from the centrosome in a kinase dependent manner when GFP-Nek2A is ectopically expressed in interphase (Bahe et al., 2005).

Interference with premature centrosome disjunction and the associated loss of rootletin in stable cell lines inducibly overexpressing GFP-Nek2A form two assays for Nek2 inhibition in cultured cells. Small molecule inhibition of Nek2A should interfere with these processes leading to cells retaining paired centrosomes and centrosomal rootletin.

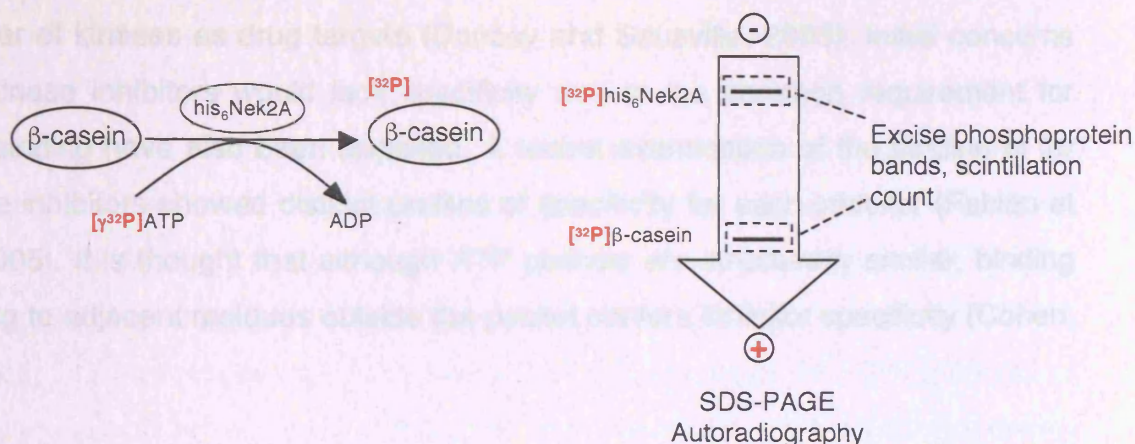
6.2 RESULTS

6.2.1 *in vitro* Nek2A kinase assays

To measure Nek2A activity *in vitro*, two assays outlined in Figure 6.2 were used, both of which measure the incorporation of radiolabelled phosphate from free ATP into control substrates, β -casein and MBP. The first is a homogenous assay whereby β -casein is incubated with ATP, P- γ^{32} -ATP and insect Sf9 cell lysate infected with a baculoviral construct encoding recombinant hexahistidine tagged Nek2A in solution. Reaction products are resolved by SDS-PAGE and ^{32}P - β -casein excised from the gel and quantified by liquid scintillation counting (Figure 6.2A). This gel-based assay is relatively rapid and the size separation of the products allows the level of other phosphoproteins, such as autophosphorylated his₆Nek2A to be determined within the same reaction. Whilst rapid when processing relatively few samples, serial loading gels and excising substrate bands becomes time consuming with multiple samples and is not amenable to the automation required for higher throughput.

To allow parallel processing of multiple reactions, such as those demanded by high throughput screening, a second assay format was employed. This similarly used radiolabelled ATP but instead relied on immobilised substrate and proximity scintillation counting with the phase separation partitioning substrate from reaction components. Scintillant coated 96 well plates, FlashPlates (Perkin Elmer), are coated with Nek2A control substrate MBP. The reaction mixture containing ATP, $\gamma^{33}\text{P}$ -ATP and purified GST-Nek2A is then added directly to the plate wells. The reaction is stopped and unincorporated radiolabel removed along with other reaction components by washing with phosphoric acid. Only $\gamma^{33}\text{P}$ -MBP immobilised on the well wall is sufficiently close to the scintillant coating to generate a positive signal (Figure 6.2B). ^{33}P - γ -ATP has a longer half-life but emits significantly less energetic β particles which makes handling the volumes required for automating screening less hazardous (25.4 days, 0.249 MeV compared to 14.3 days and 1.709 MeV for ^{32}P). Flashplate assays allow reduction in reaction volumes and microtitre plates are compatible with automated systems, significantly reducing the manual handling required.

A



B

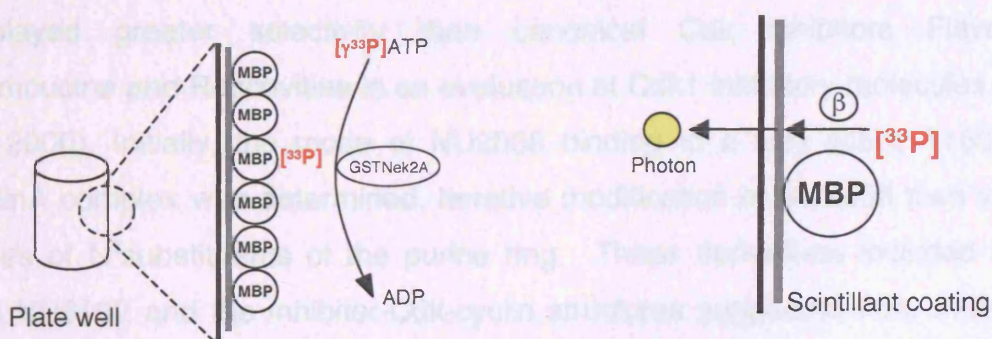


Figure 6.2 Measuring Nek2A kinase activity *in vitro*

A. $\text{his}_6\text{Nek2A}$ was incubated with β -casein and $[\gamma^{32}\text{P}]\text{ATP}$ and the reaction products resolved by SDS-PAGE to separate unincorporated $[\gamma^{32}\text{P}]\text{ATP}$ from autophosphorylated Nek2A and phosphorylated β -casein. Radiolabelled substrates are excised from the dried gel and quantified by scintillation counting. **B.** 384 well microtitre Flashplates coated with myelin basic protein (MBP) are incubated with GST-Nek2A and $[\gamma^{33}\text{P}]\text{ATP}$. The reaction is stopped and unbound reaction products and unincorporated radiolabel are removed with a PBS/pyrophosphate wash. Only the $[\text{P}^{33}]\text{MBP}$ bound to the plate wall is in sufficient proximity to the scintillant to allow emitted β particles to be converted to photons and quantified.

6.2.2 NU series molecules inhibit his₆Nek2A *in vitro*

Kinases are susceptible to inhibition by small molecules in several ways, most notably by competition with ATP for binding at the catalytic pocket or stabilisation of the kinase in an inactive conformation. This tractability has led to a burgeoning number of kinases as drug targets (Dancey and Sausville, 2003). Initial concerns that kinase inhibitors would lack specificity due to the common requirement for ATP binding have also been dispelled. A recent examination of the binding of 20 kinase inhibitors showed distinct profiles of specificity for each inhibitor (Fabian et al., 2005). It is thought that although ATP pockets are structurally similar, binding of drug to adjacent residues outside the pocket confers inhibitor specificity (Cohen, 2002).

The Newcastle University (NU) series of molecules are the products of a programme to produce inhibitors of Cdk1 and Cdk2. The lead molecule was a guanine based Cdk inhibitor O⁶-cyclo-hexylmethylguanine (NU2058) which displayed greater selectivity than canonical Cdk inhibitors Flavopiridol, Olomoucine and Roscovitine in an evaluation of Cdk1 inhibitory molecules (Arris et al., 2000). Initially, the mode of NU2058 binding to a fully active T160pCDK2-cyclinA complex was determined. Iterative modification of NU2058 then yielded a series of N²substituents of the purine ring. These derivatives included NU6094 and NU6102 and the inhibitor-Cdk-cyclin structures suggested that, while the O⁶ group is accommodated in the ribose binding motif, it is interaction of the N² substituent with residues outside of the ATP pocket which confers potency and specificity (Davies et al., 2002b; Gibson et al., 2002). The remainder of the NU series of molecules are likely further N² substituted O⁶-cyclo-hexylmethylguanine derivatives though complete structures have not been disclosed to date (Hardcastle et al., 2004; Mesguiche et al., 2003). In addition to inhibiting Cdk1 and Cdk2, a subset of the NU molecules were found to inhibit Nek2A in a specificity counter-screen (D.R. Newell, personal communication). The NU series of compounds were therefore used to develop *in vitro* assays for Nek2A inhibition in preparation for compounds identified in the Nek2A HTS.

Initially the NU series of molecules were incubated with his₆NekA T175E/F386A, a Nek2A mutant that contains two activating amino acid substitutions outside the ATP binding region and hence produces a greater signal in *in vitro* assays. The F386A mutation is thought to prevent binding of the inhibitory phosphatase PP1 and the T175E mutation (Baxter, 2006). Ten NU series compounds were provided as 10 mM stocks in DMSO: NU2058, NU6094, NU6102, NU6136, NU6140, NU6141, NU6225, NU6236, NU6242 and NU6250. Each inhibitor was added to an *in vitro* kinase assay at a final concentration of 100 μ M with 5 mM MnCl₂, 4 μ M ATP, 0.5 μ g/ μ l β -casein and 20 nCi ³²P- γ -ATP/ μ l. Total cell lysate of Sf9 insect cells expressing his₆NekA T175E/F386A was added at a final concentration of 0.1 μ l/ μ l assay. This equated to approximately 8 ng of his₆NekA T175E/F386A per μ l of reaction. DMSO alone, comprising 2.5% of the assay volume served as a carrier control. Complete reactions were incubated at 30°C for 30 minutes. Completed reactions were resolved by SDS-PAGE, stained with Coomassie Blue, dried under vacuum and the protein band corresponding to ³²P- β -casein visualised by autoradiography (Figure 6.3A). The degree of ³²P incorporation was determined by excision of the band corresponding to β -casein and liquid scintillation counting. Nek2A activity in the presence of each inhibitor was calculated as a percentage of the incorporation observed without inhibitor or DMSO present.

The majority of the inhibitors reduced Nek2A activity to approximately 10% or less of that observed with the carrier, DMSO, whilst NU2058, 6094 and 6225 effected a reduction of approximately 50% (Figure 6.3B). The same pattern emerged when the assay was repeated with purified wild-type his₆Nek2A (Upstate) (Figure 6.3C). The reaction conditions used to determine the activity of wild-type his₆Nek2A were identical to those used with the his₆NekA T175E/F386A except for the quantity of kinase. Purified wild-type his₆Nek2A was used at 2 ng/ μ l.

6.2.3 NU compounds have μ M IC₅₀ values against his₆Nek2A *in vitro*

To determine the concentration of inhibitor required to reduce Nek2A activity to 50% of maximal (IC₅₀), serial dilutions of the seven most effective inhibitors plus NU6225 were prepared in DMSO in approximately log steps. Briefly, inhibitors dissolved in DMSO were added to complete *in vitro* kinase assays at final

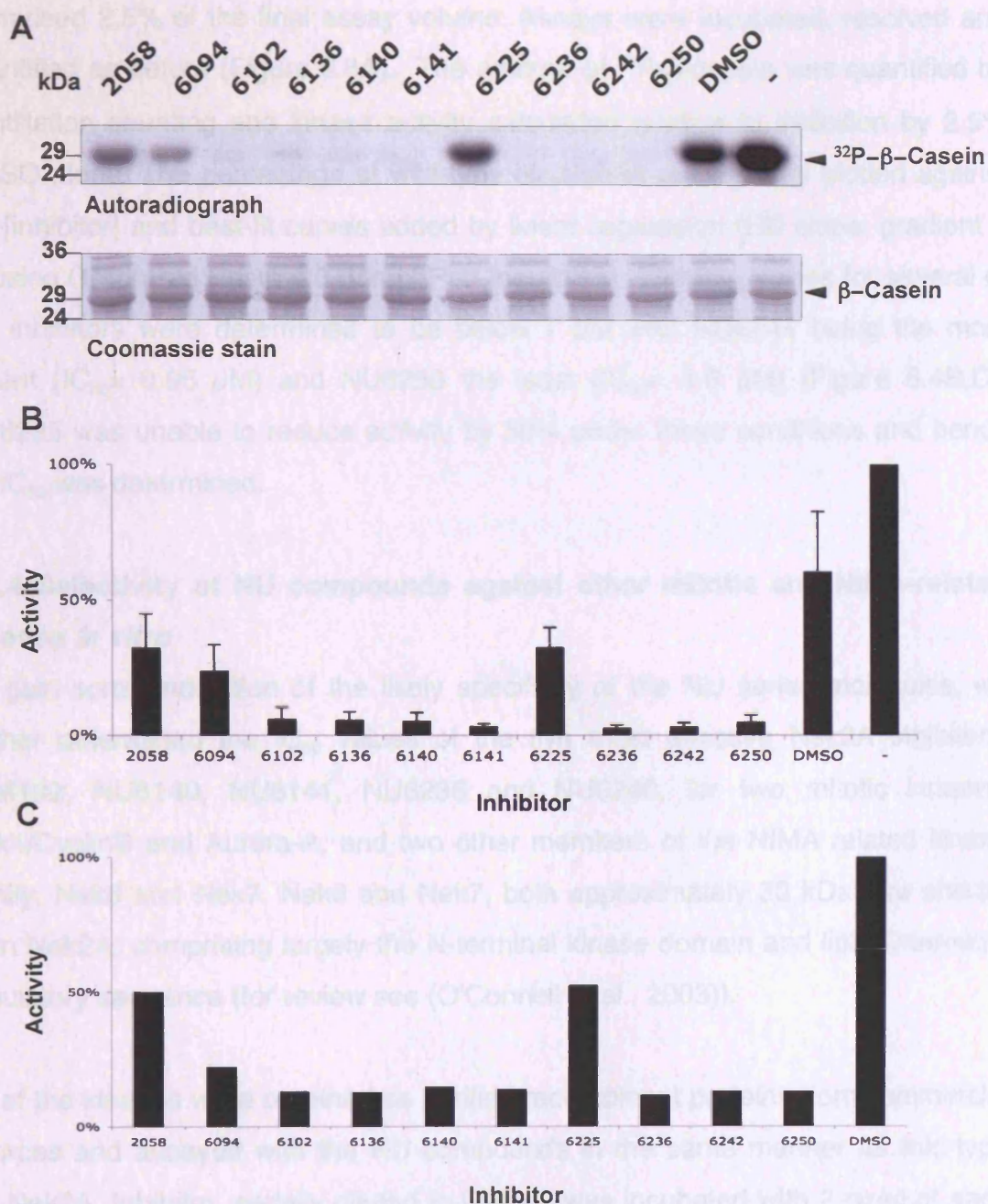


Figure 6.3 100 μ M NU series compounds inhibit Nek2A *in vitro*

A. Sf9 insect cells infected with a baculoviral construct expressing his₆Nek2A T175E, F386A were lysed and the lysate incubated with β -Casein at a final concentration of 0.5 μ g/ μ l in the presence of 100 μ M inhibitor in DMSO, DMSO alone or no carrier. The kinase reactions were stopped by boiling with an equal volume of sample buffer and an aliquot resolved by SDS-PAGE and the degree of ³²P incorporation determined by autoradiography of the dried gels. **B.** The bands corresponding to β -Casein were excised and the degree of ³²P incorporation quantified by scintillation counting. The mean percentage inhibition is shown from three independent experiments. Error bars indicate standard deviation. **C** 20 ng his₆Nek2A (Upstate) incubated with β -Casein at a final concentration of 0.5 μ g/ μ l in the presence of 100 μ M inhibitor in DMSO or DMSO alone and similarly quantified by scintillation counting. The pattern of inhibition with wild-type kinase is the same as that observed with the hyperactive mutant.

concentrations of 250 μ M, 100 μ M, 10 μ M, 5 μ M, 1 μ M, 100 nM and 10 nM and comprised 2.5% of the final assay volume. Assays were incubated, resolved and quantified as before (Figure 6.3A). The amount of 32 P- β -casein was quantified by scintillation counting and kinase activity calculated relative to inhibition by 2.5% DMSO alone. The percentage of wild-type his₆Nek2A activity was plotted against log [inhibitor] and best-fit curves added by linear regression (Hill slope, gradient = 1) using GraphPad Prism 4.0 (GraphPad Inc., USA). The IC₅₀ values for several of the inhibitors were determined to be below 7 μ M with NU6141 being the most potent (IC₅₀ = 0.95 μ M) and NU6250 the least (IC₅₀ = 6.8 μ M) (Figure 6.4B,C). NU6225 was unable to reduce activity by 50% under these conditions and hence no IC₅₀ was determined.

6.2.4 Selectivity of NU compounds against other mitotic and NIMA-related kinases *In vitro*

To gain some indication of the likely specificity of the NU series molecules, we further determined the IC₅₀ values of the five most effective Nek2A inhibitors: NU6102, NU6140, NU6141, NU6236 and NU6240, for two mitotic kinases, Cdk1/CyclinB and Aurora-A, and two other members of the NIMA related kinase family, Nek6 and Nek7. Nek6 and Nek7, both approximately 30 kDa, are shorter than Nek2A, comprising largely the N-terminal kinase domain and little C-terminal regulatory sequence (for review see (O'Connell et al., 2003)).

All of the kinases were obtained as purified recombinant proteins from commercial sources and assayed with the NU compounds in the same manner as wild-type his₆Nek2A. Inhibitor, serially diluted in DMSO, was incubated with 2 ng/ μ l of each kinase. Completed reactions were resolved by SDS-PAGE, kinase activity quantified and IC₅₀ values calculated as before. The NU compounds are all derived from a lead structure that is a potent inhibitor of both Cdk1/CyclinB and Cdk2/CyclinA, so it is reasonable to assume that molecules derived from it will retain some of that activity. Indeed NU6102, NU6141, NU6236 and NU6242 are all equipotent against Cdk1/CyclinB and Nek2A. However, whereas NU6140 inhibits Nek2A (IC₅₀ = 1.7 μ M), it surprisingly has no efficacy against Cdk1/CyclinB in this assay (IC₅₀ > 250 μ M) (Figure 6.5A). Activity against Aurora-A and Nek2A is also

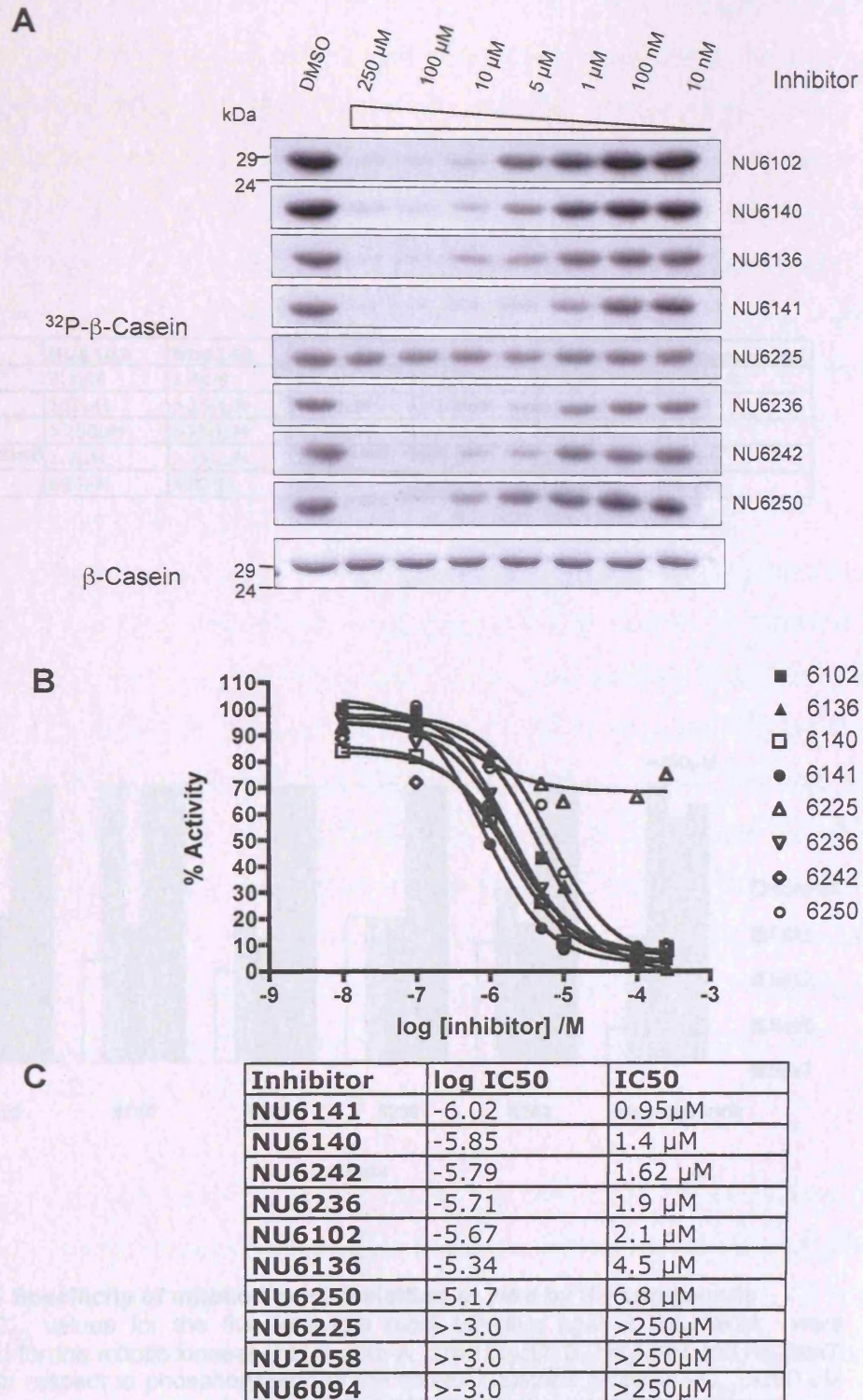


Figure 6.4 NU compounds his₆Nek2A *in vitro* IC₅₀

A. 20 ng his₆Nek2A (Upstate) was incubated with inhibitor at final concentrations from 10 nM to 100 μM as indicated. Reactions were resolved by SDS-PAGE and β-casein phosphorylation determined by autoradiography **B.** β-casein phosphorylation was quantified by scintillation counting of the excised band and the degree of phosphorylation expressed as a percentage with respect to that observed with DMSO alone and IC₅₀ determined by fitting a variable hill slope equation (Prism, Graphpad). **C.** Tabulated IC₅₀ values.

A

Enzyme	Inhibitor					
	NU6102	NU6140	NU6141	NU6236	NU6242	Staurosporine
his ₆ Nek2	2.1μM	1.4μM	950nM	1.9μM	1.6μM	>250μM
his ₆ Nek6	162μM	>250μM	>250μM	>250μM	>250μM	75μM
his ₆ Nek7	>250μM	>250μM	>250μM	>250μM	>250μM	125μM
his ₆ Cdk1/GSTcyclinB	1.2μM	>250μM	2μM	1.9μM	5.6μM	977nM
his ₆ AuroraA	695nM	430nM	280nM	2μM	800nM	34nM

B

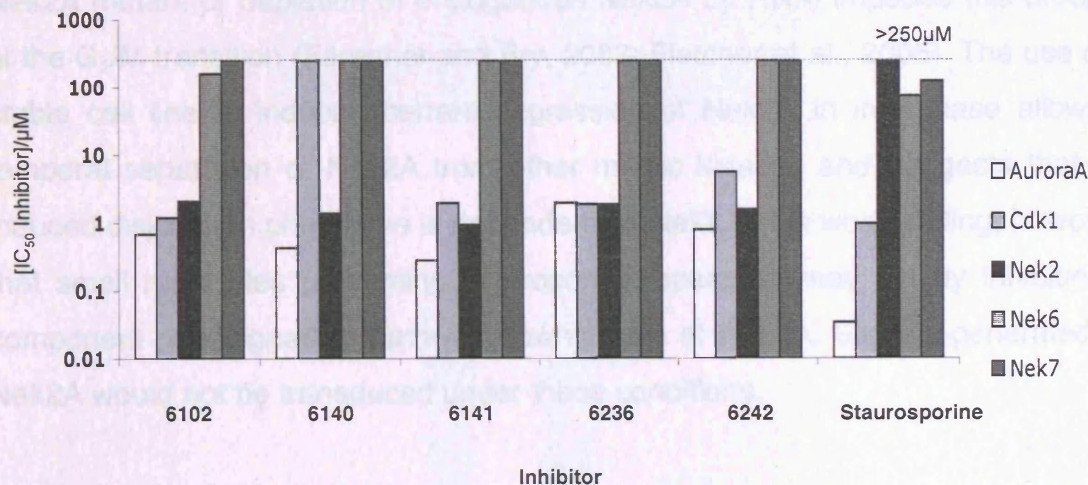


Figure 6.5 Specificity of mitotic kinase inhibition *in vitro* by NU compounds
A. The IC₅₀ values for the five inhibitors most effective against his₆Nek2A were determined for the mitotic kinases his₆Aurora-A, Cdk1/Cyclin B, his₆Nek6 and his₆Nek7 *in vitro* with respect to phosphorylation of the control substrate β-casein. IC₅₀ >250 μM denotes that no inhibition was observed at 250 μM inhibitor, the highest concentration used in the assay. **B.** Inhibitors active against Nek2A were largely equipotent against Cdk1/cyclinB and Auror-A. Nek6 and Nek7, homologous to the Nek2 kinase domain but lacking the C-terminal regulatory domain, were only inhibited to any significant degree by staurosporine

closely linked in these NU compounds. NU6102, NU6140, NU6141 and NU6242 have IC_{50} values against Aurora-A two to three fold lower than those determined for Nek2A. The exception is NU6236 which inhibits Nek2A and Aurora-A approximately equally with IC_{50} values of 1.9 μ M and 2.0 μ M, respectively. Interestingly, neither Nek6 nor Nek7 was significantly amenable to inhibition by any of the NU compounds (Figure 6.5B). The pan-kinase inhibitor staurosporine was most effective against Aurora-A (IC_{50} = 34 nM) and Cdk1/CyclinB (IC_{50} = 977 nM). The NIMA-related kinases Nek2A, Nek6 and Nek7 were relatively refractory to staurosporine with IC_{50} values of > 250 μ M, 75 μ M and 125 μ M, respectively.

6.2.5 NU6141 inhibits GFP-Nek2A induced centrosome disjunction

The most well characterised role of Nek2A is the regulation of centrosome disjunction. Ectopic overexpression of recombinant active Nek2A in interphase induces premature centrosome. Conversely, either expression of an inactive Nek2A mutant or depletion of endogenous Nek2A by RNAi impedes this process at the G₂/M transition (Faragher and Fry, 2003; Fletcher et al., 2005). The use of a stable cell line to induce aberrant expression of Nek2A in interphase allows a temporal separation of Nek2A from other mitotic kinases and suggests that the induced disjunction phenotype is dependent on Nek2A. It is worth noting, however, that small molecules preventing centrosome separation may act by inhibiting a component of a signalling pathway downstream of Nek2A. Signals generated by Nek2A would not be transduced under these conditions.

Asynchronous U2OS:GFP-Nek2A cells were induced with doxyxycycline in complete growth media supplemented with NU6141, the most effective *in vitro* Nek2A inhibitor, at a final concentration of 20 μ M or the equivalent (% v/v) of DMSO carrier. Centrosomes were considered “split” at distances greater than 2 μ m apart. Supplementation with NU6141 inhibited Nek2A dependent disjunction, as determined by staining fixed cells for the centrosomal marker γ -tubulin, with treated cells retaining paired centrosomes despite the presence of active GFP-Nek2A (Figure 6.6A). Quantification of this phenotype showed that treatment with 20 μ M NU6141 completely ablated the GFP-Nek2A induced splitting, reducing it to the basal level observed without induction of the kinase (Figure 6.6B).

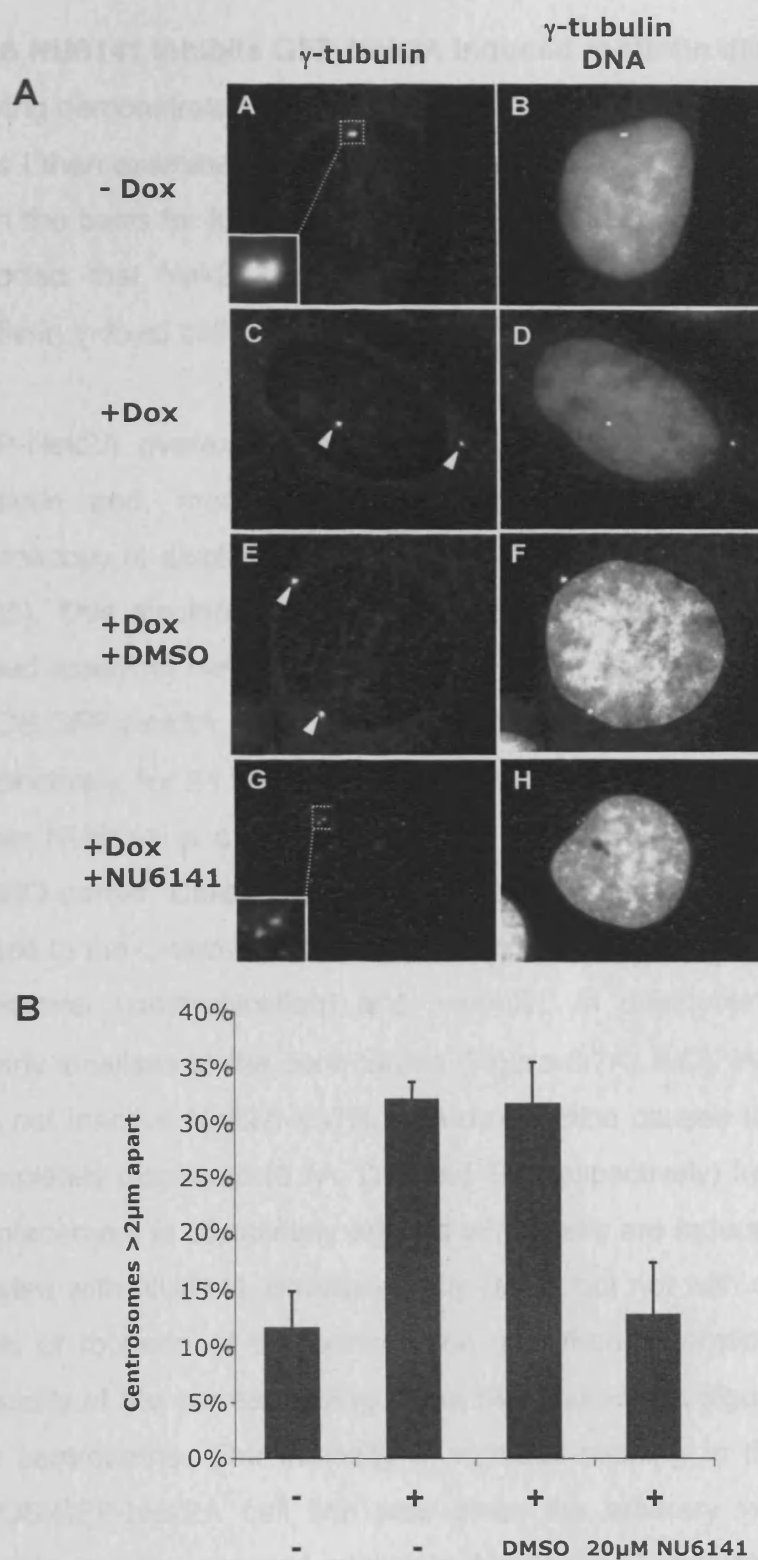


Figure 6.6 NU6141 inhibits Nek2A induced centrosome splitting.

A. U2OS:GFP-Nek2A stable cells were either untreated (A,B) or induced to express GFP-Nek2A by the addition of doxycycline (C-H) in the presence of 20 μ M NU6141 (G,H) or DMSO (E,F) for 24 hours. Cells were processed for immunofluorescence microscopy and stained for γ -tubulin and DNA. Interphase centrosomes are normally paired (A, magnified inset). However, expression of GFP-Nek2A induces splitting (arrowed, C, D); this is inhibited by NU6141 (D, magnified inset). **B.** Centrosomes greater than 2 μ m apart in interphase were scored as split for each condition. NU6141 reduces GFP-Nek2A induced splitting to control levels.

6.2.6 NU6141 inhibits GFP-Nek2A induced rootletin displacement

Having demonstrated that an *in vitro* inhibitor of Nek2A could also inhibit Nek2A in cells I then examined other known Nek2 substrates to see if their regulation could form the basis for further assays of Nek2 inhibition in cells. It has previously been reported that Nek2A interacts with rootletin, co-localising with overexpressed rootletin in fixed cells and phosphorylating it at multiple sites *in vitro*.

GFP-Nek2A overexpression results in a phosphorylation dependent upshift of rootletin and, more importantly, has been shown by immunofluorescence microscopy to displace it from the centrosome as disjunction occurs (Bahe et al., 2005). This displacement of rootletin by GFP-Nek2A comprises the second cell based assay for Nek2 inhibition. A pair of stable cell lines, U2OS:GFP-Nek2A and U2OS:GFP-Nek2A K37R were induced to overexpress active and inactive kinase, respectively, for 24 hours in the presence or absence of media supplemented with either NU6141 at a concentration of 20 μ M or an equivalent amount (1% v/v) of DMSO carrier. Cells were then fixed and stained with rabbit polyclonal antibodies raised to the C-terminus of rootletin (amino acids 1651-2017, A. Tsai and A.M. Fry, personnel communication) and γ -tubulin. In uninduced control cells, rootletin clearly localises to the centrosome (Figure 6.7A, A-C). Induction of active Nek2A, but not inactive Nek2A-K37R, with doxycycline causes rootletin to be reduced or completely displaced (6.7A, D-F and G-I, respectively) from the centrosome. This displacement is completely ablated when cells are induced with doxycycline and treated with NU6141 simultaneously (M-O) but not with carrier (J-L). The relative level of rootletin at the centrosome was then determined by quantifying mean intensity of the corresponding Alexa 594 fluorescent signal in a fixed area around the centrosome. The intensity of rootletin staining in the uninduced, untreated U2OS:GFP-Nek2A cell line was given the arbitrary value of 1 and all other conditions are expressed relative to this (6.7B). Quantification shows that while the overexpression of kinase dead Nek2A-K37R does not affect levels of centrosomal rootletin, induction of wild-type kinase either alone or in the presence of DMSO carrier reduces rootletin staining to 80 and 50% of control levels, respectively, reinforcing the dependence on kinase activity previously reported in the literature. Strikingly, upon induction of GFP-Nek2A, 20 μ M NU6141 not only prevents

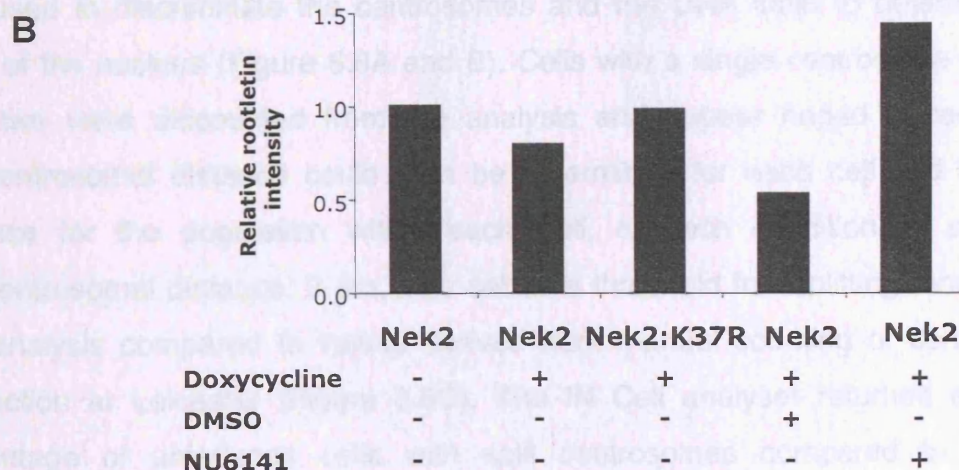
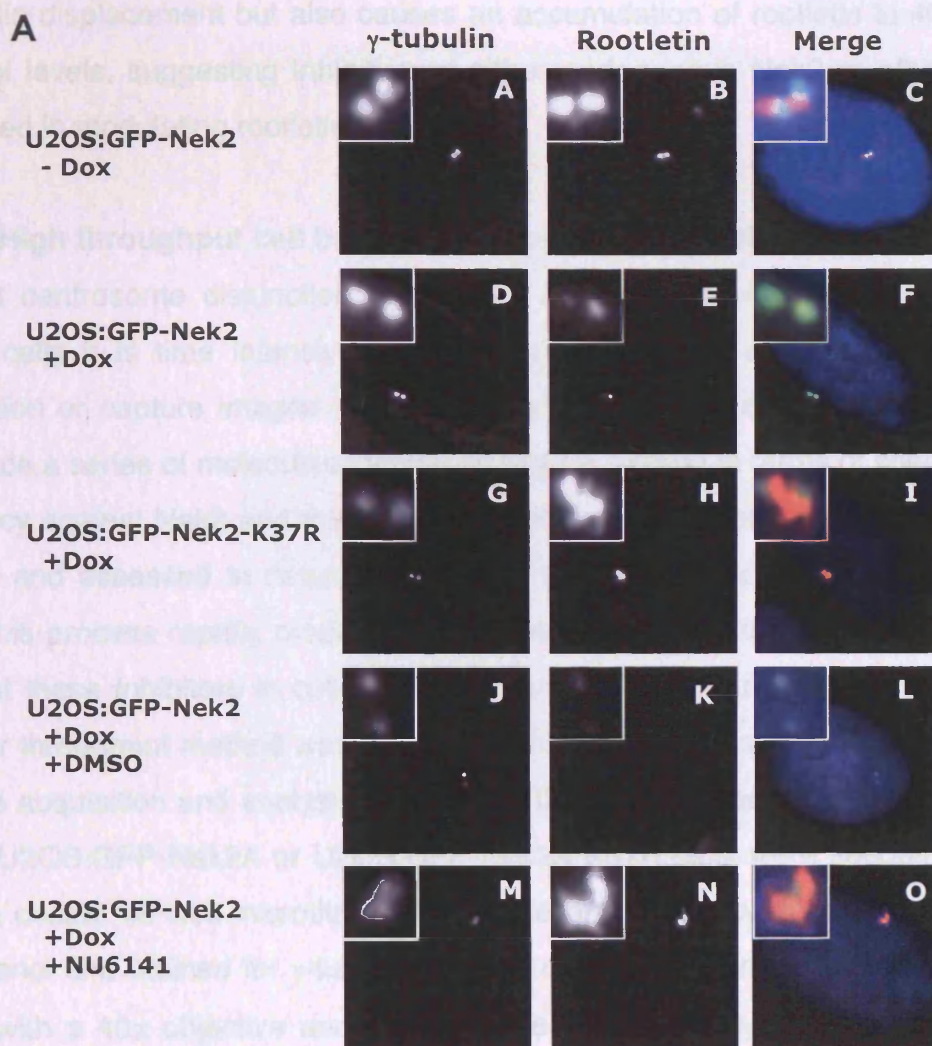


Figure 6.7 NU6141 inhibits Nek2A induced rootletin displacement

A. U2OS:GFP-Nek2A cells were induced to express GFP-Nek2-K37R (G-I) or GFP-Nek2A (D-F, J-O) by addition of doxycycline in the presence of 20 μ M NU6141 (M-O) or DMSO (J-L) for 24 hours. Cells were processed for immunofluorescence microscopy and stained for γ -tubulin, rootletin and DNA. The expression of wild type (but not kinase dead, K37R) GFP-Nek2A displaces rootletin from the centrosome (D-F, magnified inset). This displacement is inhibited by NU6141. **B.** The intensity of rootletin staining at the centrosome ($n > 50$) was quantified and is displayed as fold-change relative to uninduced cells.

rootletin displacement but also causes an accumulation of rootletin to 40% above control levels, suggesting inhibition of either endogenous Nek2 or other kinases involved in modulating rootletin localization.

6.2.7 High throughput cell based assay for Nek2A inhibition

Whilst centrosome disjunction or rootletin displacement is readily quantified in fixed cells it is time intensive to manually score fields of cells for the former condition or capture images and determine the latter. Undertaking a HTS would produce a series of molecules that would require refining in terms of specificity and potency against Nek2 and this is an iterative process. Chemical modifications are made and assessed to determine whether they improve on the parent molecule and this process rapidly produces numerous compounds to be assayed. In order to test these inhibitors in cells rapidly to inform the next round of modification a higher throughput method was sought. To this end I have assessed an automated image acquisition and analysis system, the IN Cell analyzer 1000 (GE Healthcare, UK). U2OS:GFP-Nek2A or U2OS:GFP-Nek2A K37R cells were seeded in poly-L-lysine coated 96 well microtitre plates, induced with doxycycline, fixed with -20°C methanol and stained for γ -tubulin. Images of the well were then acquired by GE staff with a 40x objective and the fluorescent signal analysed. γ -tubulin intensity was used to discriminate the centrosomes and the DNA stain to determine the limits of the nucleus (Figure 6.8A and B). Cells with a single centrosome or more than two were discounted from the analysis and appear ringed in red. The intercentrosomal distance could then be determined for each cell and a mean distance for the population within each well, or each condition. A specified intercentrosomal distance, $2\text{ }\mu\text{m}$, was set as a threshold for “splitting” and the IN Cell analysis compared to values derived from manual counting of centrosome disjunction at Leicester (Figure 6.8C). The IN Cell analyser returned a higher percentage of uninduced cells with split centrosomes compared to manual counting. This is likely due to cells with two closely spaced unsplit centrosomes presenting a single γ -tubulin focus and being excluded from subsequent analysis. This would remove a significant number of cells with unsplit centrosomes, artificially inflating the proportion of split centrosomes in cells without Nek2 induction. The automated InCell image capture and analysis has the potential to

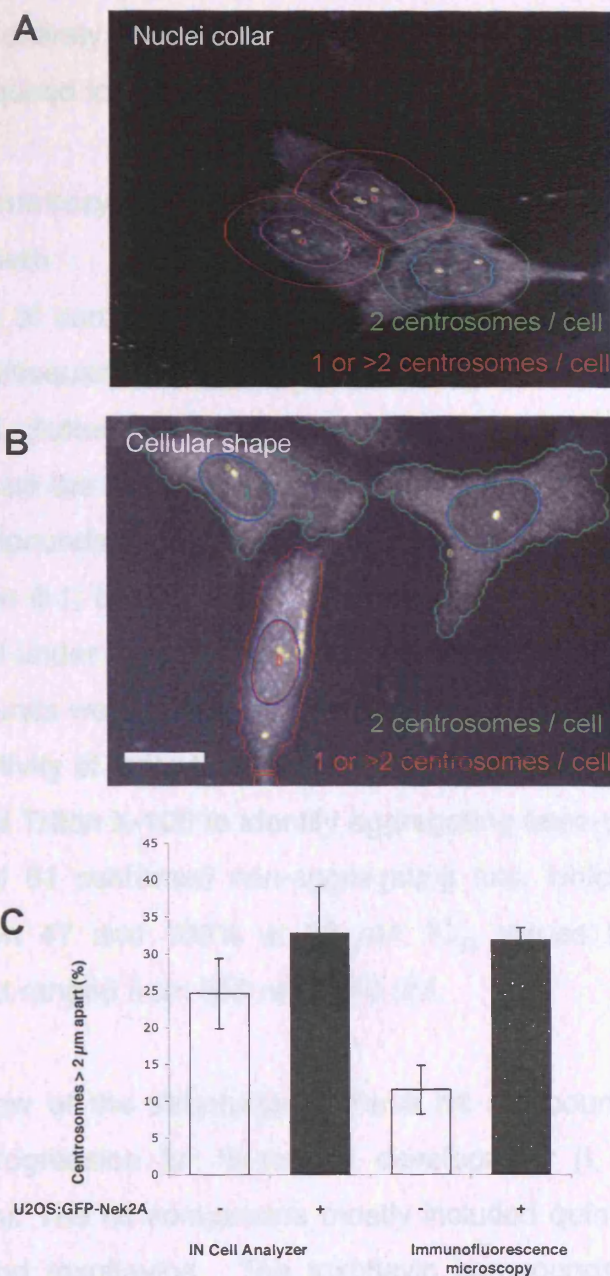


Figure 6.8. A high throughput cell based assay for Nek2: InCell Analysis of Nek2-induced centrosome splitting.

A, B. U2OS:GFP-Nek2A stable cells were induced to express GFP-Nek2A by the addition of doxycycline for 24 hours. Cells were processed for immunofluorescence microscopy and stained for γ -tubulin (Alexa 488) and DNA (Hoechst). Cells were then subject to automated analysis by an IN Cell analyzer 1000 (GE Healthcare) to discriminate centrosomes and cell nuclei. The periphery of cells was determined by considering either a uniform distance from the nucleus ("nuclear collar") or the margins of fluorescent staining ("cellular shape"). Only cells with two centrosomes are included in subsequent analyses. Scale bar 10 μ m. **C.** The inter-centrosomal distance is then defined for each cell and a user defined threshold set to produce percentage values for split and non-split centrosomes for the whole population. The reduction in centrosome splitting due to compounds inhibiting Nek2 in cells can then be assessed automatically on a whole population basis. Quantification compares splitting values determined by the IN Cell system with fluorescence microscopy and manual counting. IN Cell images and analysis courtesy M. Francis, GE healthcare.

effectively identify split and unsplit centrosomes. I am currently determining whether the entirely automated analysis can provide the accuracy and processivity required for assays of Nek2 inhibition in cells.

6.2.8 Nek2 inhibitory compounds identified in the HTS reduce HeLa and U2OS cell growth

The NU series of compounds were used to validate the conditions for the HTS which was subsequently undertaken by colleagues at the Institute for Cancer Research (ICR, Sutton). Employing purified GST-Nek2A (Stressgen, USA) and MBP as substrate the Flashplate assay returned values for the inhibition of Nek2A by the NU compounds similar to those I derived from gel-based *in vitro* assays at Leicester (Table 6.1, below). The HTS using the CRUK compound collection was then performed under the conditions optimised with the NU compounds. A total of 65,066 compounds were screened by staff at the ICR, giving 162 confirmed hits (a reduction in activity of more than 50 % at 32 μ M). These hits were re-screened in the presence of Triton X-100 to identify aggregating false-positives. This led to the identification of 61 confirmed non-aggregating hits, which inhibited GST-Nek2A kinase between 47 and 100% at 32 μ M. IC₅₀ values for these 61 hits were determined and ranged from 650 nM to 70 μ M.

Following review of the structures of these hit compounds none were deemed suitable for progression for hit-to-lead development (I. Collins, ICR, personal communication). The hit compounds mostly included quinones, metal complexes, polyphenols and toxoflavins. The toxoflavin compounds have been previously reported in patent literature as broad-spectrum kinase inhibitors (I. Collins, ICR, personal communication). Though the HTS did not identify any hits that could progress to lead development, a number of compounds did show significant inhibition of GST-Nek2A *in vitro*. Two HTS compounds, CC004731 and CC004733, are structurally related to the fungal antibiotics wortmannin and viridin and, though unsuitable for progression as lead molecules in the Nek2A inhibitor programme, were subjected to further cell based assays in Leicester. Data generated with compounds CC004731 and CC004733 will form the basis of a publication detailing the Nek2 HTS.

To determine the effects of CC004731 and CC004733 on cell viability, serial dilutions ranging from 100 μ M to 1 nM of the compounds in DMSO were incubated with cultured HeLa and U2OS cells for 72 hours. The structurally related compound wortmannin and the pan-kinase inhibitor staurosporine were included for comparison. Cell viability was measured after 72 by WST-1 assay and the GI_{50} , the concentration of compound which inhibited growth by 50%, calculated. In keeping with its broad inhibitory profile, staurosporine had the greatest effect on cell viability with a GI_{50} of 2.2 nM and 59.3 nM in U2OS and HeLa cells, respectively (Figures 6.9 and 6.10). The impact upon growth of the HTS compounds was approximately equivalent in both cell lines. The GI_{50} of CC004731 was 1.8 μ M in HeLa cells and 2.5 μ M in U2OS cells, respectively. Similarly, CC004733 reduced HeLa and U2OS cell growth with a GI_{50} of 10.2 μ M and 6.4 μ M. Lastly, the GI_{50} values for wortmannin were 15 μ M in HeLa cells and 23.7 μ M in U2OS cells.

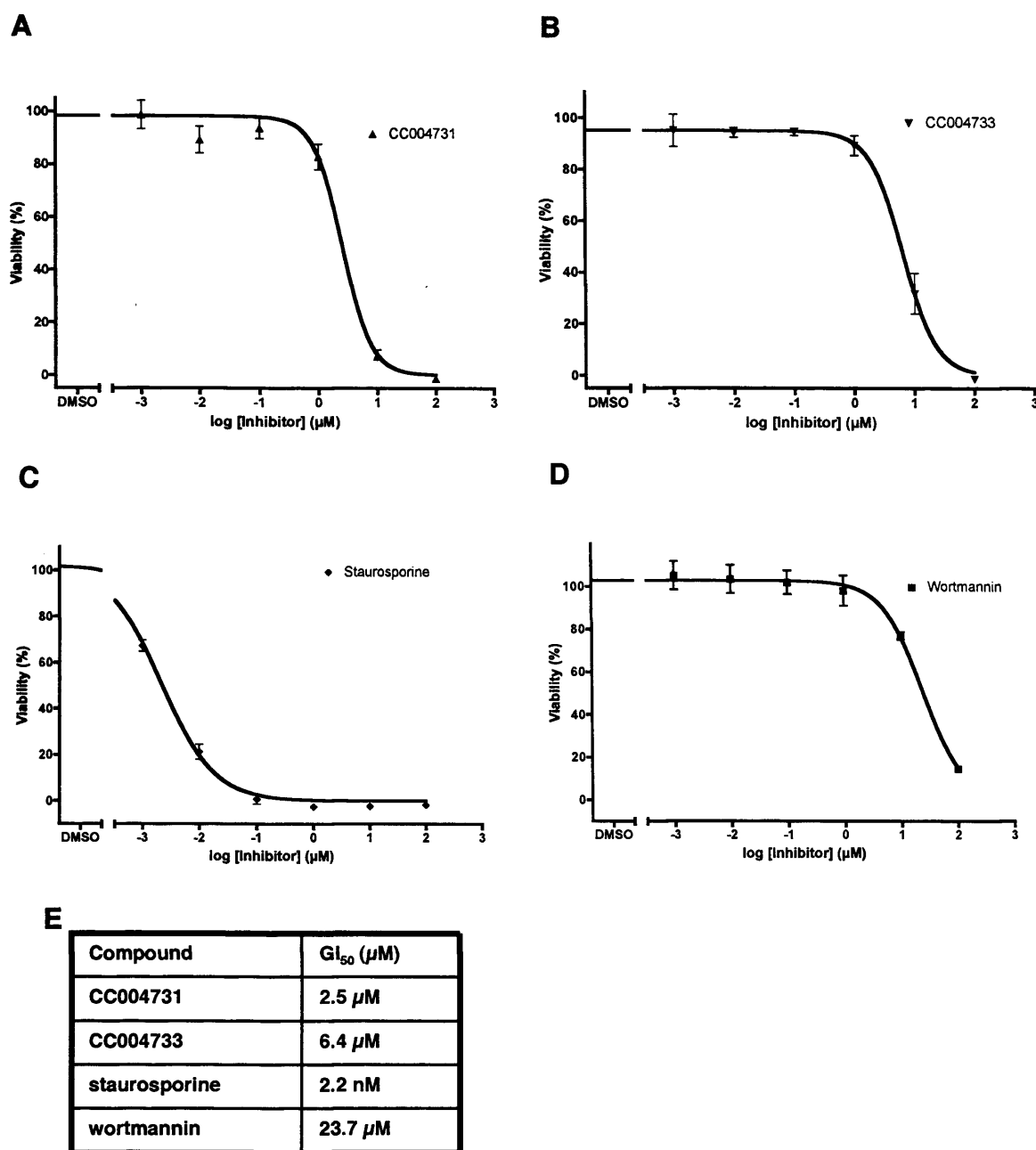


Figure 6.9 Growth inhibition of U2OS cells by HTS compounds CC004731 and CC004733
 U2OS cells were seeded in complete culture medium at a density of 6×10^3 cells / cm² in 96 well plates. Inhibitors dissolved in DMSO, or DMSO alone, were added in log steps at final concentrations of 100 μM to 1 nM. DMSO or DMSO plus inhibitor comprised 1% (v/v) of the final culture medium. To assess cell viability after 72 hours cells were first washed twice with complete medium to remove the inhibitors before the addition of 10 μl WST reagent (Merck) per well. Cells were incubated for a further two hours at 37°C before determining the OD₄₅₀ of each well in a micotitre plate reader (Bio-Rad, USA). Viability was determined as a percentage of DMSO treated cells **A**. HeLa cell viability following treatment with HTS hit compound CC004731 **B**. HTS hit compound CC004733 **C**. staurosporin **D**. wortmannin **E**. GI₅₀ values obtained for each inhibitor

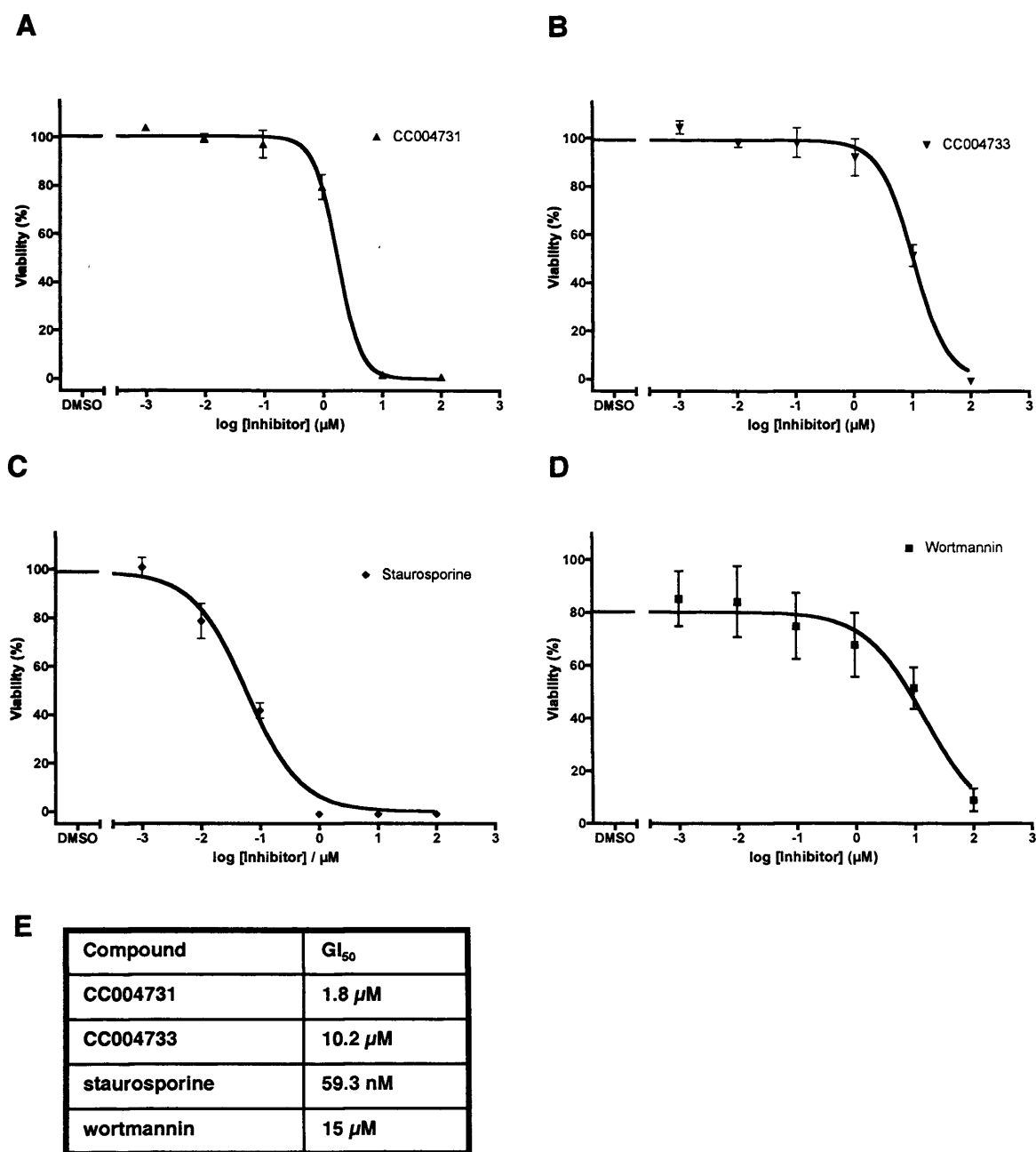


Figure 6.10 Growth inhibition of HeLa cells by HTS compounds CC004731 and CC004733

HeLa cells were seeded in complete culture medium at a density of 1×10^4 cells / cm^2 in 96 well plates. Inhibitors dissolved in DMSO, or DMSO alone, were added in log steps at final concentrations of 100 μ M to 1 nM. DMSO or DMSO plus inhibitor comprised 1% (v/v) of the final culture medium. To assess cell viability after 72 hours cells were first washed twice with complete medium to remove the inhibitors before the addition of 10 μ l WST reagent (Merck) per well. Cells were incubated for a further two hours at 37°C before determining the OD₄₅₀ of each well in a microtitre plate reader (Bio-Rad, USA). Viability was determined as a percentage of DMSO treated cells **A.** HeLa cell viability following treatment with HTS hit compound CC004731 **B.** HTS hit compound CC004733 **C.** staurosporine **D.** wortmannin **E.** GI₅₀ values obtained for each inhibitor

6.3 DISCUSSION

Centrosomes are the dominant microtubule organising centres in mammalian cells, affecting cell morphology, polarity and the fidelity of mitotic division (Doxsey et al., 2005). The presence of multiple centrosomes also correlates strongly with the pathology of human cancer (Pihan et al., 2003b; Saunders, 2005) and hence mitotic kinases governing centrosome regulation such as Plk1, Aurora-A and Aurora-B are currently the subject of considerable pharmaceutical interest. Several Aurora kinase inhibitors are progressing through to the clinic with the small molecules AZD1152 (AstraZeneca) and VX-680 (Merck & Co./Vertex Pharmaceuticals) being assessed in Phase I and II trials, respectively. Similar efforts are being made with inhibitors of Cdks such as R-roscovitine (Cyclacel) and alvocidib (Flavopiridol, NCI/Sanofi-Aventis). Both of these molecules are relatively broad pan-Cdk inhibitors and there are issues with toxicity (Benson et al., 2005).

The ultimate aim of the project is to undertake a high throughput screen and identify novel molecules which could then become the leads for development of a potent, specific inhibitor of Nek2. Whilst planning a Nek2 HTS, I was given access to a series of ATP competitive molecules originally synthesized by Newcastle University for efficacy against Cdk1/CyclinB and Cdk2/CyclinA (Arris et al., 2000; Gibson et al., 2002), which had shown some activity against Nek2A in a counterscreen of mitotic kinases (D.R. Newell, personal communication). The Newcastle University (NU) series of molecules were used to develop *in vitro* assays to facilitate the HTS and also to trial cell based assays which could be used to assess HTS hits for *in vivo* activity as well as cell membrane permeability and toxicity.

Initial experiments considered the *in vitro* efficacy of the ten NU molecules, incubating them at a single concentration, 100 μ M, with both a hyperactive mutant and wild type his₆Nek2A. The reduction in activity compared to the drug carrier demonstrated that Nek2A is indeed amenable to small molecule inhibition *in vitro* and that a range of inhibition was obtained by molecules that are all derivatives of the same chemotype, a substituted O⁶-cyclo-hexylmethylguanine, but with a

variety of substituent side chains at the N² position. The seven most potent inhibitors of both wild-type and mutant his₆Nek2A reduced activity to less than ten percent of that seen with the control, with the remaining three effecting a reduction to between twenty and thirty percent. The most effective inhibitors at 100 μ M were then examined to determine *in vitro* IC₅₀ values and allow comparison of potency.

The NU inhibitors were incubated with his₆Nek2A, constant [ATP] and inhibitor diluted in approximately log steps. The resulting IC₅₀ values fell into three groups; approximately 1 μ M, 4-8 μ M and then > 250 μ M (i.e. those compounds that were not effective at the highest concentration used in the assay). The spectrum of activities is initially encouraging, suggesting that further potency can be achieved with more chemical modifications. The NU series molecules were also used to test the FlashPlate assay format proposed for the HTS. The FlashPlate assays employed recombinant GST-Nek2A and MBP as the substrate rather than the his₆Nek2A and β -casein used in the gel-based assay. Reassuringly the IC₅₀ values derived for Nek2A inhibition by each NU compound were similar, regardless of the assay format employed (Table 6.1, below).

Compound	Nek2A IC ₅₀ (μ M)	
	Gel based assay	Flashplate assay
NU6141	0.95	2
NU6140	1.4	-
NU6242	1.62	5.5
NU6236	1.9	-
NU6102	2.1	3
NU6136	4.5	4
NU6250	6.8	12.4
NU6225	>250	No inhibition
NU2058	>250	No inhibition
NU6094	>250	No inhibition

Table 6.1 Comparison of IC₅₀ values of NU series against Nek2A generated by gel-based and flashplate assays.

Having established relative potencies for the most effective NU compounds, I then sought to determine *in vitro* specificities by testing them against two mitotic kinases, Cdk1/CyclinB and Aurora-A, and two NIMA related kinases, Nek6 and Nek7. The five most effective compounds against Nek2A: NU6102, NU6140, NU6141, NU6236 and NU6242, as well as the promiscuous pan-kinase inhibitor staurosporine, were incubated with commercially obtained recombinant Cdk1/cyclinB, Aurora-A, Nek6 and Nek7 and IC₅₀ values determined. The most obvious trend from the data is that the NU molecules show a striking discrimination between the mitotic kinases and the other NIMA related kinases, being potent against Aurora-A and Cdk1/Cyclin B, but with Nek6 and Nek7 being almost completely refractory to inhibition. The most effective inhibitor of either Nek6 or Nek7, aside from staurosporine, was NU6102 which had an IC₅₀ of 160 μ M with respect to Nek6, approximately 80 times greater than that determined for Nek2A. This is surprising and encouraging as, though Nek6 and Nek7 are severely truncated at their C-termini compared to either NIMA or Nek2A, the kinase domains are well conserved. Nek6 is similar both to Nek7, sharing 77% identity (Kimura and Okano, 2001a), and to the kinase domain of Nek2, with 38% identity at the protein level. If specificity of inhibition can be observed in such a limited examination of the Nek family it suggests that even limited divergence outside of the catalytic residues will indeed allow development of a specific Nek2A inhibitor. Conversely, whilst staurosporine inhibits both Nek6 and Nek7, it is ineffective against Nek2 in this assay, further reinforcing the possibility of specific inhibitors to related kinases. Within the scope of this investigation it also appears that β -casein is a satisfactory *in vitro* substrate for both Nek6 and Nek7, in contrast to a previous report (Hashimoto et al., 2002).

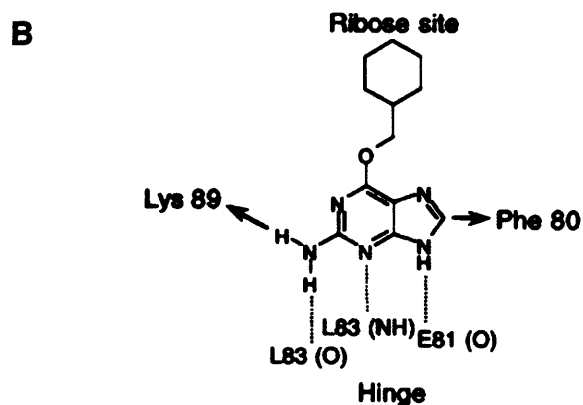
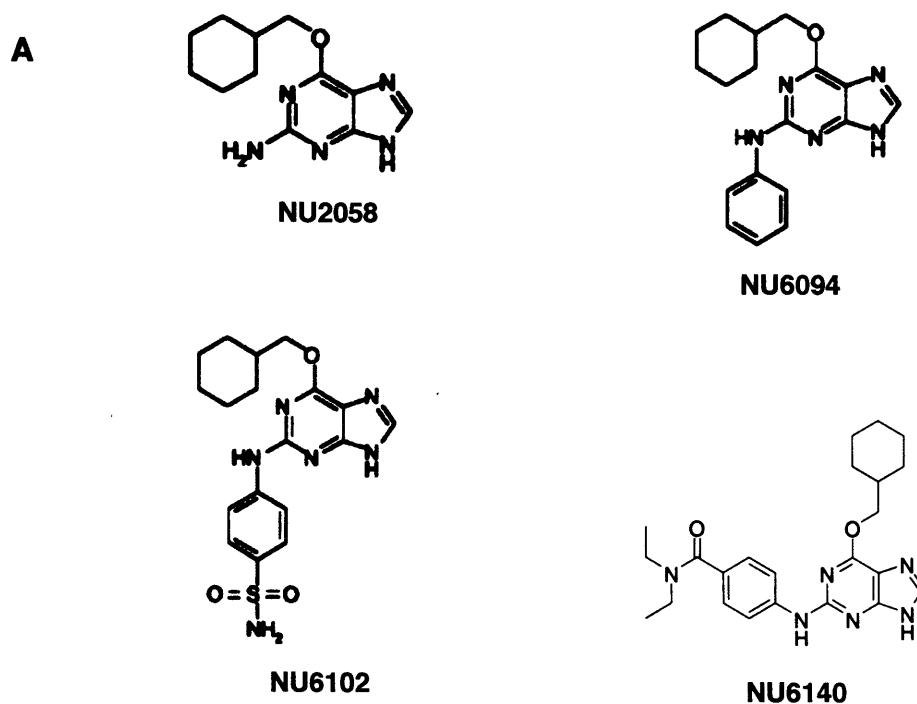
The NU molecules showed little inhibition of Nek6 or Nek7 but were generally potent inhibitors of Cdk1/Cyclin B, an expected consequence of their origin as molecules refined for activity against Cdk/Cyclin complexes. NU6102 and NU6236 were both more or equally effective against Cdk1/Cyclin B than Nek2A, whereas the opposite was true for NU6140 and NU6242 which were marginally more effective against Nek2A than Cdk1/Cyclin B. Though NU6140 did not show any efficacy against Cdk1/Cyclin B in this assay, it has been previously reported as

inhibiting Cdk1/Cyclin B with an IC_{50} of $6.6 \mu M$ *in vitro* (Pennati et al., 2005). Hence while, within an order of magnitude, the NU series molecules are equipotent against Cdk1/CyclinB and Nek2A, there are differences in potency which could be exploited to decrease activity against Cdks whilst increasing it against Nek2A.

Those structures that have been reported for the NU compounds tested here are purines that differ in the group substituted at the N² position (Figure 6.11 A). Crystal structures of phosphorylated T160pCdk2/CyclinA/NU2058 complexes suggest that this group projects out of the ATP binding cleft to interact with distal residues not directly involved with catalysis termed the specificity surface (Davies et al., 2002b). Further modification of this side chain may be the best starting point for increasing Nek2A specificity (Figure 6.11 B,C).

The last mitotic kinase to be tested with the NU compounds was Aurora-A. The NU molecules generally inhibited Aurora-A at least as effectively as Nek2A though again all the IC_{50} values for both kinases were within an order of magnitude, at approximately $1 \mu M$. The equipotent inhibition of both Nek2A and Aurora-A is unsurprising. Of the mitotic kinases with known structures, Nek2A is most similar to Aurora-A, with 31% sequence identity. The overall structures of Nek2A and Aurora A are also similar, 202 matched C α positions superimposing with an rms Δ of 1.8 angstroms (Rellos et al., 2006). In cells, Aurora inhibitors lead to failure of cytokinesis and an abrogated spindle checkpoint. It is suggested that the subsequent catastrophic mitosis, with a tetraploid genome and four centrosomes, drastically reduces cell viability and that this is exacerbated in cells lacking wild-type p53 (Ditchfield et al., 2003; Keen and Taylor, 2004). Aurora inhibitors so far characterised are not classic antimitotic agents and do not appear to affect non-cycling cells in the same manner as some Cdk inhibitors. It is therefore possible that a dual potency against both Nek2A and Aurora-A would not be therapeutically undesirable. Though a specific Nek2A inhibitor is sought, designing out Aurora-A activity is perhaps less pressing than reducing efficacy against Cdks.

The most potent Nek2A inhibitor, NU6141, was used to develop cell-based assays for Nek2 inhibition. Ectopic expression of GFP-Nek2A induces premature



C

Inhibitor	IC ₅₀				
	Nek2A Gel	Nek2A FP	CDK1/Cyclin B1	CDK2/Cyclin A3	CDK4/CyclinD1
NU2058	>250 μ M	No Inhibition	5 μ M	12 μ M	>100 μ M
NU6094	>250 μ M	No Inhibition	1.6 μ M	1 μ M	16 μ M
NU6102	2.1 μ M	3 μ M	9 <i>nm</i>	6 <i>nm</i>	1.6 μ M
NU6140	1.4 μ M	Not determined	6.6 μ M	410 <i>nM</i>	5.5 μ M

Figure 6.11 Structure and selectivity of selected NU Compounds

A. Structures of four NU series molecules. NU2058 is the parent of the chemotype, *O*⁶-cyclohexylmethylguanine. Substitution at the N2 position gives rise to NU6094 and NU6102 which is further modified to produce NU6140. **B.** Examination of NU2058 complexed with phosphorylated CDK2/CyclinA suggests that whilst the *O*⁶-cyclohexylmethyl side chain binds in the ribose site and the edge of the purine ring hydrogen bonds with the ATP binding cleft it is the N2 substituent that interacts with residues outside of the catalytic region and confers specificity of inhibition. A substituted 2-arylamino group appears to be necessary for activity against Nek2. **C.** *in vitro* IC₅₀ values for Nek2A, derived from gel based and flashplate (FP) assays, and three CDK/cyclin complexes. Values in italics are K_i. (adapted from Davies et al 2002 and Pennati et al., 2005).

disjunction, or “splitting”, of centrosomes and concomitant displacement of the proteins that putatively link them, including rootletin. Prevention of these processes can be used to assess the efficacy of an inhibitor. Both centrosome disjunction and displacement of rootletin were effectively inhibited in U2OS:GFP-Nek2A cells by supplementing growth media with 20 μ M NU6141. Inhibitor treatment effected a greater reduction in GFP-Nek2A induced centrosome splitting than rootletin displacement. Centrosome disjunction occurred in 32% of cells induced to express GFP-Nek2A and this was reduced to 10% in the presence of 20 μ M NU6141, the basal level observed in cells without overexpressed Nek2A. The intensity of centrosomal rootletin is reduced by 50% upon GFP-Nek2A induction but accumulates upon treatment with 20 μ M NU6141 to levels 40% greater than those observed in untreated cells. The accumulation of rootletin suggests an inhibition of either endogenous Nek2 or other kinases, possibly downstream of Nek2, that usually regulate levels of rootletin at the centrosome throughout the cell cycle. This would correspond with the model of rootletin being a flexible, perhaps dynamic, link between centrosomes (Bahe et al., 2005).

Centrosome disjunction induced in U2OS cells by GFP-Nek2A expression also lends itself to a higher throughput assay for Nek2 inhibition in cells. Fixed cells stained for centrosomal γ -tubulin with fluorophore conjugated antibodies can be subjected to automated image capture and analysis and the degree of splitting in response to a given drug treatment determined. Quantification of the splitting phenotype is an effective measure of Nek2A activity but it is also adversely influenced by factors affecting centrosome duplication and maturation. This is problematic when a significant proportion of the NU series of molecules are likely to have activity against Cdk2/CyclinA and Cdk2/CyclinE, both of which govern centrosome duplication (Hinchcliffe and Sluder, 2001b).

The use of recombinant kinases and ectopic GFP-Nek2A expression in stable cell lines has allowed a series of small molecules to be successfully assessed for potency of Nek2 inhibition *in vitro* and in cells, demonstrating that Nek2A is indeed a tractable target. In collaboration with colleagues at the ICR we can now undertake a Nek2A HTS. Pilot experiments with the NU compounds have

confirmed that the FlashPlate assay format accurately measures Nek2A inhibition *in vitro*. I have also suggested a high throughput cell based assay to automatically screen tens or hundreds of compounds in parallel. Future work now centres upon the execution of the Nek2A HTS and development of hit molecules into a lead Nek2 inhibitor. This work would be aided by the development of two parallel resources, the production of phosphoantibodies raised against Nek2 substrates and a solved structure of the Nek2A kinase domain complexed with an NU series or HTS inhibitor. Both centrosome splitting and rootletin displacement are well documented consequences of Nek2A activity in cultured cells but neither provide a direct molecular measure of kinase activity, a direct measure of phosphate transfer. An antibody that recognises a phosphoepitope produced by Nek2A, whether autophosphorylation or substrate phosphorylation, would be a single step measure of activity. An autophosphorylation event obligate for Nek2A activity such as that suggested to occur on threonine 175 would be especially useful (Rellos et al., 2006). The structure of Nek2A would also provide a great deal more information to refine the specificity of small molecule inhibitors. A rudimentary structure-activity relationship (SAR) can be constructed without a kinase structure by testing large numbers of inhibitors and identifying broad classes of substitutions that positively or negatively affect Nek2 inhibition, but a three dimensional structure would suggest which residues in the kinase are responsible for inhibitor binding and aid the design of more potent compounds.

The NU series compounds were invaluable in optimising and validating conditions for the HTS and cell-based assays of Nek2 inhibition. The Nek2A HTS properly screened 65,066 molecules and identified 61 “hit” compounds that significantly inhibited GST-Nek2A *in vitro* (a reduction in activity of at least 50% with the compound present at 32 μ M). Unfortunately, the structures of the hit compounds proved unattractive for further development as Nek2 inhibitors, composed mostly of quinines, metal complexes, polyphenols, pentacyclics and toxoflavins. The varied structures of the hit compounds reflect the historical origins of the CRUK HTS compound collection as an agglomeration of molecules from different cancer research campaign (CRC) and international cancer research fund (ICRF) research groups. Though unattractive for lead development, two of the reconfirmed HTS

hits, CC004731 and CC004733, were selected for further assays to form the basis of a publication reporting the Nek2 HTS. CC004731 and CC004733 were first incubated with cultured HeLa and U2OS cells to determine their impact upon cell viability.

A measure of the effect of a given compound on cell viability can be determined by calculating the fifty percent growth inhibition (GI_{50}) value, the compound concentration that reduces cell viability to half that of untreated cells. GI_{50} serves as a crude measure of growth inhibition, simply comparing compound concentrations that reduce cell growth to the same relative level. The GI_{50} value does not reflect the mechanism by which the growth inhibition is achieved, for example by apoptosis or cell cycle arrest. The GI_{50} values for an inhibitor are useful, however, for broad comparisons of potency between compounds, both within the same HTS and between different projects. Determining the GI_{50} values for CC004731 and CC004733 also allows them to be used in subsequent assays at equipotent rather than equimolar concentrations.

The GI_{50} values I obtained for CC004731 and CC004733 were similar for both HeLa and U2OS cells. The GI_{50} values for CC004731 were 1.8 μ M and 2.5 μ M for HeLa and U2OS cells, respectively. CC004733 affected cell viability to a lesser degree with correspondingly higher GI_{50} values of 10.2 μ M and 6.4 μ M for HeLa and U2OS cells, respectively. The HTS compounds CC004731 and CC004733 reduced cell viability to a greater degree than the related molecule wortmannin which had a GI_{50} of 15 μ M with respect to HeLa cells and 23.7 μ M against U2OS cells. Without further assays it is impossible to know whether the increased growth inhibition observed with CC004731 and CC004733, compared to wortmannin, simply reflects greater toxicity of these molecules rather than any consequences of Nek2 inhibition.

CHAPTER 7

DISCUSSION

7.1 Validating Nek2 as a novel drug target

The development of new strategies for effective cancer treatment is now characterised by rationality of approach; identifying the genetic lesions present in an individual patient or related subset of tumours and treating just those aberrations. The majority of current therapies are aimed at those cells that are proliferating, only a proportion of which are tumour cells, the rest comprising normal cells unnecessarily affected by the treatment. Novel chemotherapeutic targets, once identified, are subject to a process of validation followed by the development of strategies for inhibition. The most attractive new drug targets are those that exhibit greatest differential expression between normal and tumour tissue and are amenable to inhibition. This thesis demonstrates that the NIMA-related kinase Nek2 fulfils both of these criteria, being demonstrably overexpressed in primary breast tumours and susceptible to small molecule inhibition via its ATP binding pocket.

There are a number of criteria that can be applied when validating the worth of a new therapeutic target in human cancer. The first is a correlation between aberrant expression or mutation of the gene with the initiation or progression of cancer. In tandem with this, the association of the mutation with poor clinical outcome can strengthen the argument for causal involvement. A second consideration is the consequence of altered gene expression in model systems such as cultured cells: does overexpression of the gene recreate aspects of the malignant phenotype? Conversely, interference with the gene product should ideally reverse or attenuate the malignant phenotype. Lastly, the tractability of the target must be considered. In the case of protein kinases, is the kinase susceptible to small molecule inhibition, and can a specific inhibitor be developed (Workman, 2001).

7.2 Increased levels of Nek2 protein correlate with human disease and induce abnormalities in cultured cells

The implication of Nek2 in cancer was initially serendipitous. Elevated Nek2 mRNA levels were noted in a study of transcription from E2F responsive genes and further highlighted in two microarray analyses of B-cell lymphoma and paediatric osteosarcoma cells (de Vos et al., 2003a; Ren et al., 2002; Wai et al., 2002). I

undertook a more extensive examination of Nek2 levels in cancer cell lines derived from a range of tissues. A significant increase in Nek2 protein expression was identified in cells derived from breast cancer, ovarian cancer and leukaemia. Significantly, in terms of validating Nek2 as a therapeutic target, transfection of myc-Nek2A into the HBL100 normal breast cell line induced abnormal, supernumerary, centrosomes and aneuploidy, two characteristics of malignancy (Hayward et al., 2004). Aberrant centrosome number and morphology and aneuploidy been extensively reported in breast and prostate cancer, occurring in pre-invasive disease and correlating with high cytologic grade (Ghadimi et al., 2000; Kuo et al., 2000; Mayer et al., 2003; Pihan et al., 2001; Pihan et al., 2003b; Salisbury et al., 2004).

Importantly, these initial studies were then extended to encompass primary human breast tumours. Immunohistochemical staining of invasive and *in situ* breast tumours found increased levels of Nek2 protein in sixteen of twenty patients, the first report of elevated Nek2 protein levels in cancer. Additionally, within those tumour samples overexpressing Nek2, the upregulation of Nek2 was pervasive, with greater than seventy percent of cells within a given tumour sample staining strongly. It is worth noting that both the antibodies used for tumour staining were raised to regions within Nek2 that do not discriminate between the different Nek2 isoforms. In cultured cells the predominant isoform is Nek2A and this, though it cannot be concluded with certainty, is likely to be the case in tumour samples.

During the course of this thesis, one mechanism for the gross increase in Nek2 expression observed in breast tumours has also been elucidated. Analysis of 44 archival breast tumours by CGH found amplification of the Nek2 locus, 1q32, with 32 patient samples demonstrating a gain of up to six copies (Loo et al., 2004). This underlying gene amplification is in keeping with that observed for the mitotic kinases Plk1 and Aurora-A (Holtrich et al., 1994; Sen et al., 1997) and the receptor tyrosine kinase ErbB2 (Seshadri et al., 1989), all current therapeutic targets.

7.2.1 Downregulating Nek2 reduces cell viability

The correlation between increased Nek2 expression and cancer is evident, at least for a subset of breast tumours. Correspondingly, transfection of myc-Nek2A into cultured breast epithelial cells increases the incidence of aneuploidy and supernumerary and aberrant centrosomes. Conversely, the consequences of disrupting Nek2 function are less well studied.

Investigations of Nek2 depletion in the literature are limited and confined to cultured cells or simple eukaryotes. Depletion of Nek2 by RNA interference inhibited basal body separation in *T. brucei* and caused spindle defects and centrosome fragmentation in cultured embryonic *D. melanogaster* cells (Pradel et al., 2006; Prigent et al., 2005). Treating cultured human cells with Nek2 siRNA inhibited centrosome separation and specific depletion of Nek2B induced a delay in exiting mitosis (Fletcher et al., 2005). The inhibition of centrosome separation is similarly suggested by the rise in monopolar spindles observed following expression of inactive Nek2A-K37R in U2OS cells (Faragher and Fry, 2003). Interpretation of these limited data is further hindered by the realisation that Nek2 is a structural centrosome component, regardless of activity (Faragher and Fry, 2003; Twomey et al., 2004; Uto and Sagata, 2000). Broadly stated, however, loss of Nek2 activity negatively affects bipolar spindle formation and mitotic progression.

Work presented in this thesis extended these limited studies to examine the effect of Nek2 depletion on cell growth and viability. Depletion of Nek2 by siRNA in either HeLa or U2OS cell lines abolished cell growth, though this growth restriction was also observed with control siRNA duplexes (Chapter 5). Encouragingly, growth inhibition of HeLa cells by specific depletion of Nek2 was also reported independently during the course of this work (Fletcher et al., 2004). Lastly, in this thesis I demonstrate that Nek2 depletion induced apoptosis of HeLa cells, a phenotype similarly described in the same study reporting growth inhibition (Fletcher et al., 2004).

Nek2 is proposed as a target for the treatment of cancer, a disease of inappropriate proliferation. These tentative findings of growth inhibition and apoptosis are therefore encouraging. Future work should centre on characterising the nature of the growth inhibition and apoptosis, specifically whether the phenotypes are only induced in cells with existing mutations, such as the functional loss of p53 in HeLa cells. This question needs to be addressed with some urgency. If only p53^{-/-} cell lines respond to Nek2 inhibition by undergoing apoptosis this will direct the choice of cell lines used to establish xenografts or later the patients recruited to test candidate molecules for efficacy.

7.2.2 Nek2 is a tractable therapeutic target

Protein kinases are considered tractable therapeutic targets, susceptible to inhibition through their common ATP binding domains. Concerns over the specificity of inhibition possible when targeting a domain conserved in multiple kinases have been dispelled in part. *In vitro* studies examining the binding of current clinical kinase inhibitors have highlighted the role of residues distal to the ATP binding pocket (Fabian et al., 2005).

The studies of Nek2 inhibition presented in this thesis demonstrate there are several chemical series that inhibit Nek2A with *in vitro* micromolar IC₅₀ values and have GI₅₀ against U2OS and HeLa cells in the 1-10 μ M range. These series are encompassed both by the NU series of molecules and the HTS hits. In the case of the NU series of compounds they are all equipotent Cdk2 inhibitors. Consideration must be given to minimising this off-target efficacy in medicinal chemistry efforts, improving selectivity.

This thesis summarises the initial work of a project whose ultimate goal is to produce a specific, potent, well-tolerated inhibitor of Nek2 *in vivo*. The criteria for future development of the tentative hits are described briefly below and summarised in a test cascade (Figure 7.1). Satisfying the conditions of the test cascade comprises the majority of future work arising from this thesis. Whether the lead Nek2 inhibitors are developed from the NU series of molecules, or generated

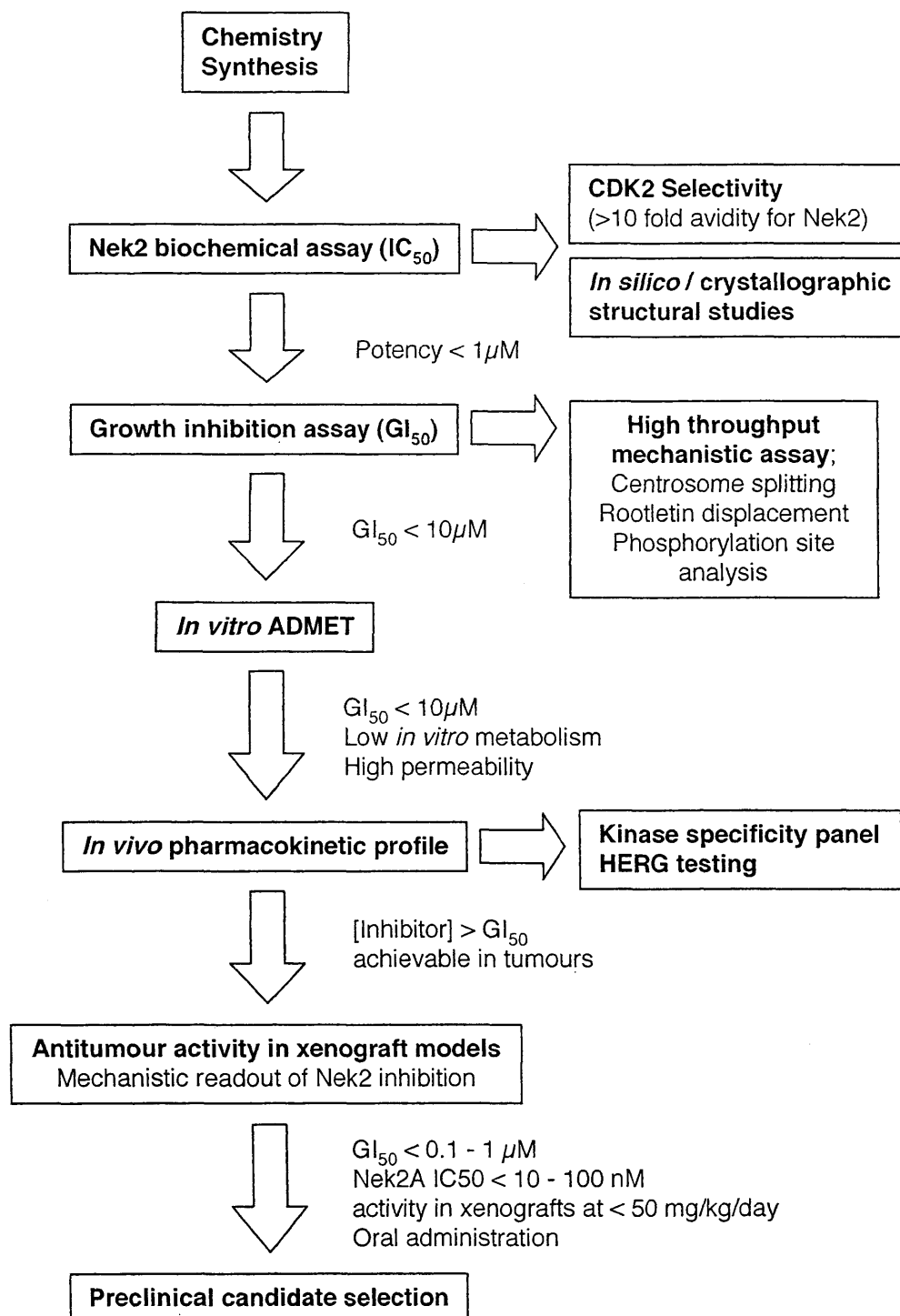


Figure 7.1 Nek2 drug discovery project test cascade

The test cascade details a series of milestones to be met in the development of a specific, potent Nek2 inhibitor. Initially molecules are screened for the simple ability to inhibit Nek2A *in vitro*. Compounds which inhibit Nek2A *in vitro* are termed “hits”. The most favourable hit molecules are progressed as “leads”. Leads are then subject to additional, specificity, toxicity and absorption criteria. The ultimate goal is to produce a selective, well tolerated compound that potently inhibits Nek2 kinase, inducing tumour regression.

from a HTS of a new compound collection, a series of developmental milestones must now be met.

The initial steps of the test cascade concentrate on refining the potency and selectivity of hit molecules as they progress to lead inhibitors. Desirable hit molecules are expected to possess an IC_{50} of approximately $1\mu M$ against Nek2A *in vitro* and a favourable chemical structure for development. Ideally, if several hit molecules from the same series are identified, a speculative structure-activity relationship (SAR) may be constructed.

Hit molecules that are progressed to leads are subject to more stringent requirements. Activity against Nek2A *in vitro* with an IC_{50} of approximately 100 nM is specified, with an additional requirement of ten-fold selectivity for Nek2 over Cdk2 for compounds originating in the NU series. The wider selectivity requirements of potential Nek2 inhibitors are also considered at this stage. Candidate molecules are assessed for their likely interaction with components of metabolic pathways involved in drug clearance. This includes the absorption, distribution, metabolism excretion and toxicity properties of the molecule (conflated as ADME^T) as well as its interaction with the oxidative cytochrome P450 enzymes. Similarly, at this stage lead compounds are also screened for specificity against a panel of related mitotic kinases. Lead compounds are also tested for inhibition of the cardiac potassium channel HERG, with an $IC_{50} > 10\mu M$ sought. The inadvertent inhibition of HERG has been implicated in cardiac arrhythmia and sudden death and has led to the withdrawal of certain drugs from the marketplace (Thomas et al., 2004). Later steps in the test cascade require the development of mechanistic assays of Nek2 activity.

Two assays of Nek2 inhibition in cultured cells have been developed, an inhibition of centrosome disjunction and inhibition of rootletin displacement, both normally induced by GFP-Nek2A expression (Bahe et al., 2005; Faragher and Fry, 2003). Both of these assays measure a phenotype induced by active Nek2 and these phenotypes have both been inhibited by the treatment of cultured cells with compounds that inhibit Nek2A *in vitro*. These assays are effective, adaptable to

automation for HTS and employ well characterised responses to increased levels of Nek2A (Bahe et al., 2005; Faragher and Fry, 2003; Fry et al., 1998c). However, neither assay directly measures Nek2 phosphorylation of a defined substrate.

The literature reflects a number of Nek2 substrates and interacting partners but a lack of a defined phosphorylation sites within them. C-Nap1 is phosphorylated on its carboxyl terminus by Nek2A *in vitro*, but the residues involved remain undefined (Fry et al., 1998b). Similarly Nek2A phosphorylates rootletin at both its C- and N-termini *in vitro* (Bahe et al., 2005). This situation is slowly beginning to change. A recent study of the Nek2 kinase domain identified residues within the T-loop that are likely autophosphorylation sites, obligate for activity *in vitro* and in cultured cells (Rellos et al., 2006). Nek2 activity has been shown to be dependent on dimerisation via its leucine zipper motif and subsequent autophosphorylation (Fry et al., 1999). Phospho-specific antibodies raised to a Nek2 autophosphorylation site, such as threonine 175, would be an excellent direct measure of Nek2 activity. A phospho-specific antibody would be invaluable in later steps of the test cascade. Directly measuring Nek2 autophosphorylation, and hence activation, would allow Nek2 inhibition to be measured in xenograft tumour models. Xenograft tumours resected from animals treated with putative inhibitors could be examined by immunohistochemistry with a Nek2 phosphospecific antibody. This allows a more rational assessment of drug administration regimes; dosing schedules whose upper limit is modulation of a specific biomarker rather than the conventional maximum tolerated dose.

7.3 Concluding remarks

There is not yet a causal role for Nek2 in cancer though there is a strong correlation between Nek2 overexpression and carcinoma. Indeed, overexpression of Nek2 in cultured cells induces aspects of neoplastic disease, namely centrosome abnormalities and aneuploidy. Experiments to determine whether Nek2 classically transforms cultured cells, conferring growth factor and anchorage independence, are still ongoing. The current lack of a causal link does not diminish the attraction of Nek2 as a novel target for the treatment of human carcinoma.

The most well characterised consequence of Nek2 overexpression in cultured cells is premature centrosome disjunction. In addition, elevated cellular levels of Nek2 promote centrosome fragmentation, mitotic spindle multipolarity, cytokinesis failure and aneuploidy. A loss of spindle bipolarity leads to a loss of genomic integrity. A multipolar spindle acting to segregate an aneuploid genome is a direct route to chromosomal instability (CIN), a constant shuffling of the tumour karyotype. This genomic plasticity provides a heterogeneous pool of tumour cells from which to select for aggressive or drug-refractory tumour development. Nek2 upregulation may represent one route by which pre-malignant cells develop a sufficiently fluid genome to allow the six main traits of tumour malignancy (expounded in (Hanahan and Weinberg, 2000) to emerge. CIN has been described as a seventh, enabling, trait that is a prerequisite for development of the other six. Increased levels of Nek2 may be central to initiating or maintaining CIN. A Nek2 inhibitor may reduce tumour viability by reducing the incidence of multipolar mitoses that can induce CIN (Figure 7.2).

Though involvement of Nek2A in human neoplastic disease is clear, much of the mechanism has yet to be resolved. The substrates and pathways that transmit an increase in Nek2 activity to malignancy are as yet unknown. However, enough is known, or can be reasonably postulated, that Nek2 should still be considered a strong candidate for therapeutic intervention. Given the lengthy process involved in transferring a hit compound through a test cascade to the clinic, it is prudent to pursue a small molecule inhibitor of Nek2 whilst simultaneously unravelling its role in the pathways of malignancy.

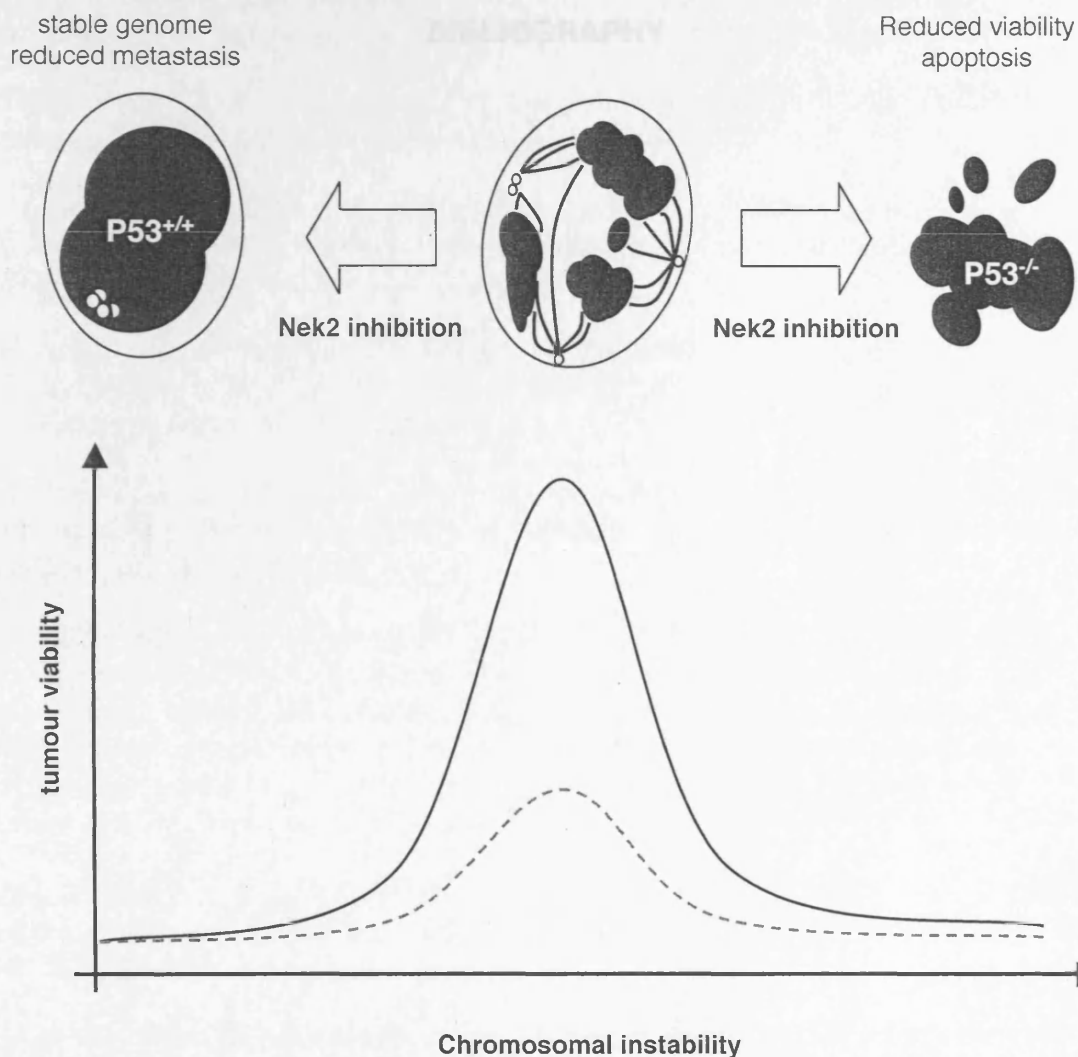


Figure 7.2 Possible consequences of Nek2 inhibition

Defects in chromosome segregation give rise to a heterogeneous population of aneuploid tumour cells, a pool from which drug refractory or aggressively metastatic cells can be selected. This heterogeneity can be considered to be in equilibrium, too little aneuploidy and carcinoma cells cannot adapt to the tumour microenvironment or evade therapy. Conversely, excessive defects in chromosome segregation reduce cell viability. Inhibitors of Nek2 may inhibit the formation of multipolar spindles, reducing the ensuing defects in chromosome segregation and disturbing this equilibrium. This would adversely affect tumour viability firstly by preventing drug resistant cells evolving. Secondly, depending on p53 status, after treatment with an inhibitor of Nek2 cells may arrest at the post mitotic checkpoint or enter successive cycles of endoreduplication and lose viability. Grey dashed line indicates a reduction in viability following Nek2 inhibitor treatment.

BIBLIOGRAPHY

- Aherne, G.W., McDonald, E. and Workman, P. (2002) Finding the needle in the haystack: why high-throughput screening is good for your health. *Breast Cancer Res*, **4**, 148-154.
- Al-Romaih, K., Bayani, J., Vorobyova, J., Karaskova, J., Park, P.C., Zielenska, M. and Squire, J.A. (2003) Chromosomal instability in osteosarcoma and its association with centrosome abnormalities. *Cancer Genet Cytogenet*, **144**, 91-99.
- Alberts, B., Johnson, A., Lewis, J., Raff, M., Roberts, K. and Walter, P. (2002) *Molecular biology of the cell*. Garland Science, New York.
- Anand, S., Penrhyn-Lowe, S. and Venkitaraman, A.R. (2003) AURORA-A amplification overrides the mitotic spindle assembly checkpoint, inducing resistance to Taxol. *Cancer Cell*, **3**, 51-62.
- Andersen, J.S., Wilkinson, C.J., Mayor, T., Mortensen, P., Nigg, E.A. and Mann, M. (2003) Proteomic characterization of the human centrosome by protein correlation profiling. *Nature*, **426**, 570-574.
- Andreassen, P.R., Lohez, O.D., Lacroix, F.B. and Margolis, R.L. (2001) Tetraploid state induces p53-dependent arrest of nontransformed mammalian cells in G1. *Mol Biol Cell*, **12**, 1315-1328.
- Arris, C.E., Boyle, F.T., Calvert, A.H., Curtin, N.J., Endicott, J.A., Garman, E.F., Gibson, A.E., Golding, B.T., Grant, S., Griffin, R.J., Jewsbury, P., Johnson, L.N., Lawrie, A.M., Newell, D.R., Noble, M.E., Sausville, E.A., Schultz, R. and Yu, W. (2000) Identification of novel purine and pyrimidine cyclin-dependent kinase inhibitors with distinct molecular interactions and tumor cell growth inhibition profiles. *J Med Chem*, **43**, 2797-2804.
- Bahe, S., Stierhof, Y.D., Wilkinson, C.J., Leiss, F. and Nigg, E.A. (2005) Rootletin forms centriole-associated filaments and functions in centrosome cohesion. *J Cell Biol*, **171**, 27-33.
- Bange, J., Zwick, E. and Ullrich, A. (2001) Molecular targets for breast cancer therapy and prevention. *Nat Med*, **7**, 548-552.
- Barnhart, R.K. (ed.). (2003) *Chambers dictionary of etymology*. Chmbers, New York.
- Barr, F.A., Sillje, H.H. and Nigg, E.A. (2004) Polo-like kinases and the orchestration of cell division. *Nat Rev Mol Cell Biol*, **5**, 429-440.
- Barton, A.B., Davies, C.J., Hutchison, C.A., 3rd and Kaback, D.B. (1992) Cloning of chromosome I DNA from *Saccharomyces cerevisiae*: analysis of the FUN52 gene, whose product has homology to protein kinases. *Gene*, **117**, 137-140.
- Baselga, J. and Arribas, J. (2004) Treating cancer's kinase 'addiction'. *Nat Med*, **10**, 786-787.

- Baxter, J.E. (2006) Phosphorylation site analysis of the centrosomal Nek2 kinase and its substrates. *Biochemistry*. University of Leicester, Leicester, p. 217.
- Belham, C., Comb, M.J. and Avruch, J. (2001) Identification of the NIMA family kinases NEK6/7 as regulators of the p70 ribosomal S6 kinase. *Curr Biol*, **11**, 1155-1167.
- Belham, C., Roig, J., Caldwell, J.A., Aoyama, Y., Kemp, B.E., Comb, M. and Avruch, J. (2003) A mitotic cascade of NIMA family kinases. Ncc1/Nek9 activates the Nek6 and Nek7 kinases. *J Biol Chem*, **278**, 34897-34909.
- Benson, C., Kaye, S., Workman, P., Garrett, M., Walton, M. and de Bono, J. (2005) Clinical anticancer drug development: targeting the cyclin-dependent kinases. *Br J Cancer*, **92**, 7-12.
- Berridge, M.V., Herst, P.M. and Tan, A.S. (2005) Tetrazolium dyes as tools in cell biology: new insights into their cellular reduction. *Biotechnol Annu Rev*, **11**, 127-152.
- Berridge, M.V., Tan, A.S., McCoy, K.D. and Wang, R. (1996) The biochemical and cellular basis of cell proliferation assays that use tetrazolium salts. *Biochemica*, **4**, 14-19.
- Berthon, P., Cussenot, O., Hopwood, L., LeDuc, A. and Maitland, N.J. (1995) Functional expression of SV40 in normal human prostatic epithelial and fibroblastic cells: differentiation pattern of non-tumorigenic cell lines. *Int. J. Oncology*, **6**, 333-343.
- Bettencourt-Dias, M., Rodrigues-Martins, A., Carpenter, L., Riparbelli, M., Lehmann, L., Gatt, M.K., Carmo, N., Balloux, F., Callaini, G. and Glover, D.M. (2005) SAK/PLK4 is required for centriole duplication and flagella development. *Curr Biol*, **15**, 2199-2207.
- Bijur, G.N., De Sarno, P. and Jope, R.S. (2000) Glycogen synthase kinase-3 β facilitates staurosporine- and heat shock-induced apoptosis. Protection by lithium. *J Biol Chem*, **275**, 7583-7590.
- Bischoff, J.R., Anderson, L., Zhu, Y., Mossie, K., Ng, L., Souza, B., Schryver, B., Flanagan, P., Clairvoyant, F., Ginther, C., Chan, C.S., Novotny, M., Slamon, D.J. and Plowman, G.D. (1998a) A homologue of *Drosophila aurora* kinase is oncogenic and amplified in human colorectal cancers. *Embo J*, **17**, 3052-3065.
- Bischoff, J.R., Anderson, L., Zhu, Y., Mossie, K., Ng, L., Souza, B., Schryver, B., Flanagan, P., Clairvoyant, F., Ginther, C., Chan, C.S.M., Novotny, M., Slamon, D.J. and Plowman, G.D. (1998b) A homologue of *Drosophila aurora* kinase is oncogenic and amplified in human colorectal cancers. *EMBO J*, **17**, 3052-3065.
- Borel, F., Lohez, O.D., Lacroix, F.B. and Margolis, R.L. (2002) Multiple centrosomes arise from tetraploidy checkpoint failure and mitotic centrosome clusters in p53 and RB pocket protein-compromised cells. *Proc. Natl. Acad. Sci. (U.S.A.)*, **99**, 9819-9824.

- Bornens, M. (2002) Centrosome composition and microtubule anchoring mechanisms. *Curr. Op. Cell Biol.*, **14**, 25-34.
- Bowers, A.J. and Boylan, J.F. (2004) Nek8, a NIMA family kinase member, is overexpressed in primary human breast tumors. *Gene*, **328**, 135-142.
- Bradley, B.A., Wagner, J.J. and Quarmby, L.M. (2004) Identification and sequence analysis of six new members of the NIMA-related kinase family in *Chlamydomonas*. *J Eukaryot Microbiol*, **51**, 66-72.
- Brinkley, B.R. (2001) Managing the centrosome numbers game: from chaos to stability in cancer cell division. *Trends Cell Biol.*, **11**, 18-21.
- Brummelkamp, T.R., Bernards, R. and Agami, R. (2002) A system for stable expression of short interfering RNAs in mammalian cells. *Science*, **296**, 550-553.
- Burns, T.F., Fei, P., Scata, K.A., Dicker, D.T. and El-Deiry, W.S. (2003) Silencing of the novel p53 target gene Snk/Plk2 leads to mitotic catastrophe in paclitaxel (taxol)-exposed cells. *Mol Cell Biol*, **23**, 5556-5571.
- Carmena, M. and Earnshaw, W.C. (2003) The cellular geography of aurora kinases. *Nat Rev Mol Cell Biol*, **4**, 842-854.
- Carmena, M., Riparbelli, M.G., Minestrini, G., Tavares, A.M., Adams, R., Callaini, G. and Glover, D.M. (1998) Drosophila polo kinase is required for cytokinesis. *J Cell Biol*, **143**, 659-671.
- Casenghi, M., Meraldi, P., Weinhart, U., Duncan, P.I., Korner, R. and Nigg, E.A. (2003) Polo-like kinase 1 regulates Nlp, a centrosome protein involved in microtubule nucleation. *Dev Cell*, **5**, 113-125.
- Castro, A., Bernis, C., Vigneron, S., Labbe, J.C. and Lorca, T. (2005) The anaphase-promoting complex: a key factor in the regulation of cell cycle. *Oncogene*, **24**, 314-325.
- Castro, A., Vigneron, S., Bernis, C., Labbe, J.C., Prigent, C. and Lorca, T. (2002) The D-Box-activating domain (DAD) is a new proteolysis signal that stimulates the silent D-Box sequence of Aurora-A. *EMBO Rep*, **3**, 1209-1214.
- Chan, C.S. and Botstein, D. (1993) Isolation and characterization of chromosome-gain and increase-in-ploidy mutants in yeast. *Genetics*, **135**, 677-691.
- Chen, H.L., Tang, C.J., Chen, C.Y. and Tang, T.K. (2005) Overexpression of an Aurora-C kinase-deficient mutant disrupts the Aurora-B/INCENP complex and induces polyploidy. *J Biomed Sci*, **12**, 297-310.
- Chen, Y., Riley, D.J., Zheng, L., Chen, P.-L. and Lee, W.-H. (2002) Phosphorylation of the mitotic regulator protein Hec1 by Nek2 kinase is essential for faithful chromosome segregation. *J. Biol. Chem.*, **277**, 49408-49416.

Cianfrocca, M. and Goldstein, L.J. (2004) Prognostic and predictive factors in early-stage breast cancer. *Oncologist*, **9**, 606-616.

Clarke, R.B., Anderson, E. and Howell, A. (2004) Steroid receptors in human breast cancer. *Trends Endocrinol Metab*, **15**, 316-323.

Clarke, R.B. and Howell, A. (2001) Applied Physiology of the Breast. In *Surgery*. The Medicine Publishing Company.

Cohen, P. (2002) Protein kinases--the major drug targets of the twenty-first century? *Nat Rev Drug Discov*, **1**, 309-315.

Cullen, B.R. (2006) Enhancing and confirming the specificity of RNAi experiments. *Nat Methods*, **3**, 677-681.

D'Assoro, A.B., Barrett, S.L., Folk, C., Negron, V.C., Boeneman, K., Busby, R., Whitehead, C.M., Stivala, F., Lingle, W.L. and Salisbury, J.L. (2002) Amplified centrosomes in breast cancer: a potential indicator of tumor aggressiveness. *Breast Cancer Research and Treatment*, **75**, 25-34.

Dancey, J. and Sausville, E.A. (2003) Issues and progress with protein kinase inhibitors for cancer treatment. *Nat Rev Drug Discov*, **2**, 296-313.

Daub, H., Specht, K. and Ullrich, A. (2004) Strategies to overcome resistance to targeted protein kinase inhibitors. *Nat Rev Drug Discov*, **3**, 1001-1010.

Davies, H., Bignell, G.R., Cox, C., Stephens, P., Edkins, S., Clegg, S., Teague, J., Woffendin, H., Garnett, M.J., Bottomley, W., Davis, N., Dicks, E., Ewing, R., Floyd, Y., Gray, K., Hall, S., Hawes, R., Hughes, J., Kosmidou, V., Menzies, A., Mould, C., Parker, A., Stevens, C., Watt, S., Hooper, S., Wilson, R., Jayatilake, H., Gusterson, B.A., Cooper, C., Shipley, J., Hargrave, D., Pritchard-Jones, K., Maitland, N., Chenevix-Trench, G., Riggins, G.J., Bigner, D.D., Palmieri, G., Cossu, A., Flanagan, A., Nicholson, A., Ho, J.W., Leung, S.Y., Yuen, S.T., Weber, B.L., Seigler, H.F., Darrow, T.L., Paterson, H., Marais, R., Marshall, C.J., Wooster, R., Stratton, M.R. and Futreal, P.A. (2002a) Mutations of the BRAF gene in human cancer. *Nature*, **417**, 949-954.

Davies, T.G., Bentley, J., Arris, C.E., Boyle, F.T., Curtin, N.J., Endicott, J.A., Gibson, A.E., Golding, B.T., Griffin, R.J., Hardcastle, I.R., Jewsbury, P., Johnson, L.N., Mesguiche, V., Newell, D.R., Noble, M.E., Tucker, J.A., Wang, L. and Whitfield, H.J. (2002b) Structure-based design of a potent purine-based cyclin-dependent kinase inhibitor. *Nat Struct Biol*, **9**, 745-749.

de Vos, S., Hofmann, W.-K., Grogan, T.M., Krug, U., Schrage, M., Miller, T.P., Braun, J.G., Wachsman, W., Koeffler, H.P. and Said, J.W. (2003a) Gene expression profile of serial samples of transformed B-cell lymphomas. *Lab. Invest.*, **83**, 271-285.

de Vos, S., Hofmann, W.K., Grogan, T.M., Krug, U., Schrage, M., Miller, T.P., Braun, J.G., Wachsman, W., Koeffler, H.P. and Said, J.W. (2003b) Gene

expression profile of serial samples of transformed B-cell lymphomas. *Lab Invest*, **83**, 271-285.

deFromentel, C.C., Nardeaux, P.C., Soussi, T., Lavielle, C., Estrade, S., Carloni, G., Chandrasekaran, K. and Cassingena, R. (1985) Epithelial HBL-100 cell line derived from milk of an apparently healthy woman harbours SV40 genetic information. *Exp. Cell Res.*, **160**, 83-94.

Di Agostino, S., Fedele, M., Chieffi, P., Fusco, A., Rossi, P., Geremia, R. and Sette, C. (2004) Phosphorylation of high-mobility group protein A2 by Nek2 kinase during the first meiotic division in mouse spermatocytes. *Mol Biol Cell*, **15**, 1224-1232.

Dietzmann, K., Kirches, E., von, B., Jachau, K. and Mawrin, C. (2001) Increased human polo-like kinase-1 expression in gliomas. *J Neurooncol*, **53**, 1-11.

Ditchfield, C., Johnson, V.L., Tighe, A., Ellston, R., Haworth, C., Johnson, T., Mortlock, A., Keen, N. and Taylor, S.S. (2003) Aurora B couples chromosome alignment with anaphase by targeting BubR1, Mad2, and Cenp-E to kinetochores. *J Cell Biol*, **161**, 267-280.

do Carmo Avides, M., Tavares, A. and Glover, D.M. (2001) Polo kinase and Asp are needed to promote the mitotic organizing activity of centrosomes. *Nat Cell Biol*, **3**, 421-424.

Doxsey, S. (2001) Re-evaluating centrosome function. *Nature Revs: Mol. Cell Biol.*, **2**, 688-698.

Doxsey, S., McCollum, D. and Theurkauf, W. (2005) Centrosomes in Cellular Regulation. *Annu Rev Cell Dev Biol*.

Dutertre, S., Cazales, M., Quaranta, M., Froment, C., Trabut, V., Dozier, C., Mirey, G., Bouche, J.P., Theis-Febvre, N., Schmitt, E., Monsarrat, B., Prigent, C. and Ducommun, B. (2004) Phosphorylation of CDC25B by Aurora-A at the centrosome contributes to the G2-M transition. *J Cell Sci*, **117**, 2523-2531.

Dutertre, S. and Prigent, C. (2003) Aurora-A overexpression leads to override of the microtubule-kinetochore attachment checkpoint. *Mol Interv*, **3**, 127-130.

Earnshaw, W.C., Martins, L.M. and Kaufmann, S.H. (1999) Mammalian caspases: structure, activation, substrates, and functions during apoptosis. *Annu Rev Biochem*, **68**, 383-424.

EBCTCG. (1998) Tamoxifen for early breast cancer: an overview of the randomised trials. Early Breast Cancer Trialists' Collaborative Group. *Lancet*, **351**, 1451-1467.

Elbashir, S.M., Harborth, J., Lendeckel, W., Yalcin, A., Weber, K. and Tuschl, T. (2001) Duplexes of 21-nucleotide RNAs mediate RNA interference in cultured mammalian cells. *Nature*, **411**, 494-498.

- Elez, R., Piiper, A., Kronenberger, B., Kock, M., Brendel, M., Hermann, E., Pliquett, U., Neumann, E. and Zeuzem, S. (2003) Tumor regression by combination antisense therapy against Plk1 and Bcl-2. *Oncogene*, **22**, 69-80.
- Elia, A.E., Cantley, L.C. and Yaffe, M.B. (2003a) Proteomic screen finds pSer/pThr-binding domain localizing Plk1 to mitotic substrates. *Science*, **299**, 1228-1231.
- Elia, A.E., Rellos, P., Haire, L.F., Chao, J.W., Ivins, F.J., Hoepker, K., Mohammad, D., Cantley, L.C., Smerdon, S.J. and Yaffe, M.B. (2003b) The molecular basis for phosphodependent substrate targeting and regulation of Plks by the Polo-box domain. *Cell*, **115**, 83-95.
- Elston, C.W. and Ellis, I.O. (1991) Pathological prognostic factors in breast cancer. I. The value of histological grade in breast cancer: experience from a large study with long-term follow-up. *Histopathology*, **19**, 403-410.
- Esteva, F.J. and Hortobagyi, G.N. (2004) Prognostic molecular markers in early breast cancer. *Breast Cancer Res*, **6**, 109-118.
- Eto, M., Elliott, E., Prickett, T.D. and Brautigan, D.L. (2002) Inhibitor-2 regulates protein phosphatase-1 complexed with NimA-related kinase to induce centrosome separation. *J Biol Chem*, **277**, 44013-44020.
- Fabian, M.A., Biggs, W.H., 3rd, Treiber, D.K., Atteridge, C.E., Azimioara, M.D., Benedetti, M.G., Carter, T.A., Ciceri, P., Edeen, P.T., Floyd, M., Ford, J.M., Galvin, M., Gerlach, J.L., Grotzfeld, R.M., Herrgard, S., Insko, D.E., Insko, M.A., Lai, A.G., Lelias, J.M., Mehta, S.A., Milanov, Z.V., Velasco, A.M., Wodicka, L.M., Patel, H.K., Zarrinkar, P.P. and Lockhart, D.J. (2005) A small molecule-kinase interaction map for clinical kinase inhibitors. *Nat Biotechnol*, **23**, 329-336.
- Faragher, A.J. and Fry, A.M. (2003) Nek2A kinase stimulates centrosome disjunction and is required for formation of bipolar mitotic spindles. *Mol Biol Cell*, **14**, 2876-2889.
- Fardilha, M., Wu, W., Sa, R., Fidalgo, S., Sousa, C., Mota, C., OA, D.A.C.E.S. and EF, D.A.C.E.S. (2004) Alternatively spliced protein variants as potential therapeutic targets for male infertility and contraception. *Ann N Y Acad Sci*, **1030**, 468-478.
- Fearon, E.R. and Pierceall, W.E. (1995) The deleted in colorectal cancer (DCC) gene: a candidate tumour suppressor gene encoding a cell surface protein with similarity to neural cell adhesion molecules. *Cancer Surv*, **24**, 3-17.
- Fearon, E.R. and Vogelstein, B. (1990) A genetic model for colorectal tumorigenesis. *Cell*, **61**, 759-767.
- Fire, A., Xu, S., Montgomery, M.K., Kostas, S.A., Driver, S.E. and Mello, C.C. (1998) Potent and specific genetic interference by double-stranded RNA in *Caenorhabditis elegans*. *Nature*, **391**, 806-811.

- Fletcher, L., Cerniglia, G.J., Nigg, E.A., Yend, T.J. and Muschel, R.J. (2004) Inhibition of centrosome separation after DNA damage: a role for Nek2. *Radiat Res*, **162**, 128-135.
- Fletcher, L., Cerniglia, G.J., Yen, T.J. and Muschel, R.J. (2005) Live cell imaging reveals distinct roles in cell cycle regulation for Nek2A and Nek2B. *Biochim Biophys Acta*, **1744**, 89-92.
- Friend, S.H., Bernards, R., Rogelj, S., Weinberg, R.A., Rapaport, J.M., Albert, D.M. and Dryja, T.P. (1986) A human DNA segment with properties of the gene that predisposes to retinoblastoma and osteosarcoma. *Nature*, **323**, 643-646.
- Fry, A.M. (2002) The Nek2 protein kinase: a novel regulator of centrosome structure. *Oncogene*, **21**, 6184-6194.
- Fry, A.M., Arnaud, L. and Nigg, E.A. (1999) Activity of the human centrosomal kinase, Nek2, depends on an unusual leucine zipper dimerization motif. *J Biol Chem*, **274**, 16304-16310.
- Fry, A.M. and Baxter, J.E. (2006) Sealed with a Kiz: How Plk1 ensures spindle pole integrity. *Dev Cell*, **11**, 431-432.
- Fry, A.M., Descombes, P., Twomey, C., Bacchieri, R. and Nigg, E.A. (2000) The NIMA-related kinase X-Nek2B is required for efficient assembly of the zygotic centrosome in *Xenopus laevis*. *J Cell Sci*, **113** (Pt 11), 1973-1984.
- Fry, A.M. and Faragher, A.J. (2001) Identification of centrosome kinases. *Methods Cell Biol*, **67**, 305-323.
- Fry, A.M., Mayor, T., Meraldi, P., Stierhof, Y.-D., Tanaka, K. and Nigg, E.A. (1998a) C-Nap1, a novel centrosomal coiled-coil protein and candidate substrate of the cell cycle-regulated protein kinase Nek2. *J. Cell Biol.*, **141**, 1563-1574.
- Fry, A.M., Mayor, T., Meraldi, P., Stierhof, Y.D., Tanaka, K. and Nigg, E.A. (1998b) C-Nap1, a novel centrosomal coiled-coil protein and candidate substrate of the cell cycle-regulated protein kinase Nek2. *J Cell Biol*, **141**, 1563-1574.
- Fry, A.M., Meraldi, P. and Nigg, E.A. (1998c) A centrosomal function for the human Nek2 protein kinase, a member of the NIMA family of cell cycle regulators. *Embo J*, **17**, 470-481.
- Fry, A.M. and Nigg, E.A. (1997) Characterization of mammalian NIMA-related kinases. *Methods Enzymol*, **283**, 270-282.
- Fry, A.M., Schultz, S.J., Bartek, J. and Nigg, E.A. (1995) Substrate specificity and cell cycle regulation of the Nek2 protein kinase, a potential human homolog of the mitotic regulator NIMA of *Aspergillus nidulans*. *J Biol Chem*, **270**, 12899-12905.
- Gadde, S. and Heald, R. (2004) Mechanisms and molecules of the mitotic spindle. *Curr Biol*, **14**, R797-805.

- Galea, M.H., Blamey, R.W., Elston, C.E. and Ellis, I.O. (1992) The Nottingham Prognostic Index in primary breast cancer. *Breast Cancer Res Treat*, **22**, 207-219.
- Ghadimi, B.M., Sackett, D.L., Difilippantonio, M.J., Schrock, E., Neumann, T., Jauho, A., Auer, G. and Ried, T. (2000) Centrosome amplification and instability occurs exclusively in aneuploid, but not in diploid colorectal cancer cell lines, and correlates with numerical chromosomal aberrations. *Genes, Chromosomes and Cancer*, **27**, 183-190.
- Gibson, A.E., Arris, C.E., Bentley, J., Boyle, F.T., Curtin, N.J., Davies, T.G., Endicott, J.A., Golding, B.T., Grant, S., Griffin, R.J., Jewsbury, P., Johnson, L.N., Mesguiche, V., Newell, D.R., Noble, M.E., Tucker, J.A. and Whitfield, H.J. (2002) Probing the ATP ribose-binding domain of cyclin-dependent kinases 1 and 2 with O(6)-substituted guanine derivatives. *J Med Chem*, **45**, 3381-3393.
- Gizatullin, F., Yao, Y., Kung, V., Harding, M.W., Loda, M. and Shapiro, G.I. (2006) The Aurora kinase inhibitor VX-680 induces endoreduplication and apoptosis preferentially in cells with compromised p53-dependent postmitotic checkpoint function. *Cancer Res*, **66**, 7668-7677.
- Glover, D.M., Leibowitz, M.H., McLean, D.A. and Parry, H. (1995) Mutations in aurora prevent centrosome separation leading to the formation of monopolar spindles. *Cell*, **81**, 95-105.
- Golsteyn, R.M., Schultz, S.J., Bartek, J., Ziemiecki, A., Ried, T. and Nigg, E.A. (1994) Cell cycle analysis and chromosomal localization of human Plk1, a putative homologue of the mitotic kinases *Drosophila* polo and *Saccharomyces cerevisiae* Cdc5. *J Cell Sci*, **107** (Pt 6), 1509-1517.
- Graf, R. (2002) DdNek2, the first non-vertebrate homologue of human Nek2, is involved in the formation of microtubule-organizing centers. *J Cell Sci*, **115**, 1919-1929.
- Grallert, A. and Hagan, I.M. (2002) *S. pombe* NIMA related kinase, Fin1, regulates spindle formation, and an affinity of Polo for the SPB. *EMBO J*, **21**, 3096-3107.
- Grallert, A., Krapp, A., Bagley, S., Simanis, V. and Hagan, I.M. (2004) Recruitment of NIMA kinase shows that maturation of the *S. pombe* spindle-pole body occurs over consecutive cell cycles and reveals a role for NIMA in modulating SIN activity. *Genes Dev*, **18**, 1007-1021.
- Gumireddy, K., Reddy, M.V., Cosenza, S.C., Boominathan, R., Baker, S.J., Papathi, N., Jiang, J., Holland, J. and Reddy, E.P. (2005) ON01910, a non-ATP-competitive small molecule inhibitor of Plk1, is a potent anticancer agent. *Cancer Cell*, **7**, 275-286.
- Habedanck, R., Stierhof, Y.D., Wilkinson, C.J. and Nigg, E.A. (2005) The Polo kinase Plk4 functions in centriole duplication. *Nat Cell Biol*, **7**, 1140-1146.
- Hames, R.S. (2002) Cell cycle regulation of the centrosomal kinase Nek2 and its substrate C-Nap1. *Biochemistry*. University of Leicester, Leicester, p. 238.

Hames, R.S., Crookes, R.E., Straatman, K.R., Merdes, A., Hayes, M.J., Faragher, A.J. and Fry, A.M. (2005) Dynamic recruitment of Nek2 kinase to the centrosome involves microtubules, PCM-1, and localized proteasomal degradation. *Mol Biol Cell*, **16**, 1711-1724.

Hames, R.S. and Fry, A.M. (2002) Alternative splice variants of the human centrosome kinase Nek2 exhibit distinct patterns of expression in mitosis. *Biochem J*, **361**, 77-85.

Hames, R.S., Wattam, S.L., Yamano, H., Bacchieri, R. and Fry, A.M. (2001) APC/C-mediated destruction of the centrosomal kinase Nek2A occurs in early mitosis and depends upon a cyclin A-type D-box. *Embo J*, **20**, 7117-7127.

Hanahan, D. and Weinberg, R.A. (2000) The hallmarks of cancer. *Cell*, **100**, 57-70.

Hannak, E., Kirkham, M., Hyman, A.A. and Oegema, K. (2001) Aurora-A kinase is required for centrosome maturation in *Caenorhabditis elegans*. *J Cell Biol*, **155**, 1109-1116.

Hardcastle, I.R., Arris, C.E., Bentley, J., Boyle, F.T., Chen, Y., Curtin, N.J., Endicott, J.A., Gibson, A.E., Golding, B.T., Griffin, R.J., Jewsbury, P., Menyerol, J., Mesguiche, V., Newell, D.R., Noble, M.E., Pratt, D.J., Wang, L.Z. and Whitfield, H.J. (2004) N2-substituted O6-cyclohexylmethylguanine derivatives: potent inhibitors of cyclin-dependent kinases 1 and 2. *J Med Chem*, **47**, 3710-3722.

Harrington, E.A., Bebbington, D., Moore, J., Rasmussen, R.K., Ajose-Adeogun, A.O., Nakayama, T., Graham, J.A., Demur, C., Hercend, T., Diu-Hercend, A., Su, M., Golec, J.M. and Miller, K.M. (2004) VX-680, a potent and selective small-molecule inhibitor of the Aurora kinases, suppresses tumor growth in vivo. *Nat Med*, **10**, 262-267.

Hashimoto, Y., Akita, H., Hibino, M., Kohri, K. and Nakanishi, M. (2002) Identification and characterization of Nek6 protein kinase, a potential human homolog of NIMA histone H3 kinase. *Biochem Biophys Res Commun*, **293**, 753-758.

Hayes, M.J., Kimata, Y., Wattam, S.L., Lindon, C., Mao, G., Yamano, H. and Fry, A.M. (2006) Early mitotic degradation of Nek2A depends on Cdc20-independent interaction with the APC/C. *Nat Cell Biol*, **8**, 607-614.

Hayward, D.G., Clarke, R.B., Faragher, A.J., Pillai, M.R., Hagan, I.M. and Fry, A.M. (2004) The centrosomal kinase Nek2 displays elevated levels of protein expression in human breast cancer. *Cancer Res*, **64**, 7370-7376.

Hayward, D.G. and Fry, A.M. (2006) Nek2 Kinase in chromosome instability and cancer. *Cancer Letters*, **237**, 155-156

Heim, S. and Mitelman, F. (1995) *Cancer cytogenetics*. Wiley-Liss, New York.

Heinrich, M.C., Corless, C.L., Demetri, G.D., Blanke, C.D., von Mehren, M., Joensuu, H., McGreevey, L.S., Chen, C.J., Van den Abbeele, A.D., Druker, B.J., Kiese, B., Eisenberg, B., Roberts, P.J., Singer, S., Fletcher, C.D., Silberman, S., Dimitrijevic, S. and Fletcher, J.A. (2003) Kinase mutations and imatinib response in patients with metastatic gastrointestinal stromal tumor. *J Clin Oncol*, **21**, 4342-4349.

Helps, N.R., Luo, X., Barker, H.M. and Cohen, P.T. (2000) NIMA-related kinase 2 (Nek2), a cell-cycle-regulated protein kinase localized to centrosomes, is complexed to protein phosphatase 1. *Biochem J*, **349**, 509-518.

Herbst, R.S. (2004) Review of epidermal growth factor receptor biology. *Int J Radiat Oncol Biol Phys*, **59**, 21-26.

Hinchcliffe, E.H. and Sluder, G. (2001a) Centrosome duplication: three kinases come up a winner! *Curr Biol*, **11**, R698-701.

Hinchcliffe, E.H. and Sluder, G. (2001b) "It takes two to tango": understanding how centrosome duplication is regulated throughout the cell cycle. *Genes Dev*, **15**, 1167-1181.

Hisamuddin, I.M. and Yang, V.W. (2004) Genetics of colorectal cancer. *MedGenMed*, **6**, 13.

Ho, P.K. and Hawkins, C.J. (2005) Mammalian initiator apoptotic caspases. *Febs J*, **272**, 5436-5453.

Holland, P.M., Milne, A., Garka, K., Johnson, R.S., Willis, C., Sims, J.E., Rauch, C.T., Bird, T.A. and Virca, G.D. (2002) Purification, cloning, and characterization of Nek8, a novel NIMA-related kinase, and its candidate substrate Bicd2. *J Biol Chem*, **277**, 16229-16240.

Holtrich, U., Wolf, G., Brauninger, A., Karn, T., Bohme, B., Rubsamen-Waigmann, H. and Strebhardt, K. (1994) Induction and down-regulation of PLK, a human serine/threonine kinase expressed in proliferating cells and tumors. *Proc. Natl. Acad. Sci. (U.S.A.)*, **91**, 1736-1740.

Horiike, S., Yokota, S., Nakao, M., Iwai, T., Sasai, Y., Kaneko, H., Taniwaki, M., Kashima, K., Fujii, H., Abe, T. and Misawa, S. (1997) Tandem duplications of the FLT3 receptor gene are associated with leukemic transformation of myelodysplasia. *Leukemia*, **11**, 1442-1446.

Hsu, J.Y., Sun, Z.W., Li, X., Reuben, M., Tatchell, K., Bishop, D.K., Grushcow, J.M., Brame, C.J., Caldwell, J.A., Hunt, D.F., Lin, R., Smith, M.M. and Allis, C.D. (2000) Mitotic phosphorylation of histone H3 is governed by Ipl1/aurora kinase and Glc7/PP1 phosphatase in budding yeast and nematodes. *Cell*, **102**, 279-291.

Huang, S.N. (1975) Immunohistochemical demonstration of hepatitis B core and surface antigens in paraffin sections. *Lab Invest*, **33**, 88-95.

- Huang, S.N., Minassian, H. and More, J.D. (1976) Application of immunofluorescent staining on paraffin sections improved by trypsin digestion. *Lab Invest*, **35**, 383-390.
- Izant, J.G. and Weintraub, H. (1984) Inhibition of thymidine kinase gene expression by anti-sense RNA: a molecular approach to genetic analysis. *Cell*, **36**, 1007-1015.
- Jacobsen, M.D., Weil, M. and Raff, M.C. (1996) Role of Ced-3/ICE-family proteases in staurosporine-induced programmed cell death. *J Cell Biol*, **133**, 1041-1051.
- Jones, D.G. and Rosamond, J. (1990) Isolation of a novel protein kinase-encoding gene from yeast by oligodeoxyribonucleotide probing. *Gene*, **90**, 87-92.
- Kambouris, N.G., Burke, D.J. and Creutz, C.E. (1993) Cloning and genetic analysis of the gene encoding a new protein kinase in *Saccharomyces cerevisiae*. *Yeast*, **9**, 141-150.
- Katayama, H., Brinkley, W.R. and Sen, S. (2003) The Aurora kinases: role in cell transformation and tumorigenesis. *Cancer Metastasis Rev*, **22**, 451-464.
- Keen, N. and Taylor, S. (2004) Aurora-kinase inhibitors as anticancer agents. *Nat Rev Cancer*, **4**, 927-936.
- Khidr, L. and Chen, P.L. (2006) RB, the conductor that orchestrates life, death and differentiation. *Oncogene*, **25**, 5210-5219.
- Kimura, M. and Okano, Y. (2001a) Identification and assignment of the human NIMA-related protein kinase 7 gene (NEK7) to human chromosome 1q31.3. *Cytogenet Cell Genet*, **94**, 33-38.
- Kimura, M. and Okano, Y. (2001b) Molecular cloning and characterization of the human NIMA-related protein kinase 3 gene (NEK3). *Cytogenet Cell Genet*, **95**, 177-182.
- Kitamura, Y., Hirota, S. and Nishida, T. (2003) Gastrointestinal stromal tumors (GIST): a model for molecule-based diagnosis and treatment of solid tumors. *Cancer Sci*, **94**, 315-320.
- Knecht, R., Oberhauser, C. and Strebhardt, K. (2000) PLK (polo-like kinase), a new prognostic marker for oropharyngeal carcinomas. *Int J Cancer*, **89**, 535-536.
- Kneisel, L., Strebhardt, K., Bernd, A., Wolter, M., Binder, A. and Kaufmann, R. (2002) Expression of polo-like kinase (PLK1) in thin melanomas: a novel marker of metastatic disease. *J Cutan Pathol*, **29**, 354-358.
- Knowles, M. and Selby, P. (2005) *Introduction to the cellular and molecular biology of cancer*. Oxford university press, Oxford.

- Knudson, A.G. (2001) Two genetic hits (more or less) to cancer. *Nat Rev Cancer*, **1**, 157-162.
- Knudson, A.G., Jr. (1986) Genetics of human cancer. *J Cell Physiol Suppl*, **4**, 7-11.
- Kramer, A., Schweizer, S., Neben, K., Giesecke, C., Kalla, J., Katzenberger, T., Benner, A., Muller-Hermelink, H.K., Ho, A.D. and Ott, G. (2003) Centrosome aberrations as a possible mechanism for chromosomal instability in non-Hodgkin's lymphoma. *Leukemia*, **17**, 2207-2213.
- Krien, M.J., Bugg, S.J., Palatsides, M., Asouline, G., Morimyo, M. and O'Connell, M.J. (1998) A NIMA homologue promotes chromatin condensation in fission yeast. *J Cell Sci*, **111** (Pt 7), 967-976.
- Kuo, K.-K., Sato, N., Mizumoto, K., Maehara, N., Yonemasu, H., Ker, C.-G., Sheen, P.-C. and Tanaka, M. (2000) Centrosome abnormalities in human carcinomas of the gallbladder and intrahepatic and extrahepatic bile ducts. *Hepatology*, **31**, 59-64.
- Kurzrock, R., Gutterman, J.U. and Talpaz, M. (1988) The molecular genetics of Philadelphia chromosome-positive leukemias. *N Engl J Med*, **319**, 990-998.
- Lacey, K.R., Jackson, P.K. and Stearns, T. (1999) Cyclin-dependent kinase control of centrosome duplication. *Proc Natl Acad Sci U S A*, **96**, 2817-2822.
- Lange, B.M. and Gull, K. (1996) Structure and function of the centriole in animal cells: progress and questions. *Trends Cell Biol*, **6**, 348-352.
- Laoukili, J., Kooistra, M.R., Bras, A., Kauw, J., Kerkhoven, R.M., Morrison, A., Clevers, H. and Medema, R.H. (2005) FoxM1 is required for execution of the mitotic programme and chromosome stability. *Nat Cell Biol*, **7**, 126-136.
- Lengauer, C., Kinzler, K.W. and Vogelstein, B. (1998) Genetic instabilities in human cancers. *Nature*, **396**, 643-649.
- Letwin, K., Mizzen, L., Motro, B., Ben-David, Y., Bernstein, A. and Pawson, T. (1992) A mammalian dual specificity protein kinase, Nek1, is related to the NIMA cell cycle regulator and highly expressed in meiotic germ cells. *Embo J*, **11**, 3521-3531.
- Levitzki, A. (2003) Protein kinase inhibitors as a therapeutic modality. *Acc Chem Res*, **36**, 462-469.
- Li, D., Zhu, J., Firozi, P.F., Abbruzzese, J.L., Evans, D.B., Cleary, K., Friess, H. and Sen, S. (2003) Overexpression of oncogenic STK15/BTAK/Aurora A kinase in human pancreatic cancer. *Clin Cancer Res*, **9**, 991-997.
- Li, M.Z., Yu, L., Liu, Q., Chu, J.Y. and Zhao, S.Y. (1999) Assignment of NEK6, a NIMA-related gene, to human chromosome 9q33. 3-->q34.11 by radiation hybrid mapping. *Cytogenet Cell Genet*, **87**, 271-272.

- Lindon, C. and Pines, J. (2004) Ordered proteolysis in anaphase inactivates Plk1 to contribute to proper mitotic exit in human cells. *J Cell Biol*, **164**, 233-241.
- Lingle, W.L., Barrett, S.L., Negron, V.C., D'Assoro, A.B., Boeneman, K., Liu, W., Whitehead, C.M., Reynolds, C. and Salisbury, J.L. (2002) Centrosome amplification drives chromosomal instability in breast tumor development. *Proc. Natl. Acad. Sci. (U.S.A.)*, **99**, 1978-1983.
- Lingle, W.L., Lutz, W.H., Ingle, J.N., Maihle, N.J. and Salisbury, J.L. (1998) Centrosome hypertrophy in human breast tumors: implications for genomic stability and cell polarity. *Proc. Natl. Acad. Sci. (U.S.A.)*, **95**, 2950-2955.
- Lingle, W.L. and Salisbury, J.L. (1999) Altered centrosome structure is associated with abnormal mitoses in human breast tumors. *Am. J. Pathol.*, **155**, 1941-1951.
- Liu, X., Lei, M. and Erikson, R.L. (2006) Normal cells, but not cancer cells, survive severe Plk1 depletion. *Mol Cell Biol*, **26**, 2093-2108.
- Lizcano, J.M., Deak, M., Morrice, N., Kieloch, A., Hastie, C.J., Dong, L., Schutkowski, M., Reimer, U. and Alessi, D.R. (2002) Molecular basis for the substrate specificity of NIMA-related kinase-6 (NEK6). Evidence that NEK6 does not phosphorylate the hydrophobic motif of ribosomal S6 protein kinase and serum- and glucocorticoid-induced protein kinase in vivo. *J Biol Chem*, **277**, 27839-27849.
- Loo, L.W., Grove, D.I., Williams, E.M., Neal, C.L., Cousens, L.A., Schubert, E.L., Holcomb, I.N., Massa, H.F., Glogovac, J., Li, C.I., Malone, K.E., Daling, J.R., Delrow, J.J., Trask, B.J., Hsu, L. and Porter, P.L. (2004) Array comparative genomic hybridization analysis of genomic alterations in breast cancer subtypes. *Cancer Res*, **64**, 8541-8549.
- Lou, Y., Yao, J., Zenreski, A., Ahmed, K., Wang, H., Hu, J., Wang, Y. and Yao, X. (2004a) Nek2A interacts with Mad1 and possibly functions as a novel integrator of the spindle checkpoint signaling. *J. Biol. Chem.*, **279**, 20049-20057.
- Lou, Y., Yao, J., Zereshki, A., Dou, Z., Ahmed, K., Wang, H., Hu, J., Wang, Y. and Yao, X. (2004b) NEK2A interacts with MAD1 and possibly functions as a novel integrator of the spindle checkpoint signaling. *J Biol Chem*, **279**, 20049-20057.
- Lowery, D.M., Lim, D. and Yaffe, M.B. (2005) Structure and function of Polo-like kinases. *Oncogene*, **24**, 248-259.
- Lu, K.P., Osmani, S.A. and Means, A.R. (1993) Properties and regulation of the cell cycle-specific NIMA protein kinase of *Aspergillus nidulans*. *J Biol Chem*, **268**, 8769-8776.
- Ma, S., Charron, J. and Erikson, R.L. (2003) Role of Plk2 (Snk) in mouse development and cell proliferation. *Mol Cell Biol*, **23**, 6936-6943.

- Mack, G.J., Rees, J., Sandblom, O., Balczon, R., Fritzler, M.J. and Rattner, J.B. (1998) Autoantibodies to a group of centrosomal proteins in human autoimmune sera reactive with the centrosome. *Arthritis Rheum*, **41**, 551-558.
- Magennis, D.P. (1997) Nuclear DNA in histological and cytological specimens: measurement and prognostic significance. *Br. J. Biomed. Sci.*, **54**, 140-148.
- Mahjoub, M.R., Qasim Rasi, M. and Quarmby, L.M. (2004) A NIMA-related kinase, Fa2p, localizes to a novel site in the proximal cilia of Chlamydomonas and mouse kidney cells. *Mol Biol Cell*, **15**, 5172-5186.
- Manche, L., Green, S.R., Schmedt, C. and Mathews, M.B. (1992) Interactions between double-stranded RNA regulators and the protein kinase DAI. *Mol Cell Biol*, **12**, 5238-5248.
- Mann, D.L. (2006) Targeted cancer therapeutics: the heartbreak of success. *Nat Med*, **12**, 881-882.
- Mao, Y., Abrieu, A. and Cleveland, D.W. (2003) Activating and silencing the mitotic checkpoint through CENP-E-dependent activation/inactivation of BubR1. *Cell*, **114**, 87-98.
- Mao, Y., Desai, A. and Cleveland, D.W. (2005) Microtubule capture by CENP-E silences BubR1-dependent mitotic checkpoint signaling. *J Cell Biol*, **170**, 873-880.
- Margolis, R.L., Lohez, O.D. and Andreassen, P.R. (2003) G1 tetraploidy checkpoint and the suppression of tumorigenesis. *J Cell Biochem*, **88**, 673-683.
- Marshall, W.F. (2001) Centrioles take center stage. *Curr Biol*, **11**, R487-496.
- Martin-Lluesma, S., Stucke, V.M. and Nigg, E.A. (2002) Role of Hec1 in spindle checkpoint signaling and kinetochore recruitment of Mad1/Mad2. *Science*, **297**, 2267-2270.
- Matsumoto, Y., Hayashi, K. and Nishida, E. (1999) Cyclin-dependent kinase 2 (Cdk2) is required for centrosome duplication in mammalian cells. *Curr Biol*, **9**, 429-432.
- Matthews, N., Visintin, C., Hartzoulakis, B., Jarvis, A. and Selwood, D.L. (2006) Aurora A and B kinases as targets for cancer: will they be selective for tumors? *Expert Rev Anticancer Ther*, **6**, 109-120.
- Mayer, F., Stoop, H., Sen, S., Bokemeyer, C., Oosterhuis, J.W. and Looijenga, L.H. (2003) Aneuploidy of human testicular germ cell tumors is associated with amplification of centrosomes. *Oncogene*, **22**, 3859-3866.
- Mayor, T., Hacker, U., Stierhof, Y.D. and Nigg, E.A. (2002) The mechanism regulating the dissociation of the centrosomal protein C-Nap1 from mitotic spindle poles. *J Cell Sci*, **115**, 3275-3284.

- Mayor, T., Stierhof, Y.D., Tanaka, K., Fry, A.M. and Nigg, E.A. (2000) The centrosomal protein C-Nap1 is required for cell cycle-regulated centrosome cohesion. *J Cell Biol*, **151**, 837-846.
- Meraldi, P., Lukas, J., Fry, A.M., Bartek, J. and Nigg, E.A. (1999) Centrosome duplication in mammalian somatic cells requires E2F and Cdk2-cyclin A. *Nat Cell Biol*, **1**, 88-93.
- Meraldi, P. and Nigg, E.A. (2001) Centrosome cohesion is regulated by a balance of kinase and phosphatase activities. *J. Cell Sci.*, **114**, 3749-3757.
- Mesguiche, V., Parsons, R.J., Arris, C.E., Bentley, J., Boyle, F.T., Curtin, N.J., Davies, T.G., Endicott, J.A., Gibson, A.E., Golding, B.T., Griffin, R.J., Jewsbury, P., Johnson, L.N., Newell, D.R., Noble, M.E., Wang, L.Z. and Hardcastle, I.R. (2003) 4-Alkoxy-2,6-diaminopyrimidine derivatives: inhibitors of cyclin dependent kinases 1 and 2. *Bioorg Med Chem Lett*, **13**, 217-222.
- Montero, C. (2003) The antigen-antibody reaction in immunohistochemistry. *J Histochem Cytochem*, **51**, 1-4.
- Morris, N.R. (1975) Mitotic mutants of *Aspergillus nidulans*. *Genet Res*, **26**, 237-254.
- Morrow, C.J., Tighe, A., Johnson, V.L., Scott, M.I., Ditchfield, C. and Taylor, S.S. (2005) Bub1 and aurora B cooperate to maintain BubR1-mediated inhibition of APC/CCdc20. *J Cell Sci*, **118**, 3639-3652.
- Mortlock, A., Keen, N.J., Jung, F.H., Heron, N.M., Foote, K.M., Wilkinson, R. and Green, S. (2005) Progress in the development of selective inhibitors of Aurora kinases. *Curr Top Med Chem*, **5**, 199-213.
- Mosmann, T. (1983) Rapid colorimetric assay for cellular growth and survival: application to proliferation and cytotoxicity assays. *J Immunol Methods*, **65**, 55-63.
- Myer, D.L., Bahassi el, M. and Stambrook, P.J. (2005) The Plk3-Cdc25 circuit. *Oncogene*, **24**, 299-305.
- Nakao, M., Yokota, S., Iwai, T., Kaneko, H., Horiike, S., Kashima, K., Sonoda, Y., Fujimoto, T. and Misawa, S. (1996) Internal tandem duplication of the *flt3* gene found in acute myeloid leukemia. *Leukemia*, **10**, 1911-1918.
- Nasmyth, K. (2005) How do so few control so many? *Cell*, **120**, 739-746.
- NICE. (2002) Guidance on the use of trastuzumab for the treatment of advanced breast cancer. In NICE (ed.). National institute for clinical excellence, London, p. 20.
- NICE. (2006) Trastazumab for the adjuvant treatment of early-stage HER2-positive breast cancer. In NICE (ed.). National institute for clinical excellence, London, p. 23.

- Nigg, E.A. (1995) Cyclin-dependent protein kinases: key regulators of the eukaryotic cell cycle. *Bioessays*, **17**, 471-480.
- Nigg, E.A. (2001) Mitotic kinases as regulators of cell division and its checkpoints. *Nature Revs: Mol. Cell Biol.*, **2**, 21-32.
- Nigg, E.A. (2002) Centrosome aberrations: cause or consequence of cancer progression? *Nat Revs Cancer*, **2**, 815-825.
- Noguchi, K., Fukazawa, H., Murakami, Y. and Uehara, Y. (2002) Nek11, a new member of the NIMA family of kinases, involved in DNA replication and genotoxic stress responses. *J Biol Chem*, **277**, 39655-39665.
- Noguchi, K., Fukazawa, H., Murakami, Y. and Uehara, Y. (2004) Nucleolar Nek11 is a novel target of Nek2A in G1/S-arrested cells. *J Biol Chem*, **279**, 32716-32727.
- Norbury, C. and Nurse, P. (1992) Animal cell cycles and their control. *Annu Rev Biochem*, **61**, 441-470.
- Nunez, G., Benedict, M.A., Hu, Y. and Inohara, N. (1998) Caspases: the proteases of the apoptotic pathway. *Oncogene*, **17**, 3237-3245.
- O'Connell, M.J., Krien, M.J. and Hunter, T. (2003) Never say never. The NIMA-related protein kinases in mitotic control. *Trends Cell Biol*, **13**, 221-228.
- O'Connell, M.J., Norbury, C. and Nurse, P. (1994) Premature chromatin condensation upon accumulation of NIMA. *Embo J*, **13**, 4926-4937.
- O.N.S. (2004) Mortality statistics. *DH2 no.31*. Office for national statistics, London, p. 312.
- Oakley, B.R. and Morris, N.R. (1983) A mutation in *Aspergillus nidulans* that blocks the transition from interphase to prophase. *J Cell Biol*, **96**, 1155-1158.
- Oshimori, N., Ohsugi, M. and Yamamoto, T. (2006) The Plk1 target Kizuna stabilizes mitotic centrosomes to ensure spindle bipolarity. *Nat Cell Biol*, **8**, 1095-1101.
- Osmani, S.A., May, G.S. and Morris, N.R. (1987) Regulation of the mRNA levels of *nimA*, a gene required for the G2-M transition in *Aspergillus nidulans*. *J Cell Biol*, **104**, 1495-1504.
- Palmer, C.J., Scott, B.T. and Jones, L.R. (1991) Purification and complete sequence determination of the major plasma membrane substrate for cAMP-dependent protein kinase and protein kinase C in myocardium. *J Biol Chem*, **266**, 11126-11130.
- Patel, D., Incassati, A., Wang, N. and McCance, D.J. (2004) Human papillomavirus type 16 E6 and E7 cause polyploidy in human keratinocytes and up-regulation of G₂-M-phase proteins. *Cancer Res.*, **64**, 1299-1306.

Pei, Y. and Tuschl, T. (2006) On the art of identifying effective and specific siRNAs. *Nat Methods*, **3**, 670-676.

Pennati, M., Campbell, A.J., Curto, M., Binda, M., Cheng, Y., Wang, L.Z., Curtin, N., Golding, B.T., Griffin, R.J., Hardcastle, I.R., Henderson, A., Zaffaroni, N. and Newell, D.R. (2005) Potentiation of paclitaxel-induced apoptosis by the novel cyclin-dependent kinase inhibitor NU6140: a possible role for survivin down-regulation. *Mol Cancer Ther*, **4**, 1328-1337.

Peters, J.M. (1999) Subunits and substrates of the anaphase-promoting complex. *Exp Cell Res*, **248**, 339-349.

Petersen, J., Paris, J., Willer, M., Philippe, M. and Hagan, I.M. (2001) The S. pombe aurora-related kinase Ark1 associates with mitotic structures in a stage dependent manner and is required for chromosome segregation. *J Cell Sci*, **114**, 4371-4384.

Pihan, G.A. and Doxsey, S.J. (1999) The mitotic machinery as a source of genetic instability in cancer. *Seminars in Cancer Biology*, **9**, 289-302.

Pihan, G.A., Purohit, A., Wallace, J., Knecht, H., Woda, B., Quesenberry, P. and Doxsey, S.J. (1998) Centrosome defects and genetic instability in malignant tumors. *Cancer Res*, **58**, 3974-3985.

Pihan, G.A., Purohit, A., Wallace, J., Malhotra, R., Liotta, L. and Doxsey, S.J. (2001) Centrosome defects can account for cellular and genetic changes that characterize prostate cancer progression. *Cancer Res*, **61**, 2212-2219.

Pihan, G.A., Wallace, J., Zhou, H. and Doxsey, S.J. (2003a) Centrosome abnormalities and chromosome instability occur together in pre-invasive carcinomas. *Cancer Res.*, **63**, 1398-1404.

Pihan, G.A., Wallace, J., Zhou, Y. and Doxsey, S.J. (2003b) Centrosome abnormalities and chromosome instability occur together in pre-invasive carcinomas. *Cancer Res*, **63**, 1398-1404.

Pines, J. and Lindon, C. (2005) Proteolysis: anytime, any place, anywhere? *Nat Cell Biol*, **7**, 731-735.

Polci, R., Peng, A., Chen, P.L., Riley, D.J. and Chen, Y. (2004) NIMA-related protein kinase 1 is involved early in the ionizing radiation-induced DNA damage response. *Cancer Res*, **64**, 8800-8803.

Pradel, L.C., Bonhivers, M., Landrein, N. and Robinson, D.R. (2006) NIMA-related kinase TbNRKC is involved in basal body separation in *Trypanosoma brucei*. *J Cell Sci*, **119**, 1852-1863.

Prigent, C., Glover, D.M. and Giet, R. (2005) Drosophila Nek2 protein kinase knockdown leads to centrosome maturation defects while overexpression causes centrosome fragmentation and cytokinesis failure. *Exp Cell Res*, **303**, 1-13.

Pu, R.T., Xu, G., Wu, L., Vierula, J., O'Donnell, K., Ye, X.S. and Osmani, S.A. (1995) Isolation of a functional homolog of the cell cycle-specific NIMA protein kinase of *Aspergillus nidulans* and functional analysis of conserved residues. *J Biol Chem*, **270**, 18110-18116.

Pugacheva, E.N. and Golemis, E.A. (2005) The focal adhesion scaffolding protein HEF1 regulates activation of the Aurora-A and Nek2 kinases at the centrosome. *Nat Cell Biol*, **7**, 937-946.

Quintyne, N.J., Reing, J.E., Hoffelder, D.R., Gollin, S.M. and Saunders, W.S. (2005) Spindle multipolarity is prevented by centrosomal clustering. *Science*, **307**, 127-129.

Ramos-Vara, J.A. (2005) Technical aspects of immunohistochemistry. *Vet Pathol*, **42**, 405-426.

Rapley, J., Baxter, J.E., Blot, J., Wattam, S.L., Casenghi, M., Meraldi, P., Nigg, E.A. and Fry, A.M. (2005) Coordinate regulation of the mother centriole component nlp by nek2 and plk1 protein kinases. *Mol Cell Biol*, **25**, 1309-1324.

Reagan-Shaw, S. and Ahmad, N. (2005) Silencing of polo-like kinase (Plk) 1 via siRNA causes induction of apoptosis and impairment of mitosis machinery in human prostate cancer cells: implications for the treatment of prostate cancer. *Faseb J*, **19**, 611-613.

Rellos, P., Ivins, F.J., Baxter, J.E., Pike, A., Nott, T., Parkinson, D.-M., Das, S., Howell, S., Fedorov, O., Shen, Q.Y., Fry, A.M., Knapp, S. and Smerdon, S.J. (2006) Structure and regulation of the human Nek2 centrosomal kinase.

Ren, B., Cam, H., Takahashi, Y., Volkert, T., Terragni, J., Young, R.A. and Dynlacht, B.D. (2002) E2F integrates cell cycle progression with DNA repair, replication, and G(2)/M checkpoints. *Genes Dev*, **16**, 245-256.

Ren, R. (2005) Mechanisms of BCR-ABL in the pathogenesis of chronic myelogenous leukaemia. *Nat Rev Cancer*, **5**, 172-183.

Reynolds, A., Anderson, E.M., Vermeulen, A., Fedorov, Y., Robinson, K., Leake, D., Karpilow, J., Marshall, W.S. and Khvorova, A. (2006) Induction of the interferon response by siRNA is cell type- and duplex length-dependent. *Rna*, **12**, 988-993.

Ring, D., Hubble, R. and Kirschner, M. (1982) Mitosis in a cell with multiple centrioles. *J Cell Biol*, **94**, 549-556.

Roig, J., Mikhailov, A., Belham, C. and Avruch, J. (2002) Nercc1, a mammalian NIMA-family kinase, binds the Ran GTPase and regulates mitotic progression. *Genes Dev*, **16**, 1640-1658.

Salisbury, J.L., D'Assoro, A.B. and Lingle, W.L. (2004) Centrosome amplification and the origin of chromosomal instability in breast cancer. *J Mammary Gland Biol Neoplasia*, **9**, 275-283.

- Samuels, Y., Diaz, L.A., Jr., Schmidt-Kittler, O., Cummins, J.M., Delong, L., Cheong, I., Rago, C., Huso, D.L., Lengauer, C., Kinzler, K.W., Vogelstein, B. and Velculescu, V.E. (2005) Mutant PIK3CA promotes cell growth and invasion of human cancer cells. *Cancer Cell*, **7**, 561-573.
- Samuels, Y., Wang, Z., Bardelli, A., Silliman, N., Ptak, J., Szabo, S., Yan, H., Gazdar, A., Powell, S.M., Riggins, G.J., Willson, J.K., Markowitz, S., Kinzler, K.W., Vogelstein, B. and Velculescu, V.E. (2004) High frequency of mutations of the PIK3CA gene in human cancers. *Science*, **304**, 554.
- Sasai, K., Katayama, H., Stenoien, D.L., Fujii, S., Honda, R., Kimura, M., Okano, Y., Tatsuka, M., Suzuki, F., Nigg, E.A., Earnshaw, W.C., Brinkley, W.R. and Sen, S. (2004) Aurora-C kinase is a novel chromosomal passenger protein that can complement Aurora-B kinase function in mitotic cells. *Cell Motil Cytoskeleton*, **59**, 249-263.
- Sato, N., Mizumoto, K., Nakamura, M., Maehara, N., Minamishima, Y.A., Nishio, S., Nagai, E. and Tanaka, M. (2001) Correlation between centrosome abnormalities and chromosomal instability in human pancreatic cancer cells. *Cancer Genetics and Cytogenetics*, **126**, 13-19.
- Saunders, W. (2005) Centrosomal amplification and spindle multipolarity in cancer cells. *Semin Cancer Biol*, **15**, 25-32.
- Schneeweiss, A., Sinn, H.-P., Ehemann, V., Khbeis, T., Neben, K., Krause, U., Ho, A.D., Bastert, G. and Kramer, A. (2003) Centrosomal aberrations in primary invasive breast cancer are associated with nodal status and hormone receptor expression. *Int. J. Cancer*, **107**, 346-352.
- Schultz, S.J., Fry, A.M., Sutterlin, C., Ried, T. and Nigg, E.A. (1994) Cell cycle-dependent expression of Nek2, a novel human protein kinase related to the NIMA mitotic regulator of *Aspergillus nidulans*. *Cell Growth Differ*, **5**, 625-635.
- Sen, S., Zhou, H. and White, R.A. (1997) A putative serine/threonine kinase encoding gene BTAK on chromosome 20q13 is amplified and overexpressed in human breast cancer cell lines. *Oncogene*, **14**, 2195-2200.
- Sen, S., Zhou, H., Zhang, R.D., Yoon, D.S., Vakar-Lopez, F., Ito, S., Jiang, F., Johnston, D., Grossman, H.B., Ruifrok, A.C., Katz, R.L., Brinkley, W. and Czerniak, B. (2002) Amplification/overexpression of a mitotic kinase gene in human bladder cancer. *J Natl Cancer Inst*, **94**, 1320-1329.
- Seshadri, R., Matthews, C., Dobrovic, A. and Horsfall, D.J. (1989) The significance of oncogene amplification in primary breast cancer. *Int J Cancer*, **43**, 270-272.
- Shah, J.V., Botvinick, E., Bonday, Z., Furnari, F., Berns, M. and Cleveland, D.W. (2004) Dynamics of centromere and kinetochore proteins; implications for checkpoint signaling and silencing. *Curr Biol*, **14**, 942-952.
- Sharp, D.J., Rogers, G.C. and Scholey, J.M. (2000) Microtubule motors in mitosis. *Nature*, **407**, 41-47.

Shay, J.W. and Bacchetti, S. (1997) A survey of telomerase activity in human cancer. *Eur J Cancer*, **33**, 787-791.

Shi, S.R., Cote, R.J. and Taylor, C.R. (1997) Antigen retrieval immunohistochemistry: past, present, and future. *J Histochem Cytochem*, **45**, 327-343.

Shi, S.R., Cote, R.J. and Taylor, C.R. (2001) Antigen retrieval techniques: current perspectives. *J Histochem Cytochem*, **49**, 931-937.

Shi, S.R., Key, M.E. and Kalra, K.L. (1991) Antigen retrieval in formalin-fixed, paraffin-embedded tissues: an enhancement method for immunohistochemical staining based on microwave oven heating of tissue sections. *J Histochem Cytochem*, **39**, 741-748.

Smith, M.R., Wilson, M.L., Hamanaka, R., Chase, D., Kung, H., Longo, D.L. and Ferris, D.K. (1997) Malignant transformation of mammalian cells initiated by constitutive expression of the polo-like kinase. *Biochem Biophys Res Commun*, **234**, 397-405.

Sonn, S., Khang, I., Kim, K. and Rhee, K. (2004) Suppression of Nek2A in mouse early embryos confirms its requirement for chromosome segregation. *J Cell Sci*, **117**, 5557-5566.

Spankuch-Schmitt, B., Bereiter-Hahn, J., Kaufmann, M. and Strebhardt, K. (2002a) Effect of RNA silencing of polo-like kinase-1 (PLK1) on apoptosis and spindle formation in human cancer cells. *J Natl Cancer Inst*, **94**, 1863-1877.

Spankuch-Schmitt, B., Wolf, G., Solbach, C., Loibl, S., Knecht, R., Stegmüller, M., von Minckwitz, G., Kaufmann, M. and Strebhardt, K. (2002b) Downregulation of human polo-like kinase activity by antisense oligonucleotides induces growth inhibition in cancer cells. *Oncogene*, **21**, 3162-3171.

Sundberg, S.A. (2000) High-throughput and ultra-high-throughput screening: solution- and cell-based approaches. *Curr Opin Biotechnol*, **11**, 47-53.

Sunkel, C.E. and Glover, D.M. (1988) polo, a mitotic mutant of *Drosophila* displaying abnormal spindle poles. *J Cell Sci*, **89** (Pt 1), 25-38.

Surpili, M.J., Delben, T.M. and Kobarg, J. (2003) Identification of proteins that interact with the central coiled-coil region of the human protein kinase NEK1. *Biochemistry*, **42**, 15369-15376.

Takahashi, T., Futamura, M., Yoshimi, N., Sano, J., Katada, M., Takagi, Y., Kimura, M., Yoshioka, T., Okano, Y. and Saji, S. (2000) Centrosomal kinases, HsAIRK1 and HsAIRK3, are overexpressed in primary colorectal cancers. *Jpn. J. Cancer Res.*, **91**, 1007-1014.

Takai, N., Miyazaki, T., Fujisawa, K., Nasu, K., Hamanaka, R. and Miyakawa, I. (2001a) Expression of polo-like kinase in ovarian cancer is associated with histological grade and clinical stage. *Cancer Lett*, **164**, 41-49.

- Takai, N., Miyazaki, T., Fujisawa, K., Nasu, K., Hamanaka, R. and Miyakawa, I. (2001b) Polo-like kinase (PLK) expression in endometrial carcinoma. *Cancer Lett*, **169**, 41-49.
- Takai, N., Miyazaki, T., K., F., Nasu, K., Hamanaka, R. and Miyakawa, I. (2001c) Expression of polo-like kinase in ovarian cancer is associated with histological grade and clinical stage. *Cancer Letts.*, **164**, 41-49.
- Tan, B.C. and Lee, S.C. (2004) Nek9, a novel FACT-associated protein, modulates interphase progression. *J Biol Chem*, **279**, 9321-9330.
- Tanaka, K. and Nigg, E.A. (1999) Cloning and characterization of the murine Nek3 protein kinase, a novel member of the NIMA family of putative cell cycle regulators. *J Biol Chem*, **274**, 13491-13497.
- Tarapore, P., Okuda, M. and Fukasawa, K. (2002) A mammalian in vitro centriole duplication system: evidence for involvement of CDK2/cyclin E and nucleophosmin/B23 in centrosome duplication. *Cell Cycle*, **1**, 75-81.
- Thomas, D., Karle, C.A. and Kiehn, J. (2004) Modulation of HERG potassium channel function by drug action. *Ann Med*, **36 Suppl 1**, 41-46.
- Tokumitsu, Y., Mori, M., Tanaka, S., Akazawa, K., Nakano, S. and Niho, Y. (1999) Prognostic significance of polo-like kinase expression in esophageal carcinoma. *Int J Oncol*, **15**, 687-692.
- Tsou, M.F. and Stearns, T. (2006a) Controlling centrosome number: licenses and blocks. *Curr Opin Cell Biol*, **18**, 74-78.
- Tsou, M.F. and Stearns, T. (2006b) Mechanism limiting centrosome duplication to once per cell cycle. *Nature*, **442**, 947-951.
- Twomey, C., Wattam, S.L., Pillai, M.R., Rapley, J., Baxter, J.E. and Fry, A.M. (2004) Nek2B stimulates zygotic centrosome assembly in *Xenopus laevis* in a kinase-independent manner. *Dev Biol*, **265**, 384-398.
- Uetake, Y. and Sluder, G. (2004) Cell cycle progression after cleavage failure: mammalian somatic cells do not possess a "tetraploidy checkpoint". *J Cell Biol*, **165**, 609-615.
- Underwood, J.C.E. (ed.). (2002) *General and systematic pathology*. Churchill Livingstone, London.
- Upadhyay, P., Birkenmeier, E.H., Birkenmeier, C.S. and Barker, J.E. (2000) Mutations in a NIMA-related kinase gene, Nek1, cause pleiotropic effects including a progressive polycystic kidney disease in mice. *Proc Natl Acad Sci U S A*, **97**, 217-221.
- Uto, K. and Sagata, N. (2000) Nek2B, a novel maternal form of Nek2 kinase, is essential for the assembly or maintenance of centrosomes in early *Xenopus* embryos. *Embo J*, **19**, 1816-1826.

van Vugt, M.A. and Medema, R.H. (2005) Getting in and out of mitosis with Polo-like kinase-1. *Oncogene*, **24**, 2844-2859.

von Ahsen, O. and Bomer, U. (2005) High-throughput screening for kinase inhibitors. *Chembiochem*, **6**, 481-490.

W.H.O. (2006) Cancer. Fact sheet 297. In Organization, W.H. (ed.), Geneva, Switzerland, p. 4.

Wai, D.H., Schaefer, K.L., Schramm, A., Korsching, E., Van Valen, F., Ozaki, T., Boecker, W., Schweigerer, L., Dockhorn-Dworniczak, B. and Poremba, C. (2002) Expression analysis of pediatric solid tumor cell lines using oligonucleotide microarrays. *Int. J. Oncol.*, **20**, 441-451.

Warnke, S., Kemmler, S., Hames, R.S., Tsai, H.L., Hoffmann-Rohrer, U., Fry, A.M. and Hoffmann, I. (2004) Polo-like kinase-2 is required for centriole duplication in mammalian cells. *Curr Biol*, **14**, 1200-1207.

Weinberg, R. (2006) *The biology of cancer*. Garland press, New York.

Weiss, M.M., Kuipers, E.J., Postma, C., Snijders, A.M., Pinkel, D., Meuwissen, S.G., Albertson, D. and Meijer, G.A. (2004) Genomic alterations in primary gastric adenocarcinomas correlate with clinicopathological characteristics and survival. *Cell Oncol*, **26**, 307-317.

Wiese, C. and Zheng, Y. (2000) A new function for the gamma-tubulin ring complex as a microtubule minus-end cap. *Nat Cell Biol*, **2**, 358-364.

Wolf, G., Elez, R., Doermer, A., Holtrich, U., Ackermann, H., Stutte, H.J., Altmannsberger, H.M., Rubsamen-Waigmann, H. and Strebhardt, K. (1997) Prognostic significance of polo-like kinase (PLK) expression in non-small cell lung cancer. *Oncogene*, **14**, 543-549.

Wonsey, D.R. and Follettie, M.T. (2005) Loss of the forkhead transcription factor FoxM1 causes centrosome amplification and mitotic catastrophe. *Cancer Res*, **65**, 5181-5189.

Workman, P. (2001) New drug targets for genomic cancer therapy: successes, limitations, opportunities and future challenges. *Curr Cancer Drug Targets*, **1**, 33-47.

Wu, W.J. (2006) Alternative Splicing regulates the nuclear localization of Nek2C.

Yamamoto, Y., Matsuyama, H., Furuya, T., Oga, A., Yoshihiro, S., Okuda, M., Kawauchi, S., Sasaki, K. and Naito, K. (2004) Centrosome hyperamplification predicts progression and tumor recurrence in bladder cancer. *Clin Cancer Res*, **10**, 6449-6455.

Yang, J., Adamian, M. and Li, T. (2006) Rootletin interacts with C-Nap1 and may function as a physical linker between the pair of centrioles/basal bodies in cells. *Mol Biol Cell*, **17**, 1033-1040.

Yang, J., Liu, X., Yue, G., Adamian, M., Bulgakov, O. and Li, T. (2002) Rootletin, a novel coiled-coil protein, is a structural component of the ciliary rootlet. *J Cell Biol*, **159**, 431-440.

Ye, X.S., Fincher, R.R., Tang, A., Osmani, A.H. and Osmani, S.A. (1998) Regulation of the anaphase-promoting complex/cyclosome by bimAAPC3 and proteolysis of NIMA. *Mol Biol Cell*, **9**, 3019-3030.

Yin, M.J., Shao, L., Voehringer, D., Smeal, T. and Jallal, B. (2003) The serine/threonine kinase Nek6 is required for cell cycle progression through mitosis. *J Biol Chem*, **278**, 52454-52460.

Zhou, H., Kuang, J., Zhong, L., Kuo, W.-L., Gray, J.W., Sahin, A., Brinkley, B.R. and Sen, S. (1998a) Tumour amplified kinase STK15/BTAK induces centrosome amplification, aneuploidy and transformation. *Nat. Genet.*, **20**, 189-193.

APPENDIX

NEK2 MUTATION SCREENING

	Sample number*	SSCP Exon 1	SSCP Exon 2	SSCP Exon 3	Sequencing Exon 3	SSCP Exon 4	SSCP Exon 5	Sequencing Exon 5	SSCP Exon 6	Sequencing Exon 6	SSCP Exon 7	Sequencing Exon 7	SSCP Exon 8	Sequencing Exon 8
Tumour Samples (MDF019/05)	2737	-	-	+	g.154159 T>C	-	-		-		-		+/-	no mutation found
	2785	-	-	+	SSCP electropherogram consistent with g.154159 T>C	-	-		+/-	no mutation found	+	g.160537 A>G	+	g.164245 A>G
	2799	-	-	+	g.154159 T>C Homozygote	-	-		+		+	g.160537 A>G	+	g.164245 A>G
	2819	-	-	+	SSCP electropherogram consistent with g.154159 T>C	-	-		-		-		+/-	no mutation found
	2914	-	-	-		-	-		-		-		+/-	no mutation found
	3206	-	-	+	SSCP electropherogram consistent with g.154159 T>C	-	-		-		-		+/-	no mutation found
	3227	-	-	+	SSCP electropherogram consistent with g.154159 T>C	-	+	g.157426 G>T	-		-		+/-	no mutation found
	3420	-	-	-		-	-		-		-		+/-	no mutation found
	3076	-	-	+	SSCP electropherogram consistent with g.154159 T>C	-	-		-		-		+/-	no mutation found
Cell Line Samples (MDF012/03)	3509	-	-	+	g.154159 T>C Homozygote	-	-		-		+	g.160537 A>G	+	g.164245 A>G
	MCF7	-	-	+	SSCP electropherogram consistent with g.154159 T>C Homozygote	-	-		-		-		+	g.164245 A>G Homozygote
	MDA MB 415	-	-	+	SSCP electropherogram consistent with g.154159 T>C Homozygote	-	-		-		-		+/-	no mutation found
	MDA MB 361	-	-	+	SSCP electropherogram consistent with g.154159 T>C Homozygote	-	-		-		-		+	g.164245 A>G Homozygote
	MDA MB 468	-	-	+	SSCP electropherogram consistent with g.154159 T>C	-	-		-		-		+/-	g.164245 A>G
	MDA 435	-	-	-		-	-		-		-		+/-	no mutation found
	BT20	-	-	-		-	-		-		-		+/-	no mutation found
	SKBR3	-	-	+	SSCP electropherogram consistent with g.154159 T>C	-	-		-		-		-	
	T47D	-	-	-		-	-		-		-		+/-	no mutation found
	MDA MB 231	-	-	-		-	-		-		-		-	
	ZR75	-	-	-		-	+/-	g.157426 G>T Homozygote	-		-		-	

N.B. MUTATIONS ARE HETEROZYGOUS UNLESS STATED OTHERWISE

DNA sequencing:

numbering based on Genbank genomic reference sequence AC096637.1

SSCP results scoring:

- : no mutation detected

+: mutation detected

+/- : equivocal result

NEK2 MUTATION SCREENING

Mutation ¹	cDNA Reference	Protein Reference	Position	Predicted Effect ⁸	Frequency (Total of 20 samples analysed)
g.154159 T>C	c.504 T>C	p.H168H	Exon 3 codon 168 ²	Silent Variation ^{3,8}	13 samples
g.157426 G>T	intronic	intronic	IVS 5 + 14 G>T	none predicted	2 samples
g.160537 A>G	c.1061 A>G	p.N354S	Exon 7 codon 76 ⁴	Asparagine(N) > Serine(S) ⁵	3 samples
g.164245 A>G	c.1317 A>G	p.R439R	Exon 8 codon 206 ⁶	Silent variation ^{7,8}	6 samples

¹ based on Genbank sequence AC096637.1

² the change in codon 168 of Exon 3 is CAT > CAC. Both sequences encode a Histidine(H) residue

³ this variation is listed in dbSNP (refSNP ID rs701929).

⁴ the change in codon 76 of Exon 7 is AAC > AGC.

⁵ this variation is listed in dbSNP (refSNP ID rs10429965)

⁶ the change in codon 206 of Exon 8 is AGA > AGG. Both sequences encode an Arginine(R) residue

⁷ this variation is listed in the dbSNP (refSNP ID rs12031285)

⁸ the predicted effect of all variations on exonic splice site enhancers was checked using software at <http://rulai.cshl.edu/tools/ESE/>
this software indicated that the variants in exons 3 and 8 may have a possible effect on splicing.

The Centrosomal Kinase Nek2 Displays Elevated Levels of Protein Expression in Human Breast Cancer

Daniel G. Hayward,¹ Robert B. Clarke,² Alison J. Faragher,¹ Meenu R. Pillai,¹ Iain M. Hagan,² and Andrew M. Fry¹

¹Department of Biochemistry, University of Leicester, Leicester; and ²Paterson Institute for Cancer Research, Manchester, United Kingdom

ABSTRACT

Aneuploidy and chromosome instability are common abnormalities in human cancer. Loss of control over mitotic progression, multipolar spindle formation, and cytokinesis defects are all likely to contribute to these phenotypes. Nek2 is a cell cycle-regulated protein kinase with maximal activity at the onset of mitosis that localizes to the centrosome. Functional studies have implicated Nek2 in regulation of centrosome separation and spindle formation. Here, we present the first study of the protein expression levels of the Nek2 kinase in human cancer cell lines and primary tumors. Nek2 protein is elevated 2- to 5-fold in cell lines derived from a range of human tumors including those of cervical, ovarian, breast, prostate, and leukemic origin. Most importantly, by immunohistochemistry, we find that Nek2 protein is significantly up-regulated in preinvasive *in situ* ductal carcinomas of the breast as well as in invasive breast carcinomas. Finally, by ectopic expression of Nek2A in immortalized HBL100 breast epithelial cells, we show that increased Nek2 protein leads to accumulation of multinucleated cells with supernumerary centrosomes. These data highlight the Nek2 kinase as novel potential target for chemotherapeutic intervention in breast cancer.

INTRODUCTION

Aneuploidy, the possession of more or less than the correct number of chromosomes, is the single most common feature of solid human tumor cells and is generally associated with poor prognostic outcome (1, 2). The underlying mechanisms for the generation of aneuploidy, although poorly understood, are likely to include defects in the mitotic machinery used to segregate duplicated chromosomes between daughter cells (3). Persistent loss of control over chromosome segregation leads to chromosome instability, which is defined as the rate of karyotypic change that occurs within a tumor over time. Ominously, chromosome instability leads to a heterogeneous population of cells with respect to genetic content and provides the tumor with a mechanism to select for cells with more malignant or drug resistant properties (4).

The centrosome plays a critical role in mitotic spindle formation and chromosome segregation, because it is the primary site of microtubule nucleation in cells (5, 6). Normal cells enter mitosis with two properly duplicated centrosomes that ensure bipolarity, as well as correct axial positioning, of the spindle. Cancer cells from a wide variety of tumor types exhibit multipolar spindles, and these are often associated with abnormal centrosome number or architecture (7–9). In addition, prematurely split centrosomes, unusually positioned centrosomes, and centrosomal proteins with aberrant levels of phosphorylation have all been detected in tumor cells (8, 10). Supernumerary

centrosomes, and thereby aneuploidy, may be generated either by a direct uncoupling of the centrosome duplication cycle from the cell division cycle or through an indirect failure of cell division that leads to tetraploidization (3, 11, 12). Cells lacking p53 or Rb pocket proteins fail to eliminate tetraploid cells allowing them to progress to the next mitosis where multipolar spindles can form (13). As a result of centrosome defects, aneuploidy, and chromosome instability being detected in early, even preinvasive, tumors (14, 15), there is considerable interest in identifying whether centrosomal proteins are either mutated or abnormally expressed in cancer cells.

A number of cell cycle-regulated protein kinases have been localized to the centrosome including Cdk1, Plk1, and Aurora-A. Each of these kinases is active in mitosis and required for mitotic progression and correct bipolar spindle formation (16). Overexpression of active and catalytically inactive versions of Plk1 and Aurora-A leads to mitotic defects, the generation of aneuploid cells, and supernumerary centrosomes (17, 18). Plk1 (*e.g.*, refs. 19–21) and Aurora-A (18, 22–25) also exhibit elevated mRNA and protein expression in a wide variety of tumors and cancer cell lines and can induce transformation on overexpression in model systems (18, 25, 26). Another centrosomal kinase that is regulated in a cell cycle-dependent manner is Nek2 (NIMA-related kinase 2; ref. 27). Nek2 is expressed in human cells as two splice variants, Nek2A and Nek2B, both of which localize to the centrosome (28). The combined abundance and activity of the two forms peaks in S and G₂ phase of the cell cycle, whereas Nek2A is specifically targeted for proteasomal destruction in mitosis (29). Nek2A also has a binding site for the catalytic subunit of PP1, and hyperactivation of Nek2A at the onset of mitosis is thought to be dependent on inactivation of PP1 (30). Overexpression of active Nek2A leads to premature centrosome splitting (31, 32), whereas overexpression of kinase-dead Nek2A causes the formation of centrosomal abnormalities, monopolar spindles, and aneuploidy (33). These data, combined with the characterization of C-Nap1 (34, 35), a centrosomal substrate of Nek2, suggest a physiologic role for Nek2A in regulating the separation of centrosomes at the G₂-M transition. Studies with the *Xenopus laevis* homologues of Nek2 indicate that Nek2B may primarily be required for assembly and maintenance of centrosomes in early embryos in a kinase-independent manner (36, 37).

Despite its importance in centrosome regulation and spindle formation, detailed analysis of Nek2 expression in tumors has not been performed. The only relevant data comes from two microarray studies that looked at the expression of a range of genes in certain cancer models. These revealed that Nek2 mRNA is significantly elevated in Ewing tumor (pediatric osteosarcoma) cell lines and upon transformation of low-grade follicular lymphoma to the more aggressive diffuse large B-cell lymphoma (38, 39). Here, we use specific Nek2 antibodies to demonstrate that Nek2 expression is elevated between 2- and 5-fold in cell lines derived from a variety of different cancer types and is significantly increased in the majority of breast tumors including early preinvasive tumors. We also show that overexpression of Nek2 in nontransformed breast cells can induce aneuploidy. These data lend support to the hypothesis that deregulation of centrosomal proteins in general, and Nek2 in particular, could be contributory factors in cancer progression.

Received 3/18/04; revised 7/19/04; accepted 8/17/04.

Grant support: Cancer Research United Kingdom (C1420/A4582). A. M. Fry is a Lister Institute Research Fellow.

The costs of publication of this article were defrayed in part by the payment of page charges. This article must therefore be hereby marked *advertisement* in accordance with 18 U.S.C. Section 1734 solely to indicate this fact.

Note: A. Faragher is currently at the MRC Toxicology Unit, Hodgkin Building, University of Leicester, University Road, Leicester LE1 7RH, United Kingdom; M. Pillai is currently at the Department of Immunology, Institute of Animal Health, Ash Road, Pirbright, Surrey GU24 0NF, United Kingdom.

Requests for reprints: Andrew M. Fry, Department of Biochemistry, University of Leicester, University Road, Leicester LE1 7RH, United Kingdom. Phone: 44-116-252-5024; Fax: 44-116-252-3369; E-mail: amf5@le.ac.uk.

©2004 American Association for Cancer Research.

MATERIALS AND METHODS

Cell Culture and Transfection. HeLa, HBL100, MCF-7, MDA-MB-231, MDA-MB-468, and T47D cells were cultured in Dulbecco's Modified Eagle's Medium (Invitrogen, Paisley, United Kingdom) supplemented with 10% fetal calf serum (FCS, Invitrogen) and 2 mmol/L glutamine (Invitrogen); ZR75-1, SKOV3, OVCAR5, DU-145, and PNT2-C2 were cultured in RPMI 1640 (Invitrogen) with 10% FCS and 4 mmol/L glutamine; K562, KCL22, U937, HL60, Ros, Rec, and Riva were cultured in RPMI 1640 (Invitrogen) with 10% FCS and 2 mmol/L glutamine; PC-3 cells were cultured in Ham's F12 (Invitrogen) with 7% FCS and 4 mmol/L glutamine (PC-3). U2OS osteosarcoma T-REx cells (Invitrogen) and tetracycline-inducible Nek2A cell lines were cultured and induced with tetracycline as described previously (33). Primary T cells were obtained as described previously (28). HBL100 cells were transfected using FuGENE 6 transfection reagent according to the manufacturer's instructions (Roche, Lewes, United Kingdom).

Cell Synchronization and Reverse Transcription-PCR. HeLa cells were chemically synchronized in different phases of the cell cycle and analyzed by flow cytometry as described previously (28). Total RNA was isolated from synchronized HeLa cells using TRI reagent (Sigma, St. Louis, MO) according to the manufacturer's instructions and treated with amplification grade DNaseI (Roche) to avoid DNA contamination. Semiquantitative reverse transcription-PCR (RT-PCR) reactions were then established as described previously (36) using primers specific for human Nek2A and Nek2B (28). Specifically, 1 μ g (for Nek2A) and 2 μ g (for Nek2B) of total RNA was used for cDNA synthesis and PCR reactions (94°C, 30 seconds; 50°C, 30 seconds; and 72°C, 45 seconds) carried out for 30 cycles.

Cell Extraction, Protein Electrophoresis, and Western Blotting. Whole cell lysates of asynchronous cell populations were prepared in radioimmunoprecipitation assay buffer [50 mmol/L Tris-HCl (pH 8.0), 150 mmol/L NaCl, 1% NP40, 0.5% sodium deoxycholate, and 0.1% SDS]. Briefly, cells were washed in ice-cold 1 \times PBS (150 mmol/L NaCl, 2.7 mmol/L KCl, 8 mmol/L disodium hydrogen P_i, and 1.5 mmol/L potassium dihydrogen phosphate) and lysed directly in radioimmunoprecipitation assay buffer on ice for 30 minutes, centrifuged at 4°C, 14,000 rpm, to remove insoluble material and total protein concentration of the resulting supernatant determined by bicinchoninic acid assay (Pierce, Rockford, United Kingdom). Lysate, 50 μ g, for each cell line was resolved by SDS-PAGE, transferred to nitrocellulose membrane, and probed with affinity-purified antibodies raised to Nek2 [antipeptide antibody (40), 1 μ g/ml], C-Nap1 [R63 (34), 1 μ g/ml], and α -tubulin (Sigma, 1 μ g/ml). Blots were developed by enhanced chemiluminescence (Amersham Biosciences, Little Chalfont, United Kingdom).

Immunohistochemistry. Four-micrometer thick sections of formalin-fixed, paraffin wax-embedded samples of resected tumor or normal breast tissue were mounted on (3-aminopropyl)triethoxysilane coated slides. Sections were dewaxed in three washes of xylene and rehydrated in graded alcohols: 100% EtOH for 10 minutes followed by 95%, 90%, and 70% for 5 minutes each, before incubation in 1 \times PBS. Slides were then incubated in a pressure cooker in 10 mmol/L citrate buffer (10 mmol/L citric acid monohydrate; pH 6.0), for 2 or 3 minutes at full pressure to recover antigenic epitopes. Slides were probed with affinity-purified polyclonal rabbit antibodies raised to Nek2 [either antipeptide (40) or R40 (31), 2 μ g/ml] or control rabbit IgGs as an appropriate control (DAKO, Ely, United Kingdom; 2 μ g/mL). For other measurements, slides were probed with antibodies raised against the Ki67 proliferation-associated nuclear antigen (clone MIB1, Dako), estrogen receptor α (clone 1D5, Dako), progesterone receptor (clone PgR636, Dako), and epidermal growth factor receptor (EGFR, NCL-EGFR, Novocastra) at concentrations recommended by the manufacturers. Bound antibodies were detected with a horseradish peroxidase-conjugated secondary antibody system (Envision, DAKO) and 3,3'-diaminobenzidine development according to the manufacturer's protocol (brown stain). Developed slides were counterstained in hematoxylin (purple stain), dehydrated through graded alcohols, incubated in Histoclear (National Diagnostics, Hesse, United Kingdom), and mounted in Pertex (Cellpath, Newtown, United Kingdom). Slide images were captured with a Zeiss Axioskop microscope using a Zeiss Axiocam and processed using Axiovision and Adobe photoshop software. EGFR expression was graded from - (zero) to +++++ (very high) intensity of membrane staining on most tumor cells. Nek2, estrogen receptor α , progesterone receptor, and Ki67 were assessed as the percentage of positively stained cells after examination of $\geq 1,000$

tumor cells in randomly selected fields. For example, in tumor sample 2196, 1,077 of 1,147 cells were positively stained for Nek2 (93.9%), 805 of 1,145 cells for estrogen receptor α (70%), 238 of 1,004 cells for progesterone receptor (24%), and 69 of 1,007 cells for Ki67 (6.9%). Intensity of staining was not assessed for these four antibodies.

Immunofluorescence microscopy. HBL100 or MDA-MB-468 cells were fixed in cold methanol and processed for indirect immunofluorescence microscopy as described previously (33). Primary antibodies used were anti-myc monoclonal (1:2,000; Cell Signaling Technologies, Beverly, MA), anti- γ -tubulin (1:2,000; Sigma), or anti-C-Nap1 (R63 1 μ g/ml; ref. 34). Secondary antibodies were Alexa Fluor 594 goat antimouse or Alexa Fluor 488 goat antirabbit (1 μ g/ml; Invitrogen). DNA was stained with Hoechst 33258 (0.2 μ g/ml; Calbiochem, San Diego, CA). Images were captured on a Nikon TE300 microscope with an ORCA-ER (Hamamatsu, Hamamatsu, Japan) CCD camera using Openlab 3.1.4 software (Improvision, Coventry, United Kingdom).

RESULTS

Nek2 Protein Expression Is Elevated in a Variety of Human Cancer Cell Lines. To determine whether the protein expression level of the Nek2 kinase is altered in human cancer, we first performed Western blots on extracts prepared from a panel of human cancer cell lines with a polyclonal anti-Nek2 antibody. This previously characterized antibody was raised against a peptide representing amino acids 278–299 of Nek2 and, therefore, detects both Nek2A and Nek2B (40). For controls, Western blots were also performed on extracts of peripheral T lymphocytes, primary human umbilical vein endothelial cells, and immortalized breast and prostate epithelial cells (HBL100 and PNT2-C2, respectively). These four nontransformed cell types showed very similar levels of expression of Nek2 proteins with Nek2A consistently expressed at higher levels than Nek2B. In contrast, elevated expression of Nek2 proteins was found in 10 of 17 (59%) cancer cell lines including those of ovarian (SKOV3 and OVCAR5), leukemic (K562, KCL22, RIVA, and Rec), breast (MCF-7 and MDA-MB-468), prostate (PC3), and cervical (HeLa) origin (Fig. 1A). Those cell lines having increased expression of Nek2A generally showed similar increases in Nek2B suggesting either amplification of the gene or up-regulated transcription (Fig. 1, B and C). None of the cell lines tested had altered expression of the centrosomal Nek2 substrate, C-Nap1 (Fig. 1A).

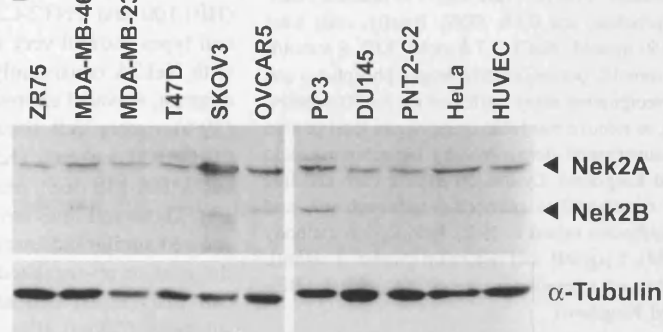
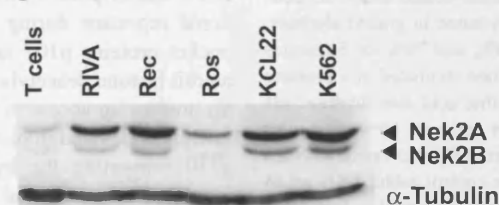
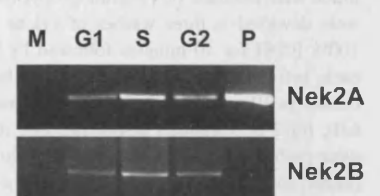
In a recent microarray study, *Nek2* was identified as a potential E2F4 transcription factor target gene (41). E2F4 acts as a transcriptional repressor during G₁ and G₀ through recruitment of the Rb pocket proteins p107 and p130. These tumor suppressors, in turn, recruit histone deacetylases, which promote a closed state of chromatin preventing access to transcriptional activators. Importantly, Nek2 mRNA is elevated in mouse embryo fibroblasts lacking both p107 and p130 supporting the hypothesis that Nek2 transcription is tightly regulated under normal cell cycle conditions (41). To directly test whether Nek2 transcription is cell cycle regulated, we performed semiquantitative RT-PCR on RNA isolated from extracts of synchronized HeLa cells (Fig. 1D). Conditions for semiquantitative RT-PCR were carefully established through serial dilution of total RNA added and optimization of PCR cycle number (36) and synchronization was confirmed by flow cytometry (data not shown). As predicted from the binding of E2F4, the abundance of both Nek2A and Nek2B mRNAs was significantly lower in G₁ than in S and G₂. The mRNAs were undetectable in mitotically arrested cells.

Nek2 Antigen Retrieval in Formaldehyde-Fixed Cells. Whereas studies on cell lines are informative, it was important to determine whether Nek2 protein levels were altered in primary human tumors. For this purpose, we decided to use an immunohistochemical staining approach with the antipeptide Nek2 polyclonal antibody (40). However, the archival tumor samples we wished to use were stored as

A

Tissue Origin	Cell Line	Nek2	C-Nap1
Umbilical Vein	HUVEC	+	ND
Breast	HBL100	+	+
	ZR75	+	+
	MDA-MB-231	+	+
	MDA-MB-468	++	+
	T47D	+	ND
	MCF7	++	ND
Prostate	PNT2-C2	+	ND
	PC3	++	ND
	DU145	+	ND
Ovary	SKOV3	+++	+
	OVCAR5	++	ND
Blood	T cells	+	ND
	K562	+++	+
	KCL22	+++	ND
	U937	+	+
	HL60	+	+
	Ros	+	+
	RIVA	+++	+
	Rec	+++	+
Cervix	HeLa	++	ND

Fig. 1. Expression of centrosomal proteins Nek2 and C-Nap1 in cancer cell lines. A. The expression levels of Nek2 and C-Nap1 were determined by Western blotting total lysates of asynchronous cell populations equalized for protein content and are presented with respect to that seen in primary cells (HUVEC). Relative expression levels were determined by densitometric scanning over the linear range of enhanced chemiluminescence autoradiographs using NIH Image 1.62 and denoted as follows: +, expressed at equal abundance to that seen in HUVECs; ++, overexpressed up to 2-fold; +++, >2-fold overexpressed; -, expressed at lower abundance than in HUVECs; ND, not determined. Each cell line was analyzed in at least three independent experiments. B and C, representative Western blots of cancer cell lysates. Total cell lysate, 50 μ g, was separated on SDS-polyacrylamide gels, Western blotted, and probed with Nek2 (antipeptide antibody; 1 μ g/mL) or α -tubulin (1 μ g/mL) antibodies. D. Semiquantitative RT-PCR was performed using specific primers against Nek2A (top) or Nek2B (bottom) on equalized amounts of total RNA collected from HeLa cells synchronized in the indicated phases of the cell cycle (M, G₁, S, and G₂) or on pGEM-Nek2A plasmid (P). Samples were separated on agarose gels and visualized with ethidium bromide. HUVEC, human umbilical vascular endothelial cell.

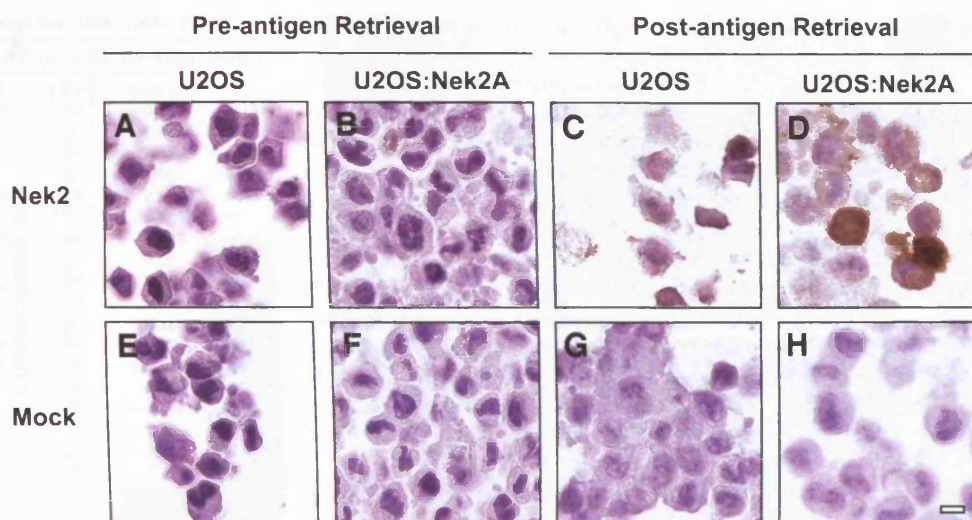
B**C****D**

formaldehyde-fixed, paraffin-embedded tissue, and we had determined previously that this antibody did not detect Nek2 after formaldehyde fixation (data not shown). To investigate a viable antigen retrieval protocol, we made use of a tetracycline-inducible Nek2A cell line generated previously in our laboratory (33). After 24-hour induction with tetracycline, parental U2OS and U2OS:Nek2A cells were harvested, fixed with formaldehyde, embedded in agarose, and sectioned. Sections were then either untreated or subjected to an antigen retrieval procedure using citrate buffer before staining with either control or anti-Nek2 antibodies (Fig. 2). After antigen retrieval, Nek2 staining was strongly detected in the U2OS:Nek2A cell line and weakly in the parental U2OS cells, whereas the control antibodies gave no stain.

A similar antigen retrieval approach was also shown to be successful on formaldehyde-fixed HBL100 breast cells (data not shown).

Nek2 Is Overexpressed in Primary Human Breast Tumors. Major karyotypic changes, including gains or losses of whole chromosomes, are by far the most common lesion in breast cancer and are strongly associated with a bleak clinical outcome (42). Using the antigen retrieval methods determined above and the polyclonal antipeptide Nek2 antibody, we therefore analyzed Nek2 protein expression in archival samples of 20 human breast cancers. Strikingly, Nek2 protein expression was elevated significantly in the majority of these breast tumor samples. Elevated Nek2 expression was clearly detected in ductal carcinoma *in situ* (DCIS) tumor

Fig. 2. Antigen retrieval enables Nek2 staining after formaldehyde fixation. U2OS osteosarcoma cells stably transformed with a construct expressing kinase-dead Nek2A-K37R-myc-His (U2OS: Nek2A; B, D, F, and H) or the parental U2OS cell line (U2OS; A, C, E, and G) were fixed with formaldehyde before embedding in paraffin wax. Sections were then cut and stained with antibodies raised to Nek2 (A–D; 3.75 μ g/mL) or control IgGs (E–H) before (A, B, E, and F) or after (C, D, G, and H) antigen retrieval. 3,3'-diaminobenzidine staining (brown) indicates that Nek2 is recognized in the stable cell line only after processing for antigen retrieval (D). The cell-to-cell variability of staining reflects the cell cycle dependent expression of Nek2A. Scale bar, 10 μ m.



cells as compared with normal breast ductal cells or stromal cells within the same sections (Fig. 3, A and C). These latter cells showed weak levels of staining as would be expected for a protein known to be ubiquitously expressed. DCIS is an early step in the pathology of breast cancer in which a luminal epithelial cell lining

the duct has undergone an early transformation event and proliferated, although the carcinoma is still bounded by the basement membrane surrounding the duct (Fig. 3, B and D). Strong Nek2 staining was both restricted to the carcinoma and dependent on the presence of primary antibodies to Nek2 as sequential DCIS tumor

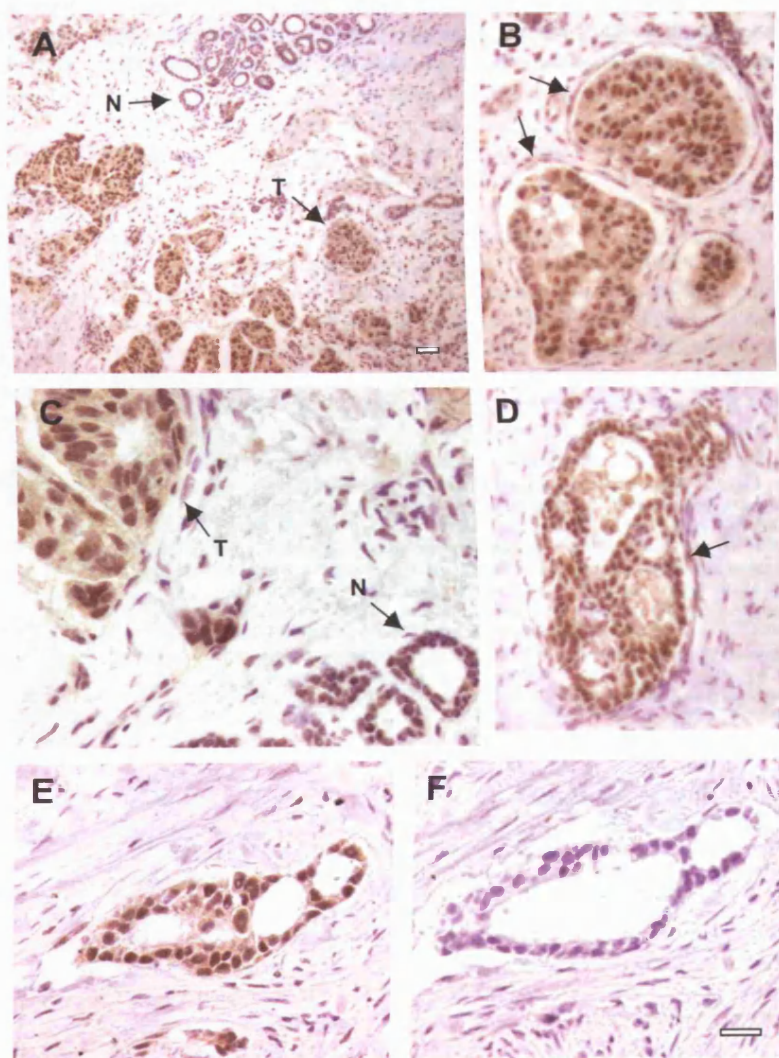


Fig. 3. Nek2 expression is elevated in DCIS breast tumors. Breast tumor sections were stained with polyclonal anti-peptide Nek2 (A–E; 2 μ g/mL) or mock antibodies (F; control IgGs, 2 μ g/mL) after antigen retrieval. Images taken at low (A) and high (B–F) magnification are shown. DCIS tumor cells (arrowed, T, A, and C) show highly elevated Nek2 expression as compared with normal breast duct tissue (arrowed, N, A, and C). The carcinoma cells in DCIS are bounded by an intact basement membrane (arrowed, B and D). To demonstrate antibody specificity, sequential tumor sections were cut and stained with Nek2 (E) or mock (F) antibodies after antigen retrieval. Scale bar in A, 100 μ m, and in F (for B–F), 30 μ m.

sections incubated with control rabbit IgG fraction exhibited no specific staining (Fig. 3, *E* and *F*).

Analysis of invasive ductal carcinoma and invasive lobular carcinoma tissue also revealed a significant increase in the expression of Nek2 protein in tumor cells compared with controls (Fig. 4, *A–D*, and data not shown). In invasive carcinomas, the tumor cells are present throughout the stroma and are no longer confined within ducts or lobules. This breakdown of normal histology and invasion of surrounding tissue is an important stage in the establishment of metastatic tumors. To verify the staining pattern that we had observed with the antipeptide Nek2 antibody, a second independent polyclonal antibody was used. This antibody was raised to a bacterially expressed fragment representing approximately the COOH-terminal two-thirds of the Nek2A protein (31). Again, after antigen retrieval, carcinoma cells in DCIS tumors stained strongly for Nek2, whereas normal ductal tissue and stromal cells did not (Fig. 4, *E* and *F*).

Thus far, we have analyzed 20 breast tumor samples, including DCIS, invasive ductal carcinoma, and invasive lobular carcinoma tumors, in which areas of both tumor and normal tissue could be detected for comparison of expression levels. Sixteen (80%) exhibited significantly elevated Nek2 protein expression, whereas 4 (20%) gave no more staining than the normal tissue (Table 1). Within those tumors that showed elevated Nek2 expression, all had increased expression in >70% of tumor cells ($n > 1000$). We compared the extent of cells overexpressing Nek2 in these breast cancers with data that had been obtained previously on estrogen, progesterone, and EGFR expression. However, no obvious correlation was apparent between the expression of Nek2 and any of these markers. For example, of the 16 tumors that were strongly Nek2 positive (>70%),

Table 1 Nek2, Ki67, and hormone receptor expression levels in breast tumors

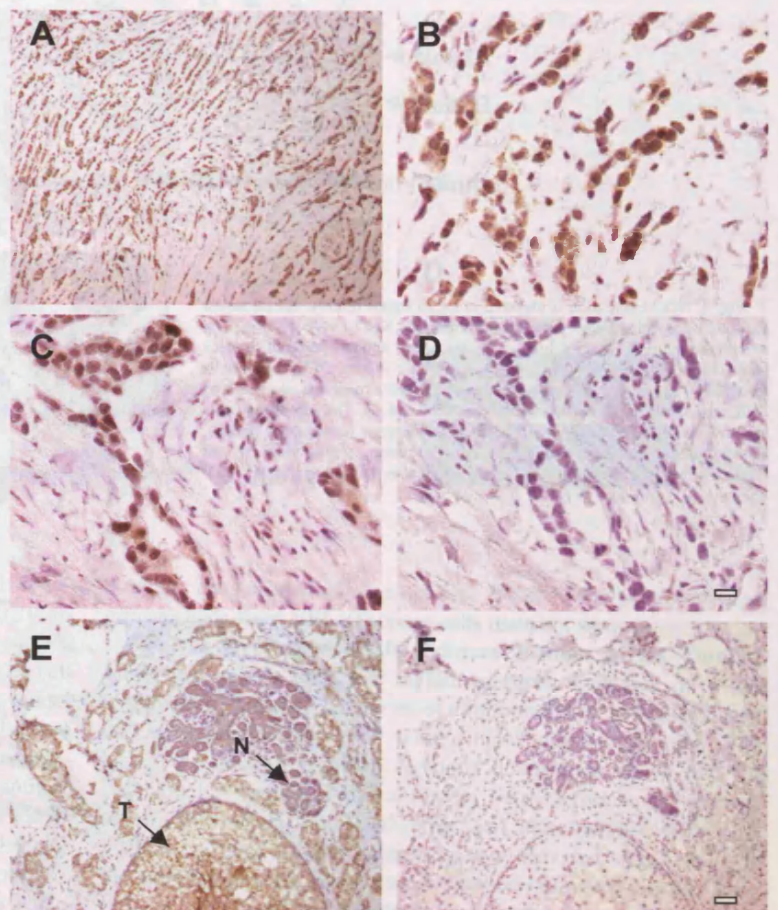
Patient	Nek2 (%)	ERα (%)	PR (%)	EGFR (+/-)	Ki67 (%)	Tumor type	Grade
8225	No stain	97	12	—	21.9	IDC	1
8226	91.0	95	95	—	44.6	IDC	2
8401	88.3	0	0	—	35.8	ILC	NK
8403	86.8	33	0	—	58.4	IDC	3
2243	90.2	78	2	—	41.7	IDC	NK
2304	72.9	95	49	—	39.3	IDC	3
2575	No stain	0	0	++	30.3	IDC	3
3000	98.0	98	37	—	16	IDC	3
2282.1	92.9	0	0	++++	52	IDC	3
2196	93.9	70	24	—	6.9	IDC	3
2210	91.6	91	8	—	9.8	IDC	3
2585	81.6	0	0	+	46.7	IDC	3
2262.2	93.7	97	98	—	18.9	ILC	3
6238	No stain	20	30	+	7.4	IDC	3
1223.2	76.0	90	15	—	37.6	IDC	3
7911	No stain	0	0	—	88.1	IDC	3
1570.2	83.0	0	0	—	34.8	IDC	3
7956	94.5	0	0	—	70.3	IDC	3
7916	75.2	80	8	—	69.9	IDC	3
1955	97.7	3	0	—	51.1	IDC	3

NOTE. The table indicates the percentage of cells ($n > 1000$) exhibiting elevated levels of Nek2 expression in randomly selected fields of 20 breast tumor samples and compares this to expression levels of ERα, PR, and EGFR and the proliferation marker Ki67. Tumor type and grade are also indicated.

Abbreviations: ER, estrogen receptor; PR, progesterone receptor; IDC, invasive ductal carcinoma; ILC, invasive lobular carcinoma; NK, not known.

9 were estrogen receptor α positive (>70%), whereas 7 were estrogen receptor α negative. Likewise, some tumors that were Nek2 positive were progesterone receptor and EGFR positive, whereas others were progesterone receptor and EGFR negative. Clearly, however, our current sample size is too small to draw any strong conclusion about

Fig. 4. Nek2 expression is elevated in invasive carcinomas of the breast. Invasive lobular carcinoma breast tumor sections were cut and stained with antibodies raised to Nek2 (*A* and *B*; 2 μg/mL) after antigen retrieval. Images taken at low (*A*) and high (*B*) magnification are shown. Sequential tumor sections stained with Nek2 (*C*) or mock (*D*) antibodies demonstrate the specificity of the response in the invasive tumor cells. Sequential tumor sections were also stained with a second independent polyclonal antibody raised to Nek2 (*E*; R40; 2 μg/mL) or mock antibodies (*F*; control IgGs; 2 μg/mL) after antigen retrieval. A DCIS carcinoma engorged with tumor cells is stained strongly for Nek2 (arrowed *T* in *E*), whereas normal ducts (arrowed *N* in *E*) and surrounding stroma are not. Scale bar in *D*, 20 μm, and in *F*, 100 μm.



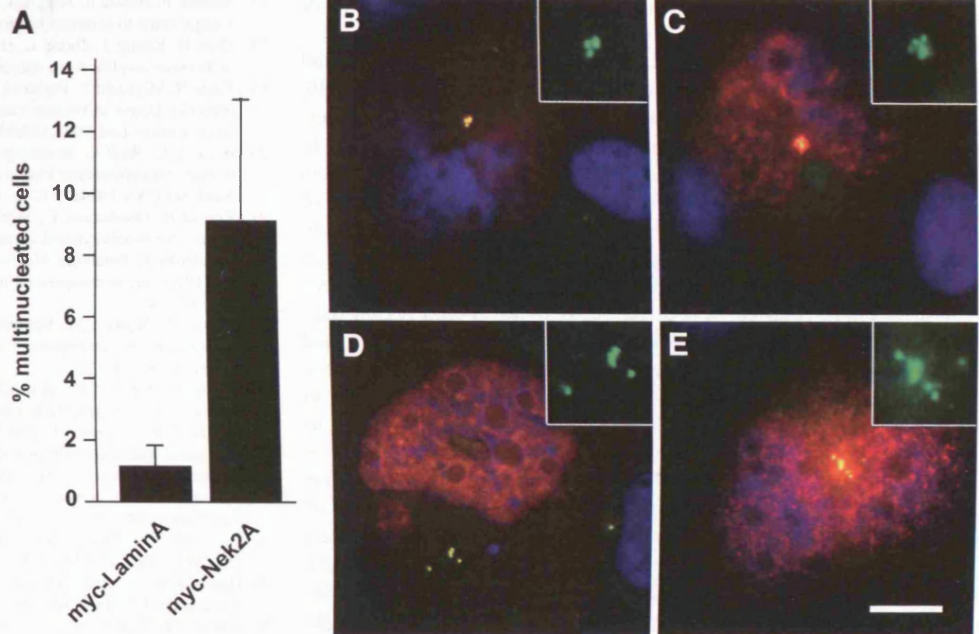


Fig. 5. Elevated expression of Nek2A induces multinucleation in HBL100 cells. **A**, histogram showing percentage of multinucleated cells after 72-hour transfection of either myc-LaminA or myc-Nek2A; 100–300 transfected cells were counted in at least four independent experiments. Bars, \pm SD and the $P = 0.01$ (Student's paired t test). **B–E**, merged images of multinucleated HBL100 cells expressing myc-Nek2A stained with antibodies against the myc tag (red) and γ -tubulin (green). DNA was stained with Hoechst 33258 (blue). An enlargement of the γ -tubulin stain is shown in the inset in each panel demonstrating the presence of supernumerary centrosomes. Scale bar, 5 μ m.

the correlative expression of these markers. Finally, no correlation was detected between expression of Nek2 and Ki67, a marker for cell proliferation. Whereas one might predict that cells expressing Nek2 would be proliferating, we note that there was no obvious correlation either between expression of proliferation markers (Ki67 or PCNA) and the overexpression of the other mitotic kinases, Plk1 and Aurora-A (19, 21, 22, 43).

Elevated Expression of Nek2A Induces Aneuploidy in Immortalized Breast Cells. To determine whether altered Nek2 expression might contribute to aneuploidy and chromosome instability in breast cancer, we analyzed the consequences of ectopic expression of Nek2A in nontransformed breast cells. HBL100 cells are derived from normal breast epithelia but are immortal due to the presence of SV40 large T antigen (44). Immunofluorescence microscopy revealed that <1% of untransfected HBL100 cells had supernumerary centrosomes or abnormal nuclei, whereas a breast cancer cell line (MDA-MB-468) had ~5% cells with supernumerary centrosomes (data not shown). After 72 hours of transfection with myc-tagged Nek2A, ~9% HBL100 cells ($n = 900$) exhibited gross nuclear abnormalities being either multinucleated or with extra chromosomal material (Fig. 5A). Staining with antibodies against γ -tubulin (Fig. 5, B–E) and C-Nap1 (data not shown) revealed that the multinucleated cells invariably contained extra centrosomes suggesting that they arose through an aborted mitosis or failed cytokinesis. Cells transfected with myc-tagged lamin A showed only ~1% nuclear defects ($n = 1200$; Fig. 5A). Ectopically expressed Nek2A colocalized with γ -tubulin at the centrosome in HBL100 cells as expected (Fig. 5, B–E). Therefore, these results support the hypothesis that elevated Nek2 levels can contribute to errors in mitotic progression and/or chromosome segregation that generate aneuploid cells.

DISCUSSION

The majority of tumor cells in human cancers exhibit centrosome abnormalities. These typically include increased centrosome size, number, and microtubule nucleation capacity (7–9). Importantly, centrosome aberrations correlate with or even precede the generation of aneuploidy and the acquisition of a chromosome instability phenotype in breast and prostate tumors (14, 15). This has led to the hypothesis that deregulation of centrosome function could be a major contribu-

tory factor to the genetic instability and loss of tissue differentiation that drive most cancer progression.

Here, we show for the first time elevated protein expression of the centrosomal kinase Nek2 in cancer cell lines and primary breast tumors. This adds to previous mRNA studies demonstrating elevated Nek2 expression in Ewing tumor cell lines and diffuse large B-cell lymphomas (38, 39). In our analysis of 17 cancer cell lines, we found up-regulated expression in breast, ovarian, leukemic, prostate, and cervical cancer cells. The level of up-regulation was 2- to 5-fold with respect to its abundance in primary or immortalized untransformed cell lines. Similar levels of protein overexpression were reported for Aurora-A in pancreatic, breast, and colorectal tumor cell lines (18, 24, 25). The HBL100 and PNT2-C2 immortalized cell lines do contain SV40 antigens that could alter expression from E2F responsive genes (44, 45). However, these cell lines had equivalent expression of Nek2 to the two primary cell types and significantly less than related cancer cell lines. In primary breast tumors, elevated Nek2 protein was detected with two independent antibodies in both *in situ* and invasive carcinomas. Its up-regulation in DCIS tumors indicates that alteration of Nek2 protein levels occurs in breast tumors before invasion and metastasis. We note that centrosomal defects, aneuploidy, and chromosome instability have all been observed with high frequency in these early stage tumors (15). From our limited data, however, we saw no correlation between Nek2 and estrogen or progesterone receptor expression.

The underlying cause for an increase in Nek2 expression is unclear. However, it is intriguing to speculate that loss of transcriptional control through inactivation of the tumor suppressors p107 and/or p130 may be one reason. By analyzing the abundance of Nek2 mRNA in synchronized cells, we found that there was a reduced amount in G₁ and M phase compared with S and G₂ phase. This result is in agreement with the observation that the promoter region of the human *Nek2* gene, located at chromosome 1q32.2–1q41 (28), binds the E2F4 transcriptional repressor (41). This would be expected to lead to a decrease in transcription in G₁ and G₀ through recruitment of the p107/p130 pocket proteins. Indeed, cells lacking p107 and p130 exhibit elevated levels of Nek2 mRNA (41). Due to the significant number of mitotic and G₂-M checkpoint proteins shown to have E2F4 binding sites, loss of p107 and p130 may well cause up-regulation of many cell cycle regulators (41). Because loss of Rb pocket proteins also promotes survival of tetraploid cells (13), we propose that these

tumor suppressors may be critical in preventing the accumulation of centrosome abnormalities and aneuploidy.

Previous studies have shown that Nek2 contributes to assembly and maintenance of centrosomes and to bipolar spindle formation (33, 36, 37). Therefore, inappropriately high expression of Nek2 might interfere with either centrosome integrity or chromosome segregation. In nondividing cells, this could contribute to the loss of differentiated cell morphology and breakdown in tissue architecture typical of invasive breast carcinomas (8, 15). In dividing cells, this could lead to aneuploidy and chromosome instability. Indeed, overexpression of Nek2A in the nontransformed HBL100 cell line did induce the generation of multinucleated cells at a level that was 9-fold higher than control transfections. Because these multinucleated cells also had supernumerary centrosomes, it seems reasonable to predict that they have failed cytokinesis, perhaps as a result of some earlier defect in mitosis. Overexpression of Aurora A and Plk1 also leads to multinucleation, and it has been proposed that this may provide a major route to both tetraploidization and centrosome amplification (17). As well as perturbing spindle formation, altered expression of Nek2 might interfere with other mitotic processes. Nek2 has been reported to interact with the kinetochore proteins Hec1 and Mad1 suggesting a role in the spindle checkpoint (46, 47). Meanwhile, studies performed on homologues of Nek2 in lower eukaryotes suggest that these kinases may promote mitotic entry through recruitment of cell cycle regulators to the centrosome and, possibly, have a direct role in triggering cytokinesis (48–50). Future studies will now be needed to determine whether inappropriate expression of Nek2A can also cause cellular transformation or tumor formation in animal models.

ACKNOWLEDGMENTS

We thank A. Cramer (Paterson Institute for Cancer Research, Manchester) for technical assistance with immunohistochemistry and Dr. S. Shackleton (University of Leicester) for the lamin A plasmid. We are most grateful to Prof. R. Walker (Glenfield, Hospital, Leicester), Drs. N. Smith, R. Chopra, and N. Clarke (Paterson Institute for Cancer Research, Manchester) and the DSMZ Cell Bank (Braunschweig, Germany) for providing cell lines.

REFERENCES

- Heim S, Mitelman F. Cancer cytogenetics. New York: Wiley-Liss, 1995.
- Magennis DP. Nuclear DNA in histological and cytological specimens: measurement and prognostic significance. *Br J Biomed Sci* 1997;54:140–8.
- Pihan GA, Doxsey SJ. The mitotic machinery as a source of genetic instability in cancer. *Semin Cancer Biol* 1999;9:289–302.
- Lengauer C, Kinzler KW, Vogelstein B. Genetic instabilities in human cancers. *Nature (Lond)* 1998;396:643–9.
- Doxsey S. Re-evaluating centrosome function. *Nature Revs Mol. Cell Biol* 2001;2:688–98.
- Bornens M. Centrosome composition and microtubule anchoring mechanisms. *Curr Op Cell Biol* 2002;14:25–34.
- Pihan GA, Purohit A, Wallace J, et al. Centrosome defects and genetic instability in malignant tumors. *Cancer Res* 1998;58:3974–85.
- Lingle WL, Lutz WH, Ingle JN, Maihle NJ, Salisbury JL. Centrosome hypertrophy in human breast tumors: implications for genomic stability and cell polarity. *Proc Natl Acad Sci. (USA)* 1998;95:2950–5.
- Pihan GA, Purohit A, Wallace J, Malhotra R, Liotta L, Doxsey SJ. Centrosome defects can account for cellular and genetic changes that characterize prostate cancer. *Cancer Res* 2001;61:2212–9.
- Lingle WL, Salisbury JL. Altered centrosome structure is associated with abnormal mitoses in human breast tumors. *Am J Pathol* 1999;155:1941–51.
- Nigg EA. Centrosome aberrations: cause or consequence of cancer progression? *Nat Revs Cancer* 2002;2:815–25.
- Brinkley BR. Managing the centrosome numbers game: from chaos to stability in cancer cell division. *Trends Cell Biol* 2001;11:18–21.
- Borel F, Lohez OD, Lacroix FB, Margolis RL. Multiple centrosomes arise from tetraploidy checkpoint failure and mitotic centrosome clusters in p53 and RB pocket protein-compromised cells. *Proc Natl Acad Sci USA* 2002;99:9819–24.
- Pihan GA, Wallace J, Zhou H, Doxsey SJ. Centrosome abnormalities and chromosome instability occur together in pre-invasive carcinomas. *Cancer Res* 2003;63:1398–404.
- Lingle WL, Barrett SL, Negron VC, et al. Centrosome amplification drives chromosomal instability in breast tumor development. *Proc Natl Acad Sci. USA* 2002;99:1978–83.
- Nigg EA. Mitotic kinases as regulators of cell division and its checkpoints. *Nat Rev Mol Cell Biol* 2001;2:21–32.
- Meraldi P, Honda R, Nigg EA. Aurora-A overexpression reveals tetraploidization as a major route to centrosome amplification in p53^{-/-} cells. *EMBO J* 2002;21:483–92.
- Zhou H, Kuang J, Zhong L, et al. Tumour amplified kinase STK15/BTAK induces centrosome amplification, aneuploidy and transformation. *Nat Genet* 1998;20:189–93.
- Takai N, Miyazaki T, Fujisawa K, Nasu K, Hamanaka R, Miyakawa I. Expression of polo-like kinase in ovarian cancer is associated with histological grade and clinical stage. *Cancer Lett* 2001;164:41–9.
- Holtrich U, Wolf G, Brauningner A, et al. Induction and down-regulation of PLK, a human serine/threonine kinase expressed in proliferating cells and tumors. *Proc Natl Acad Sci USA* 1994;91:1736–40.
- Knecht R, Oberhauser C, Strebhardt K. PLK (polo-like kinase), a new prognostic marker for oropharyngeal carcinomas. *Int J Cancer* 2000;89:535–6.
- Takahashi T, Futamura M, Yoshimi N, et al. Centrosomal kinases, HsAIRK1 and HsAIRK3, are overexpressed in primary colorectal cancers. *Jpn J Cancer Res* 2000;91:1007–14.
- Tanaka T, Kimura M, Matsunaga K, Fukada D, Mori H, Okano Y. Centrosomal kinase AIRK1 is overexpressed in invasive ductal carcinoma of the breast. *Cancer Res* 1999;59:2041–4.
- Li D, Zhu J, Firozi PF, et al. Overexpression of oncogenic STK15/BTAK/Aurora A kinase in human pancreatic cancer. *Clin Cancer Res* 2003;9:991–7.
- Bischoff JR, Anderson L, Zhu Y, et al. A homologue of Drosophila aurora kinase is oncogenic and amplified in human colorectal cancers. *EMBO J* 1998;17:3052–65.
- Smith MR, Wilson ML, Hamanaka R, et al. Malignant transformation of mammalian cells initiated by constitutive expression of the polo-like kinase. *Biochem Biophys Res Comm* 1997;234:397–405.
- Fry AM. The Nek2 protein kinase: a novel regulator of centrosome structure. *Oncogene* 2002;21:6184–94.
- Hames RS, Fry AM. Alternative splice variants of the human centrosomal kinase Nek2 exhibit distinct patterns of expression in mitosis. *Biochem J* 2002;361:77–85.
- Hames RS, Wattam SL, Yamano H, Bacchieri R, Fry AM. APC/C-mediated destruction of the centrosomal kinase Nek2A occurs in early mitosis and depends upon a cyclin A-type D-box. *EMBO J* 2001;20:7117–27.
- Helps NR, Luo X, Barker HM, Cohen PTW. NIMA-related kinase 2 (Nek2), a cell cycle-regulated protein kinase localized to centrosomes, is complexed to protein phosphatase 1. *Biochem J* 2000;349:509–18.
- Fry AM, Meraldi P, Nigg EA. A centrosomal function for the human Nek2 protein kinase, a member of the NIMA-family of cell cycle regulators. *EMBO J* 1998;17:470–81.
- Meraldi P, Nigg EA. Centrosome cohesion is regulated by a balance of kinase and phosphatase activities. *J Cell Sci* 2001;114:3749–57.
- Faragher AJ, Fry AM. Nek2 kinase stimulates centrosome disjunction and is required for formation of bipolar mitotic spindles. *Mol Biol Cell* 2003;14:2876–89.
- Fry AM, Mayor T, Meraldi P, Stierhof Y-D, Tanaka K, Nigg EA. C-Nap1, a novel centrosomal coiled-coil protein and candidate substrate of the cell cycle-regulated protein kinase Nek2. *J Cell Biol* 1998;141:1563–74.
- Mayor T, Tanaka K, Stierhof Y-D, Fry AM, Nigg EA. The centrosomal protein C-Nap1 displays properties supporting a role in cell cycle-regulated centrosome cohesion. *J Cell Biol* 2000;151:837–46.
- Twomey C, Wattam SL, Pillai MR, Rapley J, Baxter JE, Fry AM. Nek2B stimulates zygotic centrosome assembly in *Xenopus laevis* in a kinase-independent manner. *Dev Biol* 2004;265:384–98.
- Uto K, Sagata N. Nek2B, a novel maternal form of Nek2 kinase, is essential for the assembly or maintenance of centrosomes in early *Xenopus* embryos. *EMBO J* 2000;19:1816–26.
- de Vos S, Hofmann W-K, Grogan TM, et al. Gene expression profile of serial samples of transformed B-cell lymphomas. *Lab Invest* 2003;83:271–85.
- Wai DH, Schaefer KL, Schramm A, et al. Expression analysis of pediatric solid tumor cell lines using oligonucleotide microarrays. *Int J Oncol* 2002;20:441–51.
- Fry AM, Anaud L, Nigg EA. Activity of the human centrosomal kinase, Nek2, depends upon an unusual leucine zipper dimerization motif. *J Biol Chem* 1999;274:16304–10.
- Ren B, Cam H, Takahashi Y, et al. E2F integrates cell cycle progression with DNA repair, replication, and G2/M checkpoints. *Genes Dev* 2002;16:245–56.
- Pandis N, Idvall I, Bardi G, et al. Correlation between karyotypic pattern and clinicopathologic features in 125 breast cancer cases. *Int J Cancer* 1996;66:191–6.
- Kneisel L, Strebhardt K, Bernd A, Wolter M, Binder A, Kaufmann R. Expression of polo-like kinase (PLK1) in thin melanomas: a novel marker of metastatic disease. *J Cutan Pathol* 2002;29:354–8.
- deFromental CC, Nardeaux PC, Soussi T, et al. Epithelial HBL-100 cell line derived from milk of an apparently healthy woman harbours SV40 genetic information. *Exp Cell Res* 1985;160:83–94.
- Berthon P, Cussenot O, Hopwood L, LeDuc A, Maitland NJ. Functional expression of SV40 in normal human prostatic epithelial and fibroblastic cells: differentiation pattern of non-tumorigenic cell lines. *Int J Oncology* 1995;6:333–43.
- Chen Y, Riley DJ, Zheng L, Chen P-L, Lee W-H. Phosphorylation of the mitotic regulator protein Hec1 by Nek2 kinase is essential for faithful chromosome segregation. *J Biol Chem* 2002;277:49408–16.
- Lou Y, Yao J, Zenreski A, et al. Nek2A interacts with Mad1 and possibly functions as a novel integrator of the spindle checkpoint signaling. *J Biol Chem* 2004;279:20049–57.
- Wu L, Osmani SA, Mirabito PM. A role for NIMA in the nuclear localization of cyclin B in *Aspergillus nidulans*. *J. Cell Biol* 1998;141:1575–87.
- Grallert A, Hagan IM. S. pombe NIMA related kinase, Fin1, regulates spindle formation, and an affinity of Polo for the SPB. *EMBO J* 2002;21:3096–107.
- Grallert A, Krapp A, Bagley S, Simanis V, Hagan IM. Recruitment of NIMA kinase shows that maturation of the S. pombe spindle-pole body occurs over consecutive cell cycles and reveals a role for NIMA in modulating SIN activity. *Genes Dev* 2004;18:1007–21.



Available online at www.sciencedirect.com

SCIENCE @ DIRECT®

Cancer Letters 237 (2006) 155–166

CANCER
Letters

www.elsevier.com/locate/canlet

Mini-review

Nek2 kinase in chromosome instability and cancer

Daniel G. Hayward, Andrew M. Fry*

Department of Biochemistry, University of Leicester, Adrian Building, University Road, Leicester LE1 7RH, UK

Received 1 June 2005; accepted 7 June 2005

Abstract

Aneuploidy and chromosome instability are two of the most common abnormalities in cancer cells. They arise through defects in cell division and, specifically, in the unequal segregation of chromosomes between daughter cells during mitosis. A number of cell cycle dependent protein kinases have been identified that control mitotic progression and chromosome segregation. Some of these localize to the centrosome and regulate mitotic spindle formation. One such protein is Nek2, a member of the NIMA-related serine/threonine kinase family. Data are emerging that Nek2 is abnormally expressed in a wide variety of human cancers. In this review, we summarize current knowledge on the expression, regulation and function of Nek2, consider how Nek2 may contribute to chromosome instability, and ask whether it might make an attractive target for chemotherapeutic intervention in human cancer.

© 2005 Elsevier Ireland Ltd. All rights reserved.

Keywords: Nek2A; Nek2B; Centrosome; Mitosis; Aneuploidy

1. Introduction

Cancer cells invariably exhibit some degree of genetic instability. This can range from an accelerated rate of mutation, arising from defects in DNA repair, to gross changes in DNA content that result from errors in the division of chromosomes during mitosis. Chromosome segregation errors lead to an abnormal chromosome content, so called aneuploidy, usually being two to three times the content of a normal diploid cell (Rajagopalan and Lengauer, 2004). In addition, some, but not all aneuploid cells exhibit

chromosome instability (CIN), a phenotype characterized by a certain rate of gain or loss of chromosomes at each cell division. This constant shuffling of chromosomes enables a microevolutionary process to occur, with cells which acquire properties advantageous to growth and survival taking over the tumour. The loss of control over an orderly mitotic division of chromosomes is, therefore, central to the progression of many cancers to a malignant and drug resistant state.

Chromosome segregation is an extremely complex process that occurs on a microtubule-based scaffold called the mitotic spindle (Gadde and Heald, 2004). Microtubules, produced from the spindle poles, capture duplicated chromosomes such that each member of a pair of sister chromatids is attached to opposite poles, i.e. amphitelic attachment. Bipolarity

* Corresponding author. Tel.: +44 116 252 5024; fax: +44 116 252 3369.

E-mail address: amf5@le.ac.uk (A.M. Fry).

is essential for an equal segregation of genetic material and thus it is critical that cells entering mitosis have two spindle poles that can separate and migrate to opposite ends of the cell. In animal cells, the spindle poles are organized by centrosomes, as these are the dominant sites of microtubule nucleation. Importantly, the number, structure and function of centrosomes in cancer cells is frequently abnormal and correlates with the acquisition of aneuploidy and CIN in a number of cancer types (Lingle et al., 2002; Nigg, 2002; Pihan et al., 2003).

Enzymes that are active at mitosis and govern the ordered establishment of a mitotic spindle are attractive candidates for study in human cancer. A number of protein kinases localise to the centrosome and regulate different aspects of cell division. These include polo-like kinase 1 (Plk1) and Aurora-A kinase, both of which exhibit elevated expression in a wide variety of tumours and cancer cell lines and can induce transformation upon over-expression (Barr et al., 2004; Marumoto et al., 2005). Not surprisingly, major drug discovery programs are already underway to identify inhibitors of Plk1 and Aurora-A that may be effective in cancer treatment (Eckerdt et al., 2005; Keen and Taylor, 2004). Another centrosomal kinase that is active at the onset of mitosis and important for accurate chromosome segregation is Nek2 (Fry, 2002). This kinase also appears to be abnormally expressed in cancer cells and may constitute another important drug target.

2. Nek2: a conserved centrosome kinase

Nek2 is a serine/threonine protein kinase whose activity is cell cycle-regulated, peaking in S and G₂ phase (Fry, 2002). It belongs to the NIMA-related kinase, or 'Nek', family that in man consists of eleven different members (Neks1–11). These proteins share within their catalytic domain sequence similarity to the founding member of this family, the NIMA kinase of the filamentous fungus *Aspergillus nidulans* (O'Connell et al., 2003). NIMA was originally identified in a screen for *A. nidulans* cell cycle mutants that were prevented from entering mitosis, hence 'nim' for *never in mitosis*. Characterization of NIM'A', the first mutant isolated, revealed it to be

a protein kinase essential for mitotic entry (O'Connell et al., 2003).

Structurally, Neks1–11 all exhibit a broad similarity to NIMA, being comprised of an N-terminal catalytic kinase domain and a C-terminal regulatory domain (Fig. 1). However, the degree of conservation between the human kinases and *Aspergillus* NIMA is not that high compared to other cell cycle control proteins. Within the catalytic domain it never exceeds 45%, while the C-terminal domains are highly divergent in both size and domain organization (O'Connell et al., 2003). Furthermore, none of the human kinases has yet been shown to be a functional homologue of NIMA, i.e. able to rescue a *nimA* mutant, so it remains to be seen to what extent these proteins share functionality. However, initial characterization of the human Neks does support the hypothesis that they may all play important roles in cell cycle progression and/or microtubule organization.

Of all the Neks, Nek2 exhibits the greatest sequence identity to NIMA (Fry, 2002). In humans, Nek2 is expressed as at least three splice variants: Nek2A, Nek2B and Nek2A-T (Fig. 1) (Fardilha et al., 2004; Hames and Fry, 2002). Nek2A is 445 amino acids in length (48 kDa) and can be considered as the 'full-length' protein. Nek2B is 384 amino acids (44 kDa) and arises through use of an alternative polyadenylation site within the terminal intron. This means that Nek2A and Nek2B are identical up to residue 370 but differ in their extreme C-termini. Nek2A-T arises from an alternative splicing event, which excises eight amino acids (371–378) from the C-terminal domain of the full-length protein (Fardilha et al., 2004). Western blotting of most adult transformed human cell lines indicates that the predominant isoform is equivalent to the size of Nek2A/Nek2A-T, with Nek2B present but at lower abundance. This is also the case in primary T cells, human umbilical vein endothelial cells, and immortalized but non-transformed HBL100 breast and PNT2-C2 prostate epithelial cells (Hames and Fry, 2002; Hayward et al., 2004). The alternative C-termini of these splice variants leads to important differences in their cell cycle-dependent post-translational regulation (see Section 5). They are also differentially expressed in a developmental and, perhaps tissue-specific, manner (Fardilha et al., 2004; Sonn et al., 2004; Uto et al., 1999).

The most informative observation so far relating to Nek2 biology has been its subcellular localization. Biochemical, proteomic and microscopic data all

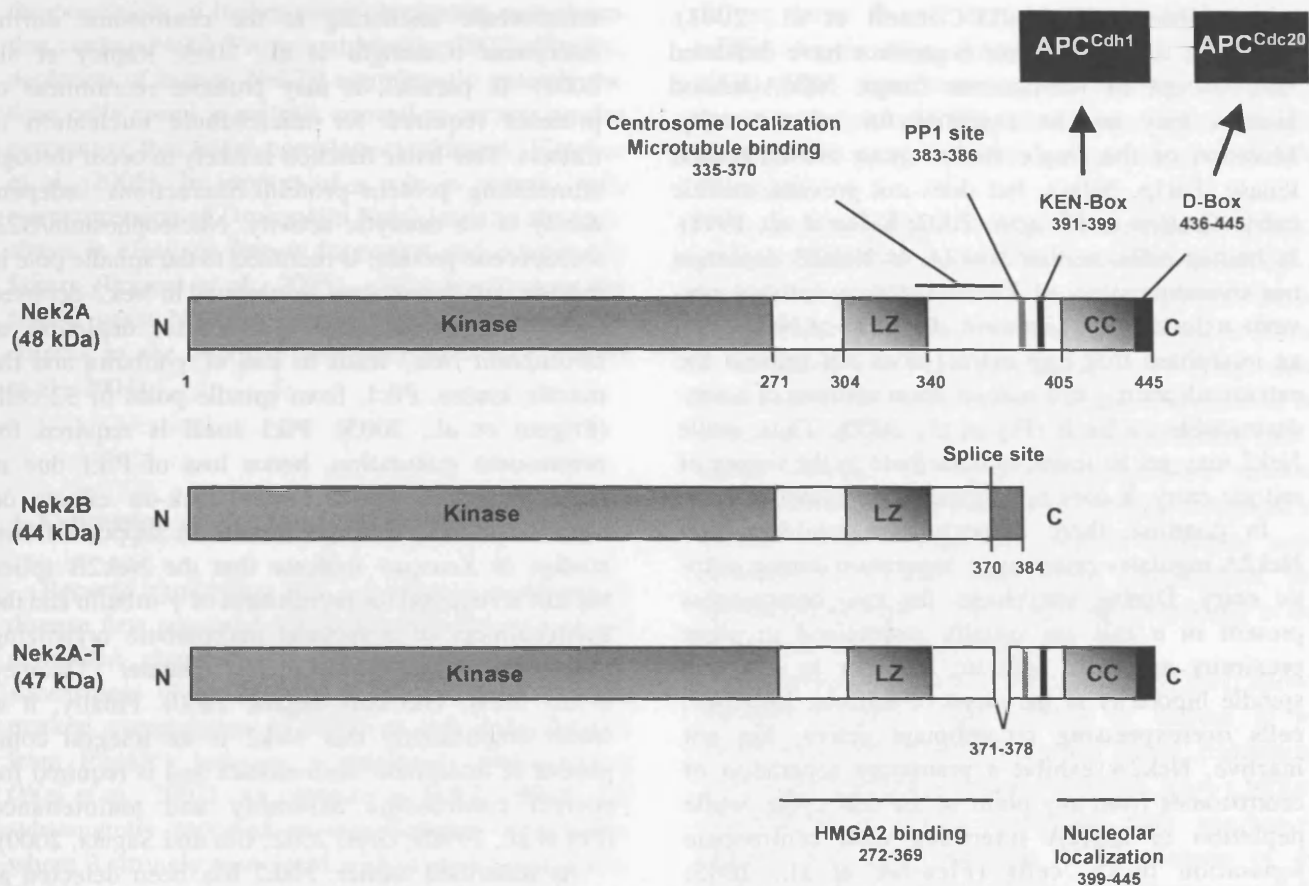


Fig. 1. Nek2 protein structure. Three splice variants of human Nek2 have been described: Nek2A, Nek2B and Nek2A-T. The domain structure of these three proteins is shown with functional regions of the protein indicated above and below the figures. Proteins are shown to scale and numbers indicate amino acid positions. The splice variants are identical in having an N-terminal catalytic kinase domain followed by a leucine zipper (LZ) dimerization motif. Nek2A and Nek2A-T contain an additional coiled-coil (CC) at the extreme C-terminus. A splice site after amino acid 370 leads to an alternative C-terminus in Nek2B and a short truncation in Nek2A-T. Both Nek2A and Nek2A-T retain motifs essential for interaction with PP1 and for protein degradation mediated by APC/C^{Cdc20} or APC/C^{Cdh1}. The non-catalytic domains of Nek2 also confer centrosome and nucleolar localization and the capacity to interact with microtubules and the HMGA2 chromatin architectural protein.

concur to show that Nek2 is a core component of the human centrosome throughout the cell cycle (Andersen et al., 2003; Fry et al., 1998b; Hames and Fry, 2002). Similar localizations have been described for homologues of Nek2 in mouse, *Xenopus*, *Drosophila* and *Dictyostelium* (Fry et al., 2000; Graf, 2002; Ha Kim et al., 2002; Prigent et al., 2005; Uto et al., 1999). Centrosomal localization of Nek2 depends upon a motif in its C-terminal regulatory domain that is also necessary for microtubule binding (Hames et al., 2005). This suggests that microtubules play a role in either delivery or anchoring of Nek2 to centrosomes. In addition to localization at the centrosome, Nek2 has been detected at nucleoli in interphase cells

(Noguchi et al., 2004), on condensed chromatin in meiotic (Fujioka et al., 2000; Rhee and Wolgemuth, 1997) and mitotic (Ha Kim et al., 2002) cells, and at the kinetochores (Lou et al., 2004) and midbody (Ha Kim et al., 2002; Prigent et al., 2005) of dividing cells. Hence, it is possible that Nek2 has substrates whose phosphorylation contributes to many aspects of cell division.

3. Nek2 function in cell division

In *Aspergillus*, NIMA is required for mitotic entry, with mutation of the *nimA* gene preventing mitotic entry and overexpression of NIMA resulting in

a premature mitosis (O'Connell et al., 2003). However, studies in other organisms have indicated that, except in filamentous fungi, NIMA-related kinases may not be essential for mitotic entry. Mutation of the single fission yeast NIMA-related kinase, Fin1p, delays, but does not prevent, mitotic entry (Grallert and Hagan, 2002; Krien et al., 1998). In human cells, neither Nek2A or Nek2B depletion nor overexpression of kinase-inactive mutants prevents mitotic entry. Likewise, depletion of Nek2 from an interphase frog egg extract does not prevent the extract advancing into mitosis upon addition of a non-destructible cyclin B (Fry et al., 2000). Thus, while Nek2 may yet be found to contribute to the timing of mitotic entry, it does not appear to be essential.

In contrast, there is persuasive evidence that Nek2A regulates centrosome separation during mitotic entry. During interphase, the two centrosomes present in a cell are usually maintained in close proximity and only separate in order to establish spindle bipolarity at the onset of mitosis. However, cells overexpressing recombinant active, but not inactive, Nek2A exhibit a premature separation of centrosomes from any point in the cell cycle, while depletion of Nek2A interferes with centrosome separation in G₂ cells (Fletcher et al., 2005; Fry et al., 1998b; Hames and Fry, 2002). Thus, one of the physiological functions of Nek2A appears to be to sever the linkage that normally holds centrosomes together during interphase. Support for this hypothesis came with the identification of C-Nap1 (also called Cep250) as a Nek2 binding partner and substrate (Fry et al., 1998a). The localization of this 280 kDa coiled coil protein is consistent with it being part of a centrosomal linker and, in line with this role, C-Nap1 is displaced from centrosomes at the G₂/M transition when Nek2 is active and centrosomes normally separate (Mayor et al., 2002, 2000). Rootletin is another protein that is displaced from centrosomes upon mitotic entry, and is both a Nek2 substrate and binding partner of C-Nap1 (S. Bahe and E. Nigg, personal communication). Thus, Nek2 may trigger centrosome separation at the onset of mitosis through phosphorylation of multiple linker components.

Besides centrosome separation, Nek2 also regulates the microtubule organization capacity of the centrosome at the time of mitotic entry. It can promote the displacement of Nlp, a protein involved in

microtubule anchoring at the centrosome during interphase (Casenghi et al., 2003; Rapley et al., 2005). In parallel, it may promote recruitment of proteins required for microtubule nucleation in mitosis. This latter function is likely to occur through stimulating protein–protein interactions independently of its catalytic activity. Nucleophosmin/B23, a chaperone protein, is recruited to the spindle pole in mitosis, but this process is inhibited in Nek2-depleted cells (Yao et al., 2004). Likewise, depletion of *Drosophila* Nek2 leads to loss of γ -tubulin and the mitotic kinase, Plk1, from spindle poles in S2 cells (Prigent et al., 2005). Plk1 itself is required for centrosome maturation, hence loss of Plk1 due to Nek2 depletion could have knock-on effects on mitotic spindle pole organization. In support of this, studies in *Xenopus* indicate that the Nek2B splice variant is required for recruitment of γ -tubulin and the establishment of a focused microtubule organizing centre in a kinase-independent manner (Twomey et al., 2004; Uto and Sagata, 2000). Finally, it is worth emphasizing that Nek2 is an integral component of interphase centrosomes and is required for correct centrosome assembly and maintenance (Fry et al., 1998b; Graf, 2002; Uto and Sagata, 2000).

As described earlier, Nek2 has been detected at several sites in mitotic cells in addition to the centrosome and, thus, it is reasonable to predict that it may contribute to other aspects of cell division. Although the evidence remains scant, there are data implicating Nek2 in chromatin condensation, mitotic checkpoint signalling and cytokinesis. HMGA2, an architectural chromatin protein, is a substrate and binding partner of Nek2 in mouse spermatocytes and phosphorylation by Nek2 may trigger its release from chromatin, promoting condensation (Di Agostino et al., 2004). This is important inasmuch as NIMA in *Aspergillus* clearly has a role in chromatin condensation (O'Connell et al., 2003). Interaction with Nek2 has also been reported for both Mad1 and Hec1, components of checkpoint complexes present at the kinetochores (Chen et al., 2002; Lou et al., 2004). Indeed, depletion of Nek2 causes premature chromosome segregation and abrogation of checkpoint signalling (Lou et al., 2004). According to a recent report, Nek2 (and fungal NIMA for that matter) can also interact with Trf1 (telomere repeat binding factor 1), which in turn can bind Mad1 suggesting

the possibility of higher order checkpoint complexes that contain Nek2 (Prime and Markie, 2005). Finally, depletion of human Nek2B significantly extends the time cells spend in mitosis as well as increasing the percentage that fail to complete cytokinesis (Fletcher et al., 2005). In support of a role in mitotic exit, overexpression of *Drosophila* Nek2 leads to abnormalities in cleavage furrow formation and cytokinesis failure (Prigent et al., 2005), while inactivating the fission yeast NIMA-related kinase, Fin1p, leads to defects in the septum initiation pathway (Grallert et al., 2004).

4. Expression of Nek2 in human cancer

Reports implicating Nek2 in human proliferative disease first appeared following microarray analysis of mRNA abundance in tumour derived cell lines. Assessment of some 1700 hundred genes revealed marked upregulation of Nek2 in cell lines derived from Ewing's tumours, a paediatric osteosarcoma (Wai et al., 2002). An increase in Nek2 mRNA was subsequently reported in non-Hodgkin lymphoma, where it strongly associated with disease progression. Profiling successive patient samples showed that, as follicular lymphoma advanced to the more aggressive

diffuse large B-cell lymphoma (DLBCL), Nek2 mRNA levels rose dramatically (de Vos et al., 2003). The transformation to DLBCL signals a decreased response to drug therapy and concomitantly bleak patient prognosis with median survival of only 22 months.

In the first study to look at the expression of Nek2 protein, rather than just mRNA, in human cancer, a 2–5 fold elevation of Nek2 was seen in cell lines derived from breast, cervical and prostate carcinomas, as well as in numerous cell lines established from lymphomas (Hayward et al., 2004). Importantly, examination of 20 archived high grade invasive ductal carcinoma (IDC) breast tumours by immunohistochemistry showed marked Nek2 upregulation in 16 samples compared to normal tissue. Though the tumours examined were confined to a single histological classification, the significant increase in Nek2 staining specifically in the carcinoma cells was striking (Fig. 2).

Comparative genomic hybridisation (CGH) allows changes of gene copy number in disease to be determined with respect to normal tissue. Examining gene copy number in disease subtypes allows further elucidation of genes associated with aggressive disease and poor outcome. CGH analysis of 44 archival breast tumours showed a common amplification of region 1q32, the locus of the human Nek2

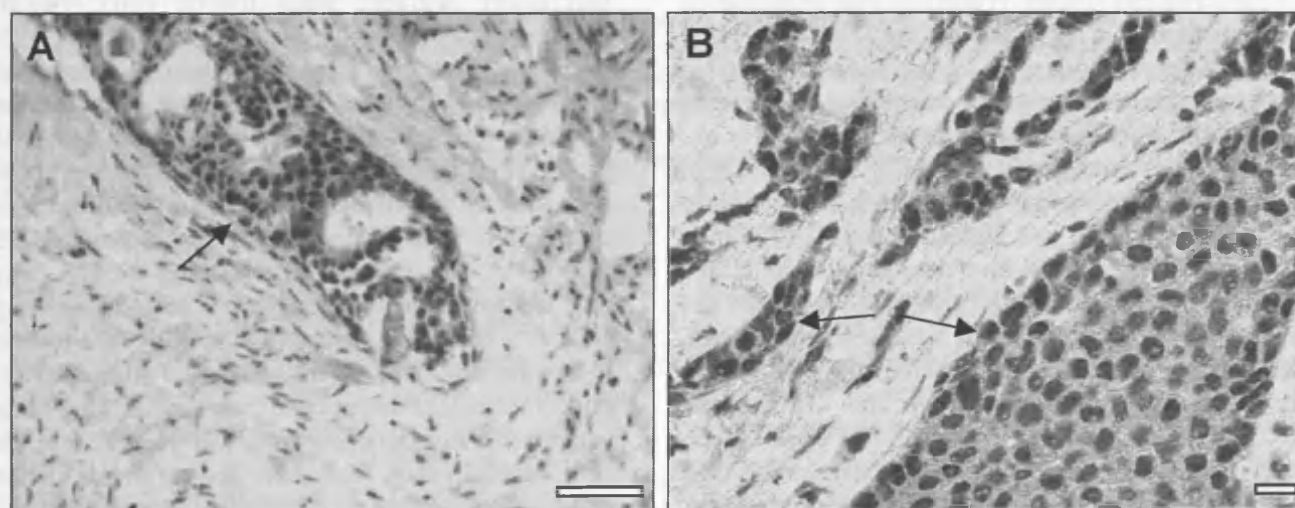


Fig. 2. Increased Nek2 protein expression in primary breast tumours. Invasive ductal carcinoma (IDC) breast tumour sections were stained with purified polyclonal anti-peptide Nek2 antibodies after antigen retrieval. Images taken at low (A) and high (B) magnification are shown. Nek2 expression is substantially increased in the carcinoma cells (arrows) compared to the surrounding stromal cells with both the nucleus and cytoplasm staining for Nek2. Scale bars: (A) 100 (B) 30 μ m.

gene (Schultz et al., 1994), with 32 patient samples showing a gain of up to six copies (Loo et al., 2004). Though 1q32 gain was widespread the degree of amplification varied slightly between histopathological tumour types, being more common in IDC and invasive lobular carcinoma (ILC). A similar gain of 1q32 has also been demonstrated in gastric cancer by CGH. Analysis of 35 primary gastric adenocarcinomas revealed a previously unreported gain of 1q32.3 in 10 cases leading the authors to propose Nek2 as a candidate gene; this common gain was significantly associated with lymph node positive disease and poor prognosis (Weiss et al., 2004).

5. Mechanisms regulating Nek2 expression and activity

Gene amplification could clearly explain the elevated levels of Nek2 mRNA and protein detected in cancer cell lines and patient samples. However, the abundance and activity of Nek2 protein is tightly controlled in a temporal and spatial manner as a result of transcriptional control, post-translational modification and protein–protein interaction. It is therefore, worth considering that one or more of these processes may be subverted in cancer cells (Fig. 3).

First of all, Nek2 transcription is regulated in a cell cycle dependent manner. A genome wide examination of transcription in HeLa cells showed Nek2 to lie in a cluster of genes with peak transcriptional activity in G₂/M phase alongside other established centrosome and spindle checkpoint components (Whitfield et al., 2002). Direct measurement of mRNA by RT-PCR in synchronized cells confirmed that Nek2 transcription is low in M and G₁ and high in S and G₂ (Twomey et al., 2004). Chromatin-immunoprecipitation (ChIP) assays further demonstrated that Nek2 is one of the genes whose promoter binds the E2F4 transcription factor in early G₁ (Ren et al., 2002). E2F4 acts as a transcriptional repressor in G₀ and G₁ through recruitment of chromatin modifiers that silence gene expression. The interaction with chromatin modifiers such as histone deacetylases is indirect and requires members of the retinoblastoma (Rb) family, notably p107 and p130. Importantly, Nek2 mRNA is elevated in mouse embryonic fibroblasts (MEFs) lacking p107 and p130 (Ren et al., 2002), and in primary

keratinocytes infected with retroviruses expressing E7, a human papillomavirus encoded protein which interferes with the repressive function of Rb family members (Patel et al., 2004). Hence, lesions in Rb pocket proteins or their abrogation by viral oncoproteins may facilitate Nek2 upregulation in tumours!

Additional insight into the transcriptional regulation of Nek2 came with the identification of Nek2 as a target for the forkhead transcription factor FoxM1, a transactivator inducing expression of a range of G₂/M specific genes (Laoukili et al., 2005). Overexpression of recombinant FoxM1 increases both the mitotic index and degree of hyperploidy of transfected U2OS osteosarcoma cells and results in a significant fold increase in Nek2 mRNA. Conversely, MEFs nullizygous for FoxM1 had reduced Nek2 expression. Though the FoxM1 transcription factor elevates Nek2 mRNA levels upon overexpression, the cell cycle pattern of Nek2 expression is preserved, maximal in G₂/M low in G₁, presumably because of E2F4 regulation. Hence, loss of pRb proteins would be predicted to be more deleterious than gain of FoxM1.

Nek2 abundance is also governed by cell cycle-dependent protein degradation. Both Nek2A and Nek2B are short-lived proteins in asynchronous cells. However, while levels of both Nek2A and Nek2B increase during S and G₂, Nek2A is specifically degraded upon mitotic entry, Nek2B persisting until the subsequent G₁ (Fry et al., 1995; Hames et al., 2001). The early mitotic destruction of Nek2A results from proteasomal degradation following ubiquitylation mediated by the anaphase promoting complex/cyclosome (APC/C). Recognition of Nek2A by the APC/C depends upon two C terminal destruction motifs that are absent from Nek2B (Hames et al., 2001). Destruction of Nek2A may also require its centrosomal localization as targeting Nek2A to the plasma membrane stabilizes the protein in mitotic cells (M. Hayes and A.M.F., unpublished observations). Furthermore, photobleaching data suggest that not only is recruitment of Nek2A to the centrosome rapid, but that its turnover at the centrosome is largely dependent upon localized degradation by the proteasome (Hames et al., 2005). What leads to the drop in Nek2B levels in G₁ is not known, but one might assume the presence of other, as yet undefined, destruction signals.

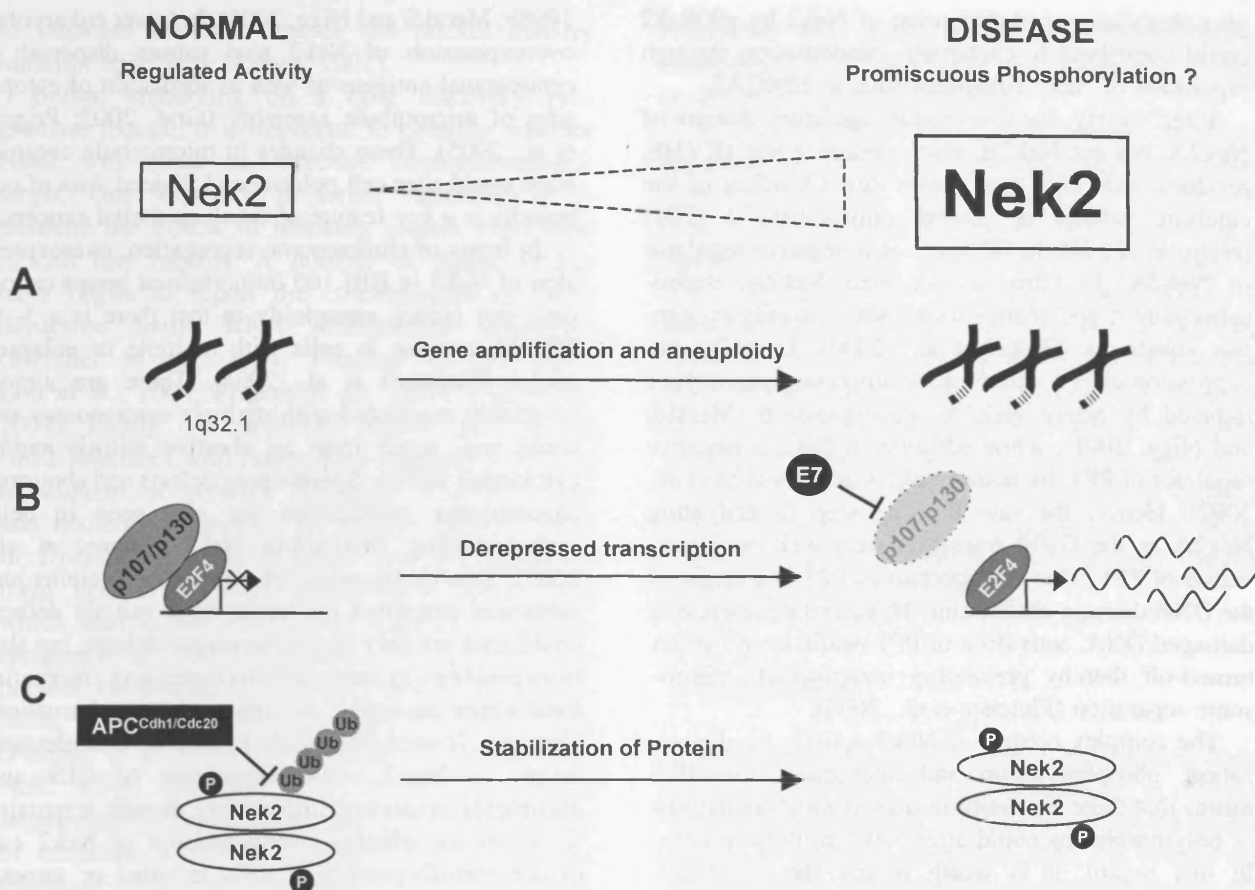


Fig. 3. Possible mechanisms leading to elevated Nek2 expression in tumours. This figure illustrates mechanisms that might lead to elevated levels of Nek2 protein in cancer cells. (A) Comparative genomic hybridisation studies reveal gain of up to six copies of the Nek2 locus 1q32.1 in breast carcinoma. (B) Expression of human papillomavirus (HPV) E7 protein leads to increased Nek2 expression in human keratinocytes. This is likely to result from E7 sequestration of the Rb pocket proteins, p107 and p130, which repress Nek2 expression via the E2F4 transcription factor. Loss of p107 and/or p130 protein would equally relieve the repression of Nek2 transcription. (C) Nek2A protein, which exists as an autophosphorylated dimer, is subject to proteasomal degradation in M, G₁ and G₀ following ubiquitylation mediated by APC/C^{Cdc20} or APC/C^{Cdh1}. Failure to degrade Nek2A, possibly as a result of destruction site mutation or downregulation of APC/C activity, would increase Nek2A protein stability and hence abundance.

Besides regulation of Nek2 protein expression, the kinase activity is further regulated by dimerization and protein phosphorylation. Downstream of the kinase domain is a coiled-coil predicted to form an unusual leucine zipper dimerization motif (residues 304–340). This is present in all Nek2 splice variants, and biophysical (R. Croasdale, M. Pfuhl and A.M.F., unpublished data) and interaction (Hames and Fry, 2002) data support the notion that Nek2 forms salt-resistant dimers via the leucine zipper. Dimerization of Nek2 leads to trans-autophosphorylation and an

increased kinase activity towards exogenous substrates (Fry et al., 1999). Autophosphorylation sites have been identified in both the catalytic and regulatory domain and studies are underway to determine their role in Nek2 activation (J. Baxter, F. Ivins, S. Smerdon and A.M.F., unpublished data). The catalytic domain of Nek2 can also be phosphorylated by p90Rsk2 in vitro (Di Agostino et al., 2002). p90Rsk2 is activated by the Erk1 MAPK pathway during meiotic G₂/M progression when both proteins are localized to condensed chromatin. Hence,

phosphorylation and activation of Nek2 by p90Rsk2 could contribute to chromatin condensation through regulation of Nek2 substrates such as HMGA2.

Interestingly, the C-terminal regulatory domain of Nek2A, but not Nek2B, also contains a site (KVHF, residues 383–386) that allows direct binding of the catalytic subunit of protein phosphatase 1 (PP1) (Helps et al., 2000). PP1 acts as a negative regulator of Nek2A. In vitro, it can bind Nek2A, dephosphorylate it and reduce its activity towards exogenous substrates (Helps et al., 2000). In cells, co-expression of PP1 with Nek2A suppresses phenotypes induced by active Nek2A overexpression (Meraldi and Nigg, 2001), while addition of Inh2, a negative regulator of PP1, increases Nek2A activity (Eto et al., 2002). Hence, the rate limiting step in activating Nek2A at the G₂/M transition may well be inactivation of PP1. This is important as PP1 is a target of the DNA damage checkpoint. Thus, in the presence of damaged DNA, activation of PP1 would keep Nek2A turned-off thereby preventing inappropriate centrosome separation (Fletcher et al., 2004).

The complex control of Nek2 activity by dimerization, phosphorylation and interaction with PP1 means that there are multiple sites at which mutations or polymorphisms could alter Nek2 activity in cells. In this regard, it is worth noting that Aurora-A displays two polymorphisms associated with increased risk of breast tumorigenesis (Lo et al., 2005).

6. Does Nek2 contribute to cancer progression?

Nek2 clearly has several putative roles in cell division, most notably in spindle formation and chromosome segregation. With evidence of Nek2 upregulation in human tumours and a mechanism for this upregulation provided by loss of transcriptional inhibitors and gene amplification, consideration must now be given to the possible impact of increased Nek2 protein on disease progression.

Experimentally, overexpression of active Nek2 in transformed human cell lines leads to defects in centrosome organization and function during interphase. This includes premature separation of centrosomes, loss of centrosomal antigens and unfocused microtubule arrays (Faragher and Fry, 2003; Fry et al.,

1998b; Meraldi and Nigg, 2001). In lower eukaryotes, overexpression of Nek2 also causes dispersal of centrosomal antigens as well as formation of ectopic sites of microtubule assembly (Graf, 2002; Prigent et al., 2005). These changes in microtubule organization could alter cell polarity and, indeed, loss of cell polarity is a key feature of many epithelial cancers.

In terms of chromosome segregation, overexpression of Nek2 in HBL100 immortalized breast cancer cells can induce aneuploidy in that there is a 5- to 10-fold increase in cells with multiple or enlarged nuclei (Hayward et al., 2004). These are almost invariably associated with multiple centrosomes and could well result from an abortive mitosis and/or cytokinesis failure. Spindle pole defects and abnormal chromosome segregation are also seen in cells overexpressing *Drosophila* Nek2 (Prigent et al., 2005). Due to the range of interacting proteins and substrates described for Nek2, these mitotic defects could arise not only from centrosome defects, but also from problems associated with condensing chromatin, kinetochore assembly, or contractile ring formation. Certainly, it seems plausible to propose that elevated levels of Nek2 could contribute to CIN and aneuploidy in cancers. Importantly, though, it remains to be shown whether overexpression of Nek2 can induce transformation of cells in vitro or tumour formation in nude mice.

7. Nek2 as a drug target in cancer?

Kinases are susceptible to inhibition by small molecules in several ways, most notably by competition with ATP for binding at the catalytic pocket or stabilisation of the kinase in an inactive conformation. This tractability has led to a burgeoning number of kinases as drug targets, with several compounds currently licensed for clinical use (Dancey and Sausville, 2003). Initial concerns that kinase inhibitors would lack specificity due to the common requirement for ATP binding have also been dispelled. A recent examination of the binding of 20 kinase inhibitors against 119 protein kinases showed distinct profiles of specificity for each inhibitor (Fabian et al., 2005). It is thought that, although ATP pockets are structurally similar, binding of drug

to adjacent residues outside the pocket confers inhibitor specificity (Cohen, 2002).

Before embarking on a drug discovery programme though, it is important to consider whether Nek2 will make an effective chemotherapeutic target. One approach to target validation is to examine the effects of blocking protein expression in cell line models. A number of recent studies have begun to report the consequences of Nek2 depletion using RNA interference strategies (Fletcher et al., 2004; Fletcher et al., 2005; Lou et al., 2004; Prigent et al., 2005; Yao et al., 2004). Firstly, as mentioned earlier, the loss of Nek2 interferes with centrosome maturation and the recruitment of proteins including γ -tubulin, Plk1 and nucleophosmin/B23, to mitotic spindle poles. In *Drosophila*, some of these proteins appear to form ectopic sites of microtubule organization which lead to the formation of multipolar spindles (Prigent et al., 2005). Secondly, Nek2 depletion can prevent centrosome separation leading, in *Drosophila*, to monopolar or monoastral bipolar spindles (Fletcher et al., 2005; Prigent et al., 2005). Thirdly, Nek2 RNAi interferes with normal chromosome segregation in human cells, causing the appearance of anaphase cells with lagging chromosomes and telophase cells with chromatin bridges (Lou et al., 2004). Fourth, specific depletion of Nek2B in human cells delays mitotic exit (Fletcher et al., 2005). Finally, and most promisingly, depletion of Nek2 leads to an apparent arrest in HeLa cell proliferation and an increase in apoptosis, possibly as a result of mitotic errors (Fletcher et al., 2004, 2005).

Similar studies have been performed to examine the consequences of expressing kinase-inactive Nek2 in cells. These, potentially dominant-negative, mutants mimic the situation of having protein present but in an inactive state, as would be the situation after administration of a small molecule inhibitor. Results in human cells show that expression of inactive Nek2A does not block cell cycle progression, but does cause mitotic defects including abnormal spindle formation and missegregation of chromosomes (Faragher and Fry, 2003; Lou et al., 2004). In U2OS cells though, kinase-inactive Nek2 expression did not appear to block cell growth or induce apoptosis (Faragher and Fry, 2003). However, it is important to

remember that these cells still contain active endogenous Nek2 and hence the consequences may be different to Nek2 depletion.

In fact, neither the consequences of Nek2 depletion by RNAi nor overexpression of kinase-inactive mutants will necessarily reflect the response of cells to small molecule kinase inhibitors. In both cases, the stoichiometry of Nek2 complexes in cells is disrupted either by depletion or overexpression; this is not the case upon drug inhibition. Likewise, kinase-independent functions of Nek2 will be abrogated by depletion but not by an inhibitor. The search for small molecule inhibitors via high throughput screening, is therefore, a necessity if researchers wish to examine directly the consequences of Nek2 inhibition on cell proliferation and cell viability in different cancer cell models.

8. Perspectives

Much has been learnt about what controls Nek2 activity in cells and how Nek2 functions in different aspects of cell division. Furthermore, from the limited number of studies performed to date, it is evident that Nek2 expression is frequently elevated in cancer cells, possibly as a result of gene amplification or loss of transcriptional control. Whether this upregulation contributes to tumour progression is an important and unresolved question, but elevated expression of Nek2 can drive aneuploidy and CIN, and there is a correlation between increased Nek2 and poor patient outcome. The key question, though, from the patient's perspective is whether tumour cells with excess Nek2 can be selectively killed by a Nek2 inhibitor. Early evidence suggests that loss of Nek2 activity may inhibit cell proliferation and trigger cell death as a result of mitotic errors. However, these data are based on depletion experiments alone and the generation of a chemical inhibitor to Nek2 would be of great value in extending these studies. Research is also needed into the consequences of Nek2 inhibition in cancer cells with different genetic backgrounds, for instance in p53 positive or negative cells. Ultimately, this will be critical to deciding in which cancers targeting Nek2 may be advantageous rather than potentially harmful to the patient.

Acknowledgements

We thank Prof M. Manson (Leicester) for critical reading of the manuscript and Prof E. Nigg (Martinsried, Germany) for communicating results prior to publication. We are also indebted to all members of our laboratory for helpful discussion. The author's laboratory is supported by grants from Cancer Research UK, the Association for International Cancer Research, the Hope Foundation for Cancer Research, The Wellcome Trust, the BBSRC and Millennium Pharmaceuticals. A.M.F. is a Lister Institute Research Fellow.

References

- [1] H. Rajagopalan, C. Lengauer, Aneuploidy and cancer, *Nature* 432 (2004) 338–341.
- [2] S. Gadde, R. Heald, Mechanisms and molecules of the mitotic spindle, *Curr. Biol.* 14 (2004) R797–R805.
- [3] W.L. Lingle, S.L. Barrett, V.C. Negron, A.B. D'Assoro, K. Boeneman, W. Liu, C.M. Whitehead, C. Reynolds, J.L. Salisbury, Centrosome amplification drives chromosomal instability in breast tumor development, *Proc. Natl Acad. Sci. (USA)* 99 (2002) 1978–1983.
- [4] E.A. Nigg, Centrosome aberrations: cause or consequence of cancer progression?, *Nat. Rev. Cancer* 2 (2002) 815–825.
- [5] G.A. Pihan, J. Wallace, Y. Zhou, S.J. Doxsey, Centrosome abnormalities and chromosome instability occur together in pre-invasive carcinomas, *Cancer Res.* 63 (2003) 1398–1404.
- [6] F.A. Barr, H.H. Sillje, E.A. Nigg, Polo-like kinases and the orchestration of cell division, *Nat. Rev. Mol. Cell Biol.* 5 (2004) 429–440.
- [7] T. Marumoto, D. Zhang, H. Saya, Aurora-A—a guardian of poles, *Nat. Rev. Cancer* 5 (2005) 42–50.
- [8] F. Eckerdt, J. Yuan, K. Strebhardt, Polo-like kinases and oncogenesis, *Oncogene* 24 (2005) 267–276.
- [9] N. Keen, S. Taylor, Aurora-kinase inhibitors as anticancer agents, *Nat. Rev. Cancer* 4 (2004) 927–936.
- [10] A.M. Fry, The Nek2 protein kinase: a novel regulator of centrosome structure, *Oncogene* 21 (2002) 6184–6194.
- [11] M.J. O'Connell, M.J. Krien, T. Hunter, Never say never. The NIMA-related protein kinases in mitotic control, *Trends Cell Biol.* 13 (2003) 221–228.
- [12] M. Fardilha, W. Wu, R. Sa, S. Fidalgo, C. Sousa, C. Mota, O.A.B. Da Cruz E Silva, E.F. Da Cruz E Silva, Alternatively spliced protein variants as potential therapeutic targets for male infertility and contraception, *Ann. NY Acad. Sci.* 1030 (2004) 468–478.
- [13] R.S. Hames, A.M. Fry, Alternative splice variants of the human centrosome kinase Nek2 exhibit distinct patterns of expression in mitosis, *Biochem. J.* 361 (2002) 77–85.
- [14] D.G. Hayward, R.B. Clarke, A.J. Faragher, M.R. Pillai, I.M. Hagan, A.M. Fry, The centrosomal kinase Nek2 displays elevated levels of protein expression in human breast cancer, *Cancer Res.* 64 (2004) 7370–7376.
- [15] S. Sonn, I. Khang, K. Kim, K. Rhee, Suppression of Nek2A in mouse early embryos confirms its requirement for chromosome segregation, *J. Cell. Sci.* 117 (2004) 5557–5566.
- [16] K. Uto, N. Nakajo, N. Sagata, Two structural variants of Nek2 kinase, termed Nek2A and Nek2B, are differentially expressed in *Xenopus* tissues and development, *Dev. Biol.* 208 (1999) 456–464.
- [17] J.S. Andersen, C.J. Wilkinson, T. Mayor, P. Mortensen, E.A. Nigg, M. Mann, Proteomic characterization of the human centrosome by protein correlation profiling, *Nature* 426 (2003) 570–574.
- [18] A.M. Fry, P. Meraldi, E.A. Nigg, A centrosomal function for the human Nek2 protein kinase, a member of the NIMA family of cell cycle regulators, *Embo. J.* 17 (1998) 470–481.
- [19] A.M. Fry, P. Descombes, C. Twomey, R. Bacchieri, E.A. Nigg, The NIMA-related kinase X-Nek2B is required for efficient assembly of the zygotic centrosome in *Xenopus laevis*, *J. Cell. Sci.* 113 (Pt 11) (2000) 1973–1984.
- [20] R. Graf, DdNek2, the first non-vertebrate homologue of human Nek2, is involved in the formation of microtubule-organizing centers, *J. Cell. Sci.* 115 (2002) 1919–1929.
- [21] Y. Ha Kim, J. Yeol Choi, Y. Jeong, D.J. Wolgemuth, K. Rhee, Nek2 localizes to multiple sites in mitotic cells, suggesting its involvement in multiple cellular functions during the cell cycle, *Biophys. Res. Commun.* 290 (2002) 730–736.
- [22] C. Prigent, D.M. Glover, R. Giet, *Drosophila* Nek2 protein kinase knockdown leads to centrosome maturation defects while overexpression causes centrosome fragmentation and cytokinesis failure, *Exp. Cell. Res.* 303 (2005) 1–13.
- [23] R.S. Hames, R.E. Crookes, K.R. Straatman, A. Merdes, M.J. Hayes, A.J. Faragher, A.M. Fry, Dynamic recruitment of Nek2 kinase to the centrosome involves microtubules, PCM-1 and localized proteasomal degradation, *Mol. Biol. Cell.* 16 (2005) 1711–1724.
- [24] K. Noguchi, H. Fukazawa, Y. Murakami, Y. Uehara, Nucleolar Nek11 is a novel target of Nek2A in G1/S-arrested cells, *J. Biol. Chem.* 279 (2004) 32716–32727.
- [25] T. Fujioka, Y. Takebayashi, M. Ito, T. Uchida, Nek2 expression and localization in porcine oocyte during maturation, *Biochem. Biophys. Res. Commun.* 279 (2000) 799–802.
- [26] K. Rhee, D.J. Wolgemuth, The NIMA-related kinase 2. Nek2, is expressed in specific stages of the meiotic cell cycle and associates with meiotic chromosomes, *Development* 124 (1997) 2167–2177.
- [27] Y. Lou, J. Yao, A. Zereshki, Z. Dou, K. Ahmed, H. Wang, J. Hu, Y. Wang, X. Yao, NEK2A interacts with MAD1 and possibly functions as a novel integrator of the spindle checkpoint signaling, *J. Biol. Chem.* 279 (2004) 20049–20057.
- [28] A. Grallert, I.M. Hagan, *S. pombe* NIMA related kinase. Fin1, regulates spindle formation, and an affinity of Polo for the SPB, *Eur. Mol. Biol. Org. J.* 21 (2002) 3096–3107.

- [29] M.J. Krien, S.J. Bugg, M. Palatsides, G. Asouline, M. Morimyo, M.J. O'Connell, A NIMA homologue promotes chromatin condensation in fission yeast, *J. Cell. Sci.* 111 (Pt 7) (1998) 967–976.
- [30] L. Fletcher, G.J. Cerniglia, T.J. Yen, R.J. Muschel. Live cell imaging reveals distinct roles in cell cycle regulation for Nek2A and Nek2B, *Biochem. Biophys. Acta* 1744 (2005) 89–92.
- [31] A.M. Fry, T. Mayor, P. Meraldi, Y.D. Stierhof, K. Tanaka, E.A. Nigg, C-Nap1, a novel centrosomal coiled-coil protein and candidate substrate of the cell cycle-regulated protein kinase Nek2, *J. Cell. Biol.* 141 (1998) 1563–1574.
- [32] T. Mayor, U. Hacker, Y.D. Stierhof, E.A. Nigg, The mechanism regulating the dissociation of the centrosomal protein C-Nap1 from mitotic spindle poles, *J. Cell. Sci.* 115 (2002) 3275–3284.
- [33] T. Mayor, K. Tanaka, Y.-D. Stierhof, A.M. Fry, E.A. Nigg, The centrosomal protein C-Nap1 displays properties supporting a role in cell cycle-regulated centrosome cohesion, *J. Cell. Biol.* 151 (2000) 837–846.
- [34] M. Casenghi, P. Meraldi, U. Weinhart, P.I. Duncan, R. Korner, E.A. Nigg, Polo-like kinase 1 regulates Nlp, a centrosome protein involved in microtubule nucleation, *Dev. Cell* 5 (2003) 113–125.
- [35] J. Rapley, J.E. Baxter, J. Blot, S.L. Wattam, M. Casenghi, P. Meraldi, E.A. Nigg, A.M. Fry, Coordinate regulation of the mother centriole component Nlp by Nek2 and Plk1 protein kinases, *Mol. Cell. Biol.* 25 (2005) 1309–1324.
- [36] J. Yao, C. Fu, X. Ding, Z. Guo, A. Zenreski, Y. Chen, K. Ahmed, J. Liao, Z. Dou, X. Yao, Nek2A kinase regulates the localization of numatrin to centrosome in mitosis, *Fed. Eur. Biol. Soc. Lett.* 575 (2004) 112–118.
- [37] C. Twomey, S.L. Wattam, M.R. Pillai, J. Rapley, J.E. Baxter, A.M. Fry, Nek2B stimulates zygotic centrosome assembly in *Xenopus laevis* in a kinase-independent manner, *Dev. Biol.* 265 (2004) 384–398.
- [38] K. Uto, N. Sagata, Nek2B, a novel maternal form of Nek2 kinase, is essential for the assembly or maintenance of centrosomes in early *Xenopus* embryos, *Eur. Mol. Biol. Org. J.* 19 (2000) 1816–1826.
- [39] S. Di Agostino, M. Fedele, P. Chieffi, A. Fusco, P. Rossi, R. Geremia, C. Sette, Phosphorylation of high-mobility group protein A2 by Nek2 kinase during the first meiotic division in mouse spermatocytes, *Mol. Biol. Cell* 15 (2004) 1224–1232.
- [40] Y. Chen, D.J. Riley, L. Zheng, P.L. Chen, W.H. Lee, Phosphorylation of the mitotic regulator protein Hec1 by Nek2 kinase is essential for faithful chromosome segregation, *J. Biol. Chem.* 277 (2002) 49408–49416.
- [41] G. Prime, D. Markie, The telomere repeat binding protein Trf1 interacts with the spindle checkpoint protein Mad1 and Nek2 mitotic kinase, *Cell. Cycle* 4 (2005) 121–124.
- [42] A. Grallert, A. Krapp, S. Bagley, V. Simanis, I.M. Hagan, Recruitment of NIMA kinase shows that maturation of the *S. pombe* spindle-pole body occurs over consecutive cell cycles and reveals a role for NIMA in modulating SIN activity, *Genes Dev.* 18 (2004) 1007–1021.
- [43] D.H. Wai, K.L. Schaefer, A. Schramm, E. Korsching, F. Van Valen, T. Ozaki, W. Boecker, L. Schweigener, B. Dockhorn-Dworniczak, C. Poremba, Expression analysis of pediatric solid tumor cell lines using oligonucleotide microarrays, *Int. J. Oncol.* 20 (2002) 441–451.
- [44] S. de Vos, W.K. Hofmann, T.M. Grogan, U. Krug, M. Schrage, T.P. Miller, J.G. Braun, W. Wachsmann, H.P. Koeffler, J.W. Said, Gene expression profile of serial samples of transformed B-cell lymphomas, *Lab. Invest.* 83 (2003) 271–285.
- [45] S.J. Schultz, A.M. Fry, C. Sutterlin, T. Ried, E.A. Nigg, Cell cycle-dependent expression of Nek2, a novel human protein kinase related to the NIMA mitotic regulator of *Aspergillus nidulans*, *Cell Growth Differ.* 5 (1994) 625–635.
- [46] L.W. Loo, D.I. Grove, E.M. Williams, C.L. Neal, L.A. Cousens, E.L. Schubert, I.N. Holcomb, H.F. Massa, J. Glogovac, C.I. Li, K.E. Malone, J.R. Daling, J.J. Delrow, B.J. Trask, L. Hsu, P.L. Porter, Array comparative genomic hybridization analysis of genomic alterations in breast cancer subtypes, *Cancer Res.* 64 (2004) 8541–8549.
- [47] M.M. Weiss, E.J. Kuipers, C. Postma, A.M. Snijders, D. Pinkel, S.G. Meuwissen, D. Albertson, G.A. Meijer, Genomic alterations in primary gastric adenocarcinomas correlate with clinicopathological characteristics and survival, *Cell. Oncol.* 26 (2004) 307–317.
- [48] M.L. Whitfield, G. Sherlock, A.J. Saldanha, J.I. Murray, C.A. Ball, K.E. Alexander, J.C. Matese, C.M. Perou, M.M. Hurt, P.O. Brown, D. Botstein, Identification of genes periodically expressed in the human cell cycle and their expression in tumors, *Mol. Biol. Cell* 13 (2002) 1977–2000.
- [49] B. Ren, H. Cam, Y. Takahashi, T. Volkert, J. Terragni, R.A. Young, B.D. Dynlacht, E2F integrates cell cycle progression with DNA repair, replication, and G2/M checkpoints, *Genes Dev.* 16 (2002) 245–256.
- [50] D. Patel, A. Incassati, N. Wang, D.J. McCance, Human papillomavirus type 16 E6 and E7 cause polyploidy in human keratinocytes and up-regulation of G2-M-phase proteins, *Cancer Res.* 64 (2004) 1299–1306.
- [51] J. Laoukili, M.R. Kooistra, A. Bras, J. Kauw, R.M. Kerkhoven, A. Morrison, H. Clevers, R.H. Medema, FoxM1 is required for execution of the mitotic programme and chromosome stability, *Nat. Cell. Biol.* 7 (2005) 126–136.
- [52] A.M. Fry, S.J. Schultz, J. Bartek, E.A. Nigg, Substrate specificity and cell cycle regulation of the Nek2 protein kinase, a potential human homolog of the mitotic regulator NIMA of *Aspergillus nidulans*, *J. Biol. Chem.* 270 (1995) 12899–12905.
- [53] R.S. Hames, S.L. Wattam, H. Yamano, R. Bacchieri, A.M. Fry, APC/C-mediated destruction of the centrosomal kinase Nek2A occurs in early mitosis and depends upon a cyclin A-type D-box, *Eur. Mol. Biol. Org. J.* 20 (2001) 7117–7127.
- [54] A.M. Fry, L. Arnaud, E.A. Nigg, Activity of the human centrosomal kinase. Nek2, depends on an unusual leucine zipper dimerization motif, *J. Biol. Chem.* 274 (1999) 16304–16310.

- [55] S. Di Agostino, P. Rossi, R. Geremia, C. Sette, The MAPK pathway triggers activation of Nek2 during chromosome condensation in mouse spermatocytes, *Development* 129 (2002) 1715–1727.
- [56] N.R. Helps, X. Luo, H.M. Barker, P.T. Cohen, NIMA-related kinase 2 (Nek2), a cell-cycle-regulated protein kinase localized to centrosomes, is complexed to protein phosphatase 1, *Biochem. J.* 349 (2000) 509–518.
- [57] P. Meraldi, E.A. Nigg, Centrosome cohesion is regulated by a balance of kinase and phosphatase activities, *J. Cell. Sci.* 114 (2001) 3749–3757.
- [58] M. Eto, E. Elliott, T.D. Prickett, D.L. Brautigan, Inhibitor-2 regulates protein phosphatase-1 complexed with NimA-related kinase to induce centrosome separation, *J. Biol. Chem.* 277 (2002) 44013–44020.
- [59] L. Fletcher, G.J. Cerniglia, E.A. Nigg, T.J. Yen, R.J. Muschel, Inhibition of centrosome separation after DNA damage: a role for Nek2, *Radiat. Res.* 162 (2004) 128–135.
- [60] Y.L. Lo, J.C. Yu, S.T. Chen, H.C. Yang, C.S. Fann, Y.C. Mau, C.Y. Shen, Breast cancer risk associated with genotypic polymorphism of the mitosis-regulating gene Aurora-A/STK15/BTAK, *Int. J. Cancer* 115 (2005) 276–283.
- [61] A.J. Faragher, A.M. Fry, Nek2A kinase stimulates centrosome disjunction and is required for formation of bipolar mitotic spindles, *Mol. Biol. Cell* 14 (2003) 2876–2889.
- [62] J. Dancey, E.A. Sausville, Issues and progress with protein kinase inhibitors for cancer treatment, *Nat. Rev. Drug. Discov.* 2 (2003) 296–313.
- [63] M.A. Fabian, W.H. Biggs, D.K. Treiber, C.E. Atteridge, M.D. Azimioara, M.G. Benedetti, T.A. Carter, P. Ciceri, P.T. Edeen, M. Floyd, J.M. Ford, M. Galvin, J.L. Gerlach, R.M. Grotzfeld, S. Herrgard, D.E. Insko, M.A. Insko, A.G. Lai, J.M. Lelias, S.A. Mehta, Z.V. Milanov, A.M. Velasco, L.M. Wodicka, H.K. Patel, P.P. Zarrinkar, D.J. Lockhart, A small molecule-kinase interaction map for clinical kinase inhibitors, *Nat. Biotechnol.* 23 (2005) 329–336.
- [64] P. Cohen, Protein kinases—the major drug targets of the twenty-first century?, *Nat. Rev. Drug Discov.* 1 (2002) 309–315.